Programa de Doctorado "Matemáticas"

PhD Dissertation

Algunas contribuciones al análisis de sistemas lineales a trozos

Some contributions to the analysis of piecewise linear systems

---

Author
Andrés Felipe Amador Rodríguez

Supervisor
Prof. Dr. Enrique Ponce Núñez

Co-supervisor
Prof. Dr. Fco. Javier Ros Padilla

Sevilla, septiembre de 2018.

A mis padres y a todos mis seres queridos

Agradecimientos

Mi agradecimiento a todos los profesores del Departamento de Matemática Aplicada II de la Universidad de Sevilla, y a la Pontificia Universidad Javeriana-Cali, institución en la cual trabajo, que me brindó la oportunidad de realizar mis estudios de doctorado.

Abstract

This thesis consists of two parts, with contributions to the analysis of dynamical systems in continuous time and in discrete time, respectively.

In the first part, we study several models of memristor oscillators of dimension three and four, providing for the first time rigorous mathematical results regarding the rich dynamics of such memristor oscillators, both in the case of piecewise linear models and polynomial models. Thus, for some families of discontinuous 3D piecewise linear memristor oscillators, we show the existence of an infinite family of invariant manifolds and that the dynamics on such manifolds can be modeled without resorting to discontinuous models. Our approach provides topologically equivalent continuous models with one dimension less but with one extra parameter associated to the initial conditions. It is possible so to justify the periodic behavior exhibited by such three dimensional memristor oscillators, by taking advantage of known results for planar continuous piecewise linear systems.

By using the first-order Melnikov theory, we derive the bifurcation set for a three-parametric family of Bogdanov-Takens systems with symmetry and deformation. As an applications of these results, we study a family of 3D memristor oscillators where the characteristic function of the memristor is a cubic polynomial. In this family we also show the existence of an infinity number of invariant manifolds. Also, we clarify some misconceptions that arise from the numerical simulations of these systems, emphasizing the important role of invariant manifolds in these models.

In a similar way than for the 3D case, we study some discontinuous 4D piecewise linear memristor oscillators, and we show that the dynamics in each stratum is topologically equivalent to a continuous 3D piecewise linear dynamical system. Some previous results on bifurcations in such reduced systems, allow us to detect rigorously for the first time a multiple focus-center-cycle bifurcation in a three-parameter space, leading to the appearance of a topological sphere in the original model, completely foliated by stable periodic orbits.

In the second part of this thesis, we show that the two-dimensional stroboscopic map defined by a second order system with a relay based control and a linear switching surface is topologically equivalent to a canonical form for discontinuous piecewise linear systems. Studying the main properties of the stroboscopic map defined by such a canonical form, the orbits of period two are completely characterized. At last, we give a conjecture about the occurrence of the *big bang* bifurcation in the previous map.

Contents

Chapter 1

Motivation and main contributions

In this thesis, concerning the bifurcation analysis of certain families of dynamical systems, two different problems are studied. Consequently, the thesis is formed of two parts. In the first part, namely Chapters 2, 3 and 4, several models of memristor oscillators of dimension three and four are investigated. In the second part, that consists of Chapter 5, a two-dimensional stroboscopic map, defined by a discontinuous piecewise linear system is considered. Detailed literature surveys are presented in the individual chapters.

1.1 Motivation

A system of ordinary differential equations or a map is said to be piecewise-smooth if the phase space can be partitioned into a finite number of regions, so that within each region the dynamical system is smooth. These regions are separated by boundaries, often called switching manifolds. In general, these systems can have two different types of bifurcations. On the one hand, there can be local bifurcations, associated to changes in a small neighborhood of the phase space belonging to the interior of a smoothness region (v.g. a stability change for one equilibrium point), and global bifurcations, which depend on qualitative changes affecting a subset of the phase space of significant size (for instance, the formation of homoclinic or heteroclinic connections). The second type of bifurcations are caused by collisions of invariant sets with the switching manifolds, and they are usually called border-collision bifurcations. These bifurcations represent one of the main features of piecewise-smooth systems as they cannot occur in smooth systems. For more details, see for instance Zusubaliev and Mosekilde [2003], Bernardo et al. [2008a], Awrejcewicz and Lamarque [2003], Di Bernardo et al. [2008].

Many dynamical systems that occur in physical processes belong to the class of piecewise-smooth systems, sometimes involving abrupt events or fast transitions. In particular, the class of piecewise-linear (PWL, for short) systems is an important class that appears naturally in realistic nonlinear engineering models, as certain devices are accurately modeled by PWL vector fields or maps, see for instance Simpson [2010], Avrutin et al. [2018]. This kind of models are frequent in applications from electronic engineering and nonlinear control systems, where PWL models cannot be

considered as idealized ones, see Tse [2003], Adamatzky and Chen [2013]. As far as we know, the pioneering investigation of PWL systems in a rigorous way is due to Andronov and coworkers (Andronov et al. [1966]). The lack of differentiability of PWL systems interferes with the standard application of the classical and powerful results that come from the theory of dynamic systems and bifurcations of differentiable dynamics, see the celebrated books by Guckenheimer and Holmes [1983] and Kuznetsov [2004]. This fact makes the endeavor of building a general theory for PWL systems to be a impressively large work, as you must proceed via a case-study approach.

The first part of this thesis is motivated by the few rigorous mathematical studies on memristor oscillators that have been reported. In fact, when memristors oscillators with continuous PWL characteristics are modeled in the usual current-voltage setting, the lack of smoothness leads to discontinuous PWL systems. Such discontinuities make it difficult to get mathematical proofs about their dynamics. Thus, for such models, many authors have described just numerically the presence of periodic orbits and chaotic behavior (see for instance Bao et al. [2017, 2016], Chen and Li [2014], Corinto and Forti [2017], Kengne et al. [2017], Wang et al. [2017], Zheng et al. [2018]).

No doubt, these devices represents an emerging topic of study in modern electronic engineering, see Itoh and Chua [2008], Messias et al. [2010], Corinto et al. [2011], Scarabello and Messias [2014], Chen and Li [2014], Corinto et al. [2015], Llibre et al. [2015]. As described in Ginoux and Llibre [2016], on April $30th$, 2008, Stan Williams and co-workers (Strukov et al. [2008]) announced in the journal *Nature* that the missing circuit element, postulated 37 years before by Leon Chua, had been found. Afterwards, the memristor has been the object of many studies and applications, see for instance Tetzlaff [2016], Radwan and Fouda [2015], Chua et al. [2012], Mehonic et al. [2012].

In Chua [1971], the memristor was defined as an electronic device characterized by a relation of type $f(\varphi, q) = 0$ between its flux φ and its charge q. Memristor is so known as the fourth basic two-terminal circuit element, where the other three are the resistance, the inductance and the capacitance. According to Itoh and Chua [2008] a memristor is characterized by a continuous function $q(\varphi)$ (respectively $\varphi(q)$) and it is passive if and only if the derivative of this function $W(\varphi)$ (respectively $M(q)$) is non-negative. The variable q represents the *current momentum* of the device

$$q(t) = \int_{-\infty}^{t} i(\tau)d\tau$$

and by analogy is usually called *charge*, while the variable φ represents the *voltage momentum*

$$\varphi(t) = \int_{-\infty}^{t} v(\tau)d\tau$$

and is called *flux*, see Corinto et al. [2015]. The voltage across a charge-controlled

memristor is given by $v(t) = M(q)i(t)$, where

$$M(q) = \frac{d\varphi(q)}{dq}$$

is measured in resistance units, being called *memristance*. The current on a flux-controlled memristor is defined by $i(t) = W(\varphi)v(t)$, where

$$W(\varphi) = \frac{dq(\varphi)}{d\varphi}$$

is measured in conductance units and is called *memductance*.

In the paper *Memristor Oscillators* by Itoh and Chua Itoh and Chua [2008] authors derive several nonlinear oscillators starting from Chua's oscillators, by replacing every Chua's diode with a memristor. They assume that the memristor is characterized by the monotone increasing and piecewise linear nonlinearity $q(\varphi) = b\varphi + 0.5(a-b)(|\varphi+1| - |\varphi-1|)$ or $\varphi(q) = dq + 0.5(c-d)(|q+1| - |q-1|)$ where $a, b, c, d > 0$. Thus, the corresponding functions $W(\varphi)$ and $M(q)$ become discontinuous piecewise-constant scalar functions. In two PWL models of third-order (see sections 3.2 and 4.2 of the quoted paper) they detect numerically the existence of some limit cycles but no global insight for the dynamics was pursued.

Later on, a deeper insight was sought in the articles by Messias and coworkers (Messias et al. [2010], Scarabello and Messias [2014]). They were conscious of the existence of a family of planes where the dynamics is to be confined, but the discontinuity issue did not allow them to completely describe the found dynamics for the different models.

The dynamics of a continuous PWL system in $\mathbb{R}^3$ with two or three zones can be rather complex. In these systems, phenomena as bistability, hysteresis, instantaneous transitions of a stable equilibrium to chaotic attractor, and the existence of invariant cones have been reported, see Carmona et al. [2006], Simpson [2016], Bernardo et al. [2008b], Freire et al. [2017, 2009, 2008].

In particular, for memristor oscillators with a dimension greater than or equal to four, cases of extreme multistability leading to coexistence of an infinite number of attractors are reported, see Bao et al. [2018], Chen et al. [2017], Wang et al. [2018], Yuan et al. [2017], Zhang et al. [2018]. However, a rigorous mathematical proof of these phenomena is still lacking.

On the other hand, the motivation of the second part of this thesis comes from the study of a conjecture given in Fossas and Granados [2013]. In such conjecture, the presence of the so-called big bang bifurcation in a two-dimensional discontinuous stroboscopic map defined by a discontinuous PWL system is discussed.

Discontinuous maps have been used in the modeling of switching phenomena in electrical circuits and as Poincaré maps associated with piecewise-smooth systems, see for instance El Aroudi et al. [2007], Avrutin et al. [2014], Olivar et al.

[2000], Kollár et al. [2004]. In Avrutin et al. [2006], the concept of big-bang bifurcation (BB bifurcation, for short) was presented, analyzing both two and three-dimensional parameter spaces. It was shown that BB bifurcations can be of three kinds: period-increasing with attractor coexistence, period-increasing with period-adding and period-increasing with chaotic inclusions. In Avrutin et al. [2007], a codimension-N BB bifurcation point is generically defined as a point in the N-dimensional parameter space ($N \geq 2$) where an infinite number of codimension $N-1$ curves intersect. In Avrutin et al. [2011], the authors gave sufficient conditions for the presence of the BB bifurcation of period incrementing type in a piecewise one-dimensional map. An excellent review of the BB bifurcation can be found in Granados et al. [2017].

The jump from dimension one to dimension two represents a really challenging problem, and few works have reported the presence of the BB bifurcation in two-dimensional maps. In Amador et al. [2014], the authors show the existence of a BB bifurcation point in a two-dimensional system defined by a Boost Converter controlled by centered pulse-width modulation and a zero average dynamics (ZAD, for short) strategy. Later on, in Fossas and Granados [2013], the authors consider the two-dimensional stroboscopic map defined by a second order system with a relay based control and a linear switching surface, giving a conjecture about the presence of a big bang bifurcation point in this map.

1.2 Outline of this thesis

Each chapter of this thesis is self-contained and has a detailed introduction and its own bibliography. Therefore, we will only give a description of the main results and tools that we use in our research.

In the first part of this thesis we study several models of memristor oscillators of dimension three and four. In Chapter 2, we provide for the first time rigorous mathematical results regarding the rich dynamics of piecewise linear memristor oscillators. In particular, for each nonlinear oscillator given in Itoh and Chua [2008], we show the existence of an infinite family of invariant manifolds and that the dynamics on such manifolds can be modeled without resorting to discontinuous models. Our approach provides topologically equivalent continuous models with one dimension less but with one extra parameter associated to the initial conditions. It is possible so to justify the periodic behavior exhibited by three dimensional memristor oscillators, by taking advantage of known results for planar continuous piecewise linear systems. The results of this chapter are already published in the journals *International Journal Bifurcation and Chaos* and *Microelectronic Engineering*, see Amador et al. [2017] and Ponce et al. [2017] respectively.

In Chapter 3, we derive the bifurcation set for a three-parametric family of

Bogdanov-Takens systems with symmetry and deformation given by

$$\begin{aligned}\dot{x} &= y,\\ \dot{y} &= \mu_1 + \mu_2 x + x^3 + y(\mu_3 - 3x^2).\end{aligned}$$

We show that it is possible to write the system as a perturbed Hamiltonian, and by using the first-order Melnikov function, we report for the first time in this system, an analytical approximation of the bifurcation curves for homoclinic and heteroclinic connections. As an application of these results, we study a family of 3D memristor oscillators, where the characteristic function of the memristor is a cubic polynomial. We show that this system has an infinity number of invariant manifolds, and by adding one parameter that stratifies the 3D dynamics, it is shown that the dynamics in each stratum is topologically equivalent to a Bogdanov-Takens system with symmetry. Also, based on the bifurcation set obtained in this chapter, we show the existence of closed surfaces in the 3D state space which are foliated by periodic orbits. Finally, we clarify some misconceptions that arise from the numerical simulations of these systems, emphasizing the important role of invariant manifolds in these models. The results of this chapter have been submitted for publication to the journal *Nonlinearity*.

In Chapter 4, we focus our analysis in the existence of multiple stable oscillations in the 4D PWL version of the canonical circuit proposed in Itoh and Chua [2008]. This oscillator is modeled by a discontinuous piecewise linear dynamical system. By adding one parameter that stratifies the 4D dynamics, it is shown that the dynamics in each stratum is topologically equivalent to a 3D continuous piecewise linear dynamical system. Some previous results on bifurcations in such reduced system, allow to detect rigorously for the first time a multiple focus-center-cycle bifurcation in a three-parameter space, leading to the appearance of a topological sphere in the original model, completely foliated by stable periodic orbits. The results of this chapter have been recently published in the journal *Nonlinear Dynamics*.

In the second part of this thesis, that consists of Chapter 5, we study the two-dimensional stroboscopic map defined by the normalized canonical form for discontinuous PWL systems introduced in Freire et al. [2014]. We rigorously study the properties of the map, and we give sufficient conditions for the existence of period two orbits. In addition, considering a special family of n-periodic orbits, we study the border collision bifurcation curves of these orbits, and we give a sufficient conditions for the admissibility of such orbits. Finally, we show that the two-dimensional stroboscopic map defined by a second order system with a relay based control and a linear switching surface, considered in Fossas and Granados [2013], is a particular case of our two-dimensional map, and by using the theory developed in this chapter, we present an extension to our map of the conjecture given in the quoted paper. In this conjecture, the presence of the big bang bifurcation is discussed. We are preparing a manuscript with the main results of this chapter, which will be submitted in a near future.

1.3 Own contributions

The scientific contributions of this thesis appear distributed along chapters, where in each one we present the notation, a revision of the terminology and the techniques used. As usual, the different results achieved during the preparation of this work have been the subject of scientific publications; some of them already appeared, but some other are still in the process of being published. Thus, we can summarize a significant part of our new results in the following five publications.

- Chapter 2:
  On Discontinuous Piecewise Linear Models for Memristor Oscillators, *International Journal of Bifurcation and Chaos*. See Amador et al. [2017].
  Unravelling the dynamical richness of 3D canonical memristor oscillators, *Microelectronic Engineering*. See Ponce et al. [2017]

- Chapter 3:
  Bifurcation set of a Bogdanov-Takens system with symmetry. Application to 3D cubic Memristor oscillators, *Submitted to Nonlinearity*. See Amador et al. [2018].

- Chapter 4:
  A multiple focus-center-cycle bifurcation in 4D discontinuous piecewise linear Memristor oscillators, *Nonlinear Dynamics*. See Ponce et al. [2018].

- Chapter 5:
  On the Big Bang Bifurcation in the stroboscopic map for discontinuous PWL Systems. An application in Discretized Sliding-mode Control Systems. *In preparation*.

Bibliography

Andrew Adamatzky and Guanrong Chen. *Chaos, CNN, memristors and beyond: a festschrift for Leon Chua*. World Scientific, 1 edition, 2013. ISBN 978-981-4434-80-5. URL https://www.worldscientific.com/worldscibooks/10.1142/8590.

A. Amador, S. Casanova, G. Olivar, and J. Hurtado. Codimension-two big-bang bifurcation in a ZAD-controlled boost DC-DC converter. *Publicacions Matematiques*, 24:1450150, 2014. URL https://doi.org/10.1142/S0218127414501508.

A. Amador, E. Freire, E. Ponce, and J. Ros. On discontinuous piecewise linear models for memristor oscillators. *International Journal of Bifurcation and Chaos*, 27 (06):1730022, jun 2017. URL https://doi.org/10.1142/s0218127417300221.

A. Amador, E. Freire, and E. Ponce. Bifurcation set of a Bogdanov-Takens system with symmetry. application to 3D cubic memristor oscillators. *submitted*, 2018.

A.A. Andronov, A. A. Vitt, and S.E. Khaikin. *Theory of oscillators*. Dover, 1 edition, 1966. ISBN 978-148-319-472-1. URL https://www.elsevier.com/books/theory-of-oscillators/andronov/978-1-4831-6724-4.

V. Avrutin, M. Schanz, and S. Banerjee. Multi-parametric bifurcations in a piecewise-linear discontinuous map. *Nonlinearity*, 19(8):1875–1906, 2006. URL http://stacks.iop.org/0951-7715/19/i=8/a=007.

V. Avrutin, M. Schanz, and S. Banerjee. Codimension-three bifurcations: Explanation of the complex one, two, and three-dimensional bifurcation structures in nonsmooth maps. *Physical Review E*, 75:066205, Jun 2007. URL https://doi.org/10.1103/PhysRevE.75.066205.

V. Avrutin, A. Granados, and M. Schanz. Sufficient conditions for a period incrementing big bang bifurcation in one-dimensional maps. *Nonlinearity*, 24(9):2575, 2011. URL http://stacks.iop.org/0951-7715/24/i=9/a=012.

V. Avrutin, I. Sushko, and L. Gardini. Cyclicity of chaotic attractors in one-dimensional discontinuous maps. *Mathematics and Computers in Simulation*, 95: 126–136, jan 2014. URL https://doi.org/10.1016/j.matcom.2012.07.019.

Viktor Avrutin, Laura Gardini, Michael Schanz, Irina Sushko, and Fabio Tramontana. *Continuous and discontinuous piecewise-smooth one-dimensional maps: invariant sets and bifurcation structures*. World Scientific, 1 edition, 2018. ISBN 978-981-436-882-7. URL https://www.worldscientific.com/worldscibooks/10.1142/8285.

Jan Awrejcewicz and Claude Lamarque. *Bifurcation and Chaos in Nonsmooth Mechanical Systems*. World Scientific, 1 edition, 2003. ISBN 978-981-256-480-1. URL https://www.worldscientific.com/worldscibooks/10.1142/5342.

B.C. Bao, Jiang Tao, Q. Xu, M. Chen, Huagan Wu, and Yihua Hu. Coexisting infinitely many attractors in active band-pass filter-based memristive circuit. *Nonlinear Dyn*, 86:17111723, 2016. URL https://doi.org/10.1007/s11071-016-2988-6.

B.C. Bao, H. Bao, N. Wang, M. Chen, and Q. Xu. Hidden extreme multistability in memristive hyperchaotic system. *Chaos, Solitons & Fractals*, 94(Supplement C): 102–111, 2017. URL https://doi.org/10.1016/j.chaos.2016.11.016.

H. Bao, T. Jiang, K. Chu, M. Chen, Q. Xu, and B. Bao. Memristor-based canonical Chua's circuit: Extreme multistability in voltage-current domain and its controllability in flux-charge domain. *Complexity*, 2018:1–13, 2018. URL https://doi.org/10.1155/2018/5935637.

M. Di Bernardo, C.J. Budd, A.R. Champneys, P. Kowalczyk, A.B. Nordmark, G. Olivar, and P.T. Piiroinen. Bifurcations in nonsmooth dynamical systems. *SIAM Review*, 50(4):629–701, 2008a. URL https://doi.org/10.1137/050625060.

M. Di Bernardo, A. Nordmark, and G. Olivar. Discontinuity-induced bifurcations of equilibria in piecewise-smooth and impacting dynamical systems. *Physica D: Nonlinear Phenomena*, 237(1):119 – 136, 2008b. ISSN 0167-2789. URL https://doi.org/10.1016/j.physd.2007.08.008.

V. Carmona, E. Freire, E. Ponce, and F. Torres. The continuous matching of two stable linear systems can be unstable. *Discrete and Continuous Dynamical Systems*, 16(3):689–703, 2006. ISSN 1078-0947. URL https://doi.org/10.3934/dcds.2006.16.689.

H. Chen and X. Li. Global phase portraits of memristor oscillators. *International Journal of Bifurcation and Chaos*, 24(12):1450152, 2014. URL https://doi.org/10.1142/S0218127414501521.

M. Chen, M. Sun, B. Bao, H. Wu, Q. Xu, and J. Wang. Controlling extreme multistability of memristor emulator-based dynamical circuit in flux-charge domain. *Nonlinear Dynamics*, 91(2):1395–1412, nov 2017. URL https://doi.org/10.1007/s11071-017-3952-9.

L.O. Chua. Memristor: The missing circuit element. *IEEE Trans. Circuit Theory*, 18:507–519, 1971. URL https://doi.org/10.1109/TCT.1971.1083337.

L.O. Chua, V. Sbitnev, and H. Kim. Hodgkin-Huxley axon is made of memristors. *International Journal of Bifurcation and Chaos*, 22(3):1230011, 2012. URL https://doi.org/10.1109/TCT.1971.1083337.

F. Corinto and M. Forti. Memristor circuits: Bifurcations without parameters. *IEEE Transactions on Circuits and Systems I: Regular Papers*, 64(6):1540–1551, jun 2017. URL https://doi.org/10.1109/tcsi.2016.2642112.

F. Corinto, A. Ascoli, and M. Gilli. Nonlinear dynamics of memristor oscillators. *IEEE Transactions on circuits and systems*, 58(6):1323–1336, 2011. URL https://doi.org/10.1109/TCSI.2010.2097731.

F. Corinto, P. Civalleri, and L.O. Chua. A theoretical approach to memristor devices. *IEEE Journal of emerging and selected topics in circuits and systems*, 5(6):123–132, 2015. URL https://doi.org/10.1109/JETCAS.2015.2426494.

M. Di Bernardo, C.J. Budd, A.R. Champneys, P. Kowalczyk, A.B. Nordmark, G. Olivar, and P.T. Piiroinen. Bifurcations in nonsmooth dynamical systems. *SIAM Review*, 50(4):629–701, jan 2008. URL https://doi.org/10.1137/050625060.

A. El Aroudi, M. Debbat, and L. Martinez-Salamero. Poincaré maps modeling and local orbital stability analysis of discontinuous piecewise affine periodically driven systems. *Nonlinear Dynamics*, 50(3):431–445, jan 2007. URL https://doi.org/10.1007/s11071-006-9190-1.

E. Fossas and A. Granados. Occurrence of big bang bifurcations in discretized sliding-mode controlled systems. *Differential Equations and Dynamical Systems*, 21:35–43, 2013. URL https://doi.org/10.1007/s12591-012-0121-y.

E. Freire, E. Ponce, and J. Ros. Bistability and hysteresis in symmetric 3D piecewise linear oscillators with three zones. *International Journal of Bifurcation and Chaos*, 18(12):3633–3645, 2008. URL https://doi.org/10.1142/S0218127408022603.

E. Freire, E. Ponce, and J. Ros. Following a saddle-node of periodic orbits bifurcation curve in Chua's circuit. *International Journal of Bifurcation and Chaos*, 19(02):487–495, 2009. URL https://doi.org/10.1142/S0218127409023147.

E. Freire, E. Ponce, and F. Torres. A general mechanism to generate three limit cycles in planar filippov systems with two zones. *Nonlinear Dynamics*, 78(1):251–263, 2014. URL https://doi.org/10.1007/s11071-014-1437-7.

E. Freire, M. Ordónez, and E. Ponce. Limit cycle bifurcation from a persistent center at infinity in 3D piecewise linear systems with two zones. *Trends in Mathematics, Extended Abstracts Spring 2016*, 18, 2017. ISSN 978-3-319-55641-3. URL https://doi.org/10.1007/978-3-319-55642-0_10.

J. Ginoux and J. Llibre. Canards existence in memristor's circuits. *Qualitative Theory of Dynamical Systems*, 15:383–431, 2016. URL https://doi.org/10.1007/s12346-015-0160-1.

A. Granados, L. Alsedà, and M. Krupa. The period adding and incrementing bifurcations: From rotation theory to applications. *SIAM Review*, 59(2):225–292, jan 2017. URL https://doi.org/10.1137/140996598.

John Guckenheimer and Philip Holmes. *Nonlinear oscillations, dynamical systems, and bifurcations of vector fields*. Springer, 1 edition, 1983. ISBN 978-1-4612-1140-2. URL https://www.springer.com/la/book/9780387908199.

M. Itoh and L.O. Chua. Memristor oscillators. *International Journal of Bifurcation and Chaos*, 18(11):3183–3206, 2008. URL http://dx.doi.org/10.1142/S0218127408022354.

J. Kengne, A. Nguomkam Negou, and D. Tchiotsop. Antimonotonicity, chaos and multiple attractors in a novel autonomous memristor-based jerk circuit. *Nonlinear Dyn*, 88:25892608, 2017. URL https://doi.org/10.1007/s11071-017-3397-1.

L. Kollár, G. Stépán, and J. Turi. Dynamics of piecewise linear discontinuous maps. *International Journal of Bifurcation and Chaos*, 14(07):2341–2351, jul 2004. URL https://doi.org/10.1142/s0218127404010837.

Yuri Kuznetsov. *Elements of applied bifurcation theory*. Springer, 1 edition, 2004. ISBN 978-1-4757-3978-7. URL https://www.springer.com/gb/book/9780387219066.

J. Llibre, E. Ponce, and C. Valls. Uniqueness and non-uniqueness of limit cycles for piecewise linear differential systems with three zones and no symmetry. *Journal of Nonlinear Science*, 25(4):861–887, 2015. URL https://doi.org/10.1007/s00332-015-9244-y.

A. Mehonic, S. Cueff, M. Wojdak, S. Hudziak, O. Jambois, C. Labbe, B. Garrido, R. Rizk, and A. Kenyon. Resistive switching in silicon suboxide films. *Journal of Applied Physics*, 111(7):074507, 2012. URL https://doi.org/10.1063/1.3701581.

M. Messias, C. Nespoli, and V.A. Botta. Hopf bifurcation from lines of equilibria without parameters in memristor oscillators. *International Journal of Bifurcation and Chaos*, 20(02):437–450, feb 2010. URL https://doi.org/10.1142/s0218127410025521.

G. Olivar, E. Fossas, and C. Batlle. Bifurcations and chaos in converters. discontinuous vector fields and singular poincaré maps. *Nonlinearity*, 13(4):1095–1121, may 2000. URL https://doi.org/10.1088/0951-7715/13/4/307.

E. Ponce, A. Amador, and J. Ros. Unravelling the dynamical richness of 3D canonical memristor oscillators. *Microelectronic Engineering*, 182:15–24, oct 2017. URL https://doi.org/10.1016/j.mee.2017.08.004.

E. Ponce, A. Amador, and J. Ros. A multiple focus-center-cycle bifurcation in 4D discontinuous piecewise linear memristor oscillators. *Nonlinear Dynamics*, 2018. URL https://doi.org/10.1007/s11071-018-4541-2.

Ahmed Radwan and Mohammed Fouda. *On the Mathematical Modeling of Memristor, Memcapacitor, and Meminductor*. Springer International Publishing, 1 edition, 2015. ISBN 978-3-319-17491-4. URL https://www.springer.com/gb/book/9783319174907.

M. Scarabello and M. Messias. Bifurcations leading to nonlinear oscillations in a 3D piecewise linear memristor oscillator. *International Journal of Bifurcation and Chaos*, 24(01):1430001, jan 2014. URL https://doi.org/10.1142/s0218127414300018.

David John Warwick Simpson. *Bifurcation in piecewise-smooth continuous systems*. World Scientific, 1 edition, 2010. ISBN 978-981-4293-85-3. URL https://www.worldscientific.com/worldscibooks/10.1142/7612.

D.J.W. Simpson. The instantaneous local transition of a stable equilibrium to a chaotic attractor in piecewise-smooth systems of differential equations. *Physics Letters A*, 380(38):3067 – 3072, 2016. ISSN 0375-9601. URL https://doi.org/10.1016/j.physleta.2016.07.033.

D.B. Strukov, G.S. Snider, G.R. Stewart, and R.S. Williams. The missing memristor found. *Nature*, 453:80–83, 2008. URL https://doi.org/10.1038/nature06932.

Ronald Tetzlaff. *Memristors and Memristive systems*. Springer-Verlag New York, 1 edition, 2016. ISBN 978-1-4614-9068-5. URL https://www.springer.com/la/book/9781461490678.

Chi Kong Tse. *Complex Behavior of Switching Power Converters*. CRC Press, 1 edition, 2003. ISBN 978-084-931-862-7. URL https://www.crcpress.com/Complex-Behavior-of-Switching-Power-Converters/Tse/p/book/9780849318627.

G. Wang, F. Yuan, G. Chen, and Y. Zhang. Coexisting multiple attractors and riddled basins of a memristive system. *Chaos: An Interdisciplinary Journal of Nonlinear Science*, 28(1):013125, jan 2018. URL https://doi.org/10.1063/1.5004001.

Z. Wang, A. Akgul, V.T. Pham, and S. Jafari. Chaos-based application of a novel no-equilibrium chaotic system with coexisting attractors. *Nonlinear Dynamics*, 89(3):1877–1887, may 2017. URL https://doi.org/10.1007/s11071-017-3558-2.

F. Yuan, G. Wang, and X. Wang. Extreme multistability in a memristor-based multi-scroll hyper-chaotic system. *Chaos*, 26(7):073107, 2017. URL https://doi.org/10.1063/1.4958296.

S. Zhang, Y. Zeng, Z. Li, M. Wang, and L. Xiong. Generating one to four-wing hidden attractors in a novel 4d no-equilibrium chaotic system with extreme multistability. *Chaos: An Interdisciplinary Journal of Nonlinear Science*, 28(1):013113, jan 2018. URL https://aip.scitation.org/doi/10.1063/1.5006214.

C. Zheng, H.C. Herbert, F. Tyrone, Y. Dongsheng, G. Hengdao, and J.K. Eshraghian. Analysis and generation of chaos using compositely connected coupled memristors. *Chaos: An Interdisciplinary Journal of Nonlinear Science*, 28(6):063115, jun 2018. URL https://aip.scitation.org/doi/10.1063/1.5023142.

Zanybai T Zusubaliev and Erik Mosekilde. *Bifurcations and chaos in piecewise-smooth dynamical systems*. World Scientific, 1 edition, 2003. ISBN 978-981-256-443-6. URL https://www.worldscientific.com/worldscibooks/10.1142/5313.

Part I

Memristor oscillators

Chapter 2

3D discontinuous PWL memristor oscillators

In this chapter, we provide for the first time rigorous mathematical results regarding the rich dynamics of piecewise linear memristor oscillators. In particular, for several nonlinear oscillators given in Itoh and Chua [2008], we show the existence of an infinite family of invariant manifolds and that the dynamics on such manifolds can be modeled without resorting to discontinuous models. Our approach provides topologically equivalent continuous models with one dimension less but with one extra parameter associated to the initial conditions. It is possible so to justify the periodic behavior exhibited by three dimensional memristor oscillators, by taking advantage of known results for planar continuous piecewise linear systems.

2.1 Continuous PWL systems with three zones

Before restricting ourselves to the class of piecewise linear systems (PWL) we are interested in, let us start with some standard definitions and properties of piecewise continuous linear systems. We start by considering a differential system defined as follows

$$\begin{aligned}
\begin{pmatrix} \dot{x} \\ \dot{y} \end{pmatrix} &= A_L \begin{pmatrix} x \\ y \end{pmatrix} + \mathbf{b}_L, \quad \text{if } x < -1, \\
\begin{pmatrix} \dot{x} \\ \dot{y} \end{pmatrix} &= A_C \begin{pmatrix} x \\ y \end{pmatrix} + \mathbf{b}_C, \quad \text{if } |x| \leq 1, \\
\begin{pmatrix} \dot{x} \\ \dot{y} \end{pmatrix} &= A_R \begin{pmatrix} x \\ y \end{pmatrix} + \mathbf{b}_R, \quad \text{if } x > 1,
\end{aligned} \tag{2.1}$$

where $A_{\{L,C,R\}}$ and $b_{\{L,C,R\}}$ are constant square matrices and vectors in dimension two and we require for the full vector field to be continuous. Namely, we must have

$$\begin{aligned}
A_L \begin{pmatrix} -1 \\ y \end{pmatrix} + \mathbf{b}_L &= A_C \begin{pmatrix} -1 \\ y \end{pmatrix} + \mathbf{b}_C, \\
A_R \begin{pmatrix} 1 \\ y \end{pmatrix} + \mathbf{b}_R &= A_C \begin{pmatrix} 1 \\ y \end{pmatrix} + \mathbf{b}_C,
\end{aligned} \tag{2.2}$$

for all $y \in \mathbb{R}$. Thus, our vector fields are in fact of differentiability class $\mathcal{C}^\infty$ except in the points with $x = \pm 1$, where the vector field is only continuous, that is of class $\mathcal{C}^0$. Note however that the vector field satisfies a Lipschitz condition on the whole $\mathbb{R}^2$ and thus, the classical theorems on existence, uniqueness and continuity of solutions with respect to initial conditions and parameters apply to these systems. In fact, solutions are differentiable with continuity and so they will be always of class $\mathcal{C}^1$ at least. Taking $y = 0$, we deduce

$$\begin{aligned} a_{11}^L - b_1^L &= a_{11}^C - b_1^C, \\ a_{21}^L - b_2^L &= a_{21}^C - b_2^C, \end{aligned}$$

and

$$\begin{aligned} a_{11}^R + b_1^R &= a_{11}^C + b_1^C, \\ a_{21}^R + b_2^R &= a_{21}^C + b_2^C. \end{aligned}$$

After canceling these terms in (2.2), we have the condition

$$A_L \begin{pmatrix} 0 \\ y \end{pmatrix} = A_C \begin{pmatrix} 0 \\ y \end{pmatrix} = A_R \begin{pmatrix} 0 \\ y \end{pmatrix} \text{ for all } y \in \mathbb{R}, \tag{2.3}$$

which implies that the last columns of A_L, A_C and A_R must be equal (see Carmona et al. [2002]). This elementary reasoning makes only 10 the number of parameters needed to define the family, instead of the 18 matrix entries initially assumed. Thus, from (2.3) we can write

$$\begin{gathered} A_L = \begin{pmatrix} a_{11}^L & a_{12} \\ a_{21}^L & a_{22} \end{pmatrix}, \quad A_C = \begin{pmatrix} a_{11}^C & a_{12} \\ a_{21}^C & a_{22} \end{pmatrix}, \quad A_R = \begin{pmatrix} a_{11}^R & a_{12} \\ a_{21}^R & a_{22} \end{pmatrix}, \\ \mathbf{b}_L = \begin{pmatrix} b_1 + a_{11}^L - a_{11}^C \\ b_2 + a_{21}^L - a_{21}^C \end{pmatrix}, \quad \mathbf{b}_C = \begin{pmatrix} b_1 \\ b_2 \end{pmatrix}, \quad \mathbf{b}_R = \begin{pmatrix} b_1 - a_{11}^R + a_{11}^C \\ b_2 - a_{21}^R + a_{21}^C \end{pmatrix}, \end{gathered} \tag{2.4}$$

but anyway, there are still a large number of parameters to consider all possible cases. In order that the theoretical development be as self-contained as possible, in the following result taken from Ponce et al. [2015], a necessary condition for existence of periodic orbits is shown.

Proposition 1. *If system (2.1)-(2.2) has periodic solutions, then* $a_{12} \neq 0$.

Proof. If we assume $a_{12} = 0$, then the dynamics in x would be decoupled from the dynamic in y, since we would have

$$\dot{x} = a_{11}^{\{L,C,R\}} x + b_1^{\{L,C,R\}},$$

that does not depend on y. Obviously this autonomous, one-dimensional equation cannot have non-constant periodic solutions. Hence, as any periodic solution of the complete system gives rise to a periodic function $x(t)$, the proof is completed. □

Next, we see that the previous necessary condition for existence of periodic orbits, which is equivalent to the so called observability condition in control theory (see Carmona et al. [2002]), is also a sufficient condition to achieve the Liénard canonical form. The following result was shown in Ponce et al. [2015].

Proposition 2. ***(Liénard form)*** *The condition $a_{12} \neq 0$ is sufficient to write system (2.1)-(2.2) in the Liénard form*

$$\dot{X} = F(X) - Y, \quad \dot{Y} = g(X) - h \tag{2.5}$$

where the piecewise linear functions F and g are defined by

$$F(X) = \begin{cases} t_L(X+1) - t_C & \text{if} \quad X < -1, \\ t_C X & \text{if} \quad |X| \leq 1, \\ t_R(X-1) + t_C & \text{if} \quad X > 1, \end{cases}$$

$$g(X) = \begin{cases} d_L(X+1) - d_C & \text{if} \quad X < -1, \\ d_C X & \text{if} \quad |X| \leq 1, \\ d_R(X-1) + d_C & \text{if} \quad X > 1, \end{cases} \tag{2.6}$$

and $t_{\{L,C,R\}}$, $d_{\{L,C,R\}}$ are the trace and determinant of the matrix $A_{\{L,C,R\}}$ given in (2.4).

Proof. First, taking into account (2.4), we make the change of variables $X = x$, $Y = a_{22}x - a_{12}y$, to obtain

$$\begin{aligned} \dot{X} &= t_{\{L,C,R\}}X - Y + b_1^{\{L,C,R\}}, \\ \dot{Y} &= d_{\{L,C,R\}}X + a_{22}b_1^{\{L,C,R\}} - a_{12}b_2^{\{L,C,R\}}, \end{aligned}$$

where we have introduced the traces

$$t_{\{L,C,R\}} = a_{11}^{\{L,C,R\}} + a_{22}$$

in each zone, and the respective determinants

$$d_{\{L,C,R\}} = a_{11}^{\{L,C,R\}}a_{22} - a_{21}^{\{L,C,R\}}a_{12}.$$

Now, a translation in the second variable $y = Y - b_1 = Y - b_1^C$, leads to the required canonical form, since from (2.4) we have

$$b_1^{\{L,R\}} - b_1^C = \pm\left(t_{\{L,R\}} - t_C\right)$$

and

$$a_{22}b_1^{\{L,R\}} - a_{12}b_2^{\{L,R\}} = -h \pm \left(d_{\{L,R\}} - d_C\right),$$

where

$$h = a_{12}b_2^C - a_{22}b_1^C.$$

Using again non-capitalized letters for variables, the proposition is shown. □

In order to analyze the dynamics of system (2.5)-(2.6) we start by considering the equilibrium points. These points are given by the solutions of the equations $F(x) = y$ and $g(x) = h$ in each zone, where F and g are defined in (2.6). As it is usual in piecewise smooth systems, these solutions can lead to real or virtual equilibrium

points, depending on whether the point belongs or not to the region whose dynamics is ruled by such equilibrium. The topological nature of these equilibrium points is determined by the linear invariants (traces and determinants) in each zone. Some boundary equilibrium bifurcations (BEB, for short) can appear when by moving the parameter h an equilibrium point changes its relative position with respect to the straight lines $x = \pm 1$.

To illustrate the interesting consequences of previous results we will focus our attention to the case where the system (2.5)-(2.6) has only one anti-saddle (focus or node) equilibrium point for any value of $h \in \mathbb{R}$ that is, $d_L, d_C, d_R > 0$. Moreover, we consider the most relevant situation from the point of view of dynamical richness, that is, dissipation in external zones ($t_L, t_R < 0$) combined with expansive dynamics in the central region ($t_C > 0$). Otherwise, periodic orbits are precluded. The following result is direct and so we omit its proof.

Proposition 3. *Consider system (2.5)-(2.6) with*

$$t_E < 0, \quad t_C > 0, \quad d_L, d_C, d_R > 0.$$

The following statements hold.

(a) The system has for $-d_C < h < d_C$ one real unstable anti-saddle (focus or node) equilibrium point in the central zone $|X| \leq 1$, with coordinates given by

$$(\overline{X}, \overline{Y}) = \left(\frac{h}{d_C}, \frac{h t_C}{d_C} \right). \tag{2.7}$$

(b) For $h > d_C$, the system has one real stable equilibrium point of anti-saddle type in one of the external zones, with coordinates given by

$$(\overline{X}, \overline{Y}) = \left(1 + \frac{h + d_C}{d_R}, t_R \frac{h + d_C}{d_R} + t_C \right). \tag{2.8}$$

(c) For $h < -d_C$, the system has one real stable equilibrium point of anti-saddle type in one of the external zones, with coordinates given by

$$(\overline{X}, \overline{Y}) = \left(-1 + \frac{h - d_C}{d_L}, t_L \frac{h - d_C}{d_L} - t_C \right). \tag{2.9}$$

(d) When $|h| = d_C$ we have a transition between the two previous situations, that is, a boundary equilibrium bifurcation.

Remark 4. *Note that if the matrices $A_E = A_L = A_R$ we obtain that for $|h| > d_C$, the system has one real stable equilibrium point of anti-saddle type in one of the external zones, with coordinates given by*

$$(\overline{X}, \overline{Y}) = \left(\pm 1 + \frac{h \pm d_C}{d_E}, t_E \frac{h \pm d_C}{d_E} \pm t_C \right), \tag{2.10}$$

where the duality of signs corresponds with the case $\pm h > 0$.

The next result assure boundedness for solutions under certain hypotheses, a property sometimes referred as dissipativeness, see the quoted reference for a proof.

Proposition 5. *Ponce et al. [2015] Consider the differential system (2.5)-(2.6) with only one equilibrium point $(\overline{X}, \overline{Y})$ in the central zone, i.e. $d_C > 0$, $-d_C < h < d_C$, and $d_L, d_R \geq 0$. If the external traces satisfy $t_L, t_R < 0$ then there exist a compact positive invariant set containing the origin, so that orbits enter the set and no orbit escapes from it. If furthermore $t_C > 0$, then the equilibrium is surrounded by a limit cycle which is unique and stable.*

Next, we recall two theorems that give a rather complete characterization for the dynamics under the hypotheses of Proposition 5.

Theorem 6. *Ponce et al. [2015]* ***(Central node dynamics)*** *Consider system (2.5)-(2.6) under the hypotheses $t_L, t_R < 0$, $t_C > 0$, $d_L, d_C, d_R > 0$ and central node dynamics, that is, $t_C^2 - 4d_C \geq 0$. The following statements hold.*

(a) For $-d_C < h < d_C$ there exists one stable limit cycle that has always points in the three linearity zones.

(b) Assuming that the right (left) dynamics is of node type, that is $t_R^2 - 4d_R \geq 0$ ($t_L^2 - 4d_L \geq 0$), the stable limit cycle of statement (a) disappears for $\delta > d_C$ ($\delta < -d_C$). In passing through the values $h = d_C$ ($h = -d_C$) we have an explosive appearance/disappearance of the stable limit cycle through a configuration determined by a bounded continuum of homoclinic connections to the equilibrium point, which is located at the right (left) corner $(1, t_C)$ (respectively, at $(-1, -t_C)$) of the graph of $F(X)$.

(c) ***(A BEB adding a new limit cycle)*** *If the right (left) dynamics is of focus type, that is $t_R^2 - 4d_R < 0$ ($t_L^2 - 4d_L < 0$), then there exists $\epsilon > 0$ such that for $d_C < h < d_C + \epsilon$ (respectively, $-d_C - \epsilon < h < -d_C$) there exists a stable focus surrounded by two limit cycles, the smaller unstable and the bigger stable. The smaller cycle is born through a BEB bifurcation at $\delta = d_C$ ($\delta = -d_C$), where the equilibrium at the corner is a repulsive node-focus while the big limit cycle persists.*

Theorem 7. *Ponce et al. [2015]* ***(Central focus dynamics)*** *Consider system (2.5)-(2.6) under the hypotheses $t_L, t_R < 0$, $t_C > 0$, $d_L, d_C, d_R > 0$ and central focus dynamics, that is, $t_C^2 - 4d_C < 0$. The following statements hold.*

(a) For $-d_C < h < d_C$ there exists one stable limit cycle..

(b) If the right (left) dynamics is of node type, that is $t_R^2 - 4d_R \geq 0$ ($t_L^2 - 4d_L \geq 0$), then the stable limit cycle of statement (a) disappears for $h > d_C$ ($h < -d_C$) in a focus-node BEB, so that the size of the limit cycle eventually decreases linearly to zero.

(c) If the right (left) dynamics is also of focus type, that is $t_E^2 - 4d_E < 0$, then three cases arise.

(c1) If we also have the condition

$$\frac{t_C}{\sqrt{d_C}}+\frac{t_R}{\sqrt{d_R}}<0 \quad \left(\frac{t_L}{\sqrt{d_L}}+\frac{t_C}{\sqrt{d_C}}<0\right),$$

the stable limit cycle of statement (a) disappears for $h=d_C$ ($h=-d_C$) in a focus-focus BEB, so that the size of the limit cycle eventually decreases linearly to zero.

(c2) If we also have the condition

$$\frac{t_C}{\sqrt{d_C}}+\frac{t_R}{\sqrt{d_R}}=0 \quad \left(\frac{t_L}{\sqrt{d_L}}+\frac{t_C}{\sqrt{d_C}}=0\right),$$

the stable limit cycle of statement (a) disappears for $h=d_C$ ($h=-d_C$) in a 'center' BEB, so that the size of the limit cycle decreases abruptly to zero for $h>d_C$ ($h<-d_C$).

(c3) ***(A BEB adding a new limit cycle)***
If we also have the condition

$$\frac{t_C}{\sqrt{d_C}}+\frac{t_R}{\sqrt{d_R}}>0 \quad \left(\frac{t_L}{\sqrt{d_L}}+\frac{t_C}{\sqrt{d_C}}>0\right),$$

then there exists $\epsilon>0$ such that for $d_C<h<d_C+\epsilon$ (respectively, $-d_C-\epsilon<h<-d_C$) there exists a stable focus surrounded by two limit cycles, the smaller unstable and the bigger stable. The smaller cycle is born through a BEB bifurcation at $h=d_C$ ($h=-d_C$), where the equilibrium at the right (left) corner of the graph of $F(X)$ is an unstable focus while the big limit cycle persists.

Note that both in the situations of central node dynamics and central focus dynamics there appear cases with two limit cycles surrounding the equilibrium point, being stable one of them and the equilibrium, so that we have bi-stability for such cases. In figure 2.1 we show the persistent BEB adding transition of Theorem 7(c).

2.2 A 3D reference model

In this section, we consider a family of 3D systems, which is general enough to capture all the mathematical models of memristor oscillators to be analyzed later in this chapter. The dynamics of such a family of three-dimensional systems presents an infinite number of equilibria, and we will show that it is essentially ruled by a family of two-dimensional systems. We consider the system

$$\begin{aligned}\dot{x} &= a_{11}W(z)x+a_{12}y,\\ \dot{y} &= a_{21}x+a_{22}y,\\ \dot{z} &= x,\end{aligned} \tag{2.11}$$

where the constants $a_{11},a_{12},a_{21},a_{22}\in\mathbb{R}$, the function W is defined by

$$W(z)=\frac{dq(z)}{dz}, \tag{2.12}$$

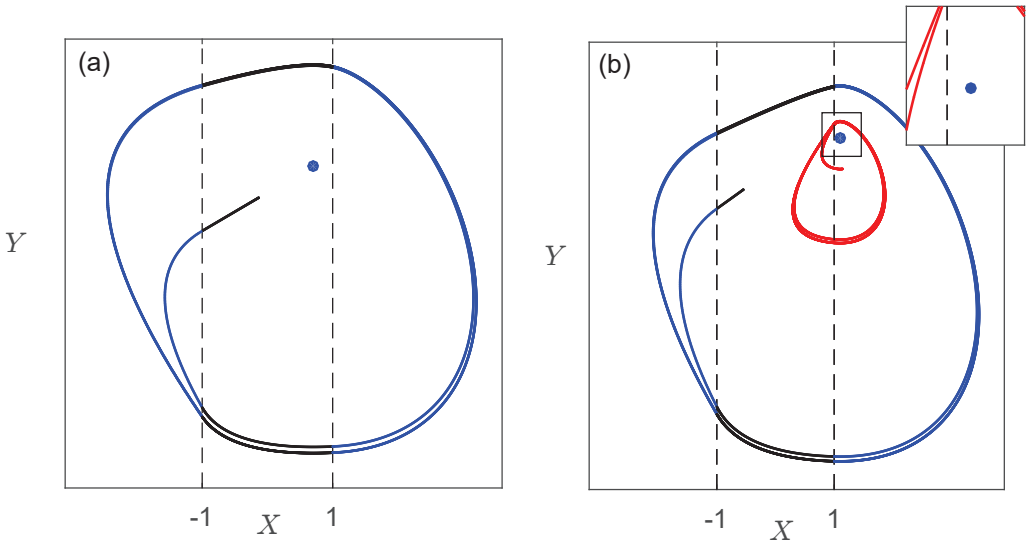

Figure 2.1: Persistent BEB adding a new limit cycle in the transition of Theorem 7(c) corresponding to a node-node-focus dynamics, with parameters $t_L = -1.5, t_C = 1.5, t_R = -1, d_L = 0.5, d_C = 0.5$ and $d_R = 1$. (a) Taking $h = 0.35$, we show in blue and black one stable limit cycle surrounding the unstable equilibrium point. (b) Taking $h = 0.6$, we show a new unstable limit cycle in red surrounding the stable equilibrium in blue.

and q is a continuous function. The equilibrium points of system (2.11) are given by the unbounded set formed by all points in the z-axis, namely

$$E = \{(x, y, z) \in \mathbb{R}^3 : x = y = 0 \text{ and } z \in \mathbb{R}\}. \tag{2.13}$$

In the following result, we show the existence of invariant manifolds for system (2.11).

Theorem 8. *Consider system (2.11) where the function W is defined as in (2.12). For any $h \in \mathbb{R}$, the set*

$$S_h = \{(x, y, z) \in \mathbb{R}^3 : -a_{22}x + a_{12}y - a_{12}a_{21}z + a_{11}a_{22}q(z) = h\} \tag{2.14}$$

is an invariant manifold for the system. Therefore, the system has an infinite family of invariant manifolds foliating the whole $\mathbb{R}^3$, and so the dynamics is essentially two-dimensional.

Proof. Define for any solution $(x(t), y(t), z(t))$ of (2.11) the function

$$h(t) = H(x(t), y(t), z(t)),$$

where

$$H(x(t), y(t), z(t)) = -a_{22}x(\tau) + a_{12}y(\tau) - a_{12}a_{21}z(\tau) + a_{11}a_{22}q(z(\tau)).$$

Then, a simple computation gives

$$h'(t) = -a_{22}(a_{11}W(z(\tau)) + a_{12}y(\tau)) + \cdots \\ + a_{12}(a_{21}x(\tau) + a_{22}y(\tau)) + (a_{11}a_{22}W(z(\tau)) - a_{12}a_{21})x(\tau) = 0,$$

so that h is constant along the orbits of (2.11) and, consequently, the level sets of H are invariant for the flow. □

The above result guarantees that the dynamics of system (2.11) is essentially two-dimensional for any continuous function q. In the next result, we show that on each invariant set S_h given in (2.14), the dynamics is topologically equivalent to a Liénard system. Furthermore, we give for any solution of the Liénard system with a given value of h, the corresponding solution of the 3D model (2.11).

Theorem 9. *Consider system (2.11) with function W defined as in (2.12). If $a_{12} \neq 0$, then on each invariant set S_h given in (2.14), the dynamics is topologically equivalent to the Liénard system*

$$\dot{X} = Y - F(X), \quad \dot{Y} = -g(X) + h, \tag{2.15}$$

where F and g are given by

$$F(X) = -a_{11}q(X) - a_{22}X, \quad g(X) = a_{11}a_{22}q(X) - a_{12}a_{21}X. \tag{2.16}$$

Moreover, $(X(\tau), Y(\tau)) \in \mathbb{R}^2$ is a solution of the Liénard system (2.15) for a given $h \in \mathbb{R}$, if and only if $E_h(X(\tau), Y(\tau)) \in \mathbb{R}^3$ is a solution of system (2.11) on S_h, where

$$E_h(X(\tau), Y(\tau)) = \begin{pmatrix} Y(\tau) - F(X(\tau)) \\ \frac{1}{a_{12}}\left[(a_{22}^2 + a_{12}a_{21})Y(\tau) - a_{22}Y(\tau) + h\right] \\ X(\tau) \end{pmatrix}. \tag{2.17}$$

Proof. First, with $a_{12} \neq 0$ the change of variables

$$\overline{x} = x, \quad \overline{y} = a_{22}x - a_{12}y, \quad \overline{z} = z \tag{2.18}$$

transforms system (2.11) into the system

$$\begin{aligned} \dot{\overline{x}} &= f_1(\overline{z})\,\overline{x} - \overline{y}, \\ \dot{\overline{y}} &= f_2(\overline{z})\,\overline{x}, \\ \dot{\overline{z}} &= \overline{x}, \end{aligned} \tag{2.19}$$

where the functions f_1 and f_2 are defined as

$$f_1(\overline{z}) = a_{11}W(\overline{z}) + a_{22}, \qquad f_2(\overline{z}) = a_{22}a_{11}W(\overline{z}) - a_{12}a_{21}. \tag{2.20}$$

From Theorem 8 and in the new variables the invariant manifolds (2.14) for system (2.19)-(2.20) can be written as

$$\widetilde{S}_h = \{(\overline{x}, \overline{y}, \overline{z}) \in \mathbb{R}^3 : -\overline{y} + g(\overline{z}) = h\}. \tag{2.21}$$

Now, replacing the condition given in (2.21) in the first equation of (2.19) and removing the unnecessary second equation, we obtain the system

$$\begin{aligned} \dot{\overline{x}} &= f_1(\overline{z})\,\overline{x} - g(\overline{z}) + h, \\ \dot{\overline{z}} &= \overline{x}, \end{aligned} \tag{2.22}$$

where the function g is defined by

$$g(x) = a_{11}a_{22}q(x) - a_{12}a_{21}x. \tag{2.23}$$

After the change of variables

$$\begin{aligned} X &= \overline{z}, \\ Y &= -\tilde{F}(\overline{z}) + \overline{x}, \end{aligned} \tag{2.24}$$

where F is given

$$\tilde{F}(z) = a_{11}q(z) + a_{22}z, \tag{2.25}$$

we obtain

$$\dot{X} = \dot{\overline{z}} = \overline{x} = Y + \tilde{F}(X) = Y - (-\tilde{F}(X)),$$

and

$$\begin{aligned} \dot{Y} &= -\tilde{F}'(\overline{z})\dot{\overline{z}} + \dot{\overline{x}} = -\left(a_{11}q'(\overline{z}) + a_{22}\right) + \left(f_1(\overline{z})\,\overline{x} - g(\overline{z}) + h\right) = \\ &= -f_1(\overline{z})\,\overline{x} + f_1(\overline{z})\,\overline{x} - g(\overline{z}) + h = -g(\overline{z}) + h \end{aligned}$$

taking $F(X) = -\tilde{F}(X)$ we obtain system (2.15)-(2.16).

If $(X(\tau), Y(\tau)) \in \mathbb{R}^2$ is a solution of system (2.15)-(2.16) for a given $h \in \mathbb{R}$, we have from (2.24) that

$$\begin{pmatrix} \overline{x}(\tau) \\ \overline{z}(\tau) \end{pmatrix} = \begin{pmatrix} Y(\tau) - F(\overline{z}(\tau)) \\ X(\tau) \end{pmatrix}$$

is a solution of system (2.22). From (2.21), we obtain on $\widetilde{S}_h$ that $\overline{y} = g(\overline{z}) - h$, with g as in (2.23). Thus,

$$\begin{pmatrix} \overline{x}(\tau) \\ \overline{y}(\tau) \\ \overline{z}(\tau) \end{pmatrix} = \begin{pmatrix} Y(\tau) - F(X(\tau)) \\ g(X(\tau)) - h \\ X(\tau) \end{pmatrix},$$

is a solution of system (2.19) on S_h. Finally, from (2.18) we obtain for system (2.11) the solution $x(\tau) = \overline{x}(\tau)$,

$$\begin{aligned} y(\tau) &= \frac{1}{a_{12}}\left[a_{22}\overline{x}(\tau) - \overline{y}(\tau)\right] = \frac{1}{a_{12}}\left[a_{22}Y(\tau) - a_{22}F(X(\tau)) - g(X(\tau)) + h\right] \\ &= \frac{1}{a_{12}}\left[a_{22}Y(\tau) + a_{22}\tilde{F}(X(\tau)) - g(X(\tau)) + h\right], \end{aligned}$$

and $z(\tau) = \overline{z}(\tau)$. The conclusion follows from the fact that for all X we have

$$a_{22}\tilde{F}(X) - g(X) = (a_{22}^2 + a_{12}a_{21})X.$$

□

These results will be of great usefulness in the analysis of the memristor oscillators as shown below. Note that function W defined in (2.12) can be discontinuous, as we will see in the next sections. However, the application of theorems in this section will not be restricted only to discontinuous functions, since in the next chapter we will apply these results in a function W defined by a quadratic polynomial.

2.3 Discontinous 3D PWL models

The three-dimensional models for piecewise linear flux-controlled memristor oscillators studied by Itoh and Chua (for details, see section 3.2 in Itoh and Chua [2008]) can be written in the form (2.11), where the function W is the derivative of the flux-charge characteristics for the memristor $q(\varphi)$. These equations are obtained from the Kirchoff laws for currents and voltages in the circuits. In what follows, we consider the case where the flux-charge characteristics function q is given by

$$q(z) = \begin{cases} b(z-1)+a, & \text{if} \quad z > 1, \\ az, & \text{if} \quad |z| \le 1, \\ b(z+1)-a, & \text{if} \quad z < -1, \end{cases} \tag{2.26}$$

so that

$$W(z) = \begin{cases} b, & \text{if} \quad |z| > 1, \\ a, & \text{if} \quad |z| \le 1, \end{cases} \quad \text{with} \quad a \neq b. \tag{2.27}$$

The piecewise linear character of the function q leads so to discontinuous models that introduce additional concerns for the mathematical analysis of the oscillators. We define the auxiliary matrices

$$A_E = \begin{pmatrix} b \cdot a_{11} & a_{12} \\ a_{21} & a_{22} \end{pmatrix}, \quad A_C = \begin{pmatrix} a \cdot a_{11} & a_{12} \\ a_{21} & a_{22} \end{pmatrix}, \tag{2.28}$$

and we introduce the notation t_E, t_C, d_E, d_C for the traces and determinants of such matrices, namely

$$\begin{aligned} t_E &= b\, a_{11} + a_{22}, & t_C &= a\, a_{11} + a_{22}, \\ d_E &= b\, a_{11} a_{22} - a_{12} a_{21}, & d_C &= a\, a_{11} a_{22} - a_{12} a_{21}. \end{aligned} \tag{2.29}$$

From Theorems 8, we obtain the piecewise linear invariant manifolds S_h defined by

$$S_h = \begin{cases} a_{12} y - a_{22} x + d_E z = h - a_{22}\,(t_C - t_E)\,, & \text{if} \quad z > 1, \\ a_{12} y - a_{22} x + d_C z = h, & \text{if} \quad |z| \le 1, \\ a_{12} y - a_{22} x + d_E z = h - a_{22}\,(t_E - t_C)\,, & \text{if} \quad z < -1, \end{cases} \tag{2.30}$$

and as a direct consequence of Theorem 9, we can state the following result.

Theorem 10. *Consider the function W defined as in (2.27). If $a_{12} \neq 0$, then on each invariant set S_h of system (2.11), the dynamics is topologically equivalent to the continuous Liénard system*

$$\dot{X} = F(X) - Y, \quad \dot{Y} = g(X) - h, \tag{2.31}$$

where F and g are given by

$$F(X) = \begin{cases} t_E(X-1) + t_C, & \textit{if} \quad X > 1, \\ t_C X, & \textit{if} \quad |X| \le 1, \\ t_E(X+1) - t_C, & \textit{if} \quad X < -1, \end{cases} \tag{2.32}$$

$$g(X) = \begin{cases} d_E(X-1) + d_C, & \textit{if} \quad X > 1, \\ d_C X, & \textit{if} \quad |X| \le 1, \\ d_E(X+1) - d_C, & \textit{if} \quad X < -1, \end{cases} \tag{2.33}$$

and t_E, t_C, d_E, d_C *are the traces and determinants* (2.29) *of the matrices defined in* (2.28). *Moreover,* $(X(\tau), Y(\tau)) \in \mathbb{R}^2$ *is a solution of the continuous reduced system* (2.31) *for a given* $h \in \mathbb{R}$, *if and only if* $E_h(X(\tau), Y(\tau)) \in \mathbb{R}^3$ *is a solution of system* (2.11) *on* S_h, *where*

$$E_h(X(\tau), Y(\tau)) = \begin{pmatrix} F(X(\tau)) - Y(\tau) \\ \frac{1}{a_{12}}\left[(a_{22}^2 + a_{12}a_{21})X(\tau) - a_{22}Y(\tau) + h\right] \\ X(\tau) \end{pmatrix}, \tag{2.34}$$

and the function F *is defined as in* (2.32).

Remark 11. *Note that each equilibrium point* $\left(\overline{X}, \overline{Y}\right)$ *given by Proposition 3 is associated to the equilibrium of coordinates* $(0, 0, \overline{X})$ *for system* (2.11).

Now, we study the existence of periodic orbits in system (2.11), using as our main tools the topologically equivalent continuous model given by Theorem 10 and the results given in Section 2.1. First, we will prove a theorem that guarantees the existence of periodic orbits in system (2.11)-(2.27)

Theorem 12. *Consider system* (2.11)-(2.27) *with* $a \neq b$, *and parameters such that*

$$t_E < 0, \quad t_C > 0, \quad d_E, d_C > 0, \tag{2.35}$$

where t_E, t_C, d_E *and* d_C *are the traces and determinants* (2.29) *of matrices defined in* (2.28). *The following statements hold.*

(a) The system has an infinite number of stable periodic orbits, each one of them contained in the set S_h *defined in* (2.30), *for any* $|h| < d_C$. *In particular, for any initial condition* $(x_0, y_0, z_0) \in \mathbb{R}^3$ *with* $x_0 \neq 0$ *or* $y_0 \neq 0$, $H(x_0, y_0, z_0) = h$ *and* $|h| < d_C$, *the steady-state solution is periodic.*

(b) The periodic orbits of statement (a) generate a tubular surface Ω *which is homeomorphic to the cylinder* $\mathbf{S^1} \times (-1, 1)$. *Such surface* Ω *is symmetric with respect to the origin.*

Proof. Since the determinants are not zero, the case $a_{12} = a_{22} = 0$ is excluded and we can apply Theorem 10, arriving at system (2.31) for a certain value of h. To show statement (a), we note that under the hypotheses, the point $(x_0, y_0, z_0) \in S_h$, where S_h is given in (2.30), is not an equilibrium point. From Proposition 3, system (2.31) has one anti-saddle equilibrium point $\left(\overline{X}, \overline{Y}\right)$ given by (2.7). We can apply Proposition 5 and conclude that the equilibrium $\left(\overline{X}, \overline{Y}\right)$ is surrounded by a limit cycle $L_h \subset \mathbb{R}^2$ which is unique and stable for the reduced system (2.31) being its global attractor. Consequently, on the invariant set S_h, we have one stable periodic orbit $O_h \subset \mathbb{R}^3$ of system (2.11)-(2.27) (see Fig 2.2(a)) corresponding to the stable limit cycle L_h (see Fig 2.2(b)). Since the initial condition $(x_0, y_0, z_0) \in S_h$ is not the equilibrium point $(0, 0, z_0)$ (see Remark 11), the solution tends to O_h and the statement is shown. Regarding statement (b), a key observation is that for any $h \in \mathbb{R}$ both system (2.11)-(2.27) and the reduced system (2.31) are Lipschitz, and so they satisfy the standard results regarding the continuous dependence of solutions

on initial conditions and parameters. Then, by varying the value of h, we produce a continuous deformation of periodic orbits L_h and so a continuous deformations of the corresponding periodic orbit O_h. In short, we can define the surface

$$\Omega = \bigcup_{|h|< d_C} O_h, \tag{2.36}$$

which is foliated, from its definition, by periodic orbits. The symmetric character of such surface comes directly from the symmetry of vector field of system (2.11)-(2.27). The theorem follows. □

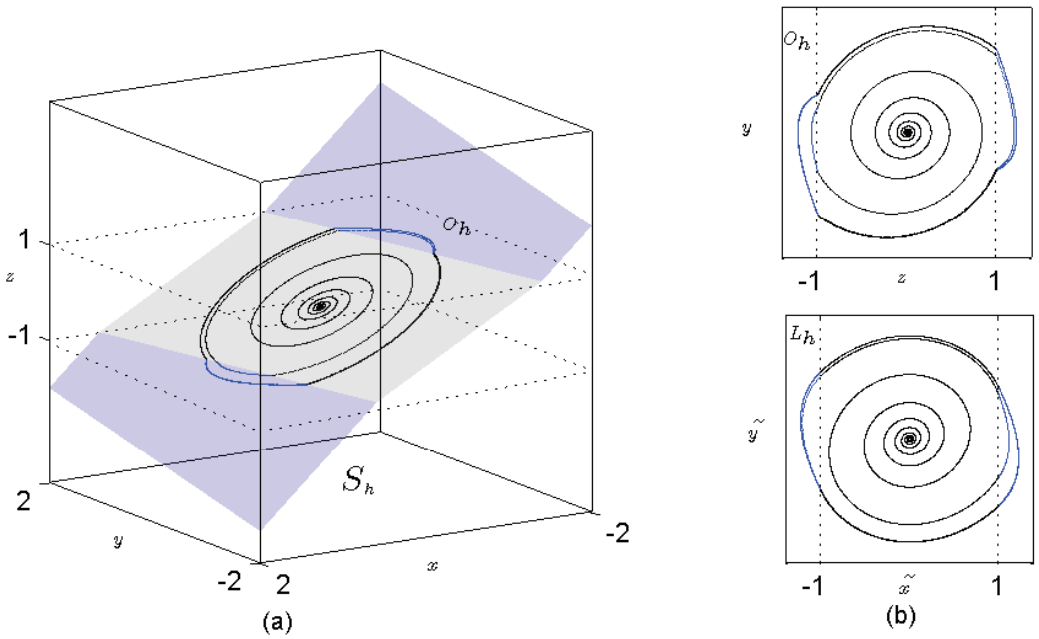

Figure 2.2: (a) The stable periodic orbit O_h of system (2.11)-(2.27) for $h = 0$ with parameters such that $a \neq b$, $d_C, d_E, t_C > 0$ and $t_E < 0$. (b) (Lower frame) Stable limit cycle L_h of system (2.31)-(2.33) in the plane $(\tilde{x}, \tilde{y})$ corresponding to periodic orbit O_h; (upper frame) the projection of the stable periodic orbit O_h on the plane (z, y).

We know that in some cases, see for instance Theorems 6(b) and 7(b), the limit cycles L_h of system (2.31) disappear for $|h| > d_C$. However, as it will be seen, there are cases where this disappearance does not take place at the exact condition $|h| = d_C$. On the other hand, in some cases, by taking into account the limit situations $|h| = d_C$, we can assure that the above cylinder Ω is in fact a closed surface which is homeomorphic to the topological sphere $\mathbf{S^2}$.

Proposition 13. ***(Central focus dynamics)*** *Consider system (2.11)-(2.27) under the assumptions of Theorem 12, and the additional condition of central focus dynamics, that is $t_C^2 - 4d_C < 0$. If we have a node dynamics in the external zones,*

that is $t_E^2 - 4d_E \geq 0$*, or a focus dynamics* ($t_E^2 - 4d_E < 0$) *with the additional condition*

$$\frac{t_C}{\sqrt{d_C}} + \frac{t_E}{\sqrt{d_E}} \leq 0,$$

then the set of periodic orbits closes at the points $(0, 0, \pm 1)$*. Therefore, for any initial condition* $(x_0, y_0, z_0) \in \mathbb{R}^3$ *with* $H(x_0, y_0, z_0) = h$ *and* $|h| \geq d_C$*, the steady state solution is not oscillatory, tending to the stationary state* $(0, 0, z_0)$*.*

Proof. It is a direct consequence of Theorem 7. □

The case of node dynamics in all zones needs a specific result, due to the existence of a continuum of homoclinic connections when $|h| = d_C$, see Theorem 6(b) and Desroches et al. [2013].

Proposition 14. ***(Node-node dynamics)*** *Consider system* (2.11)-(2.27) *under the conditions of Theorem 12, and the additional conditions of node dynamics in all zones, that is* $t_C^2 - 4d_C \geq 0$*,* $t_E^2 - 4d_E \geq 0$*. On each invariant set* S_h *with* $h = \pm d_C$*, there exists a bounded continuum of homoclinic connections to the points* $(0, 0, \pm 1)$*; such two sets of homoclinic connections allow to close the tubular surface* Ω *given in* (2.36)*.*

Proof. It is sufficient to apply Theorem 6(b). □

An important contribution of this work is the detection of bi-stable configurations, where one cannot predict the steady state behavior without a very precise knowledge of initial conditions. In fact, as shown in the next result, we can have different behavior within the same invariant set S_h for some values of h.

Proposition 15. ***(Bi-stability)*** *Consider system* (2.11)-(2.27) *under the assumptions of Theorem 12 and the additional condition of external focus dynamics, that is* $t_E^2 - 4d_E < 0$*. If we have a node dynamics in the central zone, that is* $t_C^2 - 4d_C \geq 0$*, or a focus dynamics* ($t_E^2 - 4d_E < 0$) *with the additional condition*

$$\frac{t_C}{\sqrt{d_C}} + \frac{t_E}{\sqrt{d_E}} > 0, \tag{2.37}$$

then there exists $\epsilon > 0$ *such that, for any* $h \in \mathbb{R}$ *with* $d_C < h < d_C + \epsilon$ *(resp.,* $-d_C - \epsilon < h < -d_C$*) there are two different steady-state solutions. For some initial conditions* (x_0, y_0, z_0) *with* $H(x_0, y_0, z_0) = h$*, solutions tend to a periodic solution while for others initial conditions satisfying the same equality, solutions tend to the stationary state* $(0, 0, g^{-1}(h))$*, where* g *is defined in* (2.33)*.*

Proof. If we suppose a node dynamics in the central zone, the conclusion follows after applying Theorem 6(c). If we have a focus dynamics in the central zone satisfying (2.37), it is sufficient to apply Theorem 7($c3$). □

The above results allow to characterize the dynamical behavior of the several 3D piecewise linear memristor oscillators, as we will show in the next two sections.

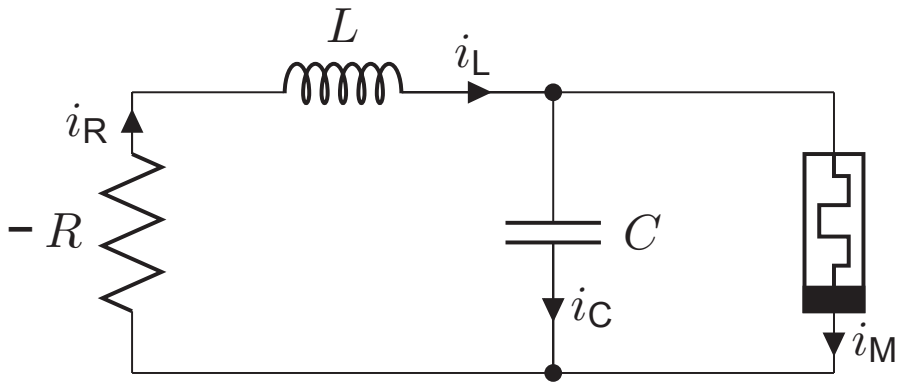

Figure 2.3: The canonical memristor oscillator, after Itoh and Chua [2008]. Note that the the only active element in the circuit is the resistor with a negative resistance $-R$.

2.4 Application to the Canonical 3D PWL memristor oscillator

Let us consider the case of the elementary memristor oscillator of Figure 2.3, which was proposed in Itoh and Chua [2008] as a canonical memristor oscillator. The circuit is endowed with one flux-controlled memristor M whose flux-charge characteristics is given by $q_M = q(\varphi_M)$, where the function q is the piecewise linear function defined in (4.31). Note that the values for the inductance L and for the capacitance C are positive, while the resistor has a negative value $-R$, being so the only active element in the circuit. From Kirchoff's laws we see that

$$\begin{aligned} i_R(\tau) - i_L(\tau) &= 0, \\ i_L(\tau) - i_C(\tau) - i_M(\tau) &= 0, \\ v_R(\tau) + v_L(\tau) + v_C(\tau) &= 0, \\ v_C(\tau) - v_M(\tau) &= 0, \end{aligned} \tag{2.38}$$

where v, i stand for the voltage and current, respectively, across the corresponding element of the circuit as indicated by the subscript.

We proceed as in Itoh and Chua [2008]. If we select the triplet (v_C, i_L, φ_M) as the set of state variables, and consider the constitutive relations in the current-voltage setting

$$v_R(\tau) = -Ri_R(\tau), \quad v_L(\tau) = L\frac{d}{d\tau}i_L(\tau), \quad i_C(\tau) = C\frac{d}{d\tau}v_C(\tau), \tag{2.39}$$

along with the relation

$$i_M = \frac{d}{d\tau}q_M(\tau) = \frac{d}{d\tau}q(\varphi_M(\tau)) = W(\varphi_M(\tau))\frac{d}{d\tau}\varphi_M(\tau) = W(\varphi_M(\tau))v_M(\tau),$$

we can take directly equations (2.38), and write

$$\begin{aligned} i_C = C\frac{dv_C}{d\tau} &= i_L - i_M = i_L - W(\varphi_M)v_C, \\ v_L = L\frac{di_L}{d\tau} &= -v_R - v_C = Ri_L - v_C, \\ v_M = \frac{d\varphi_M}{d\tau} &= v_C. \end{aligned} \tag{2.40}$$

In short, we get the 3D dynamical system

$$\begin{aligned} C\frac{dv_C}{d\tau} &= i_L - W(\varphi_M)v_C, \\ L\frac{di_L}{d\tau} &= Ri_L - v_C, \\ \frac{d\varphi_M}{d\tau} &= v_C. \end{aligned} \tag{2.41}$$

Renaming the state variables as $x = v_C$, the voltage across the capacitor; $y = i_L$, the current through the inductance L and $z = \varphi_M$ the flux of the memristor, we get a special case of system(2.11), namely

$$\begin{aligned} \frac{dx}{d\tau} &= \alpha\left(y - W(z)x\right), \\ \frac{dy}{d\tau} &= -\xi x + \beta y, \\ \frac{dz}{d\tau} &= x, \end{aligned} \tag{2.42}$$

where, following Itoh and Chua [2008], the parameters used are

$$\alpha = \frac{1}{C}, \quad \xi = \frac{1}{L}, \quad \beta = \frac{R}{L},$$

so that $\alpha, \xi, \beta > 0$. We note that, regarding (2.11),

$$a_{12} = -a_{11} = \alpha = \frac{1}{C}, \; a_{21} = -\xi = -\frac{1}{L}, \; a_{22} = \beta = \frac{R}{L}.$$

It is now direct to deduce the physical meaning of Theorem 8 for our circuit. We see that

$$H(x, y, z) = -\beta x + \alpha y - \alpha\beta q(z) + \alpha\xi z,$$

and, after introducing a factor LC and taking derivatives with respect to time, that

$$\begin{aligned} LC\dot{H} &= -RC\dot{x} + L\dot{y} - RW(z)x + \dot{z} = \\ &= -R(C\dot{x} + W(z)x) + L\dot{y} + \dot{z} = \\ &= -R(i_C + i_M) + v_L + v_M = 0, \end{aligned} \tag{2.43}$$

which is certainly not different from the Kirchoff voltage law for the circuit. Therefore, we conclude that the existence of such a conserved quantity is a direct consequence of the conservation law for the total flux (voltage momentum) in the circuit, see Section 2 of Itoh and Chua [2008]. Analogous considerations for the existence of a conserved quantity in memristor circuits had appeared in Bao et al. [2013], Riaza [2014]. An important observation is that the parameter α is not essential so that it can be removed with the change of variables and parameters

$$\begin{aligned} &\widetilde{x} = x, \quad \widetilde{y} = \alpha y, \quad \widetilde{z} = z, \quad \widetilde{\xi} = \alpha\xi, \\ &\widetilde{a} = \alpha a, \quad \widetilde{b} = \alpha b, \quad \widetilde{W} = \alpha W, \end{aligned} \tag{2.44}$$

to be assumed in the sequel, omitting also tildes to alleviate the notation. Therefore, we need to study the system

$$\begin{aligned} \dot{x} &= -W(z)x + y, \\ \dot{y} &= -\xi x + \beta y, \\ \dot{z} &= x, \end{aligned} \tag{2.45}$$

where W is as in (2.27), and we assume from now on

$$a_{11} = -1, \ a_{12} = 1, \ a_{21} = -\xi, \ a_{22} = \beta.$$

After applying Theorem 8, we obtain that

$$H(x, y, z) = -\beta x + y + \xi z - \beta q(z) \tag{2.46}$$

is a conserved quantity for system (2.45), where q is as in (4.31). Note that here

$$\begin{aligned} t_E &= \beta - b, \quad t_C = \beta - a, \\ d_E &= \xi - b\beta, \quad d_C = \xi - a\beta. \end{aligned} \tag{2.47}$$

Then, thanks to Theorem 10 we obtain a reduced system (2.31), where

$$F(X) = \beta X - q(X) = \begin{cases} (\beta - b)X + b - a, & \text{if} \quad X > 1, \\ (\beta - a)X, & \text{if} \quad |X| \leq 1, \\ (\beta - b)X - b + a, & \text{if} \quad X < -1, \end{cases} \tag{2.48}$$

$$g(X) = \xi X - \beta q(X) = \begin{cases} (\xi - b\beta)X + \beta(b - a), & \text{if} \quad X > 1, \\ (\xi - a\beta)X, & \text{if} \quad |X| \leq 1, \\ (\xi - b\beta)X - \beta(b - a), & \text{if} \quad X < -1. \end{cases} \tag{2.49}$$

Thus, by studying the properties of above reduced system, we can give a rather complete characterization of the oscillator dynamics in terms of the involved parameters. For instance, regarding equilibria of system (2.45), it is clear the existence of a continuum of points, namely

$$E = \{(x, y, z) \in \mathbb{R}^3 : x = y = 0 \text{ and } z \in \mathbb{R}\},$$

each one being an equilibrium point. Any of these equilibrium points, say $(0, 0, z_0)$, can be reached (forward or backward in time, according to its stability character)

only for solutions with initial conditions belonging to the corresponding level set S_{h_0} for the function H, namely, for $h_0 = g(z_0)$, recall (2.30). Remember that the dynamics is essentially bi-dimensional, as assured by Theorem 10. In what follows, we study the oscillatory behavior of reduced system (2.31)-(2.48)-(2.49), using the value of h, which controls the dynamical level set of system (2.45), as the main bifurcation parameter.

Obviously, for the planar system (2.31)-(2.48)-(2.49) we can resort to the results from qualitative theory of dynamical systems, and especially to all the theoretical findings recently obtained in Ponce et al. [2015] for piecewise linear systems, where a good number of useful results apply. To start with, Bendixson criterion tells us that oscillatory behavior is only possible if the divergence has not constant sign, so that a natural assumption to be assumed in the sequel is $0 < a < \beta < b$, where the inequality $a > 0$ comes from the passive character of the memristor. In Ponce et al. [2015], it is emphasized the importance of the topological type for the dynamics in each linearity region (focus, node, saddle). In particular, we must impose that in the external linearity regions the dynamics is not of saddle type; otherwise, we would have orbits going to infinity, something not allowed for realistic dissipative systems. This last assumption implies that $d_E > 0$, or equivalently $\xi > b\beta$, which leads to a dynamics of type focus or node when $|X| > 1$. However, it is easy to conclude that under the above hypotheses we have always central focus dynamics.

Lemma 16. *The dynamics in the central zone of system* (2.31)-(2.48)-(2.49) *under hypotheses*

$$0 < a < \beta < b, \quad b\beta < \xi, \tag{2.50}$$

is always of focus type.

Proof. It suffices to note that the condition $t_C^2 - 4d_C < 0$ is equivalent to

$$(\beta - a)^2 - 4(\xi - a\beta) = (\beta + a)^2 - 4\xi < 0.$$

Now, from the hypotheses (2.50) we have $(\beta + a)^2 < 4\beta^2 < 4b\beta < 4\xi$, so that the dynamics in the central zone is of focus type. □

We remark that the dynamics on the external zones with $|X| > 1$ could be of node type, if $(\beta+b)^2 \geq 4\xi$, being also of focus type when $(\beta+b)^2 < 4\xi$. Thus, under hypotheses (2.50), only two configurations are possible: we can have focus dynamics in the three linearity regions, to be denoted as the FFF case, or we can have instead the case NFN with node dynamics in external zones, see Figure 2.4.

Thanks to Theorem 10 we can characterize the possible static steady states of system (2.45), by studying instead the equilibrium points of system (2.31)-(2.48)-(2.49). The result that follows is direct so that we omit its proof. We remark that if we consider h as a bifurcation parameter then there appear some critical values where the system undergoes boundary equilibrium bifurcations (BEB, for short).

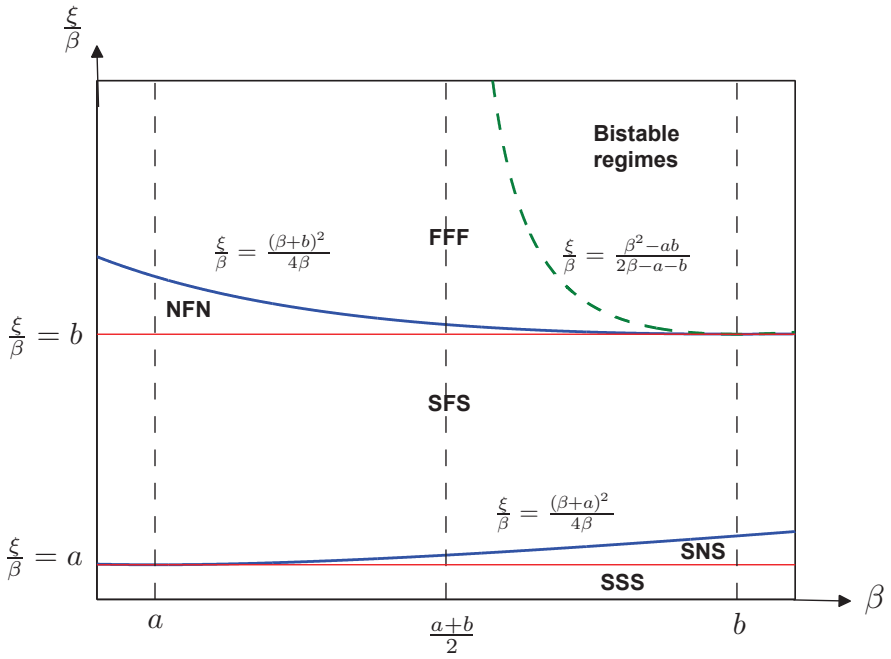

Figure 2.4: Topological type of linearity regions (F stands for focus, N for node and S for saddle) in the parameter plane $(\beta, \xi/\beta)$ for system (2.31)-(2.48)-(2.49), with emphasis in the band $a < \beta < b$, which appears at a different scale for visual purposes. Hypotheses (2.50) are valid on the upper part of the picture where we have either a NFN configuration or a FFF configuration. Within this FFF region there appears the region of bistable regimes for level sets near h_B, as will be indicated in statement (c) of Theorem 21.

Proposition 17. *For any value of $h \in \mathbb{R}$, system (2.31)-(2.48)-(2.49) with $0 < a < \beta < b < \xi/\beta$ has only one equilibrium point, and the following statements hold. We define for convenience the boundary level values $\pm h_B$ with $h_B = d_C = \xi - a\beta > 0$.*

(a) For $|h| < h_B$ the equilibrium point is one unstable focus located in the central zone $|X| < 1$, with coordinates given by

$$\left(\overline{X}, \overline{Y}\right) = \left(\frac{h}{h_B}, (\beta - a)\frac{h}{h_B}\right). \tag{2.51}$$

(b) For $|h| > h_B$, the equilibrium point is one stable anti-saddle (node or focus) located in one external zone, with coordinates given by

$$\left(\overline{X}, \overline{Y}\right) = \left(\frac{h \pm \beta(a-b)}{\xi - b\beta}, (\beta - b)\frac{h \pm \beta(a-b)}{\xi - b\beta} \pm (b - a)\right) \tag{2.52}$$

where the duality of signs must be resolved according to the cases $\pm h > 0$. Thus, for $h > h_B$ we have

$$\overline{X} = \frac{h + \beta(a-b)}{\xi - b\beta} > \frac{h_B + \beta(a-b)}{\xi - b\beta} = 1,$$

while for $h < -h_B$ we have

$$\overline{X} = \frac{h - \beta(a-b)}{\xi - b\beta} < \frac{-h_B + \beta(a-b)}{\xi - b\beta} = -1.$$

(c) If $|h| = h_B$ then we have a transition between the two previous situations, so that the equilibrium point is located at one of the boundaries $X = \pm 1$, that is, for such values of h the system undergoes a boundary equilibrium bifurcation BEB.

Remark 18. *From Theorem 10, each equilibrium point $\left(\overline{X}, \overline{Y}\right) = \left(\overline{X}, F(\overline{X})\right)$ of the above proposition corresponds to an equilibrium of coordinates $(0, 0, \overline{X})$ for system (2.45).*

A direct application of Theorem 7, gives the following result, regarding the existence of limit cycles. The appearance or disappearance of limit cycles, when the value of h is changed through some critical values, correspond to boundary equilibrium bifurcations (BEB, for short).

Proposition 19. *Consider system (2.31)-(2.48)-(2.49) under the hypotheses $0 < a < \beta < b < \xi/\beta$ and define $h_B = \xi - a\beta > 0$. The following statements hold.*

(a) For $|h| < h_B$ the unstable focus is surrounded by one stable limit cycle.

(b) If the external dynamics are of node type, that is $4\xi \leq (\beta + b)^2$, then the stable limit cycle of statement (a) disappears for $|h| \geq h_B$ in a focus-node BEB that takes place at $|h| = h_B$, so that the size of the limit cycle eventually decreases linearly to zero as $|h|$ approaches h_B from above.

(c) If the external dynamics are of focus type, that is $4\xi > (\beta + b)^2$ *, then three cases arise depending on the sign of the expression*

$$\mathbb{E}(\beta, \xi) := \frac{\beta - a}{\sqrt{\xi - a\beta}} + \frac{\beta - b}{\sqrt{\xi - b\beta}}. \tag{2.53}$$

(c1) If $\mathbb{E}(\beta, \xi) < 0$*, then the stable limit cycle of statement (a) disappears for* $|h| \geq h_B$ *in a focus-focus BEB that takes place at* $|h| = h_B$*, so that the size of the limit cycle eventually decreases linearly to zero as* $|h|$ *approaches* h_B *from above.*

(c2) If $\mathbb{E}(\beta, \xi) = 0$*, then the stable limit cycle of statement (a) disappears for* $|h| = h_B$ *in a center BEB, after colliding with the outermost periodic orbit of a bounded period annulus, and no periodic orbits appear for* $|h| > h_B$*.*

(c3) If $\mathbb{E}(\beta, \xi) > 0$*, then there exists* $\epsilon > 0$ *such that both for* $h_B < h < h_B + \epsilon$ *and for* $-h_B - \epsilon < h < -h_B$*, there exists a stable focus surrounded by two limit cycles, the smaller unstable and the bigger stable. The new smaller cycle is born through a focus-focus BEB bifurcation at* $|h| = h_B$*, so that the unstable focus that moves with* h *on the graph of* $F(X)$ *passes through one of its corners, becoming a stable focus with* $|\overline{X}| > 1$*, while the big stable limit cycle persists.*

Note that the sign of $\mathbb{E}(\beta, \xi)$ characterizes the focus-focus BEB (to be subcritical or supercritical) and the non-generic situation of the center BEB that appears when such quantity vanishes.

We state here a technical lemma, in order to facilitate the application of the above result, by characterizing the sign of the expression in (2.53).

Lemma 20. *Considering system* (2.45) *under hypotheses* (2.50) *and the additional assumption* $4\xi > (\beta + b)^2$ *(external focus dynamics). The following statements hold regarding the sign of the expression* $\mathbb{E}(\beta, \xi)$ *in* (2.53)*.*

(i) If $a < \beta \leq \dfrac{a+b}{2}$*, then* $\mathbb{E}(\beta, \xi) < 0$*.*

(ii) If $\dfrac{a+b}{2} < \beta < b$*, then* $\operatorname{sign} \mathbb{E}(\beta, \xi) = \operatorname{sign}\left(\xi - \beta \frac{\beta^2 - ab}{2\beta - a - b}\right)$*, so that* $\mathbb{E}(\beta, \xi) = 0$ *when*

$$\frac{\xi}{\beta} = \frac{\beta^2 - ab}{2\beta - a - b},$$

see the dashed green curve of Figure 2.4.

Proof. We assume now that the dynamics in the external zones is also of focus type, being our interest to control the sign of the expression (2.53). After some algebra (is suffices to multiply the above expression by $(\beta - a)/(\sqrt{\xi - a\beta}) - (\beta - b)/(\sqrt{\xi - b\beta})$, which is positive) we see that

$$\begin{aligned} \operatorname{sign} \mathbb{E}(\beta, \xi) &= \operatorname{sign}\left(\frac{(\beta - a)^2}{\xi - a\beta} - \frac{(\beta - b)^2}{\xi - b\beta}\right) = \\ &= \operatorname{sign}\left((2\beta - a - b)\xi - \beta(\beta^2 - ab)\right), \end{aligned}$$

after simplifying and grouping terms. The case when $2\beta = a+b$ comes directly from the above equality, since the last expression reduces to $-(a+b)(a-b)^2/8$. Two main cases remain. Assume the pending case of conditions in (i), that is $2\beta - a - b < 0$, we have

$$\beta\frac{\beta^2-ab}{2\beta-a-b} - \xi < \frac{\beta(\beta^2-ab)}{2\beta-a-b} - \frac{(\beta+b)^2}{4} = \\ = \frac{(\beta-b)^2(2\beta+a+b)}{4(2\beta-a-b)} < 0,$$

as assured. On the contrary, if we assume finally the cases of statement (ii), then $2\beta - a - b > 0$ and so

$$\operatorname{sign}\mathbb{E}(\beta,\xi) = \operatorname{sign}\left(\xi - \beta\frac{\beta^2-ab}{2\beta-a-b}\right)$$

as indicated, and we are done. □

Our final result characterizes completely the existence of periodic orbits for system (2.45) under above hypotheses. If we define the *periodic set* as the set of all the points belonging to the periodic orbits that appear for different values of h, including in it the two special points $(0,0,\pm1)$, then the main conclusion is that such a periodic set determines in the 3D state space a bounded and closed surface, which is homeomorphic to a topological sphere (see Figure 2.5).

Theorem 21. *Considering system (2.45) with H as defined in (2.46) under hypotheses given in (2.50) and taking $h_B = \xi - a\beta > 0$, the following statements hold.*

(a) (Dimensional reduction) For any $h \in \mathbb{R}$, the manifold $S_h = \{(x,y,z) : H(x,y,z) = h\}$ is invariant, and the dynamics on S_h is topologically equivalent to system (2.31)-(2.48)-(2.49).

Moreover, $(X(\tau), Y(\tau)) \in \mathbb{R}^2$ is a solution of the above system if and only if $E_h(X(\tau), Y(\tau))$ is a solution of system (2.45), where

$$E_h(X(\tau), Y(\tau)) = \begin{pmatrix} F(X(\tau)) - Y(\tau) \\ (\beta^2-\xi)X(\tau) - \beta Y(\tau) + h \\ X(\tau) \end{pmatrix}.$$

(b) (Oscillations) The system has infinitely many stable periodic orbits: for any initial condition $(x_0,y_0,z_0) \in \mathbb{R}^3$ with $|x_0| + |y_0| > 0$ and $|H(x_0,y_0,z_0)| < h_B$ the only stable solution is periodic. These stable periodic orbits generate a bounded tubular surface, symmetrical with respect to the origin.

(c) (Bi-stability at the same level set) If we have in system (2.31)-(2.48)-(2.49) focus dynamics in all zones, that is $4\xi > (\beta+b)^2$, and the two additional conditions

$$\beta > \frac{a+b}{2}, \quad \xi > \beta\frac{\beta^2-ab}{2\beta-a-b}, \tag{2.54}$$

hold, then there exists $\epsilon > 0$ *such that, for any* $h \in \mathbb{R}$ *with* $h_B < |h| < h_B + \epsilon$*, there are two different steady-state solutions. For some initial conditions* (x_0, y_0, z_0) *with* $H(x_0, y_0, z_0) = h$ *in the above range, there appears a periodic behavior while for others initial conditions satisfying the same equality, the solution of the system tends to a stationary state with* $x = y = 0$ *and* $|z| > 1$*, see Figure 2.6.*

(d) (Closed nature of the periodic set) If $4\xi \leq (\beta + b)^2$ *(NFN case) or* $2\beta \leq a + b$ *or, being* $2\beta > a + b$ *as in* (2.54)*, we have*

$$\xi < \beta \frac{\beta^2 - ab}{2\beta - a - b},$$

then the set of periodic orbits determines an invariant surface that closes at the points $(0, 0, \pm 1)$*, so that for any initial condition* $(x_0, y_0, z_0) \in \mathbb{R}^3$ *with* $|H(x_0, y_0, z_0)| \geq h_B$ *the steady state solution is not oscillatory, tending to a stationary state with* $x = y = 0$ *and* $|z| \geq 1$*.*

Proof. We are already able to show Theorem 21. Note first that statement (a) comes easily recalling Theorem 10. Statement (b) of Theorem 21 is a consequence of statement (a) of Proposition 19 where, by considering the different values of h, the existence of the periodic tubular surface can be deduced from the continuous dependence of solutions with respect to initial conditions and parameters. Note that non-smooth systems (2.31)-(2.48)-(2.49) are Lipschitz and so satisfy such a continuous dependence. To show statement (c) and (d), we must consider Lemma 20 and statements (b) and (c) of Proposition 19. Thus, the result is completely shown. □

We remark that the geometry of the periodic set admits different shapes. As indicated in statement (b) of Theorem 21, the part of the periodic set corresponding to $|h| < h_B$ is always a tubular surface, acting as the skeleton of the periodic set, but such surface can be closed in different ways, according to the NFN or diverse FFF cases. For instance, in the NFN case and in the FFF cases of statement (d) the tubular surface closes for $|h| = h_B$ at the two points $(0, 0, \pm 1)$, so that no periodic orbits appear for $|h| > h_B$. A special situation, not generic and not included in statement (d) for the sake of brevity, is when only the second condition (2.54) fails to become an equality; then, we have for $|h| = h_B$ a BEB of center type, and the tubular surface is closed by a bounded dihedral set of periodic orbits, see statement (c2) of Proposition 19.

Regarding Theorem 21, we can clarify some inexact sentences appearing in the final paragraph of Section 5 in Scarabello and Messias [2014]. In particular, authors postulated the existence of orbits tending to infinity in the configuration of statement (*c*) and this cannot be possible. In the quoted paper, authors say that such phenomenon can happen for $\alpha = 0.17$, $a = 1$, $b = 12$, $\xi = 50$ and $\beta = 2$. This set of parameters leads, once eliminated the non essential α by means of the change (2.44), to our parameters $\beta = 2$, $\xi = 8.5$, $a = 0.17$, $b = 2.04$, corresponding with Theorem 21(c) and possible bi-stability; in Figure 2.7, some numerical solutions for such set of parameters, corresponding to a certain value of h, indicate that this is indeed the

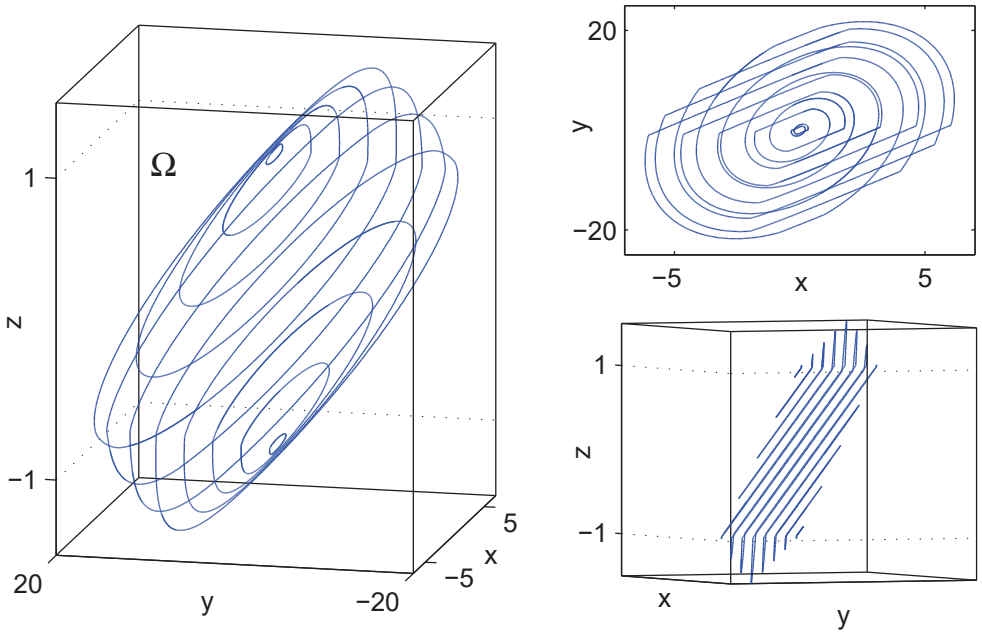

Figure 2.5: Some slices of the surface Ω given in (2.36) for system (2.45) with parameters $a = 1$, $\beta = 2$, $b = 8$, $\xi = 17$. Predicted by statement (d) of Theorem 21.

case. Effectively, in Figure 2.7 we see in the set S_h for $h = 112.41$ the existence of one stable equilibrium point surrounded by two periodic orbits, one stable (the bigger) and one unstable. In this case, as $d_C = 8.17$, we conclude that the value of ϵ in Theorem 21 (c) satisfies $\epsilon > 112.41 - 8.17 = 104.24$.

It should be also noticed that although statement (d) does not assure that the periodic set is closed under the specific hypotheses of statement (c), we have enough information to conjecture that such a property is true as well; what happens then is that two periodic orbits, one stable and another unstable, coexist in a certain range of values of h with $|h| > h_B$, and collide in a saddle-node bifurcation of periodic orbits for $|h| = h_{SN}$, with $h_{SN} > h_B$, to disappear for $|h| > h_{SN}$. Such value h_{SN} only can be detected by global techniques that go much beyond the scope of this work.

The relevance of Theorem 21 can be assessed by comparing their different statements with the simulation results achieved by M. Messias and coworkers in Messias et al. [2010], Botta et al. [2011], Scarabello and Messias [2014]. The quoted authors studied the same circuit and they were able to detect the existence of invariant manifolds, even if this fact was not shown to be connected with the existence of the first integral given in Theorem 8. However, as they did not build any reduced continuous model for the dynamics on such manifolds, only few rigorous results about oscillations were obtained.

We remark that the bi-stable regimes assured in statement (c) of Theorem 21, appearing for a same level set of the function H, have been not detected before, see Figure 2.6, and they are different from the recently obtained in Ascoli et al. [2016a,b]. The steady state depends on if the orbits, within such level set of H, start inside or

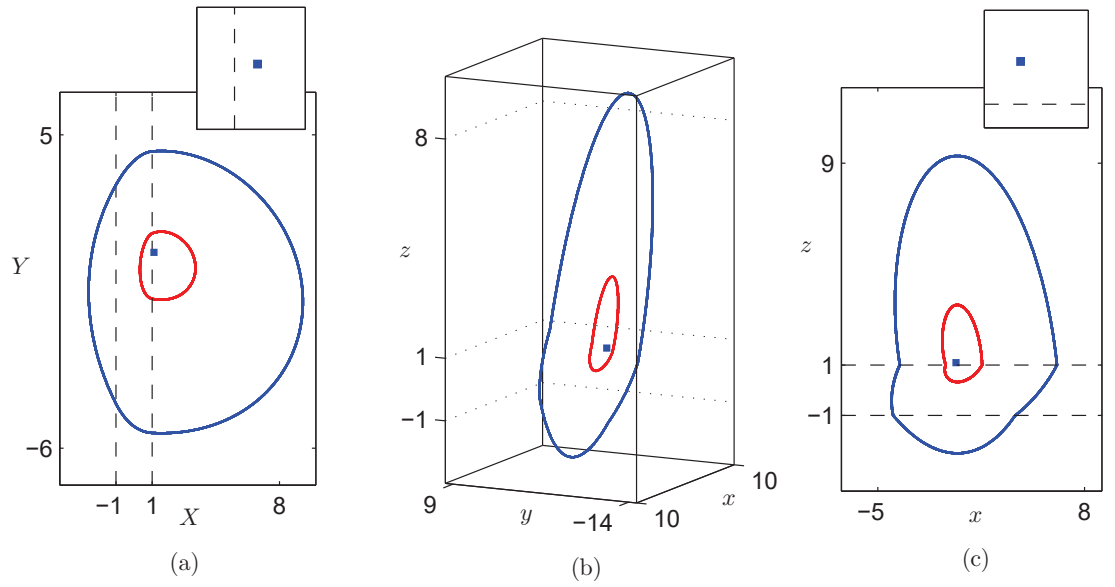

Figure 2.6: Simulation results showing the bistability phenomenon in system (2.45) predicted by statement (c) of Theorem 21. The parameters are $a = 1$, $b = 2$, $\xi = 4$, $\beta = 1.8$, and the chosen level set is $h = h_B + 0.2 = 2.4$. The stable equilibrium is surrounded by one unstable limit cycle (in red) plus one stable limit cycle (in blue). (a) The phase plane of reduced system (2.31)-(2.48)-(2.49); (b) The 3D phase space of system (2.45); (c) its projection on the (x, z) plane. The magnifications around the equilibrium point of the insets in panels (a) and (c) allow to visualize that $\overline{X} > 1$ and $\overline{z} > 1$, respectively, recall Remark 18.

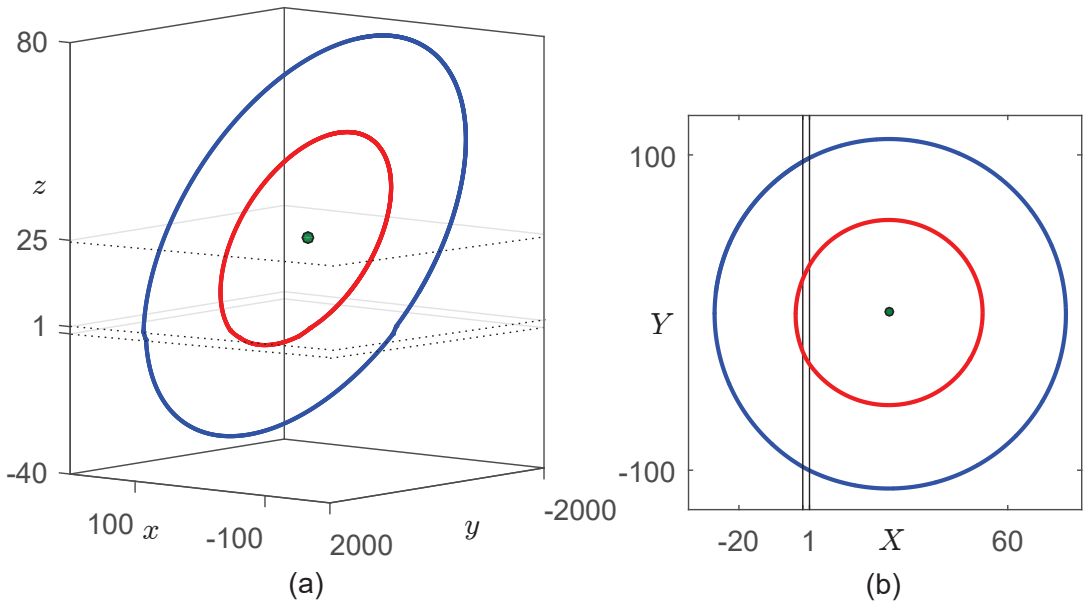

Figure 2.7: (a) The steady-state solutions of system (2.45) for $h = 112.41$. Parameters are taken like in Figure 20 of Scarabello and Messias [2014] that is $\beta = 2$, $\xi = 8.5$, $a = 0.17$, $b = 2.04$. We are in case (d) of Theorem 21, with focus dynamics in all zones. The stable periodic orbit appears in blue, the unstable periodic orbit is shown in red, and the stable equilibrium point $(0, 0, 25)$ in green. (b) Representation of the bi-stability in the reduced system (2.31)-(2.48)-(2.49).

outside the small unstable limit cycle. This fact emphasizes even more one of the main features of these oscillators: their steady states are strongly depending on the initial conditions and therefore one can get infinitely many different steady states. External perturbations changing the value H will alter the steady dynamics, not only quantitatively, but possibly also qualitatively, passing from a static regime to a periodic one or vice versa. For certain parameter values in the circuit, this is also possible, as mentioned, even when not changing the level set of the first integral.

Regarding the mathematical analysis that gives rise to Theorem 21, it relies in some recent results from the bifurcation theory of piecewise linear systems that use the value of h as the main bifurcation parameter. This can be thought as a mathematical artifact, since such a parameter is hidden in system (2.41) and so it is fair to speak of bifurcations without parameters, see Corinto and Forti [2017]. However, it is precisely such parameter who allows to classify the different qualitative behaviors one can find in the circuit, so that its control becomes a crucial matter. Clearly, to assure a desired response for the oscillator, auxiliary circuits to fix the initial values for fluxes and charges of the different elements (and so the value of h) are needed; this issue is beyond our expertise but practitioners should be aware of it.

2.4.1 Equivalence of our reduced systems and the obtained through FCAM

Here, we show how it is possible to get the same continuous reduced models by working from the beginning in the flux-charge setting instead of starting from the discontinuous 3D system (2.41). Following this method we should not need Theorem 10 to get the planar system (2.31)-(2.48)-(2.49) that has been the object under study in this section, and therefore, one can adopt any of the two modeling approaches.

Effectively, if we integrate equations (2.38) with respect to time from a given initial value τ_0 to a time $\tau \geq \tau_0$, we get

$$\begin{array}{rcl} q_R(\tau) - q_L(\tau) & = & q_R(\tau_0) - q_L(\tau_0) = Q_1, \\ q_L(\tau) - q_C(\tau) - q_M(\tau) & = & q_L(\tau_0) - q_C(\tau_0) - q_M(\tau_0) = Q_2, \\ \varphi_R(\tau) + \varphi_L(\tau) + \varphi_C(\tau) & = & \varphi_R(\tau_0) + \varphi_L(\tau_0) + \varphi_C(\tau_0) = \Phi_1, \\ \varphi_C(\tau) - \varphi_M(\tau) & = & \varphi_C(\tau_0) - \varphi_M(\tau_0) = \Phi_2, \end{array} \tag{2.55}$$

where we see the relations to be fulfilled for the different charges and fluxes, and the constants Q_1, Q_2, Φ_1 and Φ_2, give account of initial conditions in the circuit. Recalling the constitutive equations of the different elements, namely

$$\varphi_L(\tau) = L\frac{d}{d\tau}q_L(\tau), \quad q_C(\tau) = C\frac{d}{d\tau}\varphi_C(\tau), \quad q_M(\tau) = q(\varphi_M(\tau)), \tag{2.56}$$

along with the obtained after integrating the constitutive relation for the resistor $-R$ in (2.39) from time τ_0 to $\tau \geq \tau_0$, namely

$$\varphi_R(\tau) + Rq_R(\tau) = \Phi_3 = \varphi_R(\tau_0) + Rq_R(\tau_0), \tag{2.57}$$

we can describe the dynamics of the circuit with only two state variables, namely $\varphi_C(\tau)$ and $q_L(\tau)$. Effectively, from (2.55), (2.56) and (2.57) we have

$$q_C(\tau) = C\frac{d}{d\tau}\varphi_C(\tau) = q_L(\tau) - q_M(\tau) - Q_2 = q_L(\tau) - q\left(\varphi_C(\tau) - \Phi_2\right) - Q_2,$$
$$\varphi_L(\tau) = L\frac{d}{d\tau}q_L(\tau) = -\varphi_R(\tau) - \varphi_C(\tau) + \Phi_1 = R\left(q_L(\tau) + Q_1\right) - \varphi_C(\tau) + \Phi_1 - \Phi_3.$$

Clearly, it is more convenient to work with the state variables $x_1(\tau) = \varphi_M(\tau) = \varphi_C(\tau) - \Phi_2$ and $x_2(\tau) = q_L(\tau) - Q_2 = q_C(\tau) + q_M(\tau)$, to arrive at the continuous piecewise linear differential system

$$C\frac{dx_1}{d\tau} = -q(x_1) + x_2,$$
$$L\frac{dx_2}{d\tau} = -x_1 + Rx_2 + h,$$

where we introduce the constant $h = RQ_1 + RQ_2 + \Phi_1 - \Phi_2 - \Phi_3$, which depends only on the initial conditions and reduces to

$$h = -R\left(q_C(\tau_0) + q_M(\tau_0)\right) + \varphi_L(\tau_0) + \varphi_M(\tau_0).$$

Clearly, this constant is directly related with the condition derived in (2.43).

Thus, these computations lead to a one-parameter family of 2D dynamical systems, according to the flux-charge analysis method (FCAM) proposed by Corinto and Forti in Corinto and Forti [2016]. Authors emphasize in the quoted paper the usefulness of considering incremental fluxes and charges in the modeling process, see also Corinto and Forti [2017].

If we introduce the above parameters

$$\alpha = \frac{1}{C}, \quad \xi = \frac{1}{L}, \quad \beta = \frac{R}{L},$$

we get the system

$$\dot{x}_1 = -\alpha q(x_1) + \alpha x_2,$$
$$\dot{x}_2 = -\xi x_1 + \beta x_2 + \xi h.$$

Finally, the change of variables $x = x_1$, $y = \beta x_1 - \alpha x_2$ put the system in the Liénard form

$$\dot{x} = \beta x - \alpha q(x) - y,$$
$$\dot{y} = \alpha\xi x - \alpha\beta q(x) - \alpha\xi h,$$

and now, by removing the parameter α as in (2.44), we arrive exactly to the one-parameter family of 2D dynamical systems (2.31)-(2.48)-(2.49), as claimed at the beginning of this subsection.

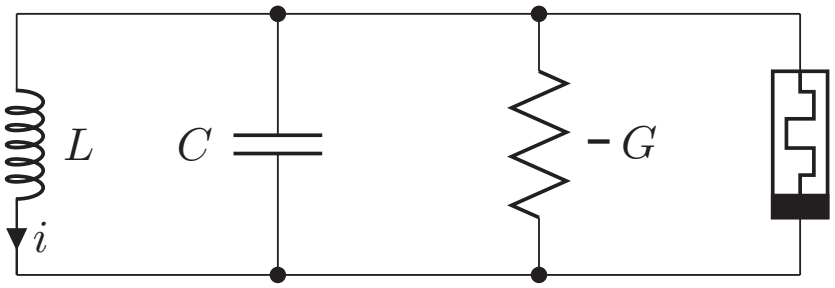

Figure 2.8: The Van der Pol oscillator, where there appears a negative conductance in parallel with a passive memristor.

2.5 Application to a 3D PWL memristor based Van der Pol oscillator

As a second example, we consider here the oscillator introduced in section 4.2 of Itoh and Chua [2008] where it is considered a Van der Pol oscillator with a two-terminal circuit consisting of a negative conductance in parallel with a flux-controlled memristor (see Figure 2.8). Recently in Messias and Maciel [2017] the authors reported numerically the existence of a sphere foliated by periodic orbits. The dynamics of this circuit is given by

$$\begin{aligned} \frac{dx}{d\tau} &= \alpha\left(-y + (\gamma - W(z))x\right), \\ \frac{dy}{d\tau} &= \beta x, \\ \frac{dz}{d\tau} &= x, \end{aligned} \tag{2.58}$$

where $\alpha, \beta, \gamma > 0$ and $W(z)$ is given by (2.27), see the quoted paper for the meaning of parameters. Authors detect numerically for a certain choice of parameters two limit cycles. Later on, in Botta et al. [2011] authors found numerically the existence of multiple oscillations and they conjectured under certain hypotheses the existence of a topological sphere foliated by such periodic orbits. Here, we show that such conjecture is true, by resorting to the previous results.

Again, we start by noticing that the parameter α is not essential. In fact, the change of variables

$$\widetilde{x} = x, \quad \widetilde{y} = \alpha y, \quad \widetilde{z} = z, \quad V(z) = \alpha(\gamma - W(z)),$$

and parameters

$$\tilde{a} = \alpha a, \quad \tilde{b} = \alpha b, \quad \tilde{\gamma} = \alpha\gamma,$$

transforms system (2.58) into the following one, where the tildes have been removed

$$\begin{aligned} \frac{dx}{d\tau} &= V(z)x - y, \\ \frac{dy}{d\tau} &= \beta x, \\ \frac{dz}{d\tau} &= x, \end{aligned} \tag{2.59}$$

with

$$V(z) = \begin{cases} \gamma - b, & \text{if} \quad |z| > 1, \\ \gamma - a, & \text{if} \quad |z| < 1. \end{cases} \tag{2.60}$$

We see that system (2.59)-(2.60) is already in the form (2.11), where $a_{11} = 1$, $a_{12} = -1$, $a_{21} = \beta$ and $a_{22} = 0$. From Theorem 8, the expression of the conserved quantity reduces to $H(x, y, z) = -y + \beta z$. The existence of this conserved quantity for the oscillator under study was already detected in Pham et al. [2012] and Buscarino et al. [2016], where some indications about its possible usefulness were mentioned.

If we replace these parameters in (2.28), we obtain

$$d_C = d_E = \beta, \quad t_C = \gamma - a, \quad t_E = \gamma - b. \tag{2.61}$$

It is immediate to state the following result.

Proposition 22. *Considering system (2.59)-(2.60) under hypotheses*

$$0 < a < \gamma < b, \quad \beta > 0,$$

and the function

$$H(x, y, z) = -y + \beta z,$$

the following statements hold.

(a) For any $h \in \mathbb{R}$, the set

$$S_h = \{(x, y, z) \, : \, H(x, y, z) = h\}$$

is invariant for the system, and the dynamics on S_h is topologically equivalent to the planar system

$$\begin{aligned} \dot{X} &= F(X) - Y, \\ \dot{Y} &= g(X) - h, \end{aligned}$$

where

$$F(X) = \begin{cases} (\gamma - b)X + b - a, & \text{if} \quad X > 1, \\ (\gamma - a)X, & \text{if} \quad |X| \leq 1, \\ (\gamma - b)X - b + a, & \text{if} \quad X < -1, \end{cases}$$

$$g(X) = \beta X.$$

Moreover, $(X(\tau), Y(\tau)) \in \mathbb{R}^2$ *is a solution of the above system if and only if* $E_h(X(\tau), Y(\tau))$ *is a solution of system* (2.45)*, where*

$$E_h(X(\tau), Y(\tau)) = \begin{pmatrix} F(X(\tau)) - Y(\tau) \\ \beta X(\tau) - h \\ X(\tau) \end{pmatrix}.$$

(b) The system has an infinite number of stable periodic orbits; in particular, for any initial condition $(x_0, y_0, z_0) \in \mathbb{R}^3$ *with* $x_0 \neq 0$ *or* $y_0 \neq 0$ *and* $|\beta z_0 - y_0| < \beta$*, the steady state solution is periodic.*

(c) The periodic orbits of statement (b) generate a tubular surface Ω *which is homeomorphic to the cylinder* $\mathbf{S^1} \times (-1, 1)$*. Such surface* Ω *is symmetric with respect to the origin.*

(d) If we have node dynamics in all zones, that is

$$\beta \leq \frac{(\gamma - a)^2}{4}, \quad \beta \leq \frac{(\gamma - b)^2}{4},$$

then, on each invariant set S_h *with* $h = \pm\beta$*, there exists a bounded continuum of homoclinic connections to the points* $(0, 0, \pm 1)$*; such two sets of homoclinic connections close the tubular surface* Ω *given in* (2.36)*.*

(e) If we have focus dynamics in all zones, that is

$$\frac{(\gamma - a)^2}{4} < \beta, \quad \frac{(\gamma - b)^2}{4} < \beta,$$

then two cases arise, as follows.

(e1) If $\gamma \leq \dfrac{a+b}{2}$ *then the set of periodic orbits determines an invariant surface that closes at the points* $(0, 0, \pm 1)$*. Therefore, for any initial condition* $(x_0, y_0, z_0) \in \mathbb{R}^3$ *with* $|\beta z_0 - y_0| > \beta$*, the steady state solution is not oscillatory, tending to a stationary state with* $x = y = 0$*, namely* $(0, 0, h/\beta)$*.*

(e2) If $\gamma > \dfrac{a+b}{2}$ *then there exists* $\epsilon > 0$ *such that, for any* $h \in \mathbb{R}$ *with* $\beta < |h| < \beta + \epsilon$ *and initial conditions* (x_0, y_0, z_0) *with* $h = \beta z_0 - y_0$*, there are two possible different steady-state solutions. For some initial conditions solutions tend to a periodic solution while for others initial conditions, the solutions of the system tend to a stationary state with* $x = y = 0$*.*

(f) If $\gamma < \dfrac{a+b}{2}$ *and we have focus dynamics in the central zone with node dynamics in external zones, that is*

$$\frac{(\gamma - a)^2}{4} < \beta \leq \frac{(\gamma - b)^2}{4},$$

then the set of periodic orbits determines a invariant surface that closes at the points $(0, 0, \pm 1)$. *Therefore, for any initial condition* $(x_0, y_0, z_0) \in \mathbb{R}^3$ *with* $|\beta z_0 - y_0| > \beta$, *the steady state solution is not oscillatory, tending to a stationary state with* $x = y = 0$.

(g) If $\gamma > \dfrac{a+b}{2}$ *and we have node dynamics in the central zone with focus dynamics in external zones, that is*

$$\frac{(\gamma - b)^2}{4} < \beta \leq \frac{(\gamma - a)^2}{4},$$

then, there exists $\epsilon > 0$ *such that, for any* $h \in \mathbb{R}$ *with* $\beta < |h| < \beta + \epsilon$ *and initial conditions* (x_0, y_0, z_0) *with* $h = \beta z_0 - y_0$, *there are two possible different steady-state solutions. For some initial conditions, there exists an oscillatory behavior while for others initial conditions, the solutions of the system tend to a stationary state with* $x = y = 0$.

Proof. The conclusion follows after applying Theorem 12 and Propositions 13, 14 and 15, taking into account that expression (2.37) simplifies here to $2\gamma > a + b$. □

We show in Fig. 2.9 some periodic orbits in the case of statement (d). The tubular surface formed by these periodic orbits is closed by two continua of homoclinic orbits, as the ones shown in Fig 4(a) of Ponce et al. [2015].

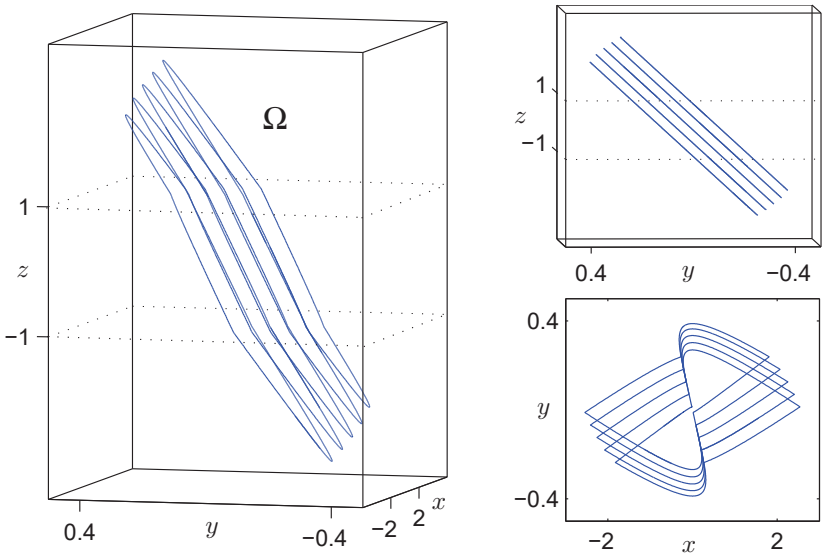

Figure 2.9: Some slices of the surface Ω given in (2.36) for system (2.59). Parameters $\beta = 1/8$, $\gamma = 2$, $a = 1$, $b = 3$. We are in case (d) of Proposition 22, with node dynamics in all zones.

Bibliography

A. Ascoli, R. Tetzlaff, and L.O. Chua. The first ever real bistable memristors-part I: Theoretical insights on local fading memory. *IEEE Transactions on Circuits and Systems II: Express Briefs*, 63(12):1091–1095, dec 2016a. URL https://doi.org/10.1109/tcsii.2016.2604567.

A. Ascoli, R. Tetzlaff, and L.O. Chua. The first ever real bistable memristors—part II: Design and analysis of a local fading memory system. *IEEE Transactions on Circuits and Systems II: Express Briefs*, 63(12):1096–1100, dec 2016b. URL https://doi.org/10.1109/tcsii.2016.2613560.

B.C. Bao, Z. Liu, and H. Leung. Is memristor a dynamic element? *Electronics Letters*, 49(24):1523–1525, 2013. URL https://ieeexplore.ieee.org/document/6680411/.

A. Botta, C. Nespoli, and M. Messias. Mathematical analysis of a third-order memristor-based Chua's oscillator. *TEMA Tend. Mat. Apl. Comput.*, 12(2):91–99, 2011. URL https://doi.org/10.5540/tema.2011.012.02.0091.

A. Buscarino, C. Corradino, L. Fortuna, M. Frasca, and L.O. Chua. Turing patterns in memristive cellular nonlinear networks. *IEEE Transactions on Circuits and Systems I: Regular Papers*, 63(8):1222–1230, Aug 2016. ISSN 1549-8328. URL https://doi.org/10.1109/TCSI.2016.2564738.

V. Carmona, E. Freire, E. Ponce, and F. Torres. On simplifying and classifying piecewise-linear systems. *IEEE Transactions in Circuits and Systems*, 49:609–620, 2002. URL https://doi.org/10.1109/TCSI.2002.1001950.

F. Corinto and M. Forti. Memristor circuits: Flux-charge analysis method. *IEEE Transactions on Circuits and Systems I: Regular Papers*, 63(11):1997–2009, nov 2016. URL https://doi.org/10.1109/tcsi.2016.2590948.

F. Corinto and M. Forti. Memristor circuits: Bifurcations without parameters. *IEEE Transactions on Circuits and Systems I: Regular Papers*, 64(6):1540–1551, jun 2017. URL https://doi.org/10.1109/tcsi.2016.2642112.

M. Desroches, E. Freire, S. Hogan, E. Ponce, and P. Thota. Canards in piecewise-linear systems: explosions and super-explosions. *Proceedings of the Royal Society of London A: Mathematical, Physical and Engineering Sciences*, 469(2154):1364–5021, 2013. URL https://doi.org/10.1098/rspa.2012.0603.

M. Itoh and L.O. Chua. Memristor oscillators. *International Journal of Bifurcation and Chaos*, 18(11):3183–3206, 2008. URL http://dx.doi.org/10.1142/S0218127408022354.

M. Messias and A.L Maciel. On the existence of limit cycles and relaxation oscillations in a 3D Van der Pol-like memristor oscillator. *International Journal of Bifurcation and Chaos*, 27(07):1750102, jun 2017. URL https://doi.org/10.1142/s0218127417501024.

M. Messias, C. Nespoli, and V.A. Botta. Hopf bifurcation from lines of equilibria without parameters in memristor oscillators. *International Journal of Bifurcation and Chaos*, 20(02):437–450, feb 2010. URL https://doi.org/10.1142/s0218127410025521.

V. Pham, A. Buscarino, L. Fortuna, and M. Frasca. Autowaves in memristive cellular neural networks. *International Journal of Bifurcation and Chaos*, 22(08):1230027, aug 2012. URL https://doi.org/10.1142/s0218127412300273.

E. Ponce, J. Ros, and E. Vela. Limit cycle and boundary equilibrium bifurcations in continuous planar piecewise linear systems. *International Journal of Bifurcation and Chaos*, 25:1530008, 2015. URL https://doi.org/10.1142/S0218127415300086.

R. Riaza. Comment: Is memristor a dynamic element? *Electronics Letters*, 50(8): 1523–1525, 2014. URL https://doi.org/10.1049/el.2014.1553.

M. Scarabello and M. Messias. Bifurcations leading to nonlinear oscillations in a 3D piecewise linear memristor oscillator. *International Journal of Bifurcation and Chaos*, 24(01):1430001, jan 2014. URL https://doi.org/10.1142/s0218127414300018.

Chapter 3

The Melnikov method in the analysis of 3D memristor oscillators

In this chapter, we derive the bifurcation set for a three-parametric family of Bogdanov-Takens systems with symmetry and deformation. We show that it is possible to write the system as a perturbed cubic Hamiltonian with a configurations of parameters not yet studied in the literature. By using the first-order Melnikov function, we report for the first time in this system an analytical approximation of the bifurcation curves for homoclinic and heteroclinic connections, which organize the parametric regions with different schemes of periodic orbits.

As a application of these results, we study a family of 3D memristor oscillators, where the characteristic function of the memristor is a cubic polynomial. We show that this system has an infinity number of invariant manifolds, and by adding one parameter that stratifies the 3D dynamics of the family previously analyzed, it is shown that the dynamics in each stratum is topologically equivalent to a Bogdanov-Takens system with symmetry. Also, based on the bifurcation set obtained in this chapter, we show the existence of closed surfaces in the 3D state space which are foliated by periodic orbits. Finally, we clarify some misconceptions that arise from the numerical simulations of these systems, emphasizing the important role of invariant manifols in these models.

3.1 Unfolding the Bogdanov-Takens normal form

In planar systems, the existence the global bifurcations may reveal the presence of other bifurcations of local character Dumortier et al. [1987]-Dumortier [1991], and the curves that determine the global phenomena are difficult to determine. This is, for instance, the case regarding the appearance of homoclinic or heteroclinic connections.

A homoclinic connection is an orbit of the system that joins a saddle equilibrium point to itself, and generally creates or destroys periodic orbits (see, for instance Wiggins [2003]). A heteroclinic connection joins two different equilibrium points of a system and the existence of this connection can determine changes in the basin

of attraction of a positively invariant set. The bifurcation curves that govern these global phenomena are very difficult to determine.

Following Freire et al. [2000], the techniques to study homoclinic orbits in planar vector fields were well developed during the 1920s in the works of Dulac. The fundamental idea is that the recurrent behavior near a connecting orbit should be studied in a fashion similar to that used in studying periodic orbits via a Poincaré return map. But there are some additional complications in the study of homoclinic orbits compared to that of periodic orbits which significantly complicate the analysis.

The normal form of the Bogdanov-Takens (see Wiggins [2003]) bifurcation is given by

$$\dot{x} = y, \quad \dot{y} = \mu_1 + \mu_2 x + x^2 \pm xy.$$

Following the classification proposed in Dumortier [1991], the deformation of codimension three of the previous normal form is given by the unfolding

$$\begin{aligned} \dot{x} &= y, \\ \dot{y} &= \mu_1 + \mu_2 x + \alpha x^3 + y(\mu_3 + \mu_4 x \pm x^2), \end{aligned} \tag{3.1}$$

where the case $\alpha > 0$ is called saddle, the cases $-1/8 < \alpha < 0$ and $\alpha < -1/8$ are called respectively elliptic and focus. The presence of this type of systems has been reported in different applications, see Freire et al. [2005]-Blank et al. [2016]-Kong and Zhu [2017]. On the study of bifurcation phenomena in these systems many contributions have been made. In Fernández et al. [1996], the authors studied the global bifurcation diagram of the three-parameter family

$$\begin{aligned} \dot{x} &= y, \\ \dot{y} &= \mu_1 + \mu_2 x - x^3 + y(\mu_3 - 3x^2), \end{aligned}$$

and fixing $\mu_3 > 0$, they obtained analytical expressions for homoclinic orbits, by using Melnikov functions. Later, the above work was quoted in Khibnik et al. [1998], where a numerical analysis of the same model was performed. In Dumortier and Li [2001]-Dumortier and Li [2003b]-Dumortier and Li [2003a], it is considered the system

$$\begin{aligned} \dot{x} &= y, \\ \dot{y} &= \mu_1 + \mu_2 x - x^3 + y(\mu_3 + \mu_4 x - x^2), \end{aligned} \tag{3.2}$$

and the authors showed that it can be written as a perturbed Hamiltonian system, reporting its maximum number of limit cycles. By taking the parameter $\mu_4 = 0$ in (3.2), the authors in Chen and Chen [2015] and Chen and Chen [2016] analyzed the system as a Liénard system, its local bifurcations are characterized, and a numerical study of the global bifurcations is done.

While all the above references dealt with the focus case, in this chapter we study the saddle case

$$\begin{aligned} \dot{x} &= y, \\ \dot{y} &= \mu_1 + \mu_2 x + x^3 + y(\mu_3 - 3x^2), \end{aligned} \tag{3.3}$$

which up to the best of our knowledge, seems to be a forgotten case, being the most interesting one for us, as shown later.

3.2 The Melnikov method

Usually, the bifurcation curves of homoclinic and heteroclinic connections are studied by numerical continuation techniques Freire et al. [1999]-Freire et al. [2000]-Dhooge et al. [2008] -Witte et al. [2012]. On the other hand, when a planar system can be written as a perturbed Hamiltonian system, we can calculate certain Melnikov functions, introduced in Melnikov [1963], and under certain hypotheses, the zeros of such Melnikov functions determine the existence of periodic orbits, homoclinic loops or heteroclinic connections, see for instance Dangelmayr and Guckenheimer [1987]-Guckenheimer et al. [1989]-Blows and Perko [1994].

Next, we review certain results that are useful in the approximation of periodic orbits, homoclinic loops and heteroclinic connections in perturbed Hamiltonian systems, see for more details Guckenheimer and Holmes [2013]. Consider the planar system given by

$$\dot{\mathbf{x}} = f(\mathbf{x}) + \varepsilon g(\mathbf{x}, \mathbf{u}), \tag{3.4}$$

with $f \in C^1(\mathbb{R}^2)$ and $g \in C^1(\mathbb{R}^2 \times \mathbb{R}^m)$, and the following assumptions.

(a) For $\varepsilon = 0$ the system (3.4) has a homoclinic orbit or a heteroclinic connection

$$\Gamma_0 : \mathbf{x} = \gamma_0(t), \quad -\infty < t < \infty,$$

to a hyperbolic saddle point $\mathbf{x}_0$.

(b) For $\varepsilon = 0$ the system (3.4) has a one-parameter family of periodic orbits $\gamma_\alpha(t)$ of period T_α on the interior of Γ_0 with $\partial\gamma_\alpha(0)/\partial\alpha \neq 0$.

The Melnikov function, $M(\mathbf{u})$, is defined by

$$M(\mathbf{u}) = \int_{-\infty}^{\infty} e^{-\int_{t_0}^{t} \nabla \cdot f(\gamma_0(s))ds} f(\gamma_0(t)) \wedge g(\gamma_0(t), \mathbf{u})dt,$$

where the wedge product of two vectors $\mathbf{w}$ and $\mathbf{v} \in \mathbb{R}^2$ is given by

$$\mathbf{w} \wedge \mathbf{v} = w_1 v_2 - w_2 v_1.$$

If f is a Hamiltonian system, statement (b) is fulfilled, and the Melnikov function has the simpler form

$$M(\mathbf{u}) = \int_{-\infty}^{\infty} f(\gamma_0(t)) \wedge g(\gamma_0(t), \mathbf{u})dt. \tag{3.5}$$

The next theorem establishes the existence of homoclinic orbits in system (3.4).

Theorem 23. *Assume that statement (a) is fulfilled and that f is a Hamiltonian system. If there exists a $\mathbf{u}_0 \in \mathbb{R}^m$ such that the function M defined in (3.5) satisfies $M(\mathbf{u}_0) = 0$, then for all sufficiently small $\varepsilon \neq 0$ there is a $\mathbf{u}_\varepsilon = \mathbf{u}_0 + O(\varepsilon)$ such that system (3.4) with $\mathbf{u} = \mathbf{u}_\varepsilon$ has a unique homoclinic orbit in an $O(\varepsilon)$ neighborhood of the homoclinic orbit Γ_0.*

3.3 Local bifurcations

In this section, we are interested in the study of local bifurcations that occur in system (3.3). First, we note that the system is symmetric under the transformation

$$(x, y, \mu_1, \mu_2, \mu_3) \to (-x, -y, -\mu_1, \mu_2, \mu_3).$$

Therefore, it is sufficient to study the bifurcation diagram for $\mu_1 > 0$. We note that the equilibrium points of the system are of the form $(\overline{x}, \overline{y}) = (\tilde{x}, 0)$, being $\tilde{x}$ a solution of the cubic $\mu_1 + \mu_2 x + x^3 = 0$.

Now, in the next result, we give a sufficient condition for the existence of three equilibrium points in system (3.3).

Proposition 24. *Consider system (3.3). If $\mu_2 < 0$ the system has three equilibrium points $\mathbf{x}_i = (s_i, 0)$ with $i \in \{L, C, R\}$, such that $s_L < s_C < s_R$ and $\mathbf{x}_L, \mathbf{x}_R$ are saddle points and $\mathbf{x}_C$ is a focus or a node (anti-saddle).*

Proof. The equilibrium points of system (3.11) are determined by roots of the polynomial $p(x) = \mu_1 + \mu_2 x + x^3$. If $\mu_2 < 0$ there exists $s_L, s_C, s_R \in \mathbb{R}$ such that $s_L < s_C < s_R$ and $p(s_i) = 0$, that is

$$\begin{aligned} p(x) &= (x - s_L)(x - s_C)(x - s_R) = \\ &= -s_C s_L s_R + (s_C s_L + s_C s_R + s_L s_R)\, x - (s_L + s_R + s_C)\, x^2 + x^3, \end{aligned}$$

and we obtain the equalities

$$\mu_1 = -s_L s_C s_R, \quad \mu_2 = s_C s_L + s_C s_R + s_L s_R, \quad s_L + s_C + s_R = 0. \tag{3.6}$$

Assuming J as the Jacobian matrix of the system (3.3), we get that $\det(J(s_i)) = -(\nu_2 + 3s_i^2)$ for $i \in \{L, C, R\}$. We need to show that $\det(J(s_L)), \det(J(s_R)) < 0$, that is $\mu_2 + 3s_i^2 > 0$ for $i \in \{L, R\}$. Assuming that $\mu_1 > 0$ and from (3.6), we obtain

$$s_C s_L s_R < 0, \quad \mu_2 = s_L s_C + s_C s_R + s_L s_R, \quad s_L + s_C = -s_R,$$

so that, from the two possibilities (all roots negative or only one) we have from the last equality that $s_L < 0 < s_C < s_R$, and

$$\begin{aligned} \mu_2 + 3s_R^2 = s_L s_C + (s_C + s_L)\, s_R + 3s_R^2 = s_L s_C - s_R^2 + 3s_R^2 = s_L s_C + 2s_R^2 = \\ = -s_C\,(s_C + s_R) + 2s_R^2 = -\,(s_C - s_R)\,(s_C + 2s_R) > 0. \end{aligned}$$

The case $\mu_1 < 0$ is analogous. Following the same kind of argument we can show that $\det(J(s_C)) > 0$, and this completes the proof. □

In the next result, we characterize the local bifurcations of the system.

Proposition 25. *The following statements hold for system (3.3).*

(a) The parameter values in the set

$$\varphi_{sn} = \{(\mu_1, \mu_2, \mu_3) : 27\mu_1^2 + 4\mu_2^3 = 0 \text{ and } \mu_3 \in \mathbb{R}\}, \tag{3.7}$$

correspond with saddle-node bifurcation points of equilibria.

(b) The system has a cusp bifurcation of equilibria along the $\mu_1 = \mu_2 = 0$.

(c) The parameter values in the set

$$\varphi_H = \{(\mu_1, \mu_2, \mu_3) : \mu_1 = \mp \left(\frac{\mu_3}{3}\right)^{3/2} \mp \left(\frac{\mu_3}{3}\right)^{1/2} \mu_2, \quad \mu_3 > 0,\ \mu_2 < -\mu_3\}, \tag{3.8}$$

represent Andronov-Hopf bifurcation points of codimension one.

(d) The system has a Bogdanov-Takens bifurcation for $\mu_1 = 2\tilde{x}^3$, $\mu_2 = -3\tilde{x}^2$, $\mu_3 = 3\tilde{x}^2$ *where* $\mu_1 + \mu_2\tilde{x} + \tilde{x}^3 = 0$.

Proof. The Jacobian matrix of system (3.3) is given by

$$J(x, y) = \begin{pmatrix} 0 & 1 \\ \mu_2 + 3x^2 - 6yx & \mu_3 - 3x^2 \end{pmatrix}.$$

Statements (a) and (b) are a direct consequence of the equations

$$x^3 + \mu_2 x + \mu_1 = 0, \quad \mu_2 + 3x^2 = 0.$$

Let $(\tilde{x}, 0)$ an equilibrium point of system (3.3). The Jacobian matrix $J(\tilde{x}, 0)$ has two purely imaginary eigenvalues when taking $\mu_3 > 0$ the equalities satisfy $\tilde{x} = \pm\sqrt{\mu_3/3}$ and $\mu_2 < -\mu_3 < 0$. Since $(\tilde{x}, 0)$ is an equilibrium point we have

$$\mu_1 + \mu_2 \left(\pm\sqrt{\frac{\mu_3}{3}}\right) + \left(\pm\sqrt{\frac{\mu_3}{3}}\right)^3 = 0,$$

and statement (c) follows. To show statement (d) is sufficient to consider the equations $trace\,(J(\tilde{x}, 0)) = \det(J(\tilde{x}, 0)) = 0$. □

Given $\mu_3 > 0$ we obtain in the parameter plane (μ_2, μ_1) two points corresponding to Bogdanov-Takens bifurcation points, namely

$$BT_\pm \equiv \left(-\mu_3, \pm\frac{2}{3}\sqrt{\frac{\mu_3^3}{3}}\right). \tag{3.9}$$

Note that we put the μ_1 axis in the plane (μ_2, μ_1) as the vertical one.

3.4 Global bifurcations

In this section we will complete the bifurcation analysis of system (3.3). We will write the system as a perturbed Hamiltonian to which the Melnikov theory can be applied. This can be done in different ways, as indicated in the next result. The possibility of resorting to one of the two next reparametrization forms will be helpful later.

Proposition 26. *System (3.3) can be written as two different perturbed Hamiltonian systems, as follows.*

(a) Taking

$$\mu_1 = \varepsilon^2\nu_1, \quad \mu_2 = \varepsilon^2\nu_2, \quad \mu_3 = \varepsilon\nu_3, \tag{3.10}$$

the system can be rewritten as

$$\begin{aligned} \dot{x} &= y, \\ \dot{y} &= \nu_2 x + x^3 + \varepsilon\left(\nu_1 + \nu_3 y - 3x^2 y\right), \end{aligned} \tag{3.11}$$

which for $\varepsilon = 0$ corresponds to the Hamiltonian

$$H_1(x,y) = \frac{y^2}{2} - \nu_2\frac{x^2}{2} - \frac{x^4}{4}. \tag{3.12}$$

(b) Taking

$$\mu_1 = \varepsilon^4\nu_1 \quad , \mu_2 = \varepsilon^2\nu_2, \quad \mu_3 = \varepsilon^2\nu_3, \tag{3.13}$$

the system can be rewritten as

$$\begin{aligned} \dot{x} &= y, \\ \dot{y} &= \nu_1 + \nu_2 x + x^3 + \varepsilon(\nu_3 y - 3x^2 y), \end{aligned} \tag{3.14}$$

which for $\varepsilon = 0$ corresponds to the Hamiltonian

$$H_2(x,y) = \frac{y^2}{2} - \nu_1 x - \nu_2\frac{x^2}{2} - \frac{x^4}{4}. \tag{3.15}$$

Proof. The blow-up transformation $x = \varepsilon x_1$, $y = \varepsilon y_1$, and $t = \varepsilon\bar{t}$, allows to rewrite the system as

$$x_1' = y_1, \quad y_1' = x_1^3 + \frac{\mu_2}{\varepsilon^2}x_1 + \frac{\mu_1}{\varepsilon^3} + \frac{\mu_3}{\varepsilon}y_1 - 3\varepsilon x_1^2 y_1,$$

where the prime denotes derivatives with respect to the new time $\tilde{t}$. Now, after some elementary algebra we obtain systems (3.11) and (3.14). □

The phase portrait for Hamiltonian systems (3.12) and (3.15) are shown in Figure 3.1. Note that when $\nu_1 = 0$ we obtain $H_1(x,y) = H_2(x,y)$, and so in that case it is sufficient to study the properties of the Hamiltonian H_2.

Now, we will consider the heteroclinic loop of Hamiltonian (3.12). The Hamiltonian has a pair of heteroclinic connections $\Gamma_{\pm}(t) = (x(t), \mp y(t))$, parameterized by

$$\begin{aligned} x(t) &= \sqrt{-\nu_2}\tanh\left(\sqrt{-\nu_2/2}t\right), \\ y(t) &= \frac{\nu_2}{\sqrt{2}}\operatorname{sech}^2\left(\sqrt{-\nu_2/2}t\right), \end{aligned} \tag{3.16}$$

where $-\infty < t < \infty$ and $\nu_2 < 0$. In the next result, we compute the Melnikov function along the heteroclinic loop Γ_+ for the perturbed Hamiltonian system (3.11), and by using (3.10), we obtain the approximate bifurcation curves for heteroclinic connections for system (3.3).

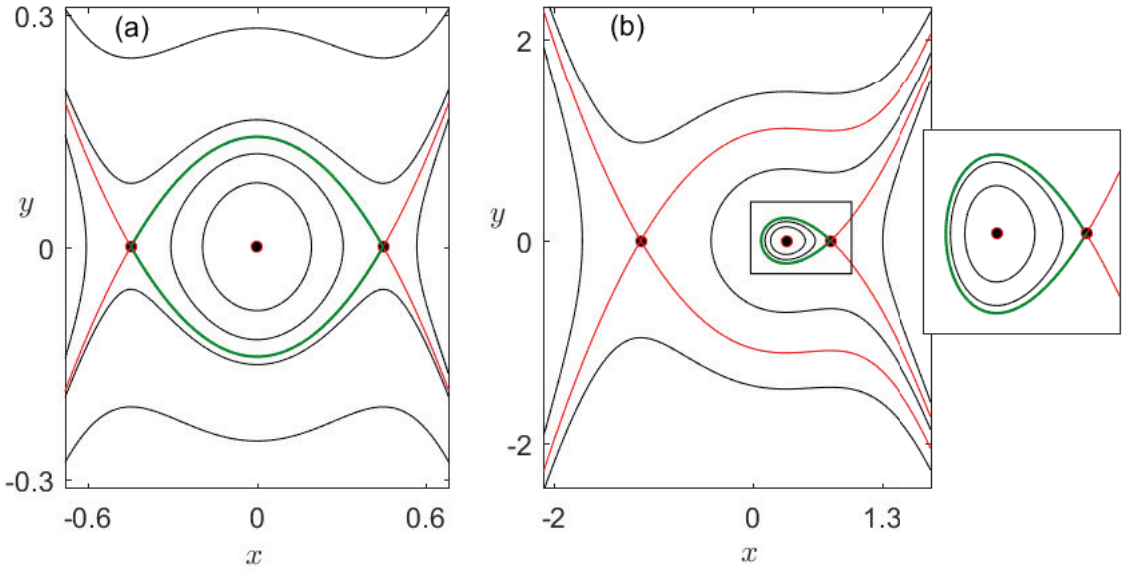

Figure 3.1: (a) Hamiltonian (3.12) with $\nu_2 = -0.2$. In green a heteroclinic orbit, the stable and unstable manifolds of the saddle points are shown in red. (b) Hamiltonian (3.15) with $\nu_1 = 0.3$ and $\nu_2 = -1$. In green a homoclinic orbit, the stable and unstable manifolds of the saddle points are shown in red.

Proposition 27. *If we consider perturbed Hamiltonian system* (3.12) *and* $\overline{\nu} = (\nu_1, \nu_2, \nu_3)$ *with* $\nu_2 < 0$, *then the Melnikov function along of the heteroclinic loop* Γ_+ *is given by*

$$M_{ht}(\overline{\nu}) = -\frac{2}{15}\sqrt{-\nu_2}\left(3\sqrt{2}\nu_2^2 + 5\sqrt{2}\nu_3\nu_2 - 15\nu_1\right) \tag{3.17}$$

Proof. The system can be written as

$$(\dot{x}, \dot{y})^T = f(x, y) + \varepsilon g(x, y),$$

where $f(x, y) = (y, \nu_2 x + x^3)^T$ and $g(x, y) = (0, \nu_1 + \nu_3 y - 3x^2 y)^T$. Thus, we have $f \wedge g = y\,(\nu_1 + \nu_3 y - 3x^2 y)$. Accordingly, the Melnikov function is defined by

$$\begin{aligned} M_{ht}(\overline{\nu}) &= \int_{-\infty}^{\infty} f(x(t), y(t)) \wedge g(x(t), y(t)) dt = \\ &= \int_{-\infty}^{\infty} y(t)\left(\nu_1 + \left(\nu_3 - 3x^2(t)\right) y(t)\right) dt, \end{aligned}$$

where $x(t)$ and $y(t)$ are given in (3.16). After a direct computation we obtain (3.17). □

By using the Menikov theory (see Section 3.2), and by fixing one parameter of system (3.3), we can give an approximation of the heteroclinic connection curves in the remaining parameters plane.

Proposition 28. *Consider system (3.3) with $\mu_3 > 0$ sufficiently small and the parametric plane (μ_2, μ_1). Then the system has a heteroclinic connection at the parameter values on the two curves*

$$\varphi_{ht} = \{(\mu_2, \mu_1) \in \mathbb{R}^2 : \mu_1 = \pm\frac{\sqrt{2}}{15}\mu_2\,(3\mu_2 + 5\mu_3)\,, \quad \mu_2 < -\frac{5}{3}\mu_3\}. \tag{3.18}$$

Moreover, for $\mu_1 = 0$ and $\mu_2 = -(5/3)\mu_3$ the system also has a heteroclinic orbit.

Proof. Fixing $\nu_3 = 1$ in the Melnikov function given in (3.17), and from the equality $M_{ht}(\nu_1, \nu_2) = 0$ we obtain

$$\nu_1 = \frac{\sqrt{2}}{15}\nu_2\,(3\nu_2 + 5)\,.$$

From (3.10) we get $\varepsilon = \mu_3$, $\mu_1 = \mu_3^2\nu_1$ and $\mu_2 = \mu_3\nu_2$, so that

$$\mu_1 = \mu_3^2\nu_1 = \mu_3^2\frac{\sqrt{2}}{15}\frac{\mu_2}{\mu_3}\left(3\frac{\mu_2}{\mu_3} + 5\right) = \frac{\sqrt{2}}{15}\mu_2\,(3\mu_2 + 5\mu_3)\,,$$

and the conclusion follows. □

When $\mu_1 = 0$ and $\mu_3 > 0$ on the parameter plane (μ_2, μ_1), we obtain the point of double heteroclinic connections

$$DHT \equiv (0, -5\mu_3/3)\,. \tag{3.19}$$

Schecter points are co-dimension two points defined by the intersection of a saddle-node curve and a homoclinic or heteroclinic curve, for more details see Schecter [1987]. Taking the intersection points of the saddle-node bifurcation curve and the heteroclinic curves given in (3.7) and (3.18) respectively, we obtain a first-order approximation of Shecter points of the system. Since the system is symmetric with respect to the parameter μ_1, the system has four Schecter points (see Figure 3.3), these points are $\pm S_1$ and $\pm S_2$ where

$$S_1 = \rho\left(\frac{\sqrt{2}}{15}\,(3\rho + 5\mu_3)\,, 1\right), \quad S_2 = \rho\left(-\frac{\sqrt{2}}{15}\,(3\rho + 5\mu_3)\,, 1\right), \tag{3.20}$$

and $\rho = -5/27\left(9\mu_3 - \sqrt{5}\sqrt{18\mu_3 + 5} + 5\right)$.

Now, by using the homoclinic connection of Hamiltonian system (3.15), we compute the associated Melnikov function for system (3.3) when $\nu_3 = 1$.

Proposition 29. *If we consider system (3.14) and $\overline{\nu} = (\nu_1, \nu_2, \nu_3)$ with $\nu_1 > 0$, $\nu_2 < 0$ and $\nu_3 = 1$, then the Melnikov function associated to the homoclinic orbit with connection point $(0, s)$, it is given by*

$$\begin{aligned} M_h(\overline{\nu}) = \sqrt{2}\frac{\cosh^2(\theta)}{\cosh^2(\theta) + 2}(&-660(3\nu_2 + 1)\theta\cosh(\theta) - 60(3\nu_2 + 1)\theta\cosh(3\theta) + \\ &+ 2\sinh(\theta)(729\nu_2 + 4(87\nu_2 + 25)\cosh(2\theta) + (3\nu_2 + 5)\cosh(4\theta) + 255)), \end{aligned} \tag{3.21}$$

and $0 < \theta < \infty$, *with*

$$\cosh\theta = \frac{2s}{\omega}, \quad \omega^2 = -2(s^2 + \nu_2) > 0,$$

being s *the biggest positive root of the equation* $\nu_1 + \nu_2 + x^3 = 0$, *see Figure 3.2.*

Proof. We consider the Hamiltonian system given in (3.15) with $\nu_2 < 0$. From Proposition 24, the system has 3 equilibrium points $\mathbf{x}_i = (s_i, 0)$, where $\mathbf{x}_L$ and $\mathbf{x}_R$ are saddle point and $\mathbf{x}_C$ is a focus or node and

$$s_L < s_C < s_R, \quad s_L + s_C + s_R = 0, \quad s_L s_C s_R = -\nu_1.$$

We study only the case $\nu_1 > 0$, for the case $\nu_1 < 0$ is analogous.
Assuming $\nu_1 > 0$ and $s_R = s > 0$, by Green's Theorem, the homoclinic Melnikov function of system (3.14) can rewritten as

$$M_h(\overline{\nu}) = \int\int_{D(\nu_1,\nu_2)} \left(\frac{-\partial g(x,y)}{\partial y}\right) dA,$$

where D is the region bounded by the homoclinic orbit which joins the equilibrium point $(s, 0)$ to itself. By fixing $\nu_3 = 1$ (that is $\mu_3 > 0$), and taking $p(x) = \nu_1 + \nu_2 x + x^3$, we get $\nu_1 + \nu_2 s + s^3 = 0$, that is

$$\nu_1 = -\left(\nu_2 s + s^3\right) = s(\nu_2 + s^2), \tag{3.22}$$

and so $\nu_2 + s^2 < 0$. Taking the auxiliary function

$$q(x) = -\int_0^x p(x)dx = \nu_1 x - \nu_2 \frac{x^2}{2} - \frac{x^4}{4},$$

and using (3.15), the homoclinic loop is given by the points $(x, y_s^{\pm}(x))$ where $\overline{x} \leq x \leq s$,

$$y_s^{\pm}(x) = \pm\sqrt{2}\sqrt{q(s) - q(x)},$$

and $y_s^{\pm}(\overline{x}) = y_s^{\pm}(s) = 0$, see Figure 3.2. Now, the Melnikov function is thanks to the symmetry of the loop

$$\begin{aligned} M_h(\overline{\nu}) &= 2\int_{\overline{x}}^{s}(1 - 3x^2)dx \int_0^{y_s^+(x)} dy = \\ &= \sqrt{2}\int_{\overline{x}}^{s}(1 - 3x^2)(s - x)\sqrt{(x + s)^2 + 2(s^2 + \nu_2)}dx = \\ &= \sqrt{2}\int_{\overline{x}}^{s}(1 - 3x^2)(s - x)\sqrt{(x + s)^2 - \omega^2}dx, \end{aligned}$$

where from (3.22) $\omega^2 = -2(s^2 + \nu_2) > 0$ and we have used that

$$q(s) - q(x) = \frac{1}{4}(x - s)^2\left((x + s)^2 - \omega^2\right).$$

Taking the change of variable

$$x + s = \omega \cosh\theta,$$

and noting that $q(s) - q(\overline{x}) = 0$ we see that $\overline{x} + s = \omega$, which corresponds to $\theta = 0$, while for $x = s$ the corresponding values of $\theta = \theta_s$ satisfy $\cosh\theta_s = 2s/\omega$, or also $\omega^2 \cosh^2\theta_s = 4s^2$, that is $(s^2 + \nu_2)\cosh^2\theta_s = 2s^2$, and so we get

$$s^2 = \frac{-\cosh^2\theta_s}{2 + \cosh^2\theta_s}\nu_2.$$

Now we arrived to

$$M_h(\overline{\nu}) = \sqrt{2}\omega^2 \int_0^{\theta_s} (1 - 3(\omega\cosh\theta - s)^2)(2s - \omega\cosh\theta)\sinh^2\theta d\theta,$$

and after some computations, we obtain (3.21), where θ_s has been simplified to θ. □

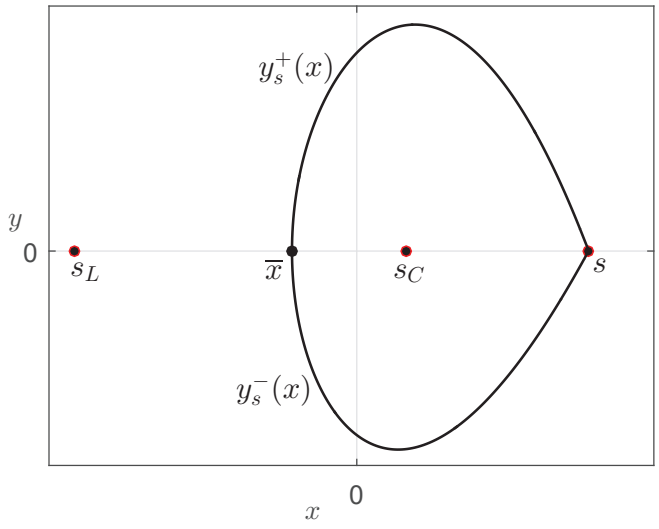

Figure 3.2: Homoclinic orbit which joins a saddle equilibrium point s to itself.

As a direct consequence of the above result, we give an analytical approximation of the bifurcation curves for homoclinic connections of system (3.3).

Proposition 30. *Consider system (3.3) with $\mu_3 > 0$ sufficiently small and the parametric plane (μ_2, μ_1). Then the system has a homoclinic orbit at the curves*

$$\varphi_h = \{(\mu_2, \mu_1) \in \mathbb{R}^2 : \mu_1 = \mu_3\nu_2(\theta), \quad \mu_2 = \pm\mu_3^{3/2}\nu_1(\theta), \quad 0 < \theta < \infty\}, \tag{3.23}$$

where

$$\begin{aligned} \nu_2(\theta) &= \frac{-10(\cosh 2\theta + 5)(9\sinh\theta + \sinh 3\theta - 12\theta\cosh\theta)}{3(370\sinh\theta + 115\sinh 3\theta + \sinh 5\theta - 60\theta(11\cosh\theta + \cosh 3\theta))}, \\ \nu_1(\theta) &= -(\nu_2(\theta)\, s + s^3), \quad s^2 = \frac{-\cosh^2\theta}{2 + \cosh^2\theta}\nu_2(\theta). \end{aligned} \tag{3.24}$$

Proof. the Melnikov function given in (3.21) vanishes at the points $(\nu_1(\theta), \nu_2(\theta))$ defined in (3.24), and from (3.13) the conclusion follows. □

Remark 31. *Note that for $\mu_3 > 0$ it can be obtained that*

$$\lim_{\theta\to\infty} \varphi_h = \left(-\mu_3, \frac{2}{3}\sqrt{\frac{\mu_3^3}{3}}\right) \equiv BT, \quad \lim_{\theta\to 0^+} \varphi_h = (0, -5\mu_3/3) \equiv DHT,$$

where the points BT and DHT are given in (3.9) and (3.19) respectively.

In Figure 3.3, the complete bifurcation set of system (3.3) is shown. Figures 3.4 and 3.5 give the different phase portrait in the labeled parameter regions, where in these figures we show the different configurations of the phase portrait of the system. In Figure 3.4 Menikov function is positive, this fact guarantees the relative position of the stable and unstable varieties of the saddle points

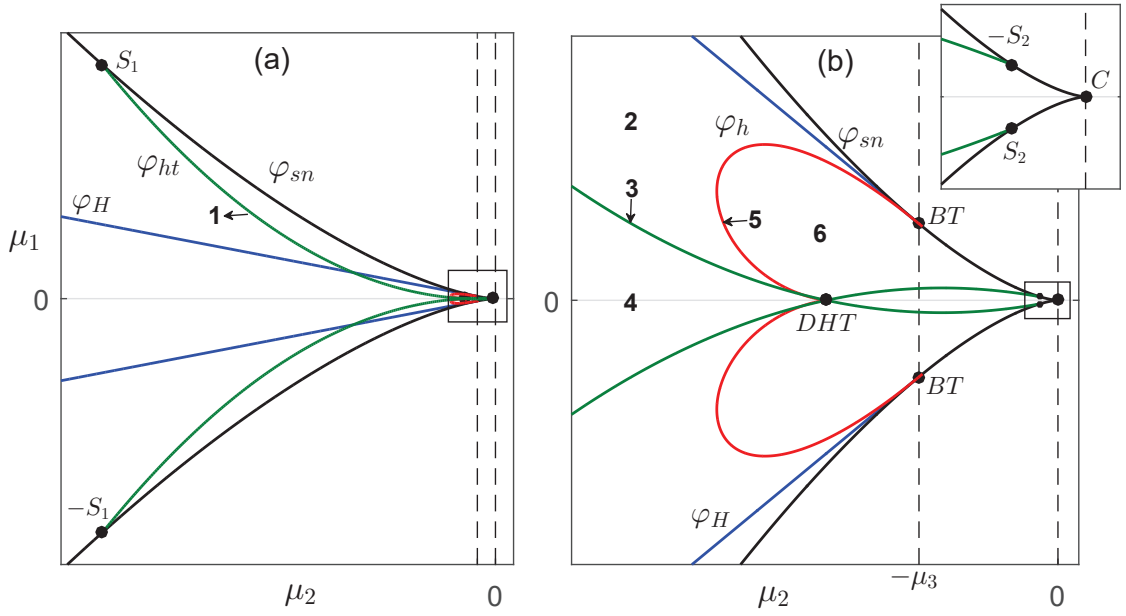

Figure 3.3: The bifurcation diagram of system (3.3), taking $\mu_3 > 0$ sufficiently small.

Remark 32. *If we consider system (3.3) with $\mu_3 > 0$ sufficiently small, then we can assume the existence of a constant $K < -(5/3)\mu_3$ such that, if*

$$|\mu_1| < \left(\frac{\mu_3}{3}\right)^{3/2} + \left(\frac{\mu_3}{3}\right)^{1/2} K,$$

then the system has a stable limit cycle. This assertion is a direct consequence of (3.8) and of the Poincaré-Bendixson Theorem (see for instance Wiggins [2003]), since the sign of the Melnikov function guarantees the existence of a compact positive invariant set with only an unstable equilibrium point in its interior.

By using the shooting method (see for instance Rodríguez-Luis et al. [1990]) and taking $\mu_3 = 0.1$, we show in Figure 3.6, the numerical continuation curve for the homoclinic orbit of system (3.3), and in red the analytic approximation curve given by (3.23).

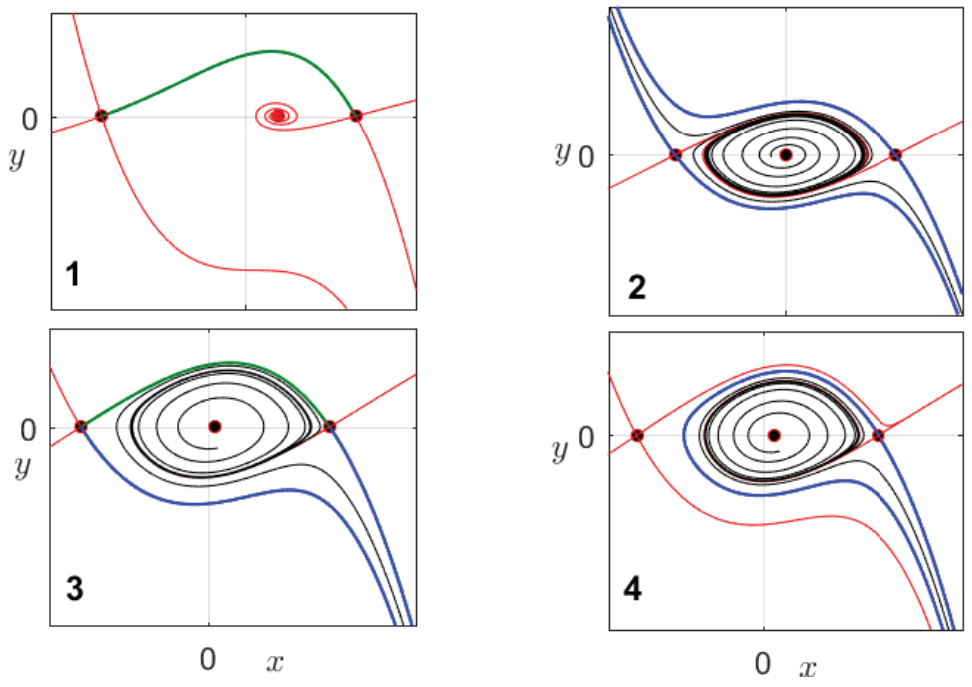

Figure 3.4: Phase portrait of system (3.3) in the parameter regions labeled with **1**,**2**, **3** and **4** in Figure 3.3. The thick lines are the boundary of the basin of attraction of a limit cycle, it is formed by the stable and unstable varieties of the saddle points. The green lines are the heteroclinic connection.

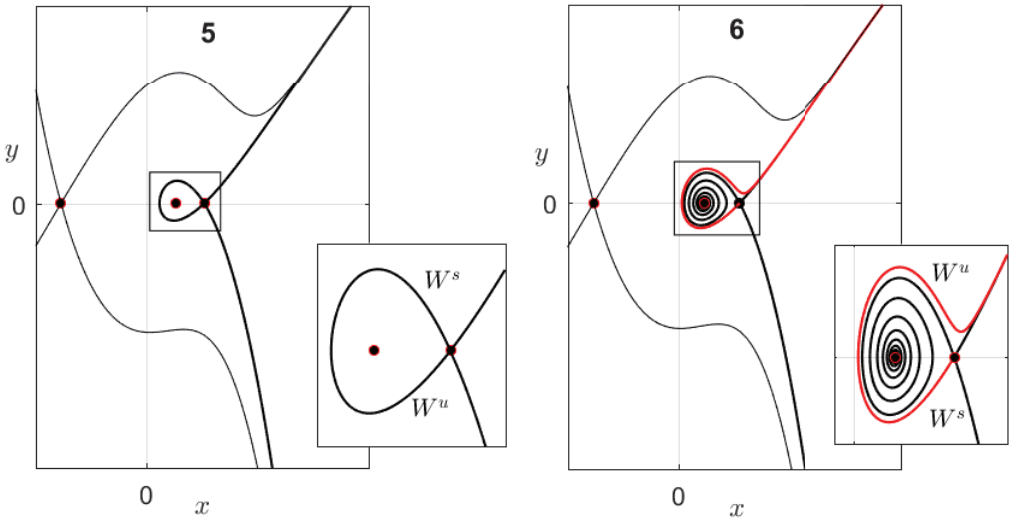

Figure 3.5: Phase portrait of system (3.3) in the parameter regions labeled with **5** and **6** in Figure 3.3. The stable and unstable varieties of the saddle points.

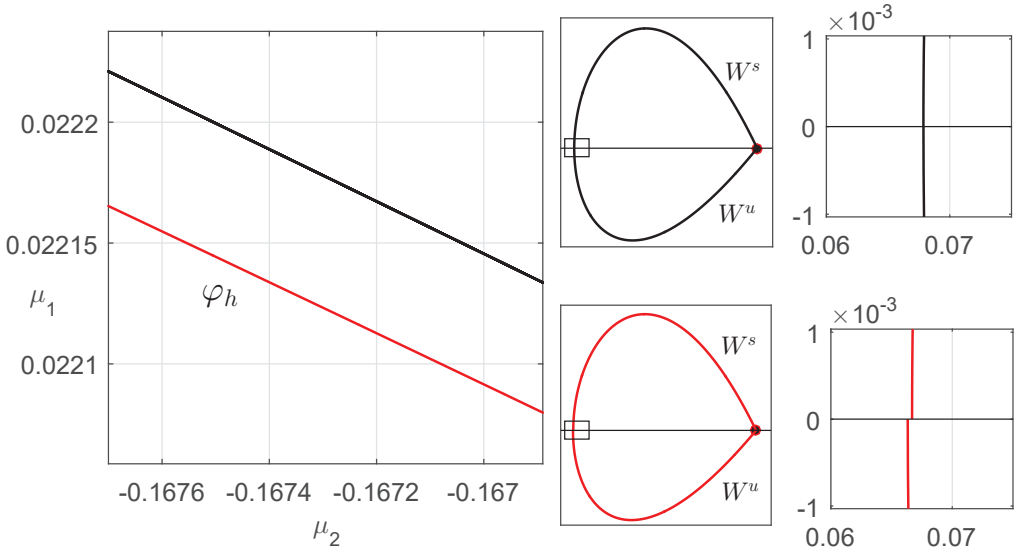

Figure 3.6: System (3.3) with $\mu_3 = 0.1$. In black (left panel), the numerical continuation curve in the parameter plane (μ_2, μ_1), and by using points of the curve, in black (right panel) the numerical computation of the stable and unstable manifold for a saddle point of the system . In red (left panel), the analytic approximation curve given by (3.23), and by using points of the curve, in red (right panel) the numerical computation of the stable and unstable manifold for a saddle point of the system.

3.5 3D Cubic memristor

In this section we consider the function q defined by the following cubic polynomial

$$q(z) = cz^3 + az^2 + bz, \tag{3.25}$$

and the function W defined as in (4.20), that is $W(z) = q'(z) = 3cz^2 + 2az + b$. As a direct consequence of Theorems 8 and 9 given in the Chapter 2, we obtain the next result.

Corollary 33. *Consider system (2.11) with the functions q and W defined as in (3.25)-(4.20). If $a_{12} \neq 0$, then on each invariant set S_h given by*

$$S_h = \{(x, y, z) \in \mathbb{R}^3 : -a_{22}x + a_{12}y + a_{11}a_{22}cz^3 + aa_{11}a_{22}z^2 + (ba_{11}a_{22} - a_{12}a_{21})z = h\}$$

the dynamics is topologically equivalent to the Liénard system

$$\begin{aligned} \dot{x} &= y + ca_{11}x^3 + aa_{11}x^2 + (ba_{11} + a_{22})\, x, \\ \dot{y} &= -a_{11}a_{22}cx^3 - a_{11}a_{22}ax^2 + (a_{12}a_{21} - a_{11}a_{22}b)x + h. \end{aligned} \tag{3.26}$$

Moreover, $(x(\tau), y(\tau)) \in \mathbb{R}^2$ is a solution of the Liénard system (3.26) for a given $h \in \mathbb{R}$, if and only if $E_h(x(\tau), y(\tau)) \in \mathbb{R}^3$ is a solution of system (2.11) on S_h, where $E_h(x(\tau), y(\tau))$ is defined by

$$E_h(X(\tau), Y(\tau)) = \begin{pmatrix} Y(\tau) - F(X(\tau)) \\ \frac{1}{a_{12}}\left[(a_{22}^2 + a_{12}a_{21})Y(\tau) - a_{22}Y(\tau) + h\right] \\ X(\tau) \end{pmatrix}. \tag{3.27}$$

In the next proposition, we show that system (3.26) can be written into the form (3.1).

Proposition 34. *The following statements hold for system (3.26).*

(a) If $a_{22} \neq 0$ and $a_{11}a_{22} < 0$ then the system can be written into the form

$$\dot{x} = y, \quad \dot{y} = \mu_1 + \mu_2 x + cx^3 + \mu_3 y + 3ca_{11}x^2 y. \tag{3.28}$$

where the new parameters μ_1, μ_2 and μ_3 are given by

$$\begin{aligned} \mu_1 &= \frac{27ch + a_{11}a_{22}a(9cb - 2a^2) - 9caa_{12}a_{21}}{27c^2\left(-a_{11}a_{22}\right)^{5/2}}, \\ \mu_2 &= \frac{a_{11}a_{22}(a^2 - 3cb) + 3ca_{12}a_{21}}{3c\left(a_{11}a_{22}\right)^2}, \quad \mu_3 = \frac{a_{11}(a^2 - 3cb) - 3ca_{22}}{3ca_{11}a_{22}}. \end{aligned} \tag{3.29}$$

(b) If $a_{22} = 0$ then the system can be written into the form

$$\dot{x} = y, \quad \dot{y} = \mu_1 + \mu_2 x + \mu_3 y + 3ca_{11}x^2 y, \tag{3.30}$$

where the new parameters μ_1, μ_2 and μ_3 are defined by

$$\mu_1 = h - \frac{aa_{12}a_{21}}{3c}, \quad \mu_2 = a_{12}a_{21}, \quad \mu_3 = ba_{11} - \frac{a^2 a_{11}}{3c}. \tag{3.31}$$

Proof. First, the change of variable

$$u = x + \frac{a}{3c}, \quad v = y + \frac{2}{27}\frac{a^3}{c^2}a_{11} - \frac{1}{3}\frac{a}{c}a_{22} - \frac{1}{3}a\frac{b}{c}a_{11},$$

transforms system (3.26) in

$$\begin{aligned} \dot{u} &= v + ca_{11}u^3 + \lambda_1 u, \\ \dot{v} &= -ca_{11}a_{22}u^3 + \lambda_2 u + \lambda_3, \end{aligned} \tag{3.32}$$

where the new parameters are

$$\begin{aligned} &\lambda_1 = a_{22} + ba_{11} - \frac{1}{3}\frac{a^2}{c}a_{11}, \quad \lambda_2 = a_{12}a_{21} - ba_{11}a_{22} + \frac{1}{3}\frac{a^2}{c}a_{11}a_{22}, \\ &\lambda_3 = h + \frac{1}{3}a\frac{b}{c}a_{11}a_{22} - \frac{1}{3}\frac{a}{c}a_{12}a_{21} - \frac{2}{27}\frac{a^3}{c^2}a_{11}a_{22}. \end{aligned} \tag{3.33}$$

If $a_{11}a_{22} < 0$, the change of variable

$$x = \frac{1}{(-a_{11}a_{22})^{1/2}}u, \quad y = v, \quad \tau = \frac{1}{-a_{11}a_{22}}t,$$

transforms system (3.32)-(3.33) in

$$\begin{aligned} \dot{x} &= \frac{1}{(-a_{11}a_{22})^{3/2}}y + ca_{11}x^3 - \frac{\lambda_1}{a_{11}a_{22}}x, \\ \dot{y} &= \frac{\lambda_3}{-a_{11}a_{22}} + \frac{\lambda_2}{(-a_{11}a_{22})^{1/2}}x + c\left(-a_{11}a_{22}\right)^{3/2}x^3 \end{aligned}$$

and taking into account that

$$\ddot{x} = \frac{1}{(-a_{11}a_{22})^{3/2}}\dot{y} + 3ca_{11}x^2\dot{x} - \frac{\lambda_1}{a_{11}a_{22}}\dot{x},$$

and after some algebra, statement (a) follows.
If $a_{22} = 0$, from system (3.32) and after a direct computation we obtain statement (b). □

3.5.1 Application to the 3D Canonical Memristor Oscillator

In order to apply the results given in the above sections, we consider in system (2.11) the parameters $a_{11} = -1$, $a_{12} = 1$, $a_{21} = -\xi$ and $a_{22} = \beta$, and $c = 1$ at the function (3.25). In Messias et al. [2010], the authors found numerically the existence of multiple oscillations in this system. As a direct consequence of Corollary 33, we get that the system has an infinite number of invariant manifolds S_h defined by

$$S_h = \{(x, y, z) \in \mathbb{R}^3 : -\beta x + y - \beta z^3 - a\beta z^2 + (\xi - b\beta)\, z = h\}, \tag{3.34}$$

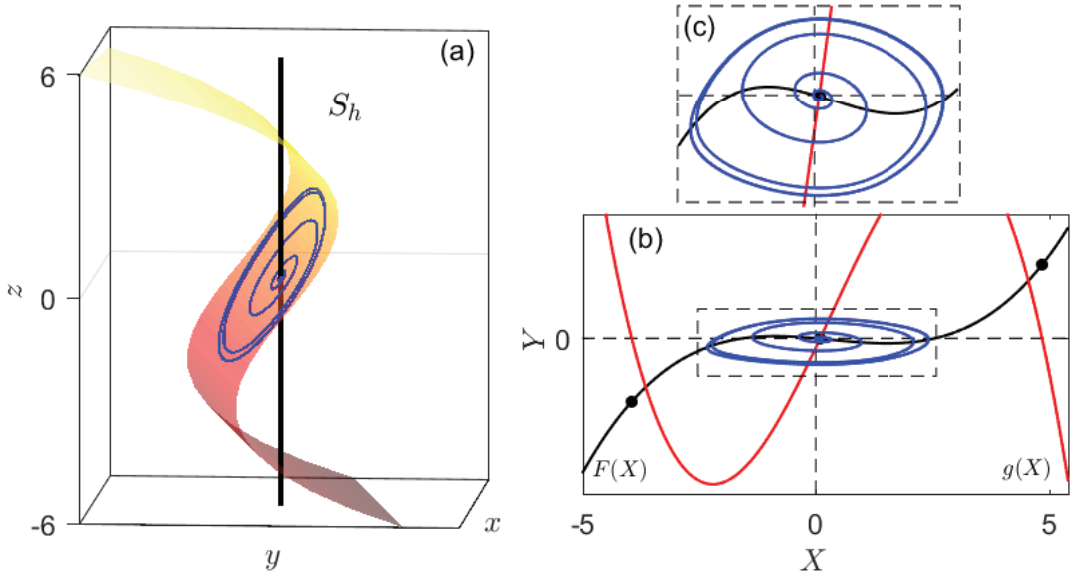

Figure 3.7: (a) The invariant manifold (3.34) corresponding to the set of parameters $\xi = 100$, $a = b = 1$, $\beta = 5$ and $h = 0.3$ is shown. In black the infinite number of equilibrium points of the system and in blue a periodic orbit of the system contained in the invariant manifold. (b) The equivalent Liénard system (3.35) corresponding to the set parameters given in (a) and the periodic orbit in blue, in red the function $g(X)$ and the function $F(X)$ in black. (c) A zoom of figure (b) is shown.

and on each S_h the system is topologically equivalent to the Liénard system

$$\begin{aligned} \dot{x} &= y - x^3 - x^2 - (b-\beta)x, \\ \dot{y} &= \beta x^3 + a\beta x^2 + (b\beta - \xi)\, x + h. \end{aligned} \tag{3.35}$$

In Figure 3.7, we show the invariant manifold (3.34) corresponding to the set of parameters $\xi = 100$, $a = b = 1$, $\beta = 5$ and $h = 0.3$, also the equivalent Liénard system (3.35) is shown. From Proposition 34 (a), the system can be rewritten as

$$\begin{aligned} \dot{x} &= y, \\ \dot{y} &= \mu_1 + \mu_2 x + \mu_3 y + x^3 - 3x^2 y, \end{aligned} \tag{3.36}$$

where the new parameter are

$$\begin{aligned} \mu_1 &= \frac{1}{27\beta^{5/2}}(27h + 9a\xi + 2a^3\beta - 9ab\beta), \\ \mu_2 &= \frac{1}{3\beta^2}\left(\beta(3b - a^2) - 3\xi\right), \quad \mu_3 = \frac{1}{3\beta}\left(a^2 - 3b + 3\beta\right). \end{aligned} \tag{3.37}$$

Now, in the next result we show the existence of a topological sphere in the 3D phase-space completely foliated by periodic orbits.

Proposition 35. *Consider system (2.45) with q defined by $q(z) = z^3 + az^2 + bz$ and $(a^2 - 3b + 3\beta)/(3\beta) > 0$ sufficiently small. Suppose that*

$$0 < 3b - a^2 < \frac{3\xi}{\beta}.$$

Then there exists $K < 0$ with

$$K < (-5/3)(a^2 - 3b + 3\beta) < 0,$$

such that the system has an infinite number of stable periodic orbits; in particular, for any initial condition $(x_0, y_0, z_0) \in \mathbb{R}^3$ with $x_0 \neq 0$ or $y_0 \neq 0$ and

$$\min\{A, B\} < -\beta x_0 - \xi y_0 + \xi z_0 - \beta q(z_0) < \max\{A, B\},$$

where

$$\begin{aligned} A &= \frac{1}{27}\left(a - \sqrt{a^2 - 3b + 3\beta}\right)\left(6b\beta - 9\xi + 3\beta^2 - a^2\beta + a\beta\sqrt{a^2 - 3b + 3\beta}\right) \\ B &= -\frac{1}{27}\left(a + \sqrt{a^2 - 3b + 3\beta}\right)\left(9\xi - 6b\beta - 3\beta^2 + a^2\beta + a\beta\sqrt{a^2 - 3b + 3\beta}\right), \end{aligned} \tag{3.38}$$

the steady state solution is periodic. Moreover, the periodic orbits generate a topological sphere Ω (see Figure 3.8) foliated by such periodic orbits.

Proof. From Remark 32 and (3.37), for $a^2 - 3b + 3\beta > 0$ sufficiently small, there exists

$$K < -(5/3)(a^2 - 3b + 3\beta),$$

such that for all h with

$$\frac{1}{27\beta^{5/2}}|(27h + 9a\xi + 2a^3\beta - 9ab\beta)| < \left(\frac{a^2 - 3b + 3\beta}{3}\right)^{3/2} + \left(\frac{a^2 - 3b + 3\beta}{3}\right)^{1/2} K,$$

the system (3.36)-(3.37) has a stable limit cycle on each S_h given in (3.34), and after a direct computation we obtain (3.38). □

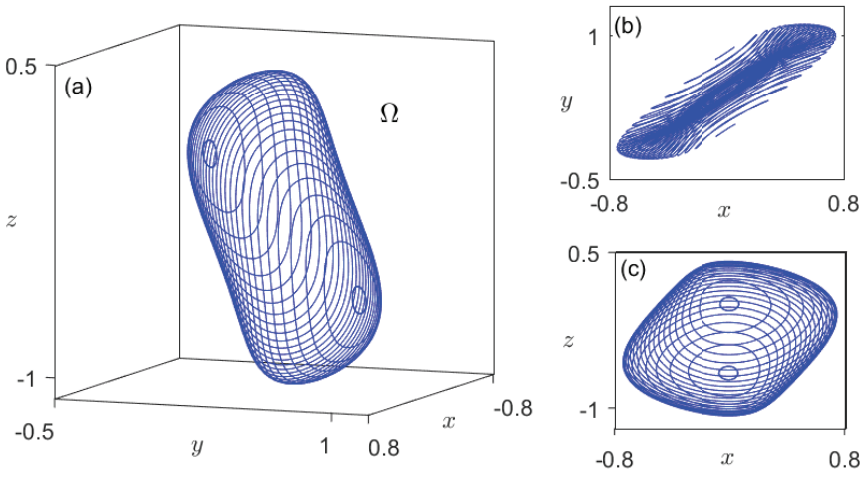

Figure 3.8: (a) Some slices of the surface Ω given by Proposition 35 for system (2.45) with parameters $a = 1, b = 4.8, \beta = 5$ and $\xi = 80$, that is $K = -2.3$, $a^2 - 3b + 3\beta = 0.1$, $A = 4.9$ and $B = -42.97$. (b) Projection of (a) in the plane (x, y). (c) Projection of (a) in the plane (x, z).

3.5.2 Application to a 3D memristor based Van der Pol oscillator

As a second example, we consider the oscillator introduced in section 2.5, that is, we take $a_{11} = 1$, $a_{12} = -1$, $a_{21} = \beta$, $a_{22} = 0$ and the function V is defined as in (2.60). We consider system (2.58) with $q(z) = z^3 + az^2 + bz$, $a^2 - 3b \leq 0$ and the function $W(z) = 3z^2 + 2az + b$, so that $V(z) = (\gamma - W(z)) = \gamma z - q(z)$. Taking into account that $\dfrac{d\overline{q}}{dz} = V(z)$ and after a direct computation we obtain that

$$\overline{q}(z) = -z^3 - az^2 - (b - \gamma)z. \tag{3.39}$$

Therefore, system (2.59) is already in the form (2.11) where $a_{11} = 1, a_{12} = -1, a_{21} = \beta$, $a_{22} = 0$ and the function $\overline{q}$ is defined in (3.39), that is $c = -1$, $a = -a$ and $b = -(b - \gamma)$. From Corollary 33, we obtain that the invariant manifolds S_h are given by

$$S_h = \{(x, y, z) \in \mathbb{R}^3 : -y + \beta z = h\}$$

and on each invariant set S_h the system is the topologically equivalent to the Liénard system

$$\begin{aligned} \dot{x} &= y - x^3 - ax^2 - (b - \gamma)x, \\ \dot{y} &= -\beta x + h. \end{aligned} \tag{3.40}$$

As a direct consequence of Proposition 34 (b), system (3.40) is topologically equivalent to the system

$$\begin{aligned} \dot{x} &= y, \\ \dot{y} &= \mu_1 + \mu_2 x + \mu_3 y + 3x^2 y, \end{aligned} \tag{3.41}$$

where the new parameters μ_1, μ_2 and μ_3 are defined by

$$\mu_1 = h + \frac{a\beta}{3}, \quad \mu_2 = -\beta, \quad \mu_3 = \frac{3b - a^2}{3}. \tag{3.42}$$

The following result is direct, so we omitted your proof.

Proposition 36. *Consider system (3.41) and the set*

$$\varphi_H = \{(\mu_1, \mu_2, \mu_3) : \mu_1^2 = \frac{\mu_2^2 \mu_3}{3},\ \mu_2 < 0,\ \mu_3 > 0.\}.$$

Then the set φ_H represents a Andronov-Hopf bifurcation of codimension one.

Now, in the next result we show the existence of a topological sphere in the 3D phase-space completely foliated by periodic orbits, its demonstration is analogous to the proof of Proposition 35, and so it is omitted.

Proposition 37. *Consider system (2.58) with q defined by $q(z) = z^3 + az^2 + bz$ and $a^2 - 3b < 0$. Suppose that*

$$0 < 3b - a^2 < 3\gamma.$$

Then the system has an infinite number of stable periodic orbits; in particular, for any initial condition $(x_0, y_0, z_0) \in \mathbb{R}^3$ with $x_0 \neq 0$ or $y_0 \neq 0$ and

$$\frac{\beta}{3}\left(-\sqrt{a^2 - 3b + 3\gamma} - a\right) < |\beta z_0 - y_0| < \frac{\beta}{3}\left(\sqrt{a^2 - 3b + 3\gamma} - a\right),$$

the steady state solution is periodic. Moreover, the periodic orbits generate a topological sphere Ω foliated by such periodic orbits.

3.6 False hidden attractors in memristor-based autonomous Duffing oscillator

An attractor is called a hidden attractor if its basin of attraction does not intersect with small neighborhoods of equilibria, otherwise it is called a self-excited attractor, for more details see Kuznetsov et al.-Leonov et al. [2011]. Recently in Varshney et al. [2018a]-Varshney et al. [2018b] was reported the existence of an infinite number of hidden attractors in Memristor-based autonomous Duffing oscillator, where the memristance function is a cubic polynomial.
The memristor based autonomous Duffing oscillator is defined by

$$\begin{aligned} \dot{x} &= y, \\ \dot{y} &= z, \\ \dot{z} &= -\alpha z - M(x)y, \end{aligned} \tag{3.43}$$

where the memristance function M (possibly discontinuous) is defined as

$$M(x) = \frac{d\phi(x)}{dx} \tag{3.44}$$

and ϕ is a continuous function. In the next result, we show that the system has an infinite number of invariant manifolds.

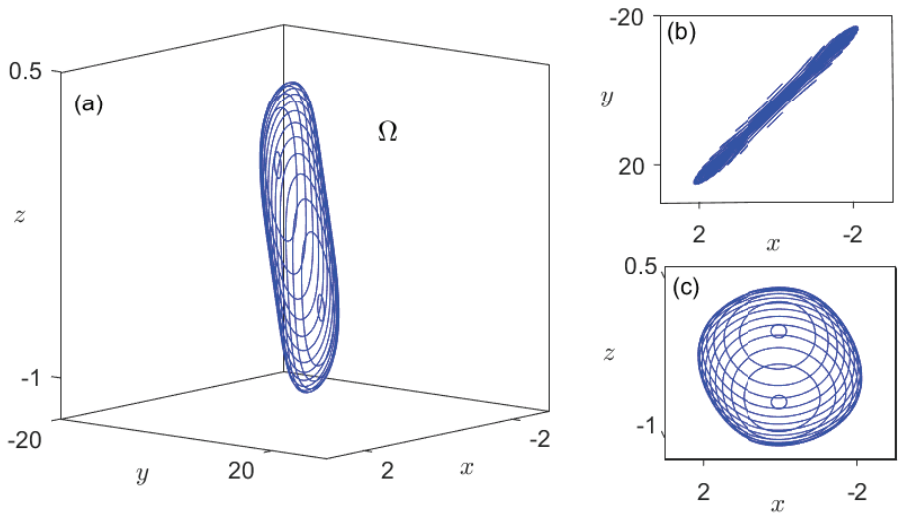

Figure 3.9: (a) Some slices of the surface Ω given by Proposition 37 with parameters $a = 1, b = 7, \beta = 10$ and $\gamma = 7$. (b) Projection of (a) in the plane (x, y). (c) Projection of (a) in the plane (x, z).

Proposition 38. *Consider system (3.43) with the function M defined as in (3.44). For any $h \in \mathbb{R}$ the set*

$$S_h = \{(x, y, z) \in \mathbb{R}^3 \colon H(x, y, z) = h\} \tag{3.45}$$

is an invariant manifold for the system, where we have introduced the continuous function

$$H(x, y, z) = \phi(x) + \alpha y + z. \tag{3.46}$$

Moreover, the system has an infinite number of invariant manifolds foliating the whole $\mathbb{R}^3$, and so the dynamics is essentially two-dimensional.

Proof. Taking H as in (3.44), define for any solution $(x(\tau), y(\tau), z(\tau))$ of (3.43) the auxiliary function

$$h(\tau) = H(x(\tau), y(\tau), z(\tau))$$

Now, a direct computation gives, excepting the points of possible non-differentiability,

$$h'(\tau) = \frac{d\phi(x)}{dx}\dot{x} + \alpha\dot{y} + \dot{z} = M(x)y + \alpha z - \alpha z - M(x)y = 0.$$

Then h is piecewise constant along the orbits of (3.43), but as h is continuous by definition, it should be globally constant. In short, the level sets of H are invariant for the flow. □

Now, by using the above result, we reduce the study of the dynamical behavior of the system, to the study of a planar system.

Proposition 39. *Consider system (3.43) with the function M defined as in (3.44). Then on each invariant set S_h defined in (3.45) the system is topologically equivalent to the planar system*

$$\begin{aligned} \dot{x} &= y, \\ \dot{y} &= -\phi(x) - \alpha y + h. \end{aligned} \tag{3.47}$$

Moreover, $(x(\tau), y(\tau)) \in \mathbb{R}^2$ is a solution of the above system if and only if $E_h(x(\tau), y(\tau))$ is a solution of system (3.43), where

$$E_h(X(\tau), Y(\tau)) = \begin{pmatrix} x(\tau) \\ y(\tau) \\ h - \phi(x(\tau)) - \alpha y(\tau) \end{pmatrix} \tag{3.48}$$

Proof. From Proposition 38 we can solve for z in the equation $H(x, y, z) = h$, and write

$$z = h - \phi(x) - \alpha y.$$

Replacing this expression into the first and second equation of (3.43) we obtain system (3.47). Suppose that $(x(\tau), y(\tau)) \in \mathbb{R}^2$ is a solution of system (3.47). Taking

$$z(\tau) = h - \alpha y(\tau) - \phi(x(\tau))$$

we obtain

$$\begin{aligned} \dot{z}(\tau) &= -\alpha \dot{y}(\tau) - \frac{d\phi(x(\tau))}{dx}\dot{x}(\tau) = -\alpha\left(h - \phi(x(\tau)) - \alpha y(\tau)\right) - M(x(\tau))y(\tau) = \\ &= -\alpha\left(z(\tau)\right) - M(x(\tau))y(\tau). \end{aligned}$$

and the proposition follows. □

In the following result, we show that for $\alpha \neq 0$, the system does not have periodic solutions.

Proposition 40. *Consider system (3.47). The following statements hold.*

(a) For $\alpha = 0$ the system is Hamiltonian.

(b) For $\alpha \neq 0$ the system does not have periodic solutions.

Proof. The divergence of the system is $\Delta = -\alpha$. Then, when $\alpha = 0$ the system corresponds to the Hamiltonian

$$H(x, y) = \frac{y^2}{2} + \phi'(x).$$

For $\alpha \neq 0$ the divergence of system (3.47) does not change sign, thus from Bendixson's criterion Hale [1991], system (3.43) does not have periodic solutions. □

Remark 41. *As a consequence of Proposition 40, the 3D system (3.43) system cannot have periodic orbits for any function ϕ and $\alpha \neq 0$. However, when $\alpha = 0$ the system could have an infinite number of periodic orbits on each invariant set S_h defined in (3.45).*

In Varshney et al. [2018a]-Varshney et al. [2018b] authors consider system (3.43) with the function $\phi(x) = \omega x + \beta x^3$ and set of parameters $\alpha = 0.0001$, $\omega = 0.35$, $\beta = 0.85$. From Propositions 38 and 39, we obtain the invariant manifolds

$$S_h = \{(x, y, z) \in \mathbb{R}^3 \colon \omega x + \beta x^3 + \alpha y + z = h\},$$

and the planar system ruling the dynamics on each S_h given by

$$\dot{x} = y, \quad \dot{y} = -\omega x - \beta x^3 - \alpha y + h.$$

In both quoted references, the authors reported the existence of an infinite number of stable periodic orbits coexisting with an infinite number of stable equilibria, by taking into account several numerical simulations.
From Remark 41 we note that, the system cannot have periodic orbits, and so, the statement made in the quoted papers is false. This show the relevance of having theoretical analysis as the obtained in this work to avoid misconceptions coming only from numerical simulations.

Bibliography

H.J. De Blank, Y. Kuznetsov, M.J. Pekkér, and D.W.M. Veldman. Degenerate Bogdanov-Takens bifurcations in a one-dimensional transport model of a fusion plasma. *Physica D: Nonlinear Phenomena*, 331:13 – 26, 2016. URL https://doi.org/10.1016/j.physd.2016.05.008.

T.R. Blows and L.M. Perko. Bifurcation of limit cycles from centers and separatrix cycles of planar analytic systems. *SIAM Review*, 36(3):341376, 1994. URL https://doi.org/10.1137/1036094.

H. Chen and X. Chen. Dynamical analysis of a cubic liénard system with global parameters. *Nonlinearity*, 28(10):35353562, Apr 2015. URL http://stacks.iop.org/0951-7715/28/i=10/a=3535.

H. Chen and X. Chen. Dynamical analysis of a cubic liénard system with global parameters (ii). *Nonlinearity*, 29(6):1798, 2016. URL http://stacks.iop.org/0951-7715/29/i=6/a=1798.

G. Dangelmayr and J. Guckenheimer. On a four parameter family of planar vector fields. *Archive for Rational Mechanics and Analysis*, 97(4):321352, 1987. URL https://doi.org/10.1007/BF00280410.

A. Dhooge, W. Govaerts, Y. Kuznetsov, H.G.E. Meijer, and B. Sautois. New features of the software matcont for bifurcation analysis of dynamical systems. *Mathematical and Computer Modelling of Dynamical Systems*, 14(2):147175, 2008. URL https://doi.org/10.1080/13873950701742754.

F. Dumortier and C. Li. Perturbations from an elliptic hamiltonian of degree four. *Journal of Differential Equations*, 175(2):209243, 2001. URL https://doi.org/10.1006/jdeq.2000.3977.

F. Dumortier and C. Li. Perturbation from an elliptic Hamiltonian of degree four-III global centre. *Journal of Differential Equations*, 188(2):473511, 2003a. URL https://doi.org/10.1016/S0022-0396(02)00110-9.

F. Dumortier and C. Li. Perturbation from an elliptic Hamiltonian of degree fourIV global centre. *Journal of Differential Equations*, 188(2):512566, 2003b. URL https://doi.org/10.1016/S0022-0396(02)00111-0.

F. Dumortier, R. Roussarie, and J. Sotomayor. Generic 3-parameter families of vector fields on the plane, unfolding a singularity with nilpotent linear part. the cusp case of codimension 3. *Ergodic Theory and Dynamical Systems*, 7(03), 1987. URL https://doi.org/10.1017/S0143385700004119.

Freddy Dumortier. *Bifurcations of planar vector fields: nilpotent singularities and Abelian integrals*. Springer-Verlag, Berlin New York, 1991. ISBN 978-3-540-38433-5. URL https://doi.org/10.1007/BFb0098353.

F. Fernández, E. Freire, L. Pizarro, and A.J. Rodríguez-Luis. Proc NDES 96: 4th workshop on nonlinear dynamics of electronic systems (seville, spain). *ed J.L. Huertas and A.J. Rodrígues-Luis*, page 3216, 1996.

E. Freire, L. Pizarro, and A.J. Rodríguez-Luis. Examples of non-degenerate and degenerate cuspidal loops in planar systems. *Dynamics and Stability of Systems*, 14(2):129161, 1999. URL https://doi.org/10.1080/026811199282038.

E. Freire, L. Pizarro, and A.J. Rodríguez-Luis. Numerical continuation of homoclinic orbits to non-hyperbolic equilibria in planar systems. *Nonlinear Dynamics*, 23(4): 353375, 2000. URL https://doi.org/10.1023/A:1008367531379.

E. Freire, L. Pizarro, A. J. Rodríguez-Luis, and F. Fernández Sánchez. Multiparametric bifurcations in an enzyme-catalyzed reaction model. *International Journal of Bifurcation and Chaos*, 15(3):905947, 2005. URL https://doi.org/10.1142/9789812774569_0012.

J. Guckenheimer and P. Holmes. *Nonlinear oscillations, dynamical systems, and bifurcations of vector field*. Springer-verlag New York Inc., 2013. URL https://www.springer.com/la/book/9780387908199.

J. Guckenheimer, R. Rand, and D. Schlomiuk. Degenerate homoclinic cycles in perturbations of quadratic hamiltonian systems. *Nonlinearity*, 2(3):405, 1989. URL http://stacks.iop.org/0951-7715/2/i=3/a=002.

Jack Hale. *Dynamics and Bifurcations*. Springer New York, New York, NY, 1991. ISBN 978-1-4612-4426-4. URL https://www.springer.com/us/book/9780387971414.

A.I. Khibnik, B. Krauskopf, and C. Rousseau. Global study of a family of cubic lienard equations. *Nonlinearity*, 11(6):1505, 1998. URL http://stacks.iop.org/0951-7715/11/i=6/a=005.

L. Kong and C. Zhu. Bogdanov-takens bifurcations of codimensions 2 and 3 in a Leslie-Gower predator-prey model with michaelis-menten-type prey harvesting. *Mathematical Methods in the Applied Sciences*, 40(18):67156731, Mar 2017. URL https://doi.org/10.1002/mma.4484.

N.V. Kuznetsov, G.A. Leonov, and S.M. Seledzhi. Hidden oscillations in nonlinear control systems. *IFAC Proceedings Volumes*. URL https://doi.org/10.3182/20110828-6-IT-1002.03316.

G.A. Leonov, N.V. Kuznetsov, and V.I. Vagaitsev. Localization of hidden Chua's attractors. *Physics Letters A*, 375(23):2230–2233, jun 2011. URL https://doi.org/10.1016/j.physleta.2011.04.037.

V.K. Melnikov. On the stability of a center for time-periodic perturbations. *Trans. Moscow Math*, 12:1–57, 1963. URL https://www.amazon.com/Transactions-Moscow-Mathematical-Sciety-Volume/dp/B000KNCUF0.

M. Messias, C. Nespoli, and V.A. Botta. Hopf bifurcation from lines of equilibria without parameters in memristor oscillators. *International Journal of Bifurcation and Chaos*, 20(02):437–450, feb 2010. URL https://doi.org/10.1142/s0218127410025521.

A.J. Rodríguez-Luis, E. Freire, and E. Ponce. A method for homoclinic and heteroclinic continuation in two and three dimensions. *Continuation and Bifurcations: Numerical Techniques and Applications, Springer Netherlands*, pages 197–210, 1990. URL https://doi.org/10.1007/978-94-009-0659-4_13.

S. Schecter. The saddle-node separatrix-loop bifurcation. *SIAM Journal on Mathematical Analysis*, 18(4):11421156, 1987. URL https://doi.org/10.1137/0518083.

V. Varshney, S. Sabarathinam, A. Prasad, and K. Thamilmaran. Infinite number of hidden attractors in memristor-based autonomous duffing oscillator. *International Journal of Bifurcation and Chaos*, 28(01):1850013, 2018a. URL https://doi.org/10.1142/S021812741850013X.

V. Varshney, S. Sabarathinam, K. Thamilmaran, M.D. Shrimali, and A. Prasad. Existence and control of hidden oscillations in a memristive autonomous duffing oscillator. *Nonlinear Dynamical Systems with Self-Excited and Hidden Attractors Studies in Systems, Decision and Control*, page 327344, 2018b. URL https://doi.org/10.1007/978-3-319-71243-7_14.

Stephen Wiggins. *Introduction to applied nonlinear dynamical systems and chaos*. Springer, 2003. URL https://www.springer.com/us/book/9780387001777.

V. Witte, W. Govaerts, Y. Kuznetsov, and M. Friedman. Interactive initialization and continuation of homoclinic and heteroclinic orbits in MATLAB. *ACM Transactions on Mathematical Software*, 38(3):134, Jan 2012. URL https://doi.org/10.1145/2168773.2168776.

Chapter 4

A multiple FCC bifurcation in 4D memristor oscillators

In this chapter, we focus our analysis in the existence of multiple stable oscillations in the 4D piecewise linear version of the canonical circuit proposed in Itoh and Chua [2008]. This oscillator is modeled by a discontinuous piecewise linear dynamical system.

By adding one parameter that stratifies the 4D dynamics, it is shown that the dynamics in each stratum is topologically equivalent to a 3D continuous piecewise linear dynamical system. Some previous results on bifurcations in such reduced system, allow to detect rigorously for the first time a multiple focus-center-cycle bifurcation in a three-parameter space, leading to the appearance of a topological sphere in the original model, completely foliated by stable periodic orbits.

4.1 PWL systems of dimension n with 2 and 3 zones

In this section, we start with a review of some basic concepts of continuous piecewise linear systems of dimension n. This material is a new elaboration of some results given in Vela [2013].

A differential equation $\dot{\mathbf{x}} = F(\mathbf{x})$ with $\mathbf{x} = (x_1, x_2, \ldots, x_n)^T$ is said to be a 3PWL$_n$ (3 zones, dimension n) system if there exist three vectors $\mathbf{b}_L, \mathbf{b}_C, \mathbf{b}_R$ and three matrices $A_L, A_C, A_R \in M_n(\mathbb{R})$ so that

$$\dot{\mathbf{x}} = F(\mathbf{x}) = \begin{cases} A_L\mathbf{x} + \mathbf{b}_L, & \text{if } \mathbf{e}_1^T\mathbf{x} < -1, \\ A_C\mathbf{x} + \mathbf{b}_C, & \text{if } |\mathbf{e}_1^T\mathbf{x}| \leq 1, \\ A_R\mathbf{x} + \mathbf{b}_R, & \text{if } \mathbf{e}_1^T\mathbf{x} > 1. \end{cases} \tag{4.1}$$

where $\mathbf{e}_1$ is the first canonical vector. If the vector field F is continuous, we have a 3CPWL$_n$ system, that is, for all $\mathbf{x} \in \mathbb{R}^n$ such that $\mathbf{e}_1^T\mathbf{x} = -1$, we have

$$A_L\mathbf{x} + \mathbf{b}_L = A_C\mathbf{x} + \mathbf{b}_C,$$

and for all $\mathbf{x} \in \mathbb{R}^n$ such that $\mathbf{e}_1^T\mathbf{x} = 1$, we get

$$A_C\mathbf{x} + \mathbf{b}_C = A_R\mathbf{x} + \mathbf{b}_R.$$

If the vector field F is discontinuous, we have a 3DPWL$_n$. When the matrices of the external regions are equal, that is $A_L = A_R$, the system is called a quasi-symmetrical 3PWL$_n$ system, and then we use the notation A_E for such common matrix.

In some control and electronic engineering applications, it is usual to have a single nonlinearity, possible appearing in several components of the vector field; then such systems are called Luré systems Afanasiev et al. [1996]. For continuous vector fields, a sufficient condition to have a Luré system is given below.

Proposition 42. *The matrices A_j, with $j \in \{L, C, R\}$ given in (4.1), when the vector field F is continuous, share the last $n-1$ columns. Furthermore, if we assume that there exists a linear dependence between the first columns of matrices $A_C - A_L$ and $A_R - A_C$, then there exist a matrix $A \in M_n(\mathbb{R})$, vectors $\mathbf{b}, \mathbf{c} \in \mathbb{R}^n$, and a continuous piecewise linear function φ, such that system (4.1) can be written in Luré form*

$$\dot{\mathbf{x}} = A\mathbf{x} + \mathbf{b}\varphi\left(\mathbf{e}_1^T\mathbf{x}\right) + \mathbf{c}. \tag{4.2}$$

Proof. First, the continuity of the vector field F assures that

$$\begin{aligned} A_L(-\mathbf{e}_1 + \mu\mathbf{e}_k) + \mathbf{b}_L &= A_C(-\mathbf{e}_1 + \mu\mathbf{e}_k) + \mathbf{b}_C, \\ A_C(-\mathbf{e}_1 + \mu\mathbf{e}_k) + \mathbf{b}_C &= A_R(-\mathbf{e}_1 + \mu\mathbf{e}_k) + \mathbf{b}_R, \end{aligned} \tag{4.3}$$

for all $\mu \in \mathbb{R}$ and $2 \leq k \leq n$. Taking $\mu = 0$ we obtain

$$\mathbf{b}_C = \mathbf{b}_L + (A_C - A_L)\mathbf{e}_1, \quad \mathbf{b}_R = \mathbf{b}_C - (A_R - A_C)\mathbf{e}_1,$$

and from (4.3) we have for $2 \leq k \leq n$ the equalities

$$A_L\mathbf{e}_k = A_C\mathbf{e}_k = A_R\mathbf{e}_k.$$

Thus, the three matrices have in common the last $n-1$ columns. As consequence, we get

$$A_C = A_L + (A_C - A_L)\mathbf{e}_1\mathbf{e}_1^T, \quad A_R = A_C + (A_R - A_C)\mathbf{e}_1\mathbf{e}_1^T,$$

and substituting $\mathbf{e}_1^T\mathbf{x} = x_1$, we obtain

$$\begin{aligned} A_C\mathbf{x} + \mathbf{b}_C &= \left(A_L + (A_C - A_L)\mathbf{e}_1\mathbf{e}_1^T\right)\mathbf{x} + \mathbf{b}_L + (A_C - A_L)\mathbf{e}_1 = \\ &= A_L\mathbf{x} + (A_C - A_L)\mathbf{e}_1 x_1 + \mathbf{b}_L + (A_C - A_L)\mathbf{e}_1 = \\ &= A_L\mathbf{x} + (A_C - A_L)\mathbf{e}_1\,(x_1 + 1) + \mathbf{b}_L, \end{aligned}$$

and similarly

$$\begin{aligned} A_R\mathbf{x} + \mathbf{b}_R &= A_C\mathbf{x} + (A_R - A_C)\mathbf{e}_1\mathbf{e}_1^T\mathbf{x} + \mathbf{b}_C - (A_R - A_C)\mathbf{e}_1 = \\ &= A_L\mathbf{x} + (A_C - A_L)\mathbf{e}_1\,(x_1 + 1) + (A_R - A_C)\mathbf{e}_1\,(x_1 - 1) + \mathbf{b}_L. \end{aligned}$$

Introducing the ramp function

$$\varphi_\delta(x) = \begin{cases} 0, & \text{if} \quad 0 \leq \delta, \\ x - \delta, & \text{if} \quad x > \delta, \end{cases}$$

we can rewrite the system into the form

$$\dot{\mathbf{x}} = A_L\mathbf{x} + (A_C - A_L)\mathbf{e}_1\varphi_{-1}(x_1) + (A_R - A_C)\mathbf{e}_1\varphi_1(x_1) + \mathbf{b}_L. \tag{4.4}$$

Under the conditional hypothesis, there exists a linear dependence between the first columns of matrices $A_C - A_L$ and $A_R - A_C$, so that

$$\mu_1(A_C - A_L)\mathbf{e}_1 + \mu_2(A_R - A_C)\mathbf{e}_1 = 0,$$

there exist a vector b and constants b_1 and b_2 such that

$$(A_C - A_L)\,\mathbf{e}_1 = b_1\mathbf{b}, \quad (A_R - A_C)\mathbf{e}_1 = b_2\mathbf{b}, \tag{4.5}$$

and then (4.4) becomes

$$\dot{\mathbf{x}} = A_L\mathbf{x} + \mathbf{b}\,(b_1\varphi_{-1}(x_1) + b_2\varphi_1(x_1)) + \mathbf{b}_L.$$

Finally, taking $A = A_L$, $\mathbf{c} = \mathbf{b}_L$ and

$$\varphi(x) = b_1\varphi_{-1}(x) + b_2\varphi_1(x),$$

we obtain system (4.2). □

As a direct consequence of Proposition 42, we get some specific cases of systems with only two or three zones.

Proposition 43. *Consider system (4.2). The following statements hold.*

(a) If either $A_L = A_C$ or $A_C = A_R$, that is, for a 2PWL$_n$ system, the function φ can be taken as follows (ramp function)

$$\varphi(v) = \begin{cases} 0, & \text{if} \quad v \le 0, \\ v, & \text{if} \quad v > 0. \end{cases} \tag{4.6}$$

(b) If $A_E = A_L = A_R$, that is, the system is a quasi-symmetrical 3PWL$_n$, then the system can be written into the form

$$\dot{\mathbf{x}} = A_E\mathbf{x} + (A_C - A_E)\,\mathbf{e}_1\mathrm{sat}\left(\mathbf{e}_1^T\mathbf{x}\right) + \mathbf{b}_C, \tag{4.7}$$

where $\mathrm{sat}\,(x)$ *is the normalized saturation function given by*

$$\mathrm{sat}\,(x) = \begin{cases} x & \text{if} \quad |x| \le 1, \\ \mathrm{sgn}(x) & \text{if} \quad |x| > 1. \end{cases}$$

Proof. If $A_L = A_C$, from (4.4) we get $\dot{\mathbf{x}} = A_L\mathbf{x} + (A_R - A_C)\mathbf{e}_1\varphi_1(x_1) + \mathbf{b}_L$, and after to adequate translation in the variable x_1 we obtain the function φ defined as in (4.6). Analogously, we can proceed for $A_C = A_R$, and the statement (a) follows. If $A_E = A_L = A_R$ we have from (4.4) and (4.5), $b_1 = -b_2 = 1$ and

$$\begin{aligned} \dot{\mathbf{x}} &= A_E\mathbf{x} + (A_C - A_E)\mathbf{e}_1\varphi_{-1}(x_1) + (A_E - A_C)\mathbf{e}_1\varphi_1(x_1) + \mathbf{b}_L = \\ &= A_E\mathbf{x} + (A_C - A_E)\mathbf{e}_1\,(\varphi_{-1}(x_1) - \varphi_1(x_1)) + \mathbf{b}_L, \end{aligned}$$

taking into account the identities

$$\begin{aligned} \text{sat}\,(x) &= \varphi_{-1}(x) - \varphi_1(x) - 1, \\ \mathbf{b}_C &= \mathbf{b}_L + (A_C - A_E)\mathbf{e}_1, \end{aligned}$$

we obtain

$$\begin{aligned} \dot{\mathbf{x}} &= A_E\mathbf{x} + (A_C - A_E)\mathbf{e}_1\left(\varphi_{-1}(x_1) - \varphi_1(x_1)\right) + \mathbf{b}_L = \\ &= A_E\mathbf{x} + (A_C - A_E)\mathbf{e}_1\left(\varphi_{-1}(x_1) - \varphi_1(x_1) - 1 + 1\right) + \mathbf{b}_L = \\ &= A_E\mathbf{x} + (A_C - A_E)\mathbf{e}_1\left(\text{sat}\,(x) + 1\right) + \mathbf{b}_L = \\ &= A_E\mathbf{x} + (A_C - A_E)\mathbf{e}_1\text{sat}\,(x) + \mathbf{b}_C, \end{aligned}$$

and the conclusion follows. □

4.2 The Focus-Center-Limit Cycle bifurcation in $\mathbb{R}^3$

In this section, we rewrite two known results regarding a mechanism for the generation of limit cycles in piecewise linear systems in $\mathbb{R}^3$, see Freire et al. [2005] and Carmona et al. [2005a], for the sake of completeness and to facilitate its application below. These theorems describes a codimension-one bifurcation analogous to the Hopf bifurcation of differentiable dynamics, in two cases, namely, in 3D PWL systems with two zones (2CPLW$_3$) and in 3D symmetrical PWL systems with 3 zones (3CPWL$_3$).

We consider the parameters t_E, m_E, d_E and t_C, m_C, d_C as the linear invariants (trace, sum of principal minors and determinant) of the matrices A_E and A_C, respectively. For the critical value $\varepsilon = m_C t_C - d_C$ with $m_C > 0$, system (4.2) has a linear center in the central zone; that is, the matrix A_C has a pair of pure imaginary eigenvalues. In the next theorem we consider systems with two zones (see Figure 4.1).

Theorem 44. *Freire et al. [2005] Consider a continuous system (4.1) with $\mathbf{b}_C = 0$ and $A_L = A_C$ (so that $A_E = A_R$ and the only separation plane is $x_1 = 1$) or $A_C = A_R$ (so that $A_E = A_L$ and the only separation plane is $x_1 = -1$) that is, the system is $2CPWL_3$. Assume that $m_C > 0$, $\varepsilon = m_C t_C - d_C$ and define the non-degeneracy parameter*

$$\rho = d_C m_C - d_C m_E + d_E m_C - m_C^2 t_E.$$

Then, for $\rho \neq 0$ and $\varepsilon = 0$ the system undergoes a focus-center-limit cycle bifurcation; that is, from the lineal center configuration in the central zone, which exists for $\varepsilon = 0$, one limit cycle appears for $\varepsilon\rho > 0$ and ε sufficiently small. The peek-to-peek amplitude a (measured for x_1), the period P_{er}, and the logarithms of characteristic

multiplier μ_r and μ_a of the periodic orbit are analytic functions at 0, in the variable $\varepsilon^{1/3}$; namely

$$a = 2 + \frac{(12\pi)^{2/3} m_C^{4/3}}{4\rho^{2/3}}\varepsilon^{2/3} + \frac{\pi m_C^{1/2}\xi}{2\rho(d_C^2 + m_C^3)\tanh\left(\frac{\pi d_C}{2m_C^{3/2}}\right)}\varepsilon + O(\varepsilon)^{4/3},$$

$$P_{er} = \frac{2\pi}{\sqrt{m_C}} + \frac{\pi(m_C - m_E)\sqrt{m_C}}{\rho}\varepsilon + \frac{12^{2/3}\pi^{5/3} m_C^{5/6} P_5}{10\rho^{8/3}}(d_C - m_C t_E)$$
$$\cdot ((d_E - m_C t_E)^2 + m_C(m_C - m_E)^2)\varepsilon^{5/3} + O(\varepsilon)^2,$$

$$\mu_r = -\frac{(12\pi)^{1/3} m_C^{7/6}\rho^{2/3}}{d_C^2 + m_C^3}\varepsilon^{1/3} + O(\varepsilon)^{1/3} + \frac{m_C}{2(d_C^2 + m_C^3)^2\tanh\left(\frac{\pi d_C}{m_C^{3/2}}\right)}\varepsilon^{2/3} + O(\varepsilon),$$

$$\mu_a = \frac{2\pi d_C}{m_C^{3/2}} + \frac{(12\pi)^{1/3}\xi}{m^{5/6}(d_C^2 + m_C^3)\rho^{1/3}}\varepsilon^{1/3} - \frac{m^{1/3}\xi\rho^{1/3}}{2(d_C^2 + m_C^3)^2\tanh\left(\frac{\pi d_C}{m_C^{3/2}}\right)}\varepsilon^{2/3} + O(\varepsilon),$$

where

$$\xi = d_C^2(m_C t_E - d_C) + m_E^2(d_E m_C - d_C m_E).$$

In particular, if $\rho > 0$ and $d_C < 0$, then the limit cycle bifurcates for $\varepsilon > 0$ and is orbitally asymptotically stable. Otherwise, if $\rho < 0$ or $d_C > 0$ the bifurcating limit cycle is unstable, being completely unstable when both inequalities hold.

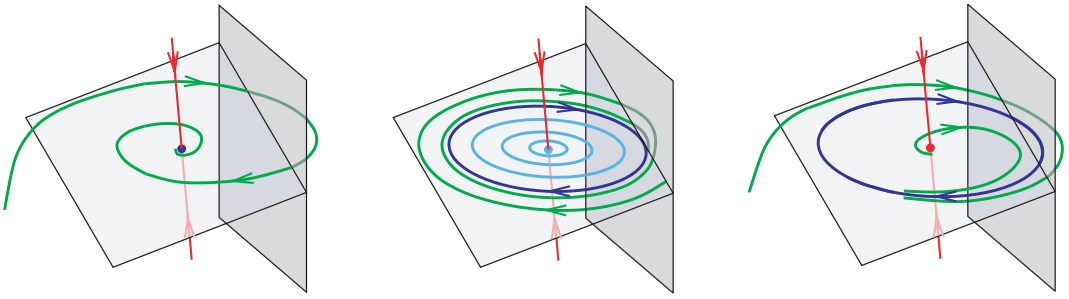

Figure 4.1: The focus-center-limit cycle bifurcation in the case $d_C < 0$ and $\rho > 0$. The focal plane and the complementary one-dimensional invariant manifold at the origin are shown, along with the plane which separates the two linear regions. Taking into account Theorem 44; the left panel correspond with the case $\varepsilon < 0$, the central panel is the case $\varepsilon = 0$ and the right panel is the case $\varepsilon > 0$. Figure used with permission, taken from Vela [2013]

Next, systems with three zones (see Figure 4.2) are studied in the following theorem.

Theorem 45. *Carmona et al. [2005a] Consider a continuous system (4.1) with* $\mathbf{b}_L = -\mathbf{b}_R$, $\mathbf{b}_C = 0$ *and* $A_E = A_L = A_R$, *that is, the system is a symmetrical 3CPWL*$_3$. *Assume that* $m_C > 0$, $\varepsilon = m_C t_C - d_C$ *and the non-degeneracy parameter*

$$\rho = d_C m_C - d_C m_E + d_E m_C - m_C^2 t_E.$$

Then, for $\rho \neq 0$ *and* $\varepsilon = 0$ *the system undergoes a focus-center-limit cycle bifurcation; that is, from the lineal center configuration in the central zone, which exists for* $\varepsilon = 0$, *one limit cycle appears for* $\varepsilon\rho > 0$ *and* ε *sufficiently small.*
The amplitude a (mesured as as the maximum of $|x_1|$*), the period* P_{er}, *and the logarithms of characteristic multiplier* μ_r *and* μ_a *of the periodic orbit are analytic functions at* 0, *in the variable* $\varepsilon^{1/3}$; *namely*

$$a = 1 + \frac{(6\pi)^{2/3} m_C^{4/3}}{8\rho}\varepsilon^{2/3} + \frac{(6\pi^4)^{1/3} a_4}{960 m_C^{1/3}\rho^{7/3}}\varepsilon^{4/3} + O(\varepsilon)^{5/3},$$

$$P_{er} = \frac{2\pi}{\sqrt{m_C}} + \frac{\pi(m_C - m_E)\sqrt{m_C}}{\rho}\varepsilon - \frac{6^{2/3}\pi^{5/3} m_C^{5/6} P_5}{20\rho^{8/3}}\varepsilon^{5/3} + O(\varepsilon)^2,$$

$$\mu_r = -\frac{(48\pi)^{1/3} m_C^{7/6}\rho^{2/3}}{d_C^2 + m_C^3}\varepsilon^{1/3} + O(\varepsilon)^{2/3},$$

$$\mu_a = \frac{2\pi d_C}{m_C^{3/2}} + \frac{(48\pi)^{1/3}}{m_C^{5/6}}\left(\frac{m_C t_E - d_C}{\rho^{1/3}} + \frac{m_C^2\rho^{2/3}}{d_C^2 + m_C^3}\right)\varepsilon^{1/3} + O(\varepsilon)^{2/3},$$

where

$$\begin{aligned} a_4 = {} & -120 t_E m_C^5 + (120 d_C + 2t_E^3 + 21 m_E t_E + 72 d_E) m_C^4 \\ & + (-(93 m_E + 27 t_E^2) d_C + (27 m_E - 2 t_E^2) d_E) m_C^3 + (2t^2 m_E + 25 d_E t_E - 27 m_E^2) d_C m_C^2 \\ & + (25 d_C^3 + 23(m_E t_E - d_E) d_C^2) m_C - 25 m_E d_C^3, \end{aligned}$$

$$P_5 = (m_C(m_C - m_E)^2 + (m_C t_E - d_E)^2)(m_C t_E - d_C).$$

In particular, if $\rho > 0$ *and* $d_C < 0$, *then the limit cycle bifurcates for* $\varepsilon > 0$ *and is orbitally asymptotically stable. Otherwise, if* $\rho < 0$ *or* $d_C > 0$ *the bifurcating limit cycle is unstable, being completely unstable when both inequalities hold.*

4.3 The dissipativeness property

In this section, we give our first result regarding quasi-symmetric 3CPWL$_3$ systems defined as in (4.7). In the important case that the matrix A_E is Hurwitz, system (4.7) have a dissipativeness property in the following sense. The following result has already been shown in dimension 2 (see Proposition 3.13.2 of Llibre and Teruel [2014]) but we include here an extended version of such result and an improved version of its proof.

Proposition 46. *Consider system (4.7). If the matrix* A_E *is Hurwitz, then all solutions are bounded.*

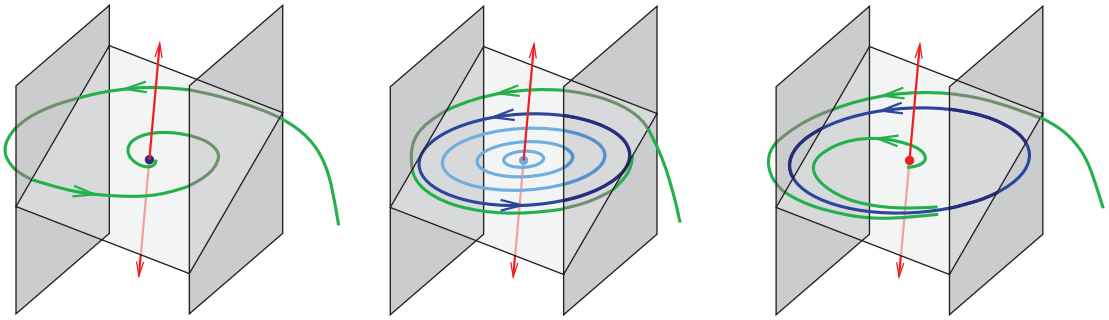

Figure 4.2: The focus-center-limit cycle bifurcation in the case $d_C < 0$ and $\rho > 0$. The focal plane and the complementary one-dimensional invariant manifold at the origin are shown, along with the two parallel planes which separate the three linear regions. Taking into account Theorem 45; the left panel correspond with the case $\varepsilon < 0$, the central panel is the case $\varepsilon = 0$ and the right panel is the case $\varepsilon > 0$. Figure used with permission, taken from Vela [2013].

Proof. The change of variables $\tilde{\mathbf{x}} = \mathbf{x} - \mathbf{x}^*$ where $\mathbf{x}^* = -A_E^{-1}\mathbf{b}_C$, transforms system (4.7) into the form $\dot{\mathbf{x}} = A_E\mathbf{x} + \varphi(\mathbf{e}_1^T\mathbf{x})\mathbf{b}$, where the tildes have been removed, the vector $\mathbf{b} = (A_C - A_E)\mathbf{e}_1$, the function φ is continuous and given by

$$\varphi(x) = \begin{cases} 1 & \text{if} \quad x > 1 + \mathbf{e}_1^T\mathbf{x}^*, \\ x & \text{if} \quad |x - \mathbf{e}_1^T\mathbf{x}^*| \leq 1, \\ -1 & \text{if} \quad x < -1 + \mathbf{e}_1^T\mathbf{x}^*, \end{cases}$$

so that we have $|\varphi(x)| \leq 1$. Since the matrix A_E is Hurwitz, there exist positive constants M and γ such that, for any $s > 0$ we get $\left\|e^{sA_E}\right\| \leq Me^{-\gamma s}$. Finally, for any solution $\mathbf{x}(t)$ we get

$$\mathbf{x}(t) = \mathbf{e}^{tA_E}\mathbf{x}(0) + \int_0^t \varphi(\mathbf{e}_1^T\mathbf{x}(r))\mathbf{e}^{(t-r)A_E}\mathbf{b}dr,$$

and taking norms, we obtain

$$\begin{aligned} \|\mathbf{x}(t)\| &\leq \left\|\mathbf{e}^{tA_E}\right\| \|\mathbf{x}(0)\| + \|\mathbf{b}\| \int_0^t \left|\varphi(\mathbf{e}_1^T\mathbf{x}(r))\right| \left\|\mathbf{e}^{(t-r)A_E}\right\| dr \leq \\ &\leq Me^{-\gamma t}\|\mathbf{x}(0)\| + \|\mathbf{b}\| M \int_0^t e^{-\gamma(t-r)}dr = \\ &= M\left(e^{-\gamma t}\|\mathbf{x}(0)\| + \|\mathbf{b}\|\frac{1}{\gamma}\left(1 - e^{-t\gamma}\right)\right) < M\left(\|\mathbf{x}(0)\| + \|\mathbf{b}\|\frac{1}{\gamma}\right), \end{aligned}$$

so that, for all $t > 0$ the solution $\mathbf{x}(t)$ is contained in the ball of radius

$$M\left(\|\mathbf{x}(0)\| + \|(A_C - A_E)\mathbf{e}_1\|\gamma^{-1}\right)$$

and the proposition follows. □

4.4 Stability of equilibria

Consider the sets $\mathbf{\Sigma}_L = \left\{\mathbf{x} \in \mathbb{R}^3 : \mathbf{e}_1^T\mathbf{x} < -1\right\}$, $\mathbf{\Sigma}_C = \left\{\mathbf{x} \in \mathbb{R}^3 : \left|\mathbf{e}_1^T\mathbf{x}\right| \leq 1\right\}$ and $\mathbf{\Sigma}_R = \left\{\mathbf{x} \in \mathbb{R}^3 : \mathbf{e}_1^T\mathbf{x} > 1\right\}$, where $\mathbf{e}_1$ is the first canonical vector. Given $k \in \{L, C, R\}$, if system (4.7) has an equilibrium point $\mathbf{x}_k^*$ with $\mathbf{x}_k^* \in \mathbf{\Sigma}_k$ then it is called real, otherwise it will be termed virtual.

When the equilibria are not at the boundaries $|\mathbf{e}_1^T\mathbf{x}| = 1$, their stability can be obtained by standard criteria, as follows. By a direct application of the Routh-Hurwitz Theorem (see for instance Afanasiev et al. [1996]) we obtain the next result.

Proposition 47. *Consider system (4.7). Assume that $\mathbf{x}_{C,E}^*$ is a real equilibrium point, then it will be asymptotically stable if $t_{\{C,E\}} < 0$, $d_{\{C,E\}} < 0$ and $t_{\{C,E\}}m_{\{C,E\}} - d_{\{C,E\}} < 0$.*

However, the stability of equilibria when they lie at the boundaries $|\mathbf{e}_1^T\mathbf{x}| = 1$ is a problem much more involved. In particular, as shown in Carmona et al. [2006], it is possible to have an unstable equilibrium point even when the two matrices A_C and A_E are Hurwitzian. The difficulties arise from the possible existence of invariant cones where the dynamics is not easy to control, see for more details Carmona et al. [2005b]. In looking for the richest dynamics persistent BEB scenarios, we will impose that the equilibrium at the boundary be stable, but such that in the transition to the central zone it becomes an unstable equilibrium. This situation is the most interesting since then it is guaranteed the appearance of a new attractor when the persistent equilibrium is within the central zone, see Theorem 5.4 of Bernardo et al. [2008a]. In this context, it turns out of interest to consider the following result, which will be given without proof, see Proposition 10 and Theorem 2(d1) of Carmona et al. [2005b], or Proposition 5.1 of Bernardo et al. [2008b]. We emphasize that it is the only case where the stability of equilibria at the boundary can be assured.

Proposition 48. *Consider system (4.7). Assume that the matrices $A_{\{C,E\}}$ have have a pair of complex eigenvalues, that is the eigenvalues are $\lambda_{\{C,E\}} \in \mathbb{R}$ and $\sigma_{\{C,E\}} \pm i\omega_{\{C,E\}}$ with $\omega_{\{C,E\}} > 0$. If there exists an equilibrium point $\mathbf{x}^*$ such that $|\mathbf{e}_1^T\mathbf{x}^*| = 1$ and*

$$(\sigma_C - \lambda_C)(\sigma_E - \lambda_E) > 0, \quad (t_E - t_C)(\sigma_E - \lambda_E) \leq 0,$$

then the equilibrium point is asymptotically stable if and only if the two real eigenvalues λ_C and λ_E are negative.

Next, following Carmona et al. [2006], we reproduce an example of a piecewise linear system with two zones, such that the two matrices are Hurwitzian, the equilibrium point is unstable and lie at the boundary. Consider the system

$$\dot{\mathbf{x}} = \begin{cases} A_E\mathbf{x}, & \text{if } \mathbf{e}_1^T\mathbf{x} \geq 0, \\ A_C\mathbf{x}, & \text{if } \mathbf{e}_1^T\mathbf{x} < 0. \end{cases} \tag{4.8}$$

where the matrices are given by

$$A_{\{C,E\}} = \begin{pmatrix} t_{\{C,E\}} & -1 & 0 \\ m_{\{C,E\}} & 0 & -1 \\ d_{\{C,E\}} & 0 & 0 \end{pmatrix}.$$

Suppose that the matrices $A_{\{C,E\}}$ has a pair of imaginary eigenvalues, that is, the eigenvalues of $A_{\{C,E\}}$ are $\lambda_{\{C,E\}} \in \mathbb{R}$ and $\sigma_{\{C,E\}} \pm i\omega_{\{C,E\}}$. The characteristic polynomials of the matrices $A_{\{C,E\}}$ are

$$p_{\{C,E\}}(\mu) = -\mu^3 + t_{\{C,E\}}\mu^2 - m_{\{C,E\}}\mu + d_{\{C,E\}},$$

and after a direct computation we get

$$\begin{aligned} t_{\{C,E\}} &= \lambda_{\{C,E\}} + 2\sigma_{\{C,E\}}, \\ m_{\{C,E\}} &= 2\lambda\sigma_{\{C,E\}} + \sigma^2_{\{C,E\}} + \omega^2_{\{C,E\}}, \\ d_{\{C,E\}} &= \lambda\left(\sigma^2_{\{C,E\}} + \omega^2_{\{C,E\}}\right). \end{aligned} \tag{4.9}$$

Fixing the parameters

$$\lambda_C = -0.5, \quad \sigma_C = -0.04 \quad \omega_C = 1, \quad \sigma_E = -0.03, \quad \omega_E = 9, \tag{4.10}$$

and taking λ_E as a bifurcation parameter, we have that for $\lambda_E = -0.1$ the equilibrium point is stable, but for $\lambda_E = -0.5$ is unstable, see Figure 4.3.

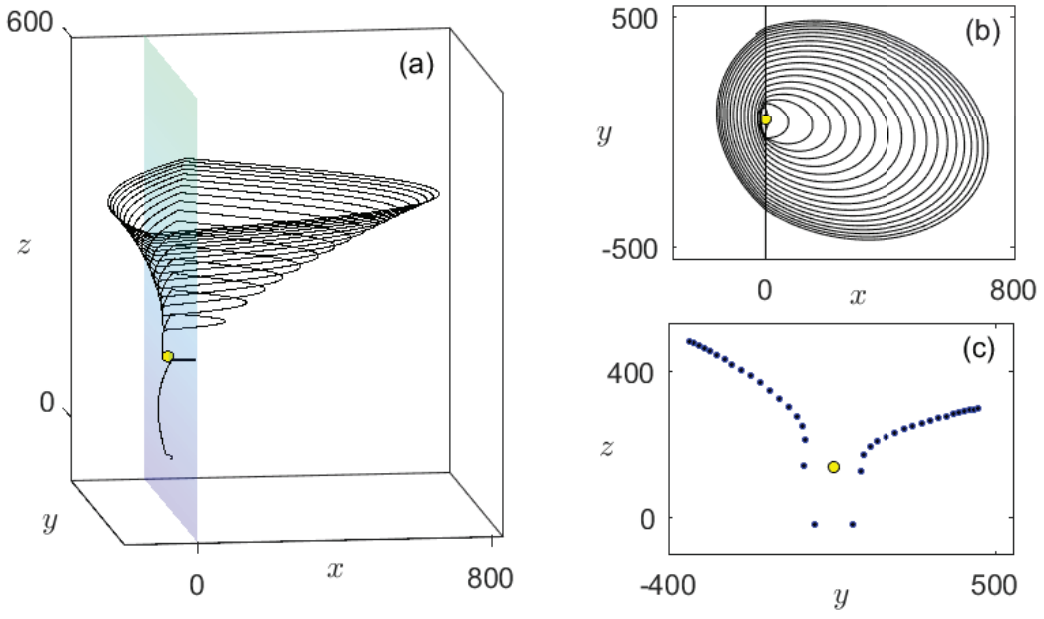

Figure 4.3: System (4.8)-(4.9) with parameters as in (4.10) and $\lambda_E = -0.5$. (a) The plane which separates the two linear regions and the unstable equilibrium point (yellow) are shown. (b) Projection of (a) in the plane (x, y). (c) The poincaré section $x = 0$ is shown.

To finish this section, we include an intersecting example. Consider the continuous quasi-symmetric 3D PWL system defined by

$$\dot{\mathbf{x}} = \begin{cases} A_E\mathbf{x} + \mathbf{b}_C + \mathbf{b}, & \text{if} \quad \mathbf{e}_1^T\mathbf{x} > 1, \\ A_C\mathbf{x} + \mathbf{b}_C, & \text{if} \quad |\mathbf{e}_1^T\mathbf{x}| < 1, \\ A_E\mathbf{x} + \mathbf{b}_C - \mathbf{b}. & \text{if} \quad \mathbf{e}_1^T\mathbf{x} < -1, \end{cases} \tag{4.11}$$

where the vectors $\mathbf{b}_C$ and $\mathbf{b}$ are

$$\mathbf{b}_C = h\mathbf{e}_3, \quad \mathbf{b} = \begin{pmatrix} t_C - t_E \\ m_C - m_E \\ d_C - d_E \end{pmatrix}. \tag{4.12}$$

Taking the set of parameters given in (4.9)-(4.10), $\lambda_E = -0.5$ and $h = d_C$, we obtain that system (4.11)-(4.12) has only one unstable equilibrium point that lies at the boundary $x_1 = 1$, while both matrices A_E and A_C are Hurwitzian. From Proposition 46 all solutions of system are bounded. Therefore, there should be a bounded attractor. In fact, by numerical simulation we see that there is a stable invariant set, see Figure 4.4. This phenomenon leads to a particular boundary equilibrium bifurcation when moving the parameter h. This example deserves a deeper study and it is out of the scope of this work.

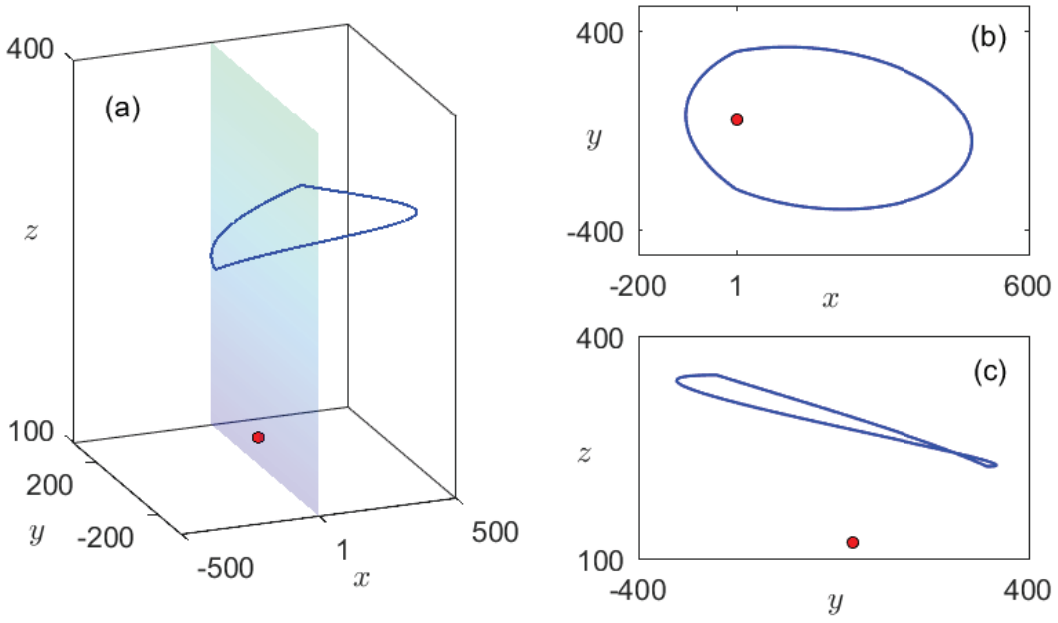

Figure 4.4: System (4.11)-(4.12) with parameters as in (4.10) and $h = d_C$. (a) The plane $x = 1$ is shown. The unstable equilibrium point is shown in red and the stable invariant set in blue. (b) Projection of (a) in the plane (x, y). (c) projection of (a) in the plane (y, z).

4.5 Liénard canonical form

Quasi-symmetric 3D piecewise linear systems given in (4.7) can be written in the generalized Liénard's form as we will show in the next theorem. First, we give an auxiliary result.

Proposition 49. *Given any matrix of order* 3 *defined by blocks*

$$A = \begin{pmatrix} a_{11} & \mathbf{r}^T \\ \mathbf{w} & B \end{pmatrix},$$

where

$$\mathbf{r} = \begin{pmatrix} a_{12} \\ a_{13} \end{pmatrix}, \quad \mathbf{w} = \begin{pmatrix} a_{21} \\ a_{31} \end{pmatrix}, \quad B = \begin{pmatrix} a_{22} & a_{23} \\ a_{32} & a_{33} \end{pmatrix},$$

the following statements hold.

(a) The linear invariants of the matrix A can be written as

$$\begin{aligned} t &= a_{11} + \operatorname{tr}(B), \\ m &= \det(B) + a_{11}\operatorname{tr}(B) - \mathbf{r}^T\mathbf{w}, \\ d &= a_{11}\det(B) + \mathbf{r}^T B\mathbf{w} - \operatorname{tr}(B)\,\mathbf{r}^T\mathbf{w}, \end{aligned}$$

where t, m and d are the trace, the sum of principal minors and the determinant respectively.

(b) If we consider the matrix

$$G = \begin{pmatrix} 1 & \mathbf{0} \\ \mathbf{s} & Q \end{pmatrix},$$

where $\mathbf{0}$ is a null row vector and

$$\mathbf{s} = \begin{pmatrix} \operatorname{tr}(B) \\ \det(B) \end{pmatrix}, \quad Q = \begin{pmatrix} -\mathbf{r}^T \\ \mathbf{r}^T B - \operatorname{tr}(B)\,\mathbf{r}^T \end{pmatrix},$$

we have

$$\begin{pmatrix} t & -1 & 0 \\ m & 0 & -1 \\ d & 0 & 0 \end{pmatrix} G = GA$$

Proof. Statement (a) can be checked by direct computation. After a direct multiplication we obtain

$$\begin{pmatrix} t & -1 & 0 \\ m & 0 & -1 \\ d & 0 & 0 \end{pmatrix} G = \begin{pmatrix} t - \operatorname{tr}(B) & \mathbf{r}^T \\ m - \det(B) & \operatorname{tr}(B)\,\mathbf{r}^T - \mathbf{r}^T B \\ d & \mathbf{0} \end{pmatrix},$$

and $GA = (\mathbf{z}, D)$ where the vector $\mathbf{z}$ and the matrix D are given by

$$\mathbf{z} = \begin{pmatrix} a_{11} \\ a_{11}\operatorname{tr}(B) - \mathbf{r}^T\mathbf{w} \\ a_{11}\det(B) + \mathbf{r}^T B\mathbf{w} - \operatorname{tr}(B)\,\mathbf{r}^T\mathbf{w} \end{pmatrix},$$

$$D = \begin{pmatrix} \mathbf{r}^T \\ \operatorname{tr}(B)\,\mathbf{r}^T - \mathbf{r}^T B \\ \mathbf{r}^T\left[B^2 - \operatorname{tr}(B)\,B + \det(B)\,I\right] \end{pmatrix}.$$

By Cayley-Hamilton's Theorem, we get $B^2 - \operatorname{tr}(B)\,B + \det(B)\,I = \mathbf{0}$, and then statement (b) follows from statement (a). □

Theorem 50. *Consider a three-dimensional quasi- symmetric continuous piecewise linear system given by*

$$\dot{\mathbf{x}} = A_E\mathbf{x} + (A_C - A_E)\,\mathbf{e}_1 \text{sat}\left(\mathbf{e}_1^T\mathbf{x}\right) + \mathbf{b}_C, \tag{4.13}$$

where the column vectors $\mathbf{w}, \mathbf{r} \in \mathbb{R}^2$ *and the matrix* B *are such that*

$$A_E = \begin{pmatrix} a_{11} & \mathbf{r}^T \\ \mathbf{w} & B \end{pmatrix}.$$

Assume that the matrix

$$C = \begin{pmatrix} \mathbf{r}^T \\ \mathbf{r}^T B \end{pmatrix} \tag{4.14}$$

has rank 2*, that is, it is nonsingular. Then, the homeomorphism* $\tilde{\mathbf{x}} = G\mathbf{x}$ *where*

$$G = \begin{pmatrix} 1 & \mathbf{0} \\ \mathbf{s} & Q \end{pmatrix}, \ \mathbf{s} = \begin{pmatrix} \text{tr}\,(B) \\ \det(B) \end{pmatrix}, \ Q = \begin{pmatrix} -\mathbf{r}^T \\ \mathbf{r}^T B - \text{tr}\,(B)\,\mathbf{r}^T \end{pmatrix} \tag{4.15}$$

transforms system (4.13) *into the generalized Liénard's form*

$$\dot{\mathbf{x}} = \begin{pmatrix} t_E & -1 & 0 \\ m_E & 0 & -1 \\ d_E & 0 & 0 \end{pmatrix} \mathbf{x} + \begin{pmatrix} t_C - t_E \\ m_C - m_E \\ d_C - d_E \end{pmatrix} \text{sat}\left(\mathbf{e}_1^T\mathbf{x}\right) + G\mathbf{b}_C, \tag{4.16}$$

where the tildes for the new variables have been removed, and the parameters t_E, m_E, d_E *and* t_C, m_C, d_C *are the linear invariants (trace, sum of principal minors and determinant) of the matrices* A_E *and* A_C*, respectively.*

Proof. From hypothesis, the matrix C has rank 2, so that the matrices Q and then G are nonsingular and the change of variables is well defined. Now, we consider the matrix

$$L_j = \begin{pmatrix} t_j & -1 & 0 \\ m_j & 0 & -1 \\ d_j & 0 & 0 \end{pmatrix} \quad \text{with} \quad j \in \{E, C\},$$

where t_j, m_j, d_j are the linear invariants (trace, sum of principal minors and determinant) of the matrices A_j with $j \in \{E, C\}$. Since system (4.13) is continuous, the matrices A_E and A_C satisfy $A_E - A_C = (A_E - A_C)\,\mathbf{e}_1\mathbf{e}_1^T$, where $\mathbf{e}_1$ is the first canonical vector, so that the matrices share the last two columns. From Proposition (49) we have $L_E G = GA_E$ and $L_C G = GA_C$. Thus, we obtain

$$\frac{d\tilde{\mathbf{x}}}{d\tau} = GA_EG^{-1}\tilde{\mathbf{x}} + (L_C - L_E)\,G\mathbf{e}_1 \text{sat}\left(\mathbf{e}_1^T G^{-1}\tilde{\mathbf{x}}\right) + G\mathbf{b}_C.$$

Taking into account that $(L_C - L_E)\,G\mathbf{e}_1 = (L_C - L_E)\,\mathbf{e}_1$ and $\mathbf{e}_1^T G^{-1} = \mathbf{e}_1^T$ we obtain the generalized Liénard's form given in (4.16) and the theorem follows. □

Remark 51. *Note that the observability matrix of the system* (4.13) *is given by*

$$O = \begin{pmatrix} \mathbf{e}_1^T \\ \mathbf{e}_1^T A_E \\ \mathbf{e}_1^T A_E^2 \end{pmatrix} = \begin{pmatrix} 1 & \mathbf{0} \\ a_{11} & \mathbf{r}^T \\ a_{11} + \mathbf{r}^T\mathbf{w} & a_{11}\mathbf{r}^T + \mathbf{r}^T B \end{pmatrix},$$

which has rank 3 *if and only if the matrix* C *has rank* 2*, so that the assumption made on the matrix* C *is by no means different from the classical observability condition (see Afanasiev et al. [1996]).*

4.6 4D canonical memristor oscillators

In this section we consider the canonical fourth-order memristor oscillator given in Itoh and Chua [2008], see Figure 4.5, where a flux-controlled memristor is the only nonlinear element. Applying Kirchhoff's laws to the upper nodes and the central loop we obtain the equations

$$i_1 = i_3 - i, \quad v_3 = v_2 - v_1, \quad i_2 = -i_3 + i_4, \tag{4.17}$$

where v_1, v_2 are the voltage across the capacitors C_1, C_2 respectively, and v_3 is the voltage across the inductance. Similarly, the current i_1, i_2, i_3 and i are as shown in Figure 4.5. Taking into account the different dipoles, and in particular that the current through the memristor satisfies

$$i = \frac{dq}{dt} = \frac{dq}{d\varphi}\frac{d\varphi}{dt},$$

it is then possible to arrive to the equations

$$\begin{aligned} C_1\frac{dv_1}{d\tau} &= i_3 - W(\varphi)v_1, \\ L\frac{di_3}{d\tau} &= v_2 - v_1, \\ C_2\frac{dv_2}{d\tau} &= -i_3 + Gv_2, \\ \frac{d\varphi}{d\tau} &= v_1, \end{aligned} \tag{4.18}$$

where C_1, C_2 denote the capacitance of the capacitors, L is the inductance of the inductor, the conductance has a negative value $-G$, $W(\varphi) = \frac{dq}{d\varphi}$ and φ denote the flux across the memristor, see section 3.1 of Itoh and Chua [2008] for more details. Taking $L = 1$ as in the quoted paper, system (4.18) can be written as

$$\begin{aligned} \frac{dx}{d\tau} &= \alpha y - \alpha W(w)x, \\ \frac{dy}{d\tau} &= z - x, \\ \frac{dz}{d\tau} &= -\beta y + \gamma z, \\ \frac{dw}{d\tau} &= x, \end{aligned} \tag{4.19}$$

where $\alpha = 1/C_1 > 0$, $\beta = 1/C_2 > 0$, $\gamma = G/C_2 > 0$ and

$$W(w) = \frac{dq(w)}{dw}, \tag{4.20}$$

being q the characteristics of the flux-controlled memristor. The new state variables are $x = v_1$ (voltage across the first capacitor); $y = i_3$ (current across the inductor L); $z = v_2$ (voltage across the second capacitor) and $w = \varphi$, the flux of the memristor.

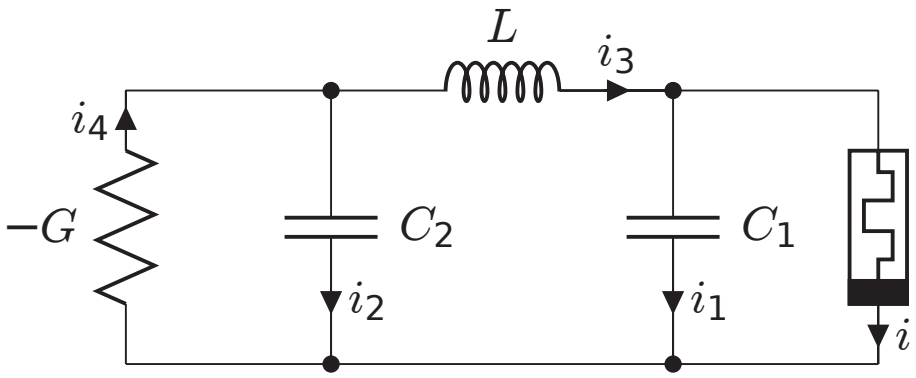

Figure 4.5: A fourth-order canonical memristor oscillator.

Remark 52. *The continuous function of the flux-charge characteristics $q(w)$ is sometimes assumed to be in the set $\mathcal{PC}^1(\mathbb{R})$ of continuous piecewise-smooth functions. Then, the vector field (4.19) becomes a discontinuous vector field at certain hyperplanes $w = w_i$ for a finite set of values w_i where $q(w)$ is not differentiable. In fact, assuming that we could compute the two lateral limits*

$$W_i^+ = \lim_{w \to w_i^+} W(w), \quad W_i^- = \lim_{w \to w_i^-} W(w),$$

at the manifold $w = w_i$, we should have the interaction of two different vector fields. However, this is not a real problem regarding the existence and uniqueness of solutions as long as such two vector fields share the normal component $\dot{w} = x$. Effectively, we can concatenate solutions in the natural way and so they become functions in $\mathcal{PC}^1(\mathbb{R})$, which exist for any $t \in \mathbb{R}$ and are uniquely defined. Therefore, here is not needed at all to invoke Filippov's theory Filippov [1988].

4.6.1 Dimensional and parameter reduction

Following a similar procedure to the one done in Theorem 8, we conclude the following result.

Theorem 53. *Consider system (4.19) where $q \in \mathcal{PC}^1(\mathbb{R})$ is given and the (possibly discontinuous) function W is defined as in (4.20). If we introduce the continuous function*

$$H(x, y, z, w) := \beta\,(x + \alpha q(w)) - \alpha\gamma\,(y + w) + \alpha z, \tag{4.21}$$

then for any $h \in \mathbb{R}$ the set

$$S_h = \{(x, y, z, w) \in \mathbb{R}^4 : H(x, y, z, w) = h\}, \tag{4.22}$$

is an invariant manifold for the system. Therefore, system (4.19) has an infinite family of invariant manifolds foliating the whole $\mathbb{R}^4$, and so the dynamics is essentially three-dimensional.

Proof. Using remark 52, we can assume the existence of solutions

$$(x(\tau), y(\tau), z(\tau), w(\tau))$$

for which the evaluation of

$$h(\tau) := H(x(\tau), y(\tau), z(\tau), w(\tau))$$

is feasible. Excepting the finite number of points where solutions are not differentiable, after a direct computation, we get that $h'(\tau) = 0$, so that h is at least piecewise constant along the solutions of (4.19). Since $h(\tau)$ is a continuous function, we obtain that the function is indeed constant everywhere. □

The existence of conserved quantity H, has a precise physical meaning for the original system (4.18). In fact, we get

$$\begin{aligned} C_1C_2\frac{dH}{d\tau} &= C_1C_2h'(\tau) \\ &= C_1\frac{dv_1}{d\tau} - G\left(\frac{di_3}{d\tau} + \frac{d\varphi}{d\tau}\right) + C_2\frac{dv_2}{d\tau} + \frac{dq}{d\tau} = 0, \end{aligned}$$

that is, $i_{C_1} + i_G + i_{C_2} + i_M = 0$ which is by no means different of the current Kirchoff law applied to the ground node of the circuit, see section 3.1 of Itoh and Chua [2008]. Thus, we deduce in this case that the conserved quantity is directly related to the conservation law for the total charge.

In the next result, we show that the parameter α is not essential and can be eliminated in system (4.19), alleviating the notation. Its proof is a direct computation which is omitted.

Proposition 54. *The change of variables*

$$\begin{aligned} &\tilde{\tau} = \alpha^{1/2}\tau, \quad \tilde{x} = \alpha^{-1/2}x, \quad \tilde{y} = y, \quad \tilde{z} = \alpha^{-1/2}z, \\ &\tilde{\beta} = \alpha^{-1/2}\beta, \quad \tilde{\gamma} = \alpha^{-1/2}\gamma, \quad \tilde{a} = \alpha^{1/2}a, \quad \tilde{b} = \alpha^{1/2}b, \end{aligned} \tag{4.23}$$

transforms system (4.19) *into the form*

$$\begin{aligned} \frac{dx}{d\tau} &= y - W(w)x, \\ \frac{dy}{d\tau} &= z - x, \\ \frac{dz}{d\tau} &= -\beta y + \gamma z, \\ \frac{dw}{d\tau} &= x, \end{aligned} \tag{4.24}$$

where the tildes for the new variables and parameters have been removed.

For convenience, we will rewrite system (4.24) as

$$\begin{aligned} \dot{y}_1 &= y_4, \\ \dot{y}_2 &= y_3 - y_4, \\ \dot{y}_3 &= -\beta y_2 + \gamma y_3, \\ \dot{y}_4 &= y_2 - W(y_1)y_4, \end{aligned} \tag{4.25}$$

where $(y_1, y_2, y_3, y_4) = (w, y, z, x)$. Note that the function H given in (4.21) can be rewritten now as

$$H(y_1, y_2, y_3, y_4) = \beta\,(y_4 + q(y_1)) - \gamma\,(y_1 + y_2) + y_3, \tag{4.26}$$

and so in the new variables we have the invariant manifolds

$$S_h = \{(y_1, y_2, y_3, y_4) \in \mathbb{R}^4 : H(y_1, y_2, y_3, y_4) = h\}. \tag{4.27}$$

The equilibrium points of system (4.25) are given by the unbounded set formed by all points in the y_1-axis, namely

$$E = \{(y_1, y_2, y_3, y_4) \in \mathbb{R}^4 : y_2 = y_3 = y_4 = 0 \text{ and } y_1 \in \mathbb{R}\}.$$

It should be noticed that all these equilibria have an eigenvalue $\lambda = 0$, since their linearization matrix has a null first column.

The following result exploits the fact that the dynamics is always confined to a certain invariant manifold S_h. We show that, by a suitable change of variables, a topologically equivalent system with a dimensional reduction and without discontinuities is achieved. The price to be payed is the introduction of an additional parameter associated to the chosen level set S_h defined in (4.22)

Theorem 55. *Consider system (4.25) with $\beta \neq 0$ and $q \in \mathcal{PC}^1(\mathbb{R})$. On any invariant set S_h the dynamics of the system is topologically equivalent to the dynamics of the continuous system*

$$\begin{aligned}
\dot{x}_1 &= \frac{\gamma}{\beta}\,(x_1 + x_2) - q(x_1) - \frac{1}{\beta}x_3 + \frac{h}{\beta},\\
\dot{x}_2 &= x_3 - \frac{\gamma}{\beta}\,(x_1 + x_2) + q(x_1) + \frac{1}{\beta}x_3 - \frac{h}{\beta},\\
\dot{x}_3 &= -\beta x_2 + \gamma x_3.
\end{aligned} \tag{4.28}$$

Proof. Solving for y_4 in the equation $H(y_1, y_2, y_3, y_4) = h$ given in (4.26), we obtain

$$y_4 = \frac{\gamma}{\beta}\,(y_1 + y_2) - q(y_1) - \frac{1}{\beta}y_3 + \frac{h}{\beta},$$

and substituting this expression in the first three equations of (4.25), we get

$$\begin{aligned}
\dot{y}_1 &= \frac{\gamma}{\beta}\,(y_1 + y_2) - q(y_1) - \frac{1}{\beta}y_3 + \frac{h}{\beta},\\
\dot{y}_2 &= y_3 - \frac{\gamma}{\beta}\,(y_1 + y_2) + q(y_1) + \frac{1}{\beta}y_3 - \frac{h}{\beta},\\
\dot{y}_3 &= -\beta y_2 + \gamma y_3.
\end{aligned} \tag{4.29}$$

Finally, making the notational change $(x_1, x_2, x_3) = (y_1, y_2, y_3)$, system (4.29) goes into the form (4.28). □

Note that $\dot{x}_1 + \dot{x}_2 = x_3$, so that, equilibria of system (4.28) satisfy $x_2 = x_3 = 0$, and the equation

$$\beta q(x_1) - \gamma x_1 = h, \tag{4.30}$$

so that generically, we will have a finite number of equilibria for each $h \in \mathbb{R}$.

Remark 56. *We note that following a similar procedure to the one done in subsection 2.4.1, it is easy to show how it is possible to get a system equivalent to the continuous reduced system (4.28), by working from the beginning in the flux-charge setting instead of starting from the discontinuous 4D system (4.18). This approach is known as Flux-Charge Analysis Method (FCAM, for short) and was proposed in Corinto and Forti [2016]-Corinto and Forti [2017].*

In what follows, we consider the function q as the continuous piecewise linear function defined by

$$q(x) = \begin{cases} b(x-1)+a, & \text{if} \quad x > 1, \\ ax, & \text{if} \quad |x| \leqslant 1, \\ b(x+1)-a, & \text{if} \quad x < -1, \end{cases} \tag{4.31}$$

so that

$$W(x) = \frac{dq(x)}{dx} = \begin{cases} b, & \text{if} \quad |x| > 1, \\ a, & \text{if} \quad |x| < 1. \end{cases} \tag{4.32}$$

Remark 57. *Note that as a first consequence of Theorem 55, when $\beta \neq 0$, $a \neq b$ and the function q is defined as in (4.31), the dynamics of system (4.25) on S_h defined in (4.27) is ruled by a continuous piecewise system of the form*

$$\dot{\mathbf{x}} = \begin{cases} A_E\mathbf{x} + \mathbf{b}_C + \mathbf{b}, & \textit{if} \quad \mathbf{x} \in \mathbf{\Sigma}_R, \\ A_C\mathbf{x} + \mathbf{b}_C, & \textit{if} \quad \mathbf{x} \in \mathbf{\Sigma}_C, \\ A_E\mathbf{x} + \mathbf{b}_C - \mathbf{b}, & \textit{if} \quad \mathbf{x} \in \mathbf{\Sigma}_L, \end{cases} \tag{4.33}$$

where

$$\begin{aligned} A_C &= \frac{1}{\beta}\begin{pmatrix} \gamma - a\beta & \gamma & -1 \\ a\beta - \gamma & -\gamma & 1+\beta \\ 0 & -\beta^2 & \gamma\beta \end{pmatrix}, \\ A_E &= \frac{1}{\beta}\begin{pmatrix} \gamma - b\beta & \gamma & -1 \\ b\beta - \gamma & -\gamma & 1+\beta \\ 0 & -\beta^2 & \gamma\beta \end{pmatrix}, \\ \mathbf{b} &= \begin{pmatrix} b-a \\ a-b \\ 0 \end{pmatrix}, \quad \mathbf{b}_C = \frac{h}{\beta}\begin{pmatrix} 1 \\ -1 \\ 0 \end{pmatrix}. \end{aligned} \tag{4.34}$$

As a consequence, the invariant manifolds S_h given in (4.27) are continuous and piecewise linear (CPWL, for short). We can obtain a canonical form (so called Liénard's generalized form). Combining Remark 57 and Theorem 50, we obtain the following result.

Proposition 58. *Consider the fourth-order discontinuous system (4.25) with $\beta \neq 0$ and the function q defined as in (4.31). On any invariant manifold S_h given in (4.27), the system is topologically equivalent to the third-order continuous canonical system*

$$\dot{\mathbf{x}} = \begin{pmatrix} t_E & -1 & 0 \\ m_E & 0 & -1 \\ d_E & 0 & 0 \end{pmatrix}\mathbf{x} + \begin{pmatrix} t_C - t_E \\ m_C - m_E \\ d_C - d_E \end{pmatrix} \text{sat}\left(\mathbf{e}_1^T\mathbf{x}\right) + \frac{h}{\beta}\begin{pmatrix} 1 \\ \gamma \\ \beta \end{pmatrix} \tag{4.35}$$

where $t_{C,E}$, $d_{C,E}$ and $m_{C,E}$ are the linear invariants of the matrices A_E and A_C given by

$$\begin{array}{lll} t_C = \gamma - a, & m_C = 1 + \beta - \gamma a, & d_C = \gamma - \beta a, \\ t_E = \gamma - b, & m_E = 1 + \beta - \gamma b, & d_E = \gamma - \beta b. \end{array} \tag{4.36}$$

Proof. From Remark 57, on any invariant manifold S_h the dynamics of system (4.25) is ruled by a continuous piecewise linear system (4.33)-(4.34). Computing the matrix C given in (4.14) we obtain

$$C = \frac{1}{\beta^2} \begin{pmatrix} \gamma\beta & -\beta \\ \beta^2 - \gamma^2 & \gamma \end{pmatrix},$$

so that $\det(C) = 1/\beta$ and C is nonsingular. From Theorem 50, there exists a matrix G given by

$$G = \frac{1}{\beta} \begin{pmatrix} \beta & 0 & 0 \\ \gamma\beta - \gamma & -\gamma & 1 \\ \beta^2 + \beta - \gamma^2 & \beta - \gamma^2 & \gamma \end{pmatrix}, \tag{4.37}$$

such that the change of variables $\tilde{\mathbf{x}} = G\mathbf{x}$ transforms system (4.33)-(4.34) into the Generalized Liénard's form (4.35) and the conclusion follows. □

Remark 59. *Note that if*

$$\mathbf{y}(\tau) = (y_1(\tau), y_2(\tau), y_3(\tau), y_4(\tau)),$$

is a solution of system (4.25), from Theorem 53 we obtain the constant value

$$h = H(y_1(\tau), y_2(\tau), y_3(\tau), y_4(\tau)), \tag{4.38}$$

where H is given in (4.26), so that $\mathbf{y}(\tau) \in S_h$. From Theorem 58, for h given in (4.38) we get that $\mathbf{x}(\tau) = G(y_1(\tau), y_2(\tau), y_3(\tau))^T$ is a solution of the canonical system (4.35)-(4.36) where the matrix G is given in (4.37). The eigenvalues of the matrices A_E and A_C are the roots of the polynomials

$$p_j(\lambda) = \lambda^3 - t_j\lambda^2 + m_j\lambda - d_j, \quad \text{with} \quad j \in \{E, C\}.$$

The numerical simulation of system (4.25) is prone to numerical errors, associated with the presence of infinite number of piecewise linear invariant manifold S_h. Thus, we need to implement a safeguard that force the solutions of system (4.25) to stay at the corresponding invariant manifold S_h. The next result avoids the numerical difficulties because we give for any solution of the continuous canonical system (4.35)-(4.36) with a given value of h the corresponding solution of the discontinuous system (4.25).

Proposition 60. *Given $h \in \mathbb{R}$ and $\beta \neq 0$, if $(x_1(\tau), x_2(\tau), x_3(\tau)) \in \mathbb{R}^3$ is a solution of canonical system (4.35)-(4.36) if and only if*

$$\mathbf{y}(\tau) = \begin{pmatrix} x_1(\tau) \\ (\gamma^2 - \beta - 1)x_1(\tau) - \gamma x_2(\tau) + x_3(\tau) \\ (\gamma^3 - 2\beta\gamma)x_1(\tau) + (\beta - \gamma^2)x_2(\tau) + \gamma x_3(\tau) \\ \gamma x_1(\tau) - x_2(\tau) - q(x_1(\tau)) + h/\beta \end{pmatrix} \tag{4.39}$$

is a solution of discontinuous system (4.25) on S_h, where the function q is defined as in (4.31).

Proof. Assume that $\mathbf{x}(\tau) = (x_1(\tau), x_2(\tau), x_3(\tau)) \in \mathbb{R}^3$ is a solution of the canonical system (4.35)-(4.36) for some $h \in \mathbb{R}$. From Theorem 58 there exists a nonsingular matrix G such that $G^{-1}\mathbf{x}(\tau)$ is a solution of non-canonical system (4.28). Taking into account that

$$G^{-1}\mathbf{x}(\tau) = \begin{pmatrix} x_1(\tau) \\ (\gamma^2 - \beta - 1)\, x_1(\tau) - \gamma x_2(\tau) + x_3(\tau) \\ (\gamma^3 - 2\beta\gamma)\, x_1(\tau) + (\beta - \gamma^2)\, x_2(\tau) + \gamma x_3(\tau) \end{pmatrix} = \begin{pmatrix} y_1(\tau) \\ y_2(\tau) \\ y_3(\tau) \end{pmatrix},$$

and defining

$$\begin{aligned} y_4(\tau) &= \frac{\gamma}{\beta}(y_1(\tau) + y_2(\tau)) - q(y_1(\tau)) - \frac{1}{\beta} y_3(\tau) + \frac{h}{\beta} = \\ &= \gamma x_1(\tau) - x_2(\tau) - q(x_1(\tau)) + \frac{h}{\beta}, \end{aligned}$$

we obtain trivially $H(y_1(\tau), y_2(\tau), y_3(\tau), y_4(\tau)) = h$, where H is given in (4.26), that is $(G^{-1}\mathbf{x}(\tau), y_4(\tau)) \in S_h$. Now, after to direct computation we get $\dot{y}_1 = y_4$, $\dot{y}_2 = y_3 - y_4$, $\dot{y}_3 = -\beta y_2 + \gamma y_3$ and taking into account that $\dot{y}_1 + \dot{y}_2 = y_3$ we obtain

$$\dot{y}_4 = \frac{\gamma}{\beta}(\dot{y}_1 + \dot{y}_2) - W(y_1(\tau))\dot{y}_1 - \frac{1}{\beta}\dot{y}_3 = y_2(\tau) - W(y_1(\tau))y_4(\tau).$$

Thus $\mathbf{y}(\tau)$ defined as in (4.39) is a solution of discontinuous system (4.25) and the conclusion follows. □

4.6.2 Boundary equilibrium bifurcations

In the following result we study the existence of real equilibrium points and their transitions between the central zone and the externals zones. The proof is a direct computation and is omitted.

Proposition 61. *Consider canonical system (4.35)-(4.36) with $a \neq b$. The following statements hold.*

(a) The system has for $|h| \leq |d_C|$ one real equilibrium point in the central zone $\left|\mathbf{e}_1^T\mathbf{x}\right| \leq 1$, with coordinates

$$\mathbf{x}_C^* = h \begin{pmatrix} -\frac{1}{d_C} \\ \frac{1}{\beta} - \frac{t_C}{d_C} \\ \frac{\gamma}{\beta} - \frac{m_C}{d_C} \end{pmatrix}. \tag{4.40}$$

(b) For $\frac{h+d_C}{d_E} < 0$ the system has one real equilibrium point in the right external zone $\mathbf{e}_1^T\mathbf{x} > 1$, with coordinates

$$\mathbf{x}_R^* = \begin{pmatrix} 1 - \frac{h+d_C}{d_E} \\ t_C - \frac{t_E}{d_E} d_C + \left(\frac{1}{\beta} - \frac{t_E}{d_E}\right) h \\ m_C - \frac{m_E}{d_E} d_C + \left(\frac{\gamma}{\beta} - \frac{m_E}{d_E}\right) h \end{pmatrix}. \tag{4.41}$$

(c) For $\frac{h-d_C}{d_E} > 0$ *the system has one real equilibrium point in the left external zone* $\mathbf{e}_1^T\mathbf{x} < -1$*, with coordinates*

$$\mathbf{x}_L^* = \begin{pmatrix} -1 - \frac{h-d_C}{d_E} \\ -t_C + \frac{t_E}{d_E} d_C + \left(\frac{1}{\beta} - \frac{t_E}{d_E}\right) h \\ -m_C + \frac{m_E}{d_E} d_C + \left(\frac{\gamma}{\beta} - \frac{m_E}{d_E}\right) h \end{pmatrix}. \tag{4.42}$$

Following the terminology introduced in section 5.1.1 of Bernardo et al. [2008b], in the next result we study, by taking h as a bifurcation parameter, the boundary-equilibrium bifurcation (BEB, for short) of system (4.35)-(4.36). Such bifurcation can be of two different types, namely persistence (the number of equilibria does not change) and non-smooth fold, when the number of equilibria changes by two. The non-generic cases $d_C = 0$ or $d_E = 0$ are excluded for brevity.

Proposition 62. *The following statements hold for canonical system* (4.35)-(4.36) *with* $\beta \neq 0$.

(a) If $d_C \cdot d_E > 0$ *the system has for any* $h \in \mathbb{R}$ *only one real equilibrium point so that for* $h = \pm d_C$ *we have a persistence BEB, see figure 4.6 (a).*

(b) If $d_C \cdot d_E < 0$ *the system has for* $|h| > |d_C|$ *only one real equilibrium point and for* $|h| < |d_C|$ *three real equilibrium points. Therefore, for* $h = \pm d_C$ *the system has two equilibrium points and a non-smooth fold BEB, see figure 4.6 (b).*

Proof. From Proposition 61 we have

$$\mathbf{e}_1^T\mathbf{x}_C^* = -\frac{h}{dc}, \quad \mathbf{e}_1^T\mathbf{x}_L^* = -1 + \frac{d_C}{d_E} - \frac{h}{d_E},$$
$$\mathbf{e}_1^T\mathbf{x}_R^* = 1 - \frac{d_C}{d_E} - \frac{h}{d_E},$$

where $\mathbf{e}_1$ is the canonical vector. Assuming that $d_C > 0$ and $d_E < 0$ we obtain

$$\begin{aligned} |\mathbf{e}_1^T\mathbf{x}_C^*| \leq 1, &\quad \text{for } -d_C \leq h \leq d_C, \\ \mathbf{e}_1^T\mathbf{x}_R^* > 1, &\quad \text{for } -d_C < h, \\ \mathbf{e}_1^T\mathbf{x}_L^* < -1, &\quad \text{for } h < d_C. \end{aligned}$$

Thus, for $|h| < d_C$ the system has three real equilibrium points while for $h = d_C$ we get $\mathbf{e}_1^T\mathbf{x}_C^* = \mathbf{e}_1^T\mathbf{x}_L^*$, so that the system has two equilibrium points and passing through at $h = d_C$ we have a non-smooth fold boundary equilibrium bifurcation. Analogously, for $h = -d_C$ we have $\mathbf{e}_1^T\mathbf{x}_C^* = \mathbf{e}_1^T\mathbf{x}_R^*$. The case $d_C < 0$ and $d_E > 0$ is analogous and statement (a) follows.
If $d_C > 0$ and $d_E > 0$ the system has only one real equilibrium point for any $h \in R$ so that there exists a persistence of the equilibrium point at $h = d_C$ and $h = -d_C$. The case $d_C < 0$ and $d_E < 0$ is analogous and the proof is completed. □

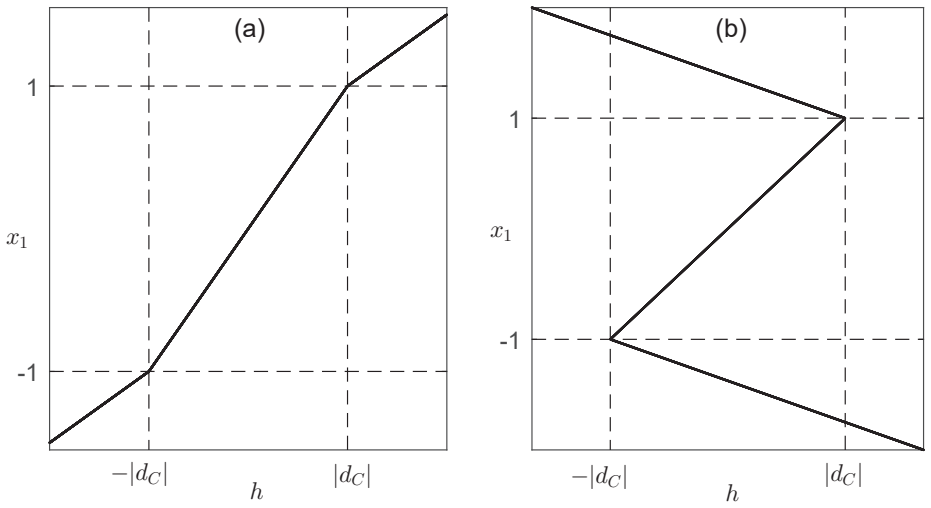

Figure 4.6: Real equilibrium points of canonical system (4.35)-(4.36) varying parameter h. (a) Parameters as in statement (a) of Proposition 62 showing a persistence BEB at $h = \pm d_C$. (b) Parameters as in statement (b) of Proposition 62 showing a non-smooth fold BEB at $h = \pm d_C$.

Note that, the above BEB's could be detected by applying Theorem 5.1 of Bernardo et al. [2008b] or Di Bernardo et al. [2008], but here is not necessary thanks to the canonical form (4.35)-(4.36) which facilitates the required computations.

When the equilibria are not at the boundaries $|\mathbf{e}_1^T \mathbf{x}| = 1$, their stability can be obtained by standard criteria (see section 4.4), as follows.

Proposition 63. *Consider system (4.35)-(4.36) with $a \neq b$, $|h| \neq |d_C|$ and the equilibrium points given in (4.40)-(4.41)-(4.42). The following statements hold.*

(a) When equilibrium point $\mathbf{x}_C^*$ is real, it will be asymptotically stable if $t_C < 0$, $d_C < 0$ and $m_C t_C - d_C < 0$, that is

$$\gamma - a < 0, \quad \gamma - a\beta < 0, \quad a^2\gamma - a\gamma^2 + \beta\gamma - a < 0.$$

(b) When a external equilibrium point ($\mathbf{x}_R^*$ or $\mathbf{x}_L^*$) is real, it will be asymptotically stable if $t_E < 0$, $d_E < 0$ and $m_E t_E - d_E < 0$, that is

$$\gamma - b < 0, \quad \gamma - b\beta < 0, \quad b^2\gamma - b\gamma^2 + \beta\gamma - b < 0.$$

In figure 4.7, we show the stable region for the origin on the parameter plane (a, γ).

4.7 Multiple FCC Bifurcation

The equilibria of system (4.28) are of the form $(x_1, 0, 0)$ where x_1 is a solution of (4.30). When $|x_1| < 1$ the stability of such equilibrium is determined by the

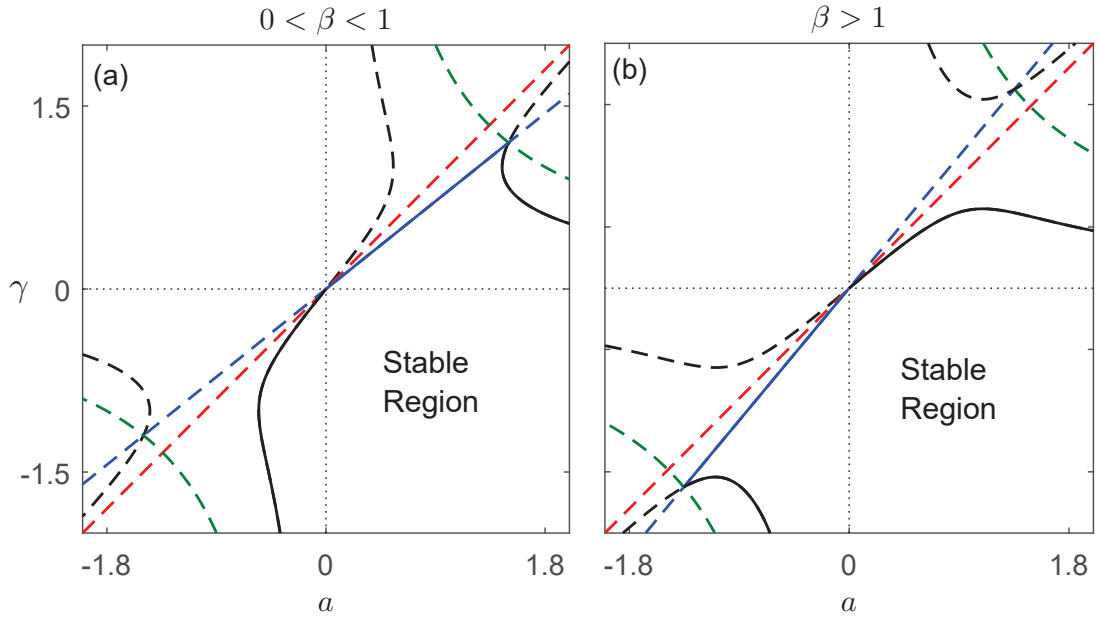

Figure 4.7: In solid line the stability region for the origin is plotted. The dashed red (blue, green) line represents the curve $t_{\{C,E\}} = 0$ ($d_{\{C,E\}} = 0$, $m_{\{C,E\}} = 0$), in black dashed line $t_{\{C,E\}} m_{\{C,E\}} = d_{\{C,E\}}$. (a) case $\beta = 0.8$, (b) case $\beta = 1.2$.

roots of the polynomial $\lambda^3 - t_C\lambda^2 + m_C\lambda - d_C$. These equilibria can undergo the so-called focus-center-limit cycle (FCLC, for short) bifurcation Freire et al. [2005, 2008], Carmona et al. [2005a], Freire et al. [2009] under the conditions

$$m_C > 0, \quad m_C t_C = d_C. \tag{4.43}$$

Such conditions assure that the matrix A_C has a pair of pure imaginary eigenvalues. Effectively, under the hypothesis of the existence of a complex eigenvalue pair, if we introduce the parameter $\varepsilon = m_C t_C - d_C$, then we conclude that it is associated to the sign of the real part of such complex eigenvalues. Effectively, if λ, and $\sigma \pm i\omega$ are the three eigenvalues a straightforward computation gives

$$\varepsilon = m_C t_C - d_C = 2\sigma \left[(\sigma + \lambda)^2 + \omega^2\right].$$

Therefore, for $\varepsilon = 0$ we have a linear center in the central zone on the corresponding focal plane. Since $d_C = \lambda(\sigma^2 + \omega^2)$, we observe that when $d_C < 0$, such focal plane is attractive because we have a dynamics approaching the plane along the transversal direction associated to the λ-eigenvector.
Assuming β fixed, we start by analyzing the auxiliary expression $\varepsilon(a, \gamma) = m_C t_C - d_C$ that leads to the bifurcation when it vanishes, where m_C, t_C and d_C are given in (4.36). We have

$$\varepsilon\,(a, \gamma) = a^2\gamma - a\gamma^2 + \beta\gamma - a. \tag{4.44}$$

For $\beta = 1$ we get $\varepsilon(a, \gamma) = (1 - a\gamma)(\gamma - a)$. If $\gamma = a$ then we have $t_C = d_C = 0$, so that we do not have any equilibrium point for $h \neq 0$; anyway, $m_C = 2 - a^2$, and so for

$|a| < \sqrt{2}$ we get a Hopf-zero bifurcation if $h = 0$, see Ponce et al. [2013]. The other possibility given by $\gamma = 1/a$ is not so problematic but we will not consider anymore the case $\beta = 1$, see Figure 4.7. As it is a non-generic situation, to be investigated elsewhere.

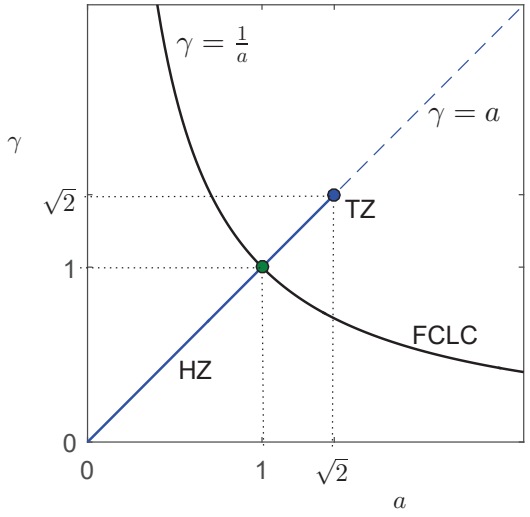

Figure 4.8: The two parametric plane (a, γ) with $\beta = 1$ is shown. The Hopf-zero point is shown in green and the triple-zero point in blue. The curve $\gamma = 1/a$ is drawn in black.

For $\beta \neq 1$, the condition $\varepsilon(a, \gamma) = 0$ is equivalent to the equality $a\gamma(a - \gamma) = a - \beta\gamma$, which is only possible for $a\gamma > 0$. Effectively, if $a\gamma < 0$, then

$$\operatorname{sgn}(a - \gamma) = \operatorname{sgn}(a - \beta\gamma)$$

and the previous equality can not be fulfilled. Therefore, the points where (4.44) vanishes are in the first or third quadrant of the parameter plane (a, γ). In Figure 4.9, we show for the first quadrant of parameter plane the locus $\varepsilon(a, \gamma) = 0$, which is formed by two disconnected branches. As will be later detailed, not all the points in such branches are FCLC bifurcation points. See Theorems 69 and 70, below.
We observe that system (4.35)-(4.36) is invariant under the symmetry

$$(x, y, x, h) \to (-x, -y, -z, -h), \tag{4.45}$$

so that for the analysis of the FCLC bifurcation, we only need to consider the dynamics of the system for $h \geq 0$. When $h = 0$ the vector field of the system is indeed symmetric, and then for the equilibrium at the origin Theorem 1.1 of Freire et al. [2005] on the FCLC bifurcation applies. This result assures under certain hypotheses, to be detailed later, the bifurcation of a limit cycle from a linear center configuration that exists at the critical bifurcation value in the central zone.
When $0 < h < |d_C|$ the only equilibrium of system (4.35)-(4.36) in the central zone is not at the origin any longer, but is nearer to one of the two planes $x = \pm 1$, see Figure 4.6. Then a similar FCLC Theorem applies (see Theorem 1 of Carmona et al.

[2005a]) that involves two linear zones.
We note that the FCLC bifurcation condition (4.43) does not depend on the concrete value of h, so that the FCLC bifurcation takes place simultaneously for all values of $|h| < |d_C|$. Therefore, we can state as a consequence the following result, where a new criticality parameter ρ is introduced to characterize the bifurcation.

Theorem 64. *Consider the canonical system (4.35)-(4.36) with $|h| < |d_C| \neq 0$, $m_C > 0$, $\varepsilon = m_C t_C - d_C$, and the non-degeneracy parameter*

$$\rho = d_C m_C - d_C m_E + d_E m_C - m_C^2 t_E. \tag{4.46}$$

Then, for $\rho \neq 0$ and $\varepsilon = 0$ the system undergoes a focus-center-limit cycle bifurcation; that is, from the lineal center configuration in the central zone, which exists for $\varepsilon = 0$, one limit cycle appears for $\varepsilon\rho > 0$ and ε sufficiently small. In particular, if $\rho > 0$ and $d_C < 0$, then the limit cycle bifurcates for $\varepsilon > 0$ and is orbitally asymptotically stable. Otherwise, if $\rho < 0$ or $d_C > 0$ the bifurcating limit cycle is unstable, being completely unstable when both inequalities hold.

In all the cases, the bifurcating limit cycle comes from the most external periodic orbit of the linear center that exist for $\varepsilon = 0$, which is tangent to one of the planes $\mathbf{e}_1^T\mathbf{x} = \pm 1$ or to both of them if $h = 0$.
Now, given the value of h, the FCLC bifurcation is characterized in the parameter plane (a, γ), see Figure 4.9. The golden ratio $\phi = \frac{1+\sqrt{5}}{2}$ appears in some statements.

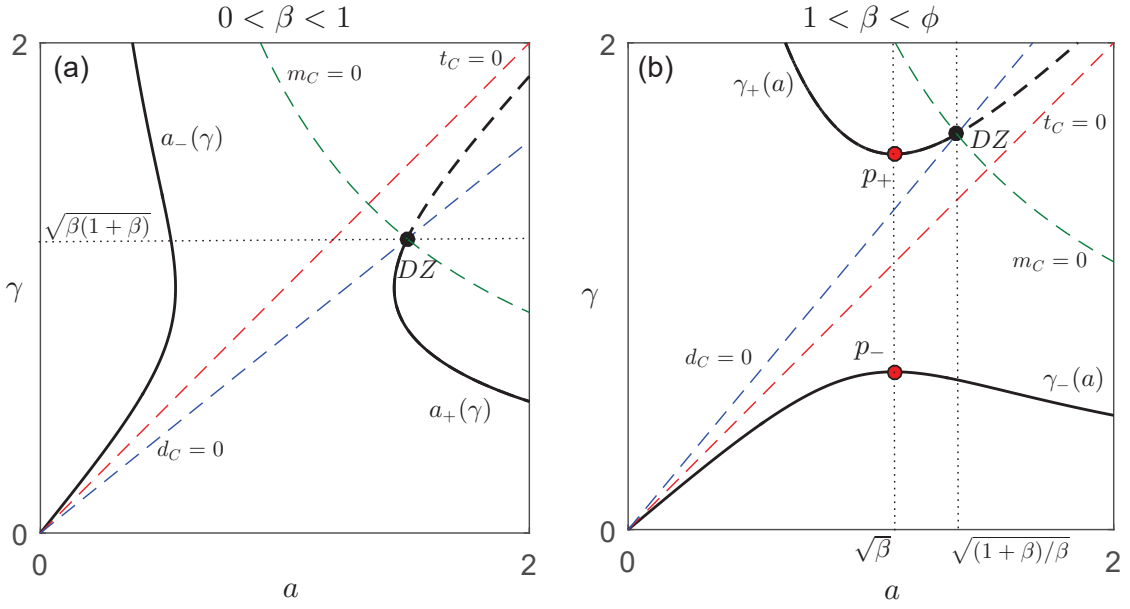

Figure 4.9: The thin dashed lines represents the locus $t_C = 0$ (red), $d_C = 0$ (blue) and $m_C = 0$ (green). The thick black curves corresponds to FCLC bifurcation points, excepting the dashed points where $m_C < 0$. The panel (a) it is shown the case $0 < \beta < 1$ ($\beta = 0.8$), while in (b) there appears the case $\beta < 1$ ($\beta = 1.2$).

First some auxiliary results. Assuming β fixed, we start by analyzing the auxiliary expression $\varepsilon(a,\gamma) = m_C t_C - d_C$ that leads to the bifurcation when it vanishes, where m_C, t_C and d_C are given in (4.36).

For $\beta \neq 1$, the condition $\varepsilon(a,\gamma) = 0$ is equivalent to $a\gamma\,(a-\gamma) = a - \beta\gamma$, which is only possible for $a\gamma > 0$, so that the points where (4.44) vanishes are in the first or third quadrant of the parameter plane (a,γ). The following Lemma is direct and so we omit its proof.

Lemma 65. *Consider for the reduced system (4.35)-(4.36) the auxiliary expression (4.44), where t_C, m_C and d_C are given in (4.36) and $a > 0$, $\beta \neq 1$. The following statements hold.*

(a) The points of the parameter plane (a,γ) where ε vanishes satisfy $\gamma \neq a$.

(b) If $0 < \beta < 1$ then $(\gamma^2+1)^2 > 4\beta\gamma^2$ and we have the factorization

$$\varepsilon(a,\gamma) = \gamma\,(a - a_+(\gamma))\,(a - a_-(\gamma))\,, \tag{4.47}$$

where

$$a_\pm(\gamma) = \frac{\gamma^2+1}{2\gamma} \pm \sqrt{\left(\frac{\gamma^2+1}{2\gamma}\right)^2 - \beta}, \tag{4.48}$$

so that $a_-(\gamma) < \gamma < a_+(\gamma)$. Thus at the points $(a_-(\gamma),\gamma)$ we have $t_C > 0$ and $d_C > 0$, while for $(a_+(\gamma),\gamma)$ we have $t_C < 0$. Furthermore, for $\gamma < \sqrt{\beta(1+\beta)}$ we also have $\gamma < a_+(\gamma)\beta$, that is, $d_C < 0$ at such points $(a_+(\gamma),\gamma)$, see Figure 4.9 (a).

(c) If $\beta > 1$ then $\beta + a^2 > 2a$ and we have the factorization

$$\varepsilon(a,\gamma) = -a\,(\gamma - \gamma_+(a))\,(\gamma - \gamma_-(a))\,, \tag{4.49}$$

where

$$\gamma_\pm(a) = \frac{a^2+\beta}{2a} \pm \sqrt{\left(\frac{a^2+\beta}{2a}\right)^2 - 1}, \tag{4.50}$$

so that $\gamma_-(a) < a < \gamma_+(a)$. Thus at the points $(a,\gamma_-(a))$ we have $t_C < 0$ and $d_C < 0$, while for $(a,\gamma_+(a))$ we have $t_C > 0$. Furthermore, for $a < \sqrt{(1+\beta)/\beta}$ we also have $a\beta < \gamma_+(a)$, that is $d_C > 0$ at such points $(a,\gamma_+(a))$, see Figure 4.9 (b).

Remark 66. *Regarding conditions (4.43), we need in the bifurcation that* $\operatorname{sgn}(t_C) = \operatorname{sgn}(d_C)$. *Therefore, we note that for $\beta > 1$ the points on the curve $\varepsilon(a,\gamma) = 0$ with $a < \gamma < a\beta$ do not represent FCLC bifurcation points. Analogously, for $\beta < 1$ we must neglect the points with $a\beta < \gamma < a$.*
The point (a,γ) at the curve $\varepsilon(a,\gamma) = 0$ with $\gamma = a\beta$ namely

$$DZ = \left(\sqrt{\frac{1+\beta}{\beta}}, \sqrt{\beta\,(1+\beta)}\right), \tag{4.51}$$

represents a higher codimension bifurcation point (a double zero, since $d_C = m_C = 0$) from which the curve of FCLC bifurcation emanates (see Figure 4.9).

In the next Lemma we study the sign of parameters m_C and ρ on the bifurcation curve $\varepsilon(a,\gamma)=0$, in order to apply Theorem 64.

Lemma 67. *Consider the canonical system (4.35)-(4.36) with $|h|<|d_C|\neq 0$ and $a\neq b$, where we also assume $a,\gamma>0$, $0<\beta\neq 1$ and ε given in (4.44). The following statements hold.*

(a) For m_C and ρ defined in (4.36) and (4.46) respectively, we have

$$\begin{aligned} m_0 &:= m_C|_{f=0} = \frac{\gamma-\beta a}{\gamma-a}, \\ \rho_0 &:= \rho|_{f=0} = m_0\frac{\gamma\,(b-a)}{a}\left(\beta-a^2\right). \end{aligned} \tag{4.52}$$

(b) When $m_0\neq 0$ and $\beta<1$, we have $\rho_0\neq 0$.

(c) When $m_0\neq 0$ and $\beta>1$ there exist two points at the bifurcation curve given by

$$p_\pm = \left(\sqrt{\beta},\sqrt{\beta}\pm\sqrt{\beta-1}\right), \tag{4.53}$$

such that $\rho_0\left(p_\pm\right)=0$.

Proof. To show statement (a), we note that $\varepsilon(a,\gamma)=0$ is equivalent to $d_C=m_Ct_C$, so that the expression for m_0 is direct. Also, on the curve $\varepsilon(a,\gamma)=0$, we have

$$\gamma^2+1=\frac{\gamma}{a}\left(a^2+\beta\right). \tag{4.54}$$

Now, we obtain from (4.46)

$$\rho|_{f=0}=m_0\left(d_C-m_Et_C+d_E-m_0t_E\right).$$

Using (4.54) and after some algebra we obtain

$$\begin{aligned} d_C-m_Et_C+d_E-m_Ct_E &= \frac{\gamma\left(a^2+\beta\right)}{a}(a+b)-2\gamma\left(ab+\beta\right)= \\ &= \frac{\gamma}{a}(b-a)\left(\beta-a^2\right), \end{aligned}$$

and the statement (a) follows.
If $m_0\neq 0$ and in (4.52) we assume $a^2=\beta$, from (4.44) we get that $\varepsilon(a,\gamma)=0$ is equivalent to the condition $\gamma^2+1=2a\gamma$, so that for all $\gamma>0$ we have

$$a=\frac{\gamma^2+1}{2\gamma}=\frac{1}{2}\left(\gamma+\frac{1}{\gamma}\right)>1, \tag{4.55}$$

which implies $\beta>1$, getting a contradiction. Statement (b) follows.
Finally, if $m_0\neq 0$ the only posibility for $\rho_0=0$ is $a^2=\beta>1$. From (4.50) we obtain $\gamma_\pm(\sqrt{\beta})=\sqrt{\beta}\pm\sqrt{\beta-1}$ and the lemma follows. □

Remark 68. *According to Remark 66 the point p_+ given in (4.53) must be neglected when at such point $a < \gamma < a\beta$*

$$\sqrt{\beta} < \sqrt{\beta} + \sqrt{\beta - 1} < \beta\sqrt{\beta},$$

and this fails when $\sqrt{\beta} + \sqrt{\beta - 1} > \beta\sqrt{\beta}$. Multiplying by $\sqrt{\beta} - \sqrt{\beta - 1} > 0$ and after some algebra, we obtain the equivalent inequality

$$0 > \beta^3 - 2\beta^2 + 1 = (\beta - 1)(\beta - \phi)\left(\beta + \frac{1}{\phi}\right),$$

where $\phi = \frac{1+\sqrt{5}}{2}$ is the golden ratio. Thus, for $\beta > \phi$, the point p_+ lies on the portion of the curve $\gamma = \gamma_+(a)$ that does not represents FCLC bifurcation points.

In the next theorem we give a complete characterization of the FCLC bifurcation for $0 < a < b$.

Theorem 69. *Consider the reduced system (4.35)-(4.36) with $|h| < |d_C| \neq 0$, $0 < a < b$, $\beta \neq 1$, and $\gamma > 0$. Additionally, consider the functions $a_\pm(\gamma)$ and $\gamma_\pm(a)$ defined in (4.48)-(4.50) respectively. The following statements hold.*

(a) If $0 < \beta < 1$ then at the points $(a, \gamma) = (a_-(\gamma), \gamma)$ the system undergoes a FCLC bifurcation, so that an unstable limit cycle bifurcates for $a < a_-(\gamma)$.

(b) If $0 < \beta < 1$ then at the points $(a, \gamma) = (a_+(\gamma), \gamma)$ with $\gamma < \sqrt{\beta(1+\beta)}$ the system undergoes a FCLC bifurcation, so that an unstable limit cycle bifurcates for $a < a_+(\gamma)$.

(c) If $\beta > 1$ then at the points $(a, \gamma) = (a, \gamma_-(a))$ with $a < \sqrt{\beta}$ ($a > \sqrt{\beta}$) the system undergoes a FCLC bifurcation, so that a stable (unstable) limit cycle bifurcates for $\gamma > \gamma_-(a)$ ($\gamma < \gamma_-(a)$).

(d) If $1 < \beta < \phi$ then at the points $(a, \gamma) = (a, \gamma_+(a))$ with $a < \sqrt{\beta}$ ($\sqrt{\beta} < a < \sqrt{(1+\beta)/\beta}$) the system undergoes a FCLC bifurcation, so that an unstable (completely unstable) limit cycle bifurcates for $\gamma < \gamma_+(a)$ ($\gamma > \gamma_+(a)$).

(e) If $\beta \geq \phi$ then at the points $(a, \gamma) = (a, \gamma_+(a))$ with $a < \sqrt{(1+\beta)/\beta}$ the system undergoes a FCLC bifurcation, so that an unstable limit cycle bifurcates for $\gamma < \gamma_+(a)$.

In all the above cases, the system has for the critical values of parameters indicated a linear center in the region $|\mathbf{e}_1^T \mathbf{x}| \leq 1$ and the limit cycle bifurcates from the most external periodic orbit of the center.

Proof. Under the hypothesis $\beta < 1$, the points in the branch $(a, \gamma) = (a_-(\gamma), \gamma)$ satisfy $a_-(\gamma)\beta < a_-(\gamma) < \gamma$ and $m_0 > 0$ from (4.52). Furthermore, we know from statement (b) of Lemma 67 that the sign of ρ_0 does not change for all the points of the branch. To discriminate this sign, from (4.52) we only need to check the sign of $\beta - a^2$. Taking $\gamma = 1$, we see after some algebra that $\beta > a_-(1)^2 = \left(1 - \sqrt{1-\beta}\right)^2$ and so $\rho_0 > 0$. The conclusion follows from Theorem 64, since $a < a_+(\gamma)$ and

$\varepsilon(a,\gamma) = \gamma\,(a - a_+(\gamma))\,(a - a_-(\gamma)) > 0$ for $a - a_-(\gamma) < 0$ indicating that the limit cycle appears for $a < a_-(\gamma)$ and is unstable since $a_-(\gamma)\beta < \gamma$ and so $d_C > 0$. Statement (a) follows.
Analogously, we know that only for $\gamma < \sqrt{\beta\,(1+\beta)}$ the points in the branch $(a,\gamma) = (a_+(\gamma),\gamma)$ satisfy $\gamma < a_+(\gamma)\beta < a_+(\gamma)$ and so $m_0 > 0$ from (4.52). The sign of the ρ_0 will also be determined by the sign of $\beta - a^2$. Taking $\gamma = 1$, we see that $\beta - (1+\sqrt{1-\beta})^2 < 0$ and so $\rho_0 < 0$. So that the bifurcation does not involve stable limit cycles. In this branch we have $a - a_-(\gamma) > 0$, then the limit cycle bifurcates for $a < a_+(\gamma)$ and it is unstable although $d_C = \gamma - a_+(\gamma)\beta < 0$, according to Theorem 64.
To show statement (c) we start with the case $a < \sqrt{\beta}$, that is, on the left of point p_-, see Figure 4.9 (b). Then, we have that $\gamma_-(a) < a < a\beta$, so that from (4.52) we get that $m_0 > 0$. Then, under our hypothesis $a < \sqrt{\beta}$ we deduce that $\rho_0 > 0$ and then the bifurcating limit cycle predicted by Theorem 64 will appear for $\gamma > \gamma_-(a)$, since $\varepsilon(a,\gamma) = -a\,(\gamma - \gamma_+(a))\,(\gamma - \gamma_-(a))$ and $\gamma - \gamma_+(a) < 0$. The stability comes from the inequalities $\rho_0 > 0$ and $d_C < 0$. The case $a > \sqrt{\beta}$ is the dual case where $\rho_0 < 0$ and the bifurcation appears for $\gamma < \gamma_-(a)$ leading to an unstable limit cycle.
To show statement (d) we consider first the case $a < \sqrt{\beta}$. Now, from statement (c) of Lemma 65, we have $a < a\beta < \gamma_+(a)$ and so $m_0 > 0$. Here $\rho_0 > 0$, and as $\gamma - \gamma_-(a) < 0$, the limit cycle bifurcates for $\gamma > \gamma_+(a)$ but it is unstable because $d_C = \gamma - a\beta > 0$. The case $\sqrt{\beta} < a < \sqrt{(1+\beta)/\beta}$, which is only possible when $\beta < \phi$, is the dual case with $\rho_0 < 0$, also leading to an completely unstable limit cycle.
Regarding statement (e), we see that

$$a^2 < \frac{1+\beta}{\beta} = 1 + \frac{1}{\beta} \leq 1 + \frac{1}{\phi} = \phi \leq \beta,$$

so that $\rho_0 < 0$ as before, along with $d_C > 0$, and the Theorem follows. □

A similar result can be stated for $0 < b < a$, its proof is analogous and so it is omitted.

Theorem 70. *Consider the reduced system (4.35)-(4.36) with $|h| < |d_C| \neq 0$, $0 < b < a$, $\beta \neq 1$, and $\gamma > 0$. Additionally, consider the functions $a_\pm(\gamma)$ and $\gamma_\pm(a)$ defined in (4.48)-(4.50) respectively. The following statements hold.*

(a) If $0 < \beta < 1$ then at the points $(a,\gamma) = (a_-(\gamma),\gamma)$ the system undergoes a FCLC bifurcation, so that a completely unstable limit cycle bifurcates for $a > a_-(\gamma)$.

(b) If $0 < \beta < 1$ then at the points $(a,\gamma) = (a_+(\gamma),\gamma)$ with $\gamma < \sqrt{\beta(1+\beta)}$ the system undergoes a FCLC bifurcation, so that a stable limit cycle bifurcates for $a > a_+(\gamma)$.

(c) If $\beta > 1$ then at the points $(a,\gamma) = (a,\gamma_-(a))$ with $a < \sqrt{\beta}$ $(a > \sqrt{\beta})$ the system undergoes a FCLC bifurcation, so that an unstable (stable) limit cycle bifurcates for $\gamma < \gamma_-(a)$ $(\gamma > \gamma_-(a))$.

(d) If $1 < \beta < \phi$ then at the points $(a, \gamma) = (a, \gamma_+(a))$ with $a < \sqrt{\beta}$ $(\sqrt{\beta} < a < \sqrt{(1+\beta)/\beta})$ the system undergoes a FCLC bifurcation, so that an completely unstable (unstable) limit cycle bifurcates for $\gamma < \gamma_+(a)$ $(\gamma > \gamma_+(a))$.

(e) If $\beta \geq \phi$ then at the points $(a, \gamma) = (a, \gamma_+(a))$ with $a < \sqrt{(1+\beta)/\beta}$ the system undergoes a FCLC bifurcation, so that an unstable limit cycle bifurcates for $\gamma < \gamma_+(a)$.

In all the above cases, the system has for the critical values of parameters indicated a linear center in the region $|\mathbf{e}_1^T \mathbf{x}| \leq 1$ and the limit cycle bifurcates from the most external periodic orbit of the center.

In Figure 4.7, we give a schematic view of the different FCLC bifurcations predicted by Theorems 69 and 70. We denote by s,u, cu the stable, unstable and completely unstable character of the bifurcating limit cycle. The arrows across the branches of the curve $\varepsilon(a, \gamma) = 0$ denote the reported bifurcations.

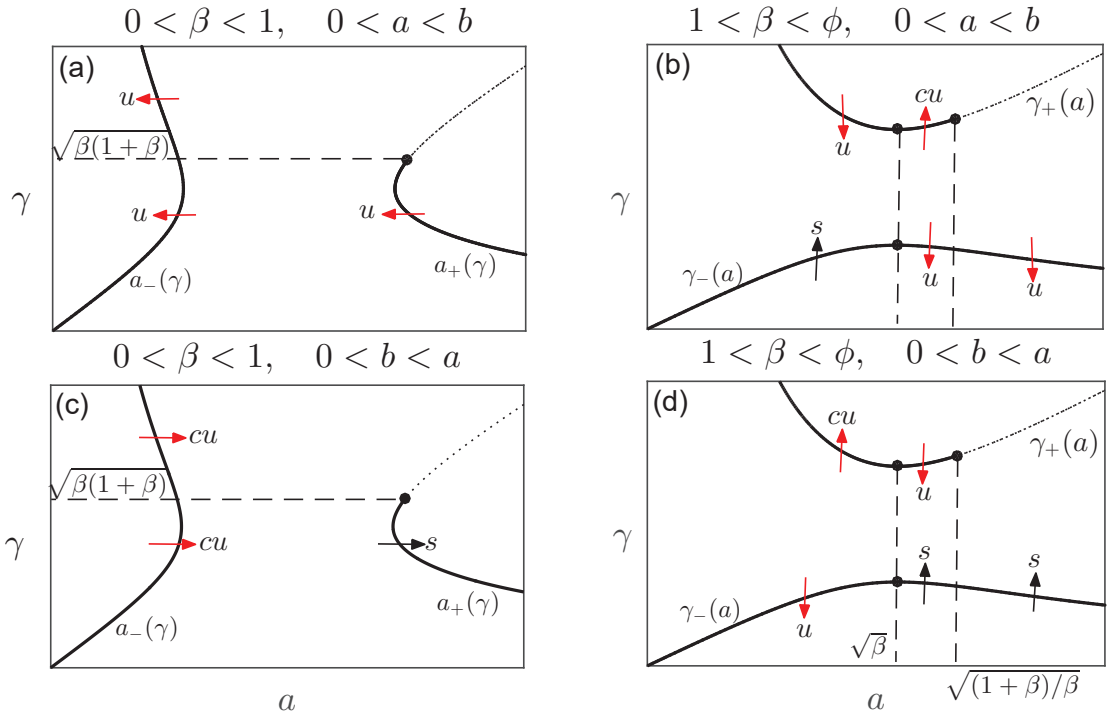

Figure 4.10: Scheme of the bifurcations reported in Theorems 69 and 70. Panels (a) and (b) correspond to Theorem 69, while panels (c) and (d) to Theorem 70.

Next, we give our last main result for the 4D discontinuous system (4.25), which emphasizes three cases of simultaneous appearance of an infinite number of stable periodic orbits in what can be called a multiple focus-center-cycle (for short, MFCC) bifurcation. This bifurcation, to be reported for the first time up to the best of our knowledge, is a consequence of the standard focus-center-limit cycle bifurcations that occur in such invariant CPWL manifold S_h for the values of h with $|h| < |d_C|$.

Note that the multiple stable oscillations that are predicted cannot be called limit cycles as long as they are non isolated when one thinks of the 4D system (4.25).

Theorem 71. *Consider the discontinuous system (4.25) with $\beta \neq 1$. Additionally, consider the functions a_+ and γ_- defined in (4.48)-(4.50) respectively. The following statements hold.*

(a) If $\beta > 1$, $a < \sqrt{\beta}$ and $0 < a < b$ then for $\gamma = \gamma_-(a)$ the system undergoes a MFCC bifurcation, so that when $\gamma \leq \gamma_-(a)$ all the equilibria in central segment are stable, becoming unstable for $\gamma > \gamma_-(a)$. When $\gamma = \gamma_-(a)$ there appears a bounded, simply connected set, symmetric with respect to the origin and completely full of periodic orbits that surrounds such set of central equilibria. For $\gamma - \gamma_-(a) > 0$ and sufficiently small, the above set of periodic orbits disappears giving rise to a bounded hypersurface $\Omega \subset \mathbb{R}^4$ foliated by stable periodic orbits.

(b) If $0 < \beta < 1$, $\gamma < \sqrt{\beta(1+\beta)}$ and $0 < b < a$ then for $a = a_+(\gamma)$ the system undergoes a MFCC bifurcation, so that when $a \leq a_+(\gamma)$ all the equilibria in central segment are stable, becoming unstable for $a > a_+(\gamma)$. When $a = a_+(\gamma)$ there appears a bounded, simply connected set, symmetric with respect to the origin and completely full of periodic orbits that surrounds such set of central equilibria. For $a - a_+(\gamma) > 0$ and sufficiently small, the above set of periodic orbits disappears giving rise to a bounded hypersurface $\Omega \subset \mathbb{R}^4$ foliated by stable periodic orbits.

(c) If $0 < \beta < 1$, $a > \sqrt{\beta}$ and $0 < b < a$ then for $\gamma = \gamma_-(a)$ the system undergoes a MFCC bifurcation, so that when $\gamma \leq \gamma_-(a)$ all the equilibria in central segment are stable, becoming unstable for $\gamma > \gamma_-(a)$. When $\gamma = \gamma_-(a)$ there appears a bounded, simply connected set, symmetric with respect to the origin and completely full of periodic orbits that surrounds such set of central equilibria. For $\gamma - \gamma_-(a) > 0$ and sufficiently small, the above set of periodic orbits disappears giving rise to a bounded hypersurface $\Omega \subset \mathbb{R}^4$ foliated by stable periodic orbits.

In Figure 4.11, we show the effect of the reported MFCC bifurcation on system (4.25). Before the bifurcation we have stable equilibria (Figure 4.11(a)) in the central segment. After Figure 4.11(b), these equilibria are unstable with a sudden appearance of a hypersurface of stable periodic orbits.

4.8 Numerical examples

Just to demonstrate the dynamical richness of these memristor oscillators, we select two numerical examples. In the first example, we show another case of the existence of hypersurfaces of periodic orbits, this time related to boundary equilibrium bifurcations (BEB). Furthermore, we also show a case where have detected a h-route to chaos in the reduced model.

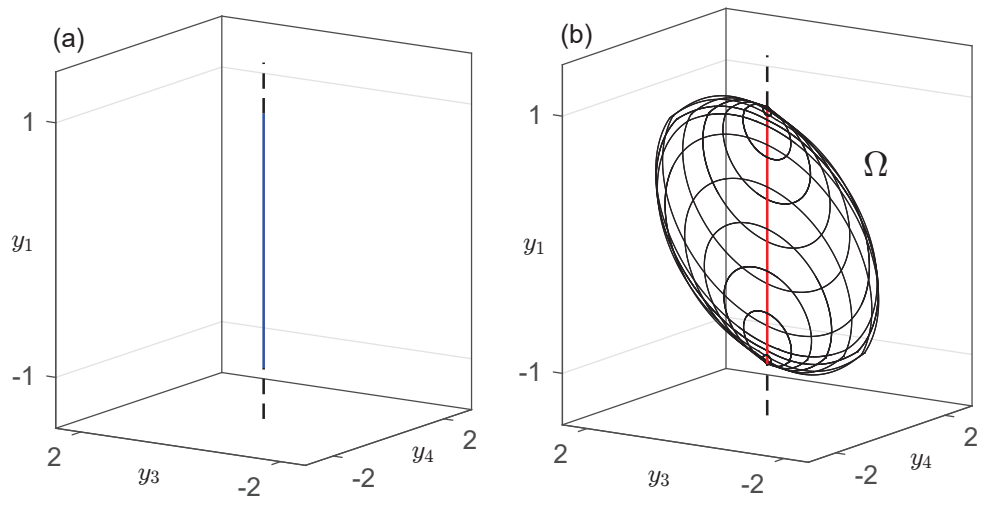

Figure 4.11: The MFCC bifurcation predicted by Theorem 71(a) in the discontinuous system (4.25). In panel (a) points in the blue line correspond to the stable equilibria in the central zone. In panel (b) for $\gamma > \gamma_-(a)$, we show the 3D projection of some slices of the hypersurface Ω that bifurcate from the multiple center when $\gamma = \gamma_-(a)$. Parameters are $\beta = 1.2$, $a = 0.8$, $\gamma = \gamma_-(a) + 0.02$, $b = 2$. The equilibrium points of the system are unstable in all zones, the red line shows the unstable equilibria in the central zone.

4.8.1 Non-smooth fold BEB with unstable zones and stable periodic orbits.

Consider system (4.35)-(4.36) with parameters

$$\beta = 0.5, \quad \gamma = 0.325, \quad a = 0.2, \quad b = 3.5. \tag{4.56}$$

In this case, the system has the linear invariants $t_C = 0.125$, $d_C = 0.225$, $t_E = -3.175$, $d_E = -1.425$ and the eigenvalues of matrices $A_{C,E}$ are $\lambda_{C,E} \in \mathbb{R}$ and $\sigma_{C,E} \pm i\omega_{C,E}$ given by

$$\begin{aligned}
&\lambda_C = 0.1562624, \quad \sigma_C = -0.0156312,\\
&\omega_C = 1.1998503298,\\
&\lambda_E = -3.2008358, \quad \sigma_E = 0.0129179,\\
&\omega_E = 0.6671051.
\end{aligned}$$

From Propositions 62 and 63 the system has for $|h| > d_C$ only one unstable real equilibrium point and for $|h| < d_C$ three unstable real equilibrium points and at $h = \pm d_C$ we have a non-smooth fold BEB of unstable equilibrium points. In Figure 4.12, we have in dashed red line the real equilibrium points. When $h = \pm d_C$ a stable periodic orbit is created and for $|h| < |d_C|$ two stable periodic orbits coexist.

From Proposition 60 this set of periodic orbits can be translated to the 4D original model leading to certain hypersurface foliated by periodic orbits. Although the lack

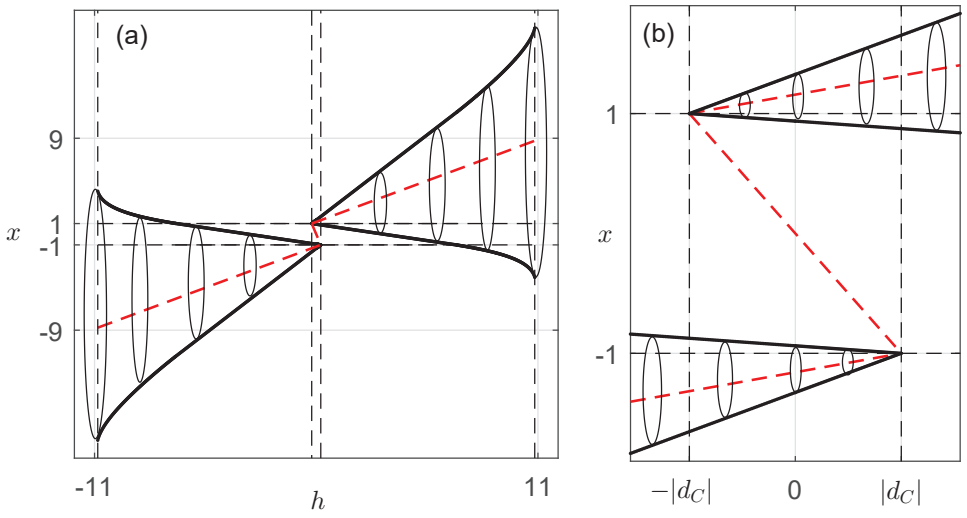

Figure 4.12: (a) Fixed parameters as in (4.56), showing the bifurcation diagram of the canonical system (4.35)-(4.36) varying parameter h, its minimum and maximum x-values are plotted, in black the schematic stable periodic orbits are drawn. The dashed red line represents the coordinate x of the real unstable equilibrium points. (b) A zoom into the bifurcation diagram (a).

of theoretical results for these BEB precludes at this moment any non-numerical justification, we can advance that it is possible to show the sudden appearance of these hypersurfaces in a MFCC bifurcation similar to the one included in this paper. This will be the subject of future work.

4.8.2 Route to chaos without parameters

In section 3.1 of Itoh and Chua [2008], authors consider the discontinuous system (4.19) with the function q defined as in (4.31). They detect numerically a chaotic attractor for the set of parameters $\alpha = 4$, $\beta = 1$, $\gamma = 0.65$, $a = 0.2$ and $b = 10$. The change of variables given in (4.23) transforms the system into the form (4.35)-(4.36) where the new parameters are given by

$$\beta = 0.5, \quad \gamma = 0.325, \quad a = 0.4, \quad b = 20. \tag{4.57}$$

For these parameters we obtain the linear invariants $t_C = -0.075$, $d_C = 0.125$, $t_E = -19.675, d_E = -9.675$ and the eigenvalues of matrices $A_{C,E}$ are $\lambda_{C,E} \in \mathbb{R}$ and $\sigma_{C,E} \pm i\omega_{C,E}$ given by

$$\begin{aligned} &\lambda_C = 0.09025818, \quad \sigma_C = -0.0826290, \\ &\omega_C = 1.17392007, \\ &\lambda_E = -19.949936, \quad \sigma_E = 0.13746820, \\ &\omega_E = 0.68269059. \end{aligned}$$

From Propositions 62 and 63 the system has for $|h| > d_C$ only one unstable real equilibrium point and for $|h| < d_C$ three unstable real equilibrium points. As in

the previous example, and at $h = \pm d_C$ we have a non-smooth fold BEB of unstable equilibrium points.

Following Tucker [2002], by computing the Poincaré map on the plane $x = 1$, and taking h as the bifurcation parameter of system (4.35)-(4.36), we obtain the numerical bifurcation diagram given in Figure 4.13(a).
We observe that the system undergoes several period-doubling bifurcations, see the corresponding periodic orbits of Figure 4.13 (b),(c),(d). Finally, for $h_0 = 0$ the system has a symmetric pair strange attractors of two zones, see Figure 4.13(e).

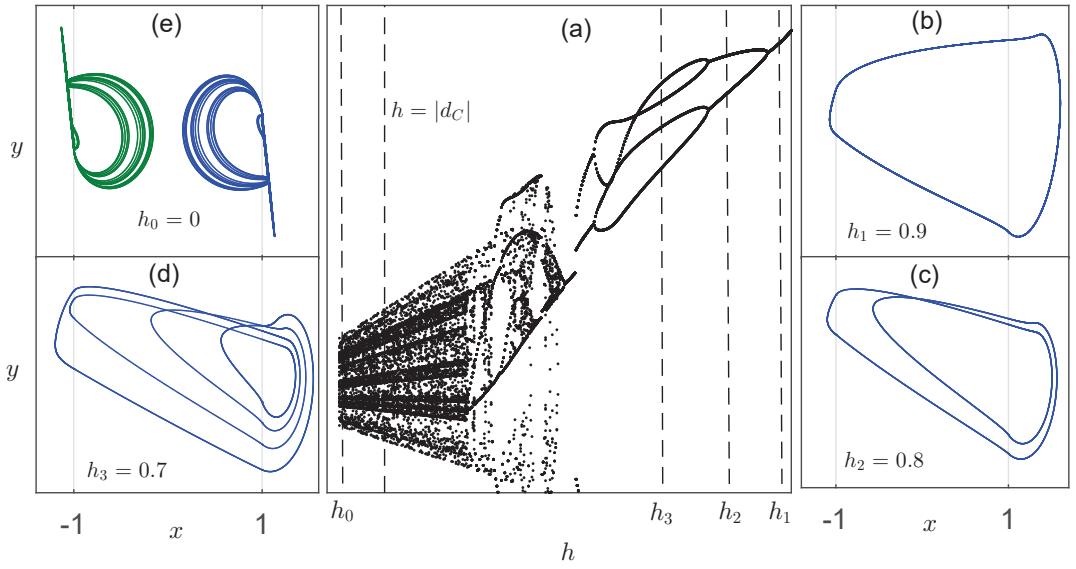

Figure 4.13: Parameters fixed as in (4.57) (a) The coordinate y of the poincaré section $x = 1$. Bifurcation diagram of the canonical system (4.35)-(4.36) varying parameter h. (b) For $h_1 = 0.9$ we shown a stable periodic orbit of three zones. (c) For $h_2 = 0.8$ we have a stable 2-periodic orbit of three zones. (d) For $h_3 = 0.7$ we have a stable 4-periodic orbit of three zones. (e) When $h_0 = 0$ the system has two symmetric strange attractors of two zones.

Since the parameter h is not present in the original model, but it is associated to the initial conditions, we can speak of a route to chaos without parameters or a phase-space route to chaos. In fact, more than multistability in the 4D model, we should better speak of the existence of a non-denumerable set of attractors.

For instance, in Figure 4.14, using the initial conditions in each invariant set $S_{0.9}$, S_0 and Proposition 60, we show in the discontinuous system (4.25), two symmetric stable periodic orbits that coexist with two symmetric strange attractors.

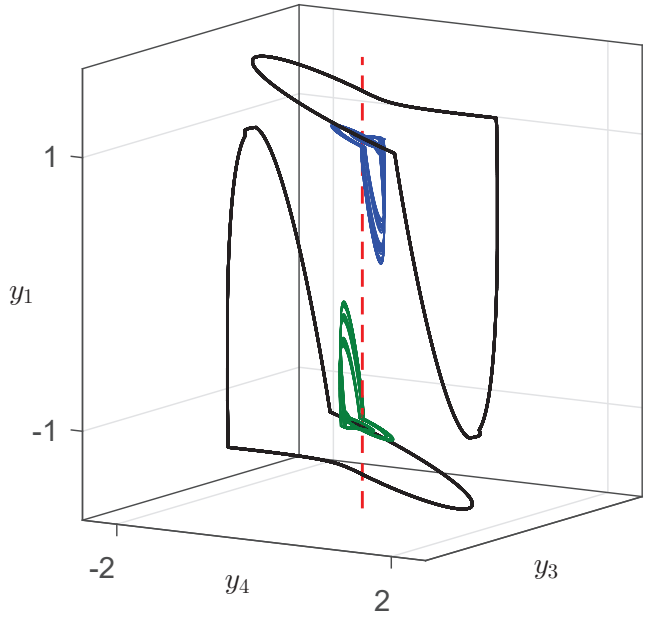

Figure 4.14: Parameters fixed as in (4.57). Using Proposition 60, the coexistence of the two strange attractors and of two stable periodic orbits in the discontinuous system (4.25) is shown. The dashed red line represents the coordinate x of the unstable equilibrium points.

Bibliography

V.N. Afanasiev, V.B. Kolmanovskii, and V.R. Nosov. *Mathematical Theory of Control Systems Design*. Springer Netherlands, 1 edition, 1996. ISBN 978-94-017-2203-2. URL https://www.springer.com/us/book/9780792337249.

M. Di Bernardo, A. Nordmark, and G. Olivar. Discontinuity-induced bifurcations of equilibria in piecewise-smooth and impacting dynamical systems. *Physica D: Nonlinear Phenomena*, 237(1):119 – 136, 2008a. ISSN 0167-2789. URL https://doi.org/10.1016/j.physd.2007.08.008.

Mario Di Bernardo, Chris Budd, Alan Richard Champneys, and Piotr Kowalczyk. *Piecewise-smooth Dynamical Systems*. Springer-Verlag London, 1 edition, 2008b. ISBN 978-1-84628-708-4. URL https://www.springer.com/la/book/9781846280399.

V. Carmona, E. Freire, E. Ponce, J. Ros, and F. Torres. Limit cycle bifurcation in 3D continuous piecewise linear systems with two zones: Application to Chua's circuit. *International Journal of Bifurcation and Chaos*, 15(10):3153–3164, 2005a. URL https://doi.org/10.1142/S0218127405014027.

V. Carmona, E. Freire, E. Ponce, and F. Torres. Bifurcation of invariant cones in piecewise linear homogeneous systems. *International Journal of Bifurcation and Chaos*, 15(08):2469–2484, 2005b. URL https://doi.org/10.1142/S0218127405013423.

V. Carmona, E. Freire, E. Ponce, and F. Torres. The continuous matching of two stable linear systems can be unstable. *Discrete and Continuous Dynamical Systems*, 16(3):689–703, 2006. ISSN 1078-0947. URL https://doi.org/10.3934/dcds.2006.16.689.

F. Corinto and M. Forti. Memristor circuits: Flux-charge analysis method. *IEEE Transactions on Circuits and Systems I: Regular Papers*, 63(11):1997–2009, nov 2016. URL https://doi.org/10.1109/tcsi.2016.2590948.

F. Corinto and M. Forti. Memristor circuits: Bifurcations without parameters. *IEEE Transactions on Circuits and Systems I: Regular Papers*, 64(6):1540–1551, jun 2017. URL https://doi.org/10.1109/tcsi.2016.2642112.

M. Di Bernardo, D.J. Pagano, and E. Ponce. Nonhyperbolic boundary equilibrium bifurcations in planar filippov systems: A case study approach. *International Journal of Bifurcation and Chaos*, 18(05):1377–1392, 2008. URL https://doi.org/10.1142/S0218127408021051.

A.F. Filippov. *Differential Equations with Discontinuous Righthand Sides*. Springer Netherlands, 1 edition, 1988. ISBN 978-90-277-2699-5. URL https://www.springer.com/us/book/9789027726995.

E. Freire, E. Ponce, and J. Ros. The focus-center-limit cycle bifurcation in symmetric 3D piecewise linear systems. *SIAM J. Appl. Math*, 65(6):1933–1951, 2005. URL https://doi.org/10.1137/040606107.

E. Freire, E. Ponce, and J. Ros. Bistability and hysteresis in symmetric 3D piecewise linear oscillators with three zones. *International Journal of Bifurcation and Chaos*, 18(12):3633–3645, 2008. URL https://doi.org/10.1142/S0218127408022603.

E. Freire, E. Ponce, and J. Ros. Following a saddle-node of periodic orbits bifurcation curve in Chua's circuit. *International Journal of Bifurcation and Chaos*, 19(02): 487–495, 2009. URL https://doi.org/10.1142/S0218127409023147.

M. Itoh and L.O. Chua. Memristor oscillators. *International Journal of Bifurcation and Chaos*, 18(11):3183–3206, 2008. URL http://dx.doi.org/10.1142/S0218127408022354.

Jaume Llibre and Antonio E. Teruel. *Introduction to the qualitative theory of differential systems: planar, symmetric and continuous piecewise linear systems*. Birkhauser, 2014. URL https://www.springer.com/us/book/9783034806565.

E. Ponce, J. Ros, and E. Vela. Unfolding the fold-Hopf bifurcation in piecewise linear continuous differential systems with symmetry. *Physica D: Nonlinear Phenomena*, 250:34–46, 2013. URL https://doi.org/10.1016/j.physd.2013.01.010.

W. Tucker. Computing accurate Poincaré maps. *Physica D: Nonlinear Phenomena*, 171(3):127 – 137, 2002. ISSN 0167-2789. URL https://doi.org/10.1016/S0167-2789(02)00603-6.

Elísabet Vela. *Piecewise linear differential systems: Limit cycles and analysis of bifurcations*. PhD thesis, University of Sevilla, Spain, 2013. URL https://idus.us.es/xmlui/bitstream/handle/11441/55165/111112013velafsiste.pdf?sequence=1.

Part II

Two-dimensional stroboscopic maps

Chapter 5

On the BB bifurcation in stroboscopic maps of DPWL systems

In this chapter, we consider the two-dimensional stroboscopic map defined by the normalized canonical form for discontinuous piecewise linear (DPWL, for short) systems introduced in Freire et al. [2014]. We rigorously study the properties of the map and we give sufficient conditions for the existence of two-periodic orbits. In addition, considering a special family of n-periodic orbits, we study the border collision bifurcation curves of these orbits, and we give a sufficient conditions for the admissibility of such orbits.

In Fossas and Granados [2013], authors consider a two-dimensional stroboscopic map defined by a second order system with a relay based control and a linear switching surface, giving a conjecture about the presence of a big bang bifurcation point in this map. We show that this stroboscopic map is a particular case of our two-dimensional map, and by using the theory developed in this chapter, we present a conjecture about the presence of a Big Bang (BB, for short) bifurcation point of codimension-two in our map.

5.1 Introduction

In Avrutin and Schanz [2006], the discrete one-dimensional dynamical system

$$x_{n+1} = \begin{cases} bx_n + c, & \text{if} \quad x_n < 0, \\ x_n - a, & \text{if} \quad x_n > 0, \end{cases}$$

is considered. Despite its simplicity, the intersection of an infinite number of codimension-one bifurcation lines was shown both in two and three-dimensional parameter spaces. Later, in Avrutin et al. [2006], the concept of big-bang bifurcation (BB bifurcation, for short) was presented, analyzing both two and three-dimensional parameter space and it was shown that BB bifurcations can be classified in three kinds: period-increasing with attractor coexistence, period-increasing with period-adding and period-increasing with chaotic inclusions. In Avrutin et al. [2007], a

codimension-N BB bifurcation point is defined as a point in the N-dimensional parameter space ($N \geq 2$) where an infinite number of codimension $N-1$ curves intersect. In Avrutin et al. [2011], the authors gave sufficient conditions for the presence of the big bang bifurcation of the period incrementing type in a piecewise one-dimensional map. An excellent review of the BB bifurcation can be found in Granados et al. [2017].

In this context, the jump from dimension one to dimension two represents a really challenging problem. The presence of BB bifurcations in two-dimensional maps are reported in some works. In Fossas and Granados [2013], a BB bifurcation point of codimension two is shown in a second order system with a relay based control and a linear switching surface. In Amador et al. [2014], the authors show the existence of a BB bifurcation point in a two-dimensional system defined by a Boost Converter controlled by centered pulse-width modulation and a ZAD (Zero Average Dynamics) strategy.

Following Fossas and Granados [2013], we start by considering a second order system with a relay based control and a linear switching surface defined by

$$\dot{\mathbf{x}} = \begin{cases} A\mathbf{x} + \mathbf{b}, & \text{if} \quad \sigma(\mathbf{x}) \geq 0, \\ A\mathbf{x} - \mathbf{b}, & \text{if} \quad \sigma(\mathbf{x}) < 0, \end{cases} \tag{5.1}$$

where the matrix A and vector $\mathbf{b}$ are defined by

$$A = \begin{pmatrix} 0 & 1 \\ -a_0 & -a_1 \end{pmatrix}, \quad \mathbf{b} = \begin{pmatrix} 0 \\ bk \end{pmatrix}, \tag{5.2}$$

and the switching surface is defined as

$$\sigma(\mathbf{x}) = \mathbf{e}_1^T \mathbf{x} + c\,\mathbf{e}_2^T \mathbf{x} - y_c. \tag{5.3}$$

where $\mathbf{e}_1^T = (1,0), \mathbf{e}_2^T = (0,1)$ and b, k, c and y_c are real numbers.

First, in the next result, we put system (5.1)-(5.2) into the normal form for the border collision bifurcation proposed in Nusse and Yorke [1992].

Proposition 72. *System (5.1)-(5.2) can by rewritten into the form*

$$\dot{\mathbf{x}} = \mathbf{F}(\mathbf{x}) = \begin{cases} \mathbf{F}_L(\mathbf{x}) = A\mathbf{x} + \mathbf{b}_L, & \text{if} \quad \mathbf{e}_1^T \mathbf{x} \leq 0, \\ \mathbf{F}_R(\mathbf{x}) = A\mathbf{x} + \mathbf{b}_R, & \text{if} \quad \mathbf{e}_1^T \mathbf{x} > 0, \end{cases} \tag{5.4}$$

where the new matrix A and vectors $\mathbf{b}_{\{L,R\}}$ are

$$A = \begin{pmatrix} -ca_0 & a_0c^2 - a_1c + 1 \\ -a_0 & ca_0 - a_1 \end{pmatrix}, \ \mathbf{b}_R = \begin{pmatrix} bkc - ca_0y_c \\ bk - a_0y_c \end{pmatrix}, \ \mathbf{b}_L = \begin{pmatrix} -bkc - ca_0y_c \\ -bk - a_0y_c \end{pmatrix}, \tag{5.5}$$

and $\mathbf{e}_1$ is the first canonical vector.

Proof. It is sufficient to consider the change of variables

$$\tilde{\mathbf{x}} = \begin{pmatrix} 1 & c \\ 0 & 1 \end{pmatrix} \mathbf{x} - \begin{pmatrix} y_c \\ 0 \end{pmatrix}.$$

□

When the condition $\mathbf{F}_L(0,y) = \mathbf{F}_R(0,y)$ is fulfilled for every value of y, then system (5.4)-(5.5) turn out to be continuous, otherwise the system is discontinuous. In what follows we assume that the system is discontinuous.

Although both functions $\mathbf{F}_L$ and $\mathbf{F}_R$ are defined in every point of $\mathbb{R}^2$, the vector field $\mathbf{F}$ is not explicitly defined when $x = 0$, and so the definition of a solution for discontinuous system (5.4)-(5.5) needs to be clarified. As usual, we will adopt the Filippov convex method, so that solutions can be uniquely defined in forward time, although they can be nonsmooth, see Kuznetsov et al. [2003] for more details.

If $\mathbf{F}_L(0,y) \cdot \mathbf{F}_R(0,y) > 0$, then both vector fields are transversal to the discontinuity line and their normal components have the same sign. In this case, we will assume that orbits are concatenated in the natural way. Following the terminology introduced in Freire et al. [2012], we say that this point is a crossing point, so that the crossing set Σ^c is defined by

$$\Sigma^c = \{(0,y) \,:\, \mathbf{F}_L(0,y) \cdot \mathbf{F}_R(0,y) > 0\}.$$

If $\mathbf{F}_L(0,y) \cdot \mathbf{F}_R(0,y) \leq 0$, then either the normal components of vector fields to the discontinuity line have opposite sign or at least one of them vanishes. We say that $(0,y)$ is a sliding point, and the set

$$\Sigma^s = \{(0,y) \,:\, \mathbf{F}_L(0,y) \cdot \mathbf{F}_R(0,y) \leq 0\}$$

is the sliding set.

The dynamics of system (5.4)-(5.5) can be discretized by using a fixed sampling time what produces a stroboscopic map, see for instance Granados et al. [2014] for more details. Now, for a fixed $t > 0$ and taking into account the solutions of system (5.4)-(5.5), the stroboscopic map is defined as

$$P(\mathbf{x};t) = \begin{cases} e^{At}\mathbf{x} + (e^{At} - I)A^{-1}\mathbf{b}_L, & \text{if} \quad \mathbf{e}_1^T\mathbf{x} \leq 0, \\ e^{At}\mathbf{x} + (e^{At} - I)A^{-1}\mathbf{b}_R, & \text{if} \quad \mathbf{e}_1^T\mathbf{x} > 0, \end{cases} \tag{5.6}$$

where from here we assume that the matrix A is invertible.

Note that the previous map always has two fixed points given by

$$\mathbf{x}^*_{\{L,R\}} = -A^{-1}\mathbf{b}_{\{L,R\}}.$$

As usual, when $\mathbf{e}_1^T\mathbf{x}^*_L < 0$ or $\mathbf{e}_1^T\mathbf{x}^*_R > 0$ the fixed point are real, otherwise these are virtual fixed points.

In Fossas and Granados [2013], the authors consider the stroboscopic map (5.5)-(5.6) and take variables y_c and k as main bifurcation parameters. They numerically detected the presence of an infinite number of periodic orbits with arbitrarily large periods near to the point $(0,0)$ of the parameter plane (y_c,k), see Figure 5.1. These periodic orbits exist when both fixed points are virtual and the sliding set Σ^s is attractive. Such a point in the parameter plane (y_c,k) seems to be a BB bifurcation point of codimension two. As the main consequence of the quoted paper, it is

conjectured that when the eigenvalues of the matrix e^{At} are real and lower than 1, both fixed point are virtual and the sliding set Σ^s is attractive, then the stroboscopic map (5.6)-(5.5) has a BB bifurcation point at $(y_c, k) = (0, 0)$.

In Figure 5.1(a) we show the border collision bifurcation curves separating existence regions of periodic orbits on the parameter plane (y_c, k) for the map (5.5)-(5.6) and for parameter values $a_0 = 1$, $a_1 = 5$, $b = 1$, $c = 1.5$ and $t = 0.1$. On the red lines, the fixed points change from real to virtual, that is, $\mathbf{e}_1^T\mathbf{x}_L^* = 0$ or $\mathbf{e}_1^T\mathbf{x}_R^* = 0$. The blue line is a circular arc on the two-parametric plane. In (b) we show a bifurcation diagram along the circular arc parametrized by the angle θ. In Figure (c) we show a period diagram of the bifurcation diagram given in (b).

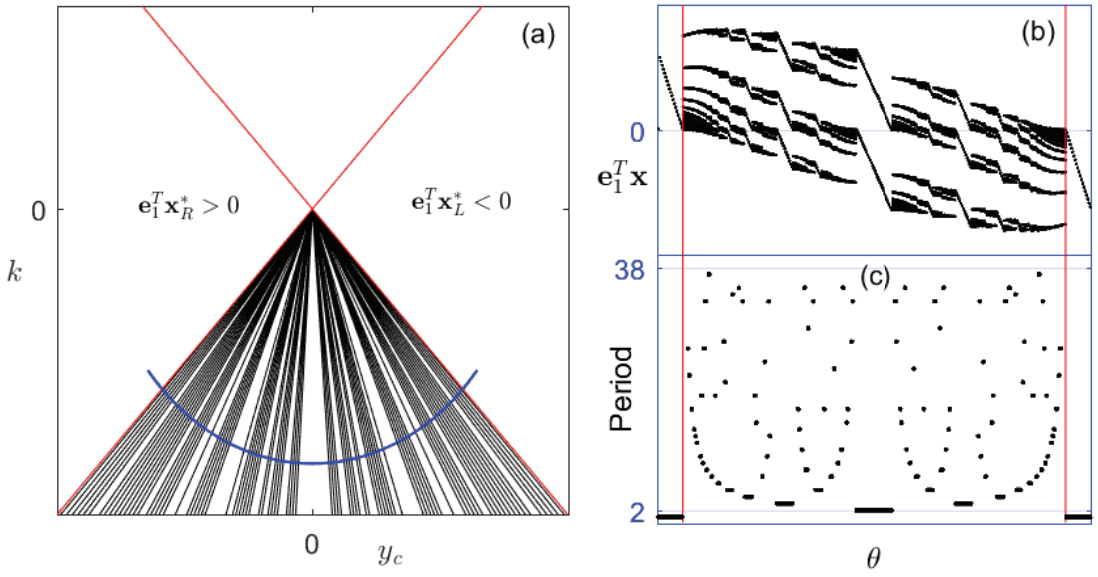

Figure 5.1: (a) The border collision bifurcation curves separating existence regions of periodic orbits on the parameter plane (y_c, k) for the map (5.5)-(5.6) and for parameter values $a_0 = 1$, $a_1 = 5$, $b = 1$, $c = 1.5$ and $t = 0.1$. (b) Bifurcation diagram along the blue curve in (a) parametrized by the angle θ. (c) Periods (numerically computed) of the periodic orbits found along the blue curve in (a) parametrized by the angle θ.

Note that system (5.4) is a discontinuous piecewise linear system, and therefore, the discontinuous canonical forms defined in Freire et al. [2012] and Freire et al. [2014] can be applied. These canonical forms allow us to reduce the number of parameters and also, to characterize the sliding set and its stability with only one parameter.

In what follows, we will study the stroboscopic map defined by the normalized canonical form, the general properties of this map and the existence and stability of its periodic orbits.

5.2 Canonical forms for DPWL systems

In this section we present the canonical forms for discontinuous piecewise linear (DPWL, for short) systems, which were defined in Freire et al. [2012] and Freire et al. [2014]. This material uses a slightly different notation from the notation used in the quoted works. Consider the sets $\mathbf{\Sigma}_L$ and $\mathbf{\Sigma}_R$ defined as

$$\mathbf{\Sigma}_L = \left\{\mathbf{x} \in \mathbb{R}^2 : \mathbf{e}_1^T\mathbf{x} < 0\right\}, \quad \mathbf{\Sigma}_R = \left\{\mathbf{x} \in \mathbb{R}^2 : \mathbf{e}_1^T\mathbf{x} \geq 0\right\}. \tag{5.7}$$

where $\mathbf{e}_1$ is the first canonical vector. We start by considering the differential system

$$\dot{\mathbf{x}} = \begin{cases} A_L\mathbf{x} + \mathbf{b}_L, & \text{if} \quad \mathbf{x} \in \mathbf{\Sigma}_L, \\ A_R\mathbf{x} + \mathbf{b}_R, & \text{if} \quad \mathbf{x} \in \mathbf{\Sigma}_R, \end{cases} \tag{5.8}$$

where $A_L = (a_{ij}^L)$, $A_R = (a_{ij}^R)$ are constant matrices of order 2, and $\mathbf{b}_L = (b_1^L, b_2^L)^T$, $\mathbf{b}_R = (b_1^R, b_2^R)^T$ are constant vectors of $\mathbb{R}^2$.

In Freire et al. [2012], a Liénard-like canonical form for general discontinuous planar piecewise linear (DPWL, for short) systems with two linear regions separated by a straight line is defined. This canonical form reduce the number of parameters and concentrate the sliding set and its stability in only one parameter b, see the quoted reference for more details. In the next proposition the Liénard canonical form is shown.

Proposition 73. *Freire et al. [2012] Assume that $a_{12}^R a_{12}^L > 0$ in system (5.8). Then the change of variables*

$$\overline{\mathbf{x}} = \begin{cases} \begin{pmatrix} 1 & 0 \\ a_{22}^L & -a_{12}^L \end{pmatrix}\mathbf{x} - \begin{pmatrix} 0 \\ b_1^L \end{pmatrix}, & \text{if} \quad \mathbf{x} \in \mathbf{\Sigma}_L, \\ \dfrac{1}{a_{12}^R}\begin{pmatrix} a_{12}^L & 0 \\ a_{12}^L a_{22}^R & -a_{12}^L a_{12}^R \end{pmatrix}\mathbf{x} - \begin{pmatrix} 0 \\ b_1^L \end{pmatrix}, & \text{if} \quad \mathbf{x} \in \mathbf{\Sigma}_R, \end{cases} \tag{5.9}$$

after dropping tildes, transforms system (5.8) into the Liénard canonical form

$$\dot{\mathbf{x}} = \begin{cases} \begin{pmatrix} t_L & -1 \\ d_L & 0 \end{pmatrix}\mathbf{x} - \begin{pmatrix} 0 \\ c_L \end{pmatrix}, & \text{if} \quad \mathbf{x} \in \mathbf{\Sigma}_L, \\ \begin{pmatrix} t_R & -1 \\ d_R & 0 \end{pmatrix}\mathbf{x} - \begin{pmatrix} -b \\ c_R \end{pmatrix}, & \text{if} \quad \mathbf{x} \in \mathbf{\Sigma}_R, \end{cases} \tag{5.10}$$

where t_L, t_R and d_L, d_R are the trace and determinant of matrices A_L and A_R respectively, while the new constants c_L, c_R and b are

$$c_L = a_{12}^L b_2^L - a_{22}^L b_1^L, \quad c_R = \frac{a_{12}^L}{a_{12}^R}\left(a_{12}^R b_2^R - a_{22}^R b_1^R\right), \quad b = \frac{a_{12}^L}{a_{12}^R} b_1^R - b_1^L. \tag{5.11}$$

Besides the invariance of the discontinuity line, the crossing and sliding sets, tangency points, and boundary equilibria of the original system are transformed by the

change of variables (5.9) *into sets and points of the same type for system* (5.10)-(5.11).
Moreover, there is a topological equivalence between systems (5.8) *and* (5.10)-(5.11) *for only all their orbits not having points in common with the sliding set. However, the change of variables preserves the attractive or repulsive character of the sliding set*

The sliding set of canonical form (5.10)-(5.11) is determined by the inequality $\mathbf{F}_L(0,y)\cdot\mathbf{F}_R(0,y) = y(y-b) \leq 0$. When $b<0$ the sliding set is attractive and it is defined by the segment

$$\Sigma^s = \{(x,y) \,:\, x=0, \quad b \leq y \leq 0\}.$$

If $b>0$ the sliding set is unstable and

$$\Sigma^s = \{(x,y) \,:\, x=0, \quad 0 \leq y \leq b\}.$$

By considering the sign of the discriminants of the characteristic equation matrices involved in (5.10),

$$\Delta_{\{L,R\}} = t^2_{\{L,R\}} - 4d_{\{L,R\}}, \tag{5.12}$$

a modal parameter $m_{\{L,R\}} \in \{0,1,i\}$ defined in each zone by

$$m_{\{L,R\}} = \begin{cases} i, & \text{if} \quad \Delta_{\{L,R\}} < 0, \\ 0, & \text{if} \quad \Delta_{\{L,R\}} = 0, \\ 1 & \text{if} \quad \Delta_{\{L,R\}} > 0, \end{cases} \tag{5.13}$$

where i is the unit imaginary, was introduced in Freire et al. [2014]. Then, by using a piecewise linear change of variables and by normalizing the time in a different way for each zone, we can rewrite the Liénard canonical form (5.10)-(5.11) into the so-called normalized canonical form.

Proposition 74. *Freire et al. [2014] Consider canonical form* (5.10)-(5.11)*, the modal parameter* $m_{\{L,R\}}$ *defined as in* (5.13)*, the discriminant* $\Delta_{\{L,R\}}$ *given in* (5.12) *and*

$$\omega_{\{L,R\}} = \begin{cases} 1, & \text{if} \quad m_{\{L,R\}} = 0, \\ \dfrac{\sqrt{|\Delta_{\{L,R\}}|}}{2}, & \text{if} \quad m_{\{L,R\}} \neq 0. \end{cases} \tag{5.14}$$

Then the change of variable

$$\left(\overline{x},\overline{y},\overline{t}\right) = \begin{cases} \left(\dfrac{x}{\omega_L}, y, \dfrac{t}{\omega_L}\right), & \text{if} \quad \mathbf{x} \in \mathbf{\Sigma}_L, \\ \left(\dfrac{x}{\omega_R}, y, \dfrac{t}{\omega_R}\right), & \text{if} \quad \mathbf{x} \in \mathbf{\Sigma}_R, \end{cases} \tag{5.15}$$

where $\mathbf{x} = (x, y)$, *transforms system* (5.10)-(5.11) *into the normalized canonical form*

$$\dot{\mathbf{x}} = \begin{cases} A_L\mathbf{x} - \mathbf{b}_L, & \text{if } \mathbf{x} \in \mathbf{\Sigma}_L, \\ A_R\mathbf{x} - \mathbf{b}_R, & \text{if } \mathbf{x} \in \mathbf{\Sigma}_R, \end{cases} \tag{5.16}$$

where the bars for the new variables have been removed, the new matrices and vectors are

$$A_j = \begin{pmatrix} 2\gamma_j & -1 \\ \gamma_j^2 - m_j^2 & 0 \end{pmatrix}, \quad \mathbf{b}_R = \begin{pmatrix} -b \\ a_R \end{pmatrix}, \quad \mathbf{b}_L = \begin{pmatrix} 0 \\ a_L \end{pmatrix}, \quad j = \{L, R\}. \tag{5.17}$$

and the new constants are defined by

$$a_{\{L,R\}} = \frac{c_{\{L,R\}}}{\omega_{\{L,R\}}}, \quad \gamma_{\{L,R\}} = \frac{t_{\{L,R\}}}{2\omega_{\{L,R\}}}. \tag{5.18}$$

The parameter m_j determines the type of dynamics, for $m = i$ we have a focus, for $m = 0$ we have a improper node, for $m = 1$ we have a node if $|\gamma| \geq 1$ or a saddle if $|\gamma| < 1$. The condition $\gamma^2 - m^2 < 0$ leads to saddle cases, while the condition $\gamma^2 - m^2 \geq 0$ corresponds to anti-saddle cases.

We emphasize that system (5.4)-(5.5) studied in Fossas and Granados [2013] can be rewritten into the canonical form and normalized form defined in (5.10)-(5.11) and (5.16)-(5.17) respectively.

5.3 On the exponential matrix e^{At}

In this section, we will study some properties of the exponential matrix $\Phi = e^{tA}$ when matrix A has the special form given in (5.17), that is

$$A = \begin{pmatrix} 2\gamma & -1 \\ \gamma^2 - m^2 & 0 \end{pmatrix},$$

with $m \in \{0, 1, i\}$. First, we introduce for $k \geq 1$ the functions $C_k(mt)$ and $S_k(mt)$ defined by

$$C_k(mt) = \cosh(kmt), \quad S_k(mt) = \begin{cases} \dfrac{\sinh(kmt)}{m}, & \text{if } m \neq 0, \\ kt, & \text{if } m = 0. \end{cases}$$

Note that for $m = 0$ we have $C_k(mt) = 1$ and that for $m = i$ we get

$$C_k(it) = \cosh(kit) = \cos(kt), \quad S_k(it) = \frac{\sinh(kit)}{i} = \sin kt.$$

Thus, functions C_k and S_k can be rewritten as follows

$$C_k(mt) = \begin{cases} \cosh(kt), & \text{if } m = 1, \\ \cos(kt), & \text{if } m = i, \\ 1, & \text{if } m = 0, \end{cases}, \quad S_k(mt) = \begin{cases} \sinh(kt), & \text{if } m = 1, \\ \sin(kt), & \text{if } m = i, \\ kt, & \text{if } m = 0. \end{cases} \tag{5.19}$$

In order to alleviate notation, we define for $k \geq 1$ and $m \in \{0, 1, i\}$, the auxiliary functions

$$\mu_k^{\pm}(mt) = C_k(mt) \pm \gamma S_k(mt). \tag{5.20}$$

Note that for any $k \geq 1$ we have the identities

$$S_1(kmt) = S_k(mt), \quad C_1(kmt) = C_k(mt), \quad \mu_1^{\pm}(kmt) = \mu_k^{\pm}(mt). \tag{5.21}$$

Now, for $\gamma \in \mathbb{R}$, we can give an expression for the exponential matrix

$$\Phi = e^{tA} = \Phi(mt) = e^{t\gamma} \begin{pmatrix} \mu_1^+(mt) & -S_1(mt) \\ S_1(mt)\, D & \mu_1^-(mt) \end{pmatrix},$$

where $D = \gamma^2 - m^2$. Fixing the parameters m, t which $t > 0$ and by dropping the variables, we will write for convenience

$$\Phi = \Phi(mt), \quad C_k = C_k(mt), \quad S_k = S_k(mt), \quad \mu_k^{\pm} = \mu_k^{\pm}(mt). \tag{5.22}$$

By using the identities given in (5.21), the matrix $\Phi^k = \left(e^{tA}\right)^k$ can be written as

$$e^{tkA} = \Phi(kmt) = e^{kt\gamma} \begin{pmatrix} \mu_k^+ & -S_k \\ S_k D & \mu_k^- \end{pmatrix}. \tag{5.23}$$

In the next result, some identities of the functions defined above are given. The proof is a direct consequence of the definitions and so it is omitted.

Proposition 75. *Given $m \in \{0, 1, i\}$ and $\gamma \in \mathbb{R}$, consider the function C_k, S_k and $\mu_k^{\pm}$ defined in (5.19)-(5.20)-(5.22) and $D = \gamma^2 - m^2 \neq 0$. The following identities hold.*
For any $k \geq 1$

$$C_k^2 - m^2 S_k^2 = \mu_k^+ \mu_k^- + S_k^2 D = 1, \tag{5.24}$$
$$\mu_k^+ + \mu_k^- = 2C_k, \quad \mu_{-k}^{\pm} = \mu_k^{\mp}, \tag{5.25}$$
$$S_{-k} = -S_k, \quad \mu_k^+ \mu_k^- = C_k^2 - \gamma^2 S_k^2, \tag{5.26}$$
$$S_1 = S_k C_{k-1} - C_k S_{k-1}, \quad C_1 = C_k C_{k-1} - m^2 S_k S_{k-1}, \tag{5.27}$$
$$\mu_{k-1}^+ = \mu_k^+ \mu_1^- + S_k S_1 D, \tag{5.28}$$
$$S_{k-1} = S_k \mu_1^+ - \mu_k^+ S_1. \tag{5.29}$$

For any $k \geq 2$

$$\mu_{k-2}^- = \mu_{k-1}^- \mu_1^+ + S_{k-1} S_1 D, \tag{5.30}$$
$$\mu_{k-2}^+ = \mu_k^+ \mu_2^- + S_k S_2 D, \tag{5.31}$$
$$S_{k-2} = S_k \mu_2^+ - \mu_k^+ S_2 = C_1 S_{k-1} - S_1 C_{k-1}, \tag{5.32}$$
$$\mu_{k-2}^- = \mu_1^+ \mu_{k-1}^- + S_1 S_{k-1} D, \tag{5.33}$$

Given $n \geq 2$ and $2 \leq k \leq n$

$$\mu_{n-k+1}^+ = 2C_n \mu_{k-2}^- - \mu_{n-1}^- \mu_{k-1}^- + S_{n-1} S_{k-1} D, \tag{5.34}$$
$$\mu_{n-k+2}^+ = 2C_n \mu_{k-1}^- - \mu_n^- \mu_{k-1}^- + S_n S_{k-1} D, \tag{5.35}$$
$$S_{n-k+1} = S_n C_{k-1} - C_n S_{k-1}, \tag{5.36}$$
$$S_{n-k+2} = S_{n-1} C_{k-1} + C_{n-1} S_{k-1} - 2C_n S_{k-2}. \tag{5.37}$$

In the following result some properties of the k-power of the exponential matrix Φ, see (5.23), are studied.

Proposition 76. *Consider the function C_k defined in (5.19)-(5.20)-(5.22). The following statements hold for any $k \in \mathbb{N}$ and $m \in \{0, 1, i\}$.*

(a) The determinant and trace of the matrix Φ^k are

$$\det\left(\Phi^k\right) = e^{kt\gamma}, \quad \operatorname{tr}\left(\Phi^k\right) = 2e^{kt\gamma}C_k. \tag{5.38}$$

(b) The characteristic polynomial of the matrix Φ^k is

$$\det\left(\Phi^k - \lambda I\right) = \lambda^2 - 2\lambda e^{kt\gamma}C_k + e^{2kt\gamma}. \tag{5.39}$$

Moreover, the two eigenvalues of matrix Φ^k are $\lambda_m^{\pm}(\gamma) = e^{kt(\gamma \pm m)}$. Additionally, when $\gamma^2 - m^2 > 0$ and $\gamma < 0$, we have

$$\left|\lambda_m^{\pm}(\gamma)\right| < 1.$$

(c) For any $k \in \mathbb{R}$ the matrix Φ^k is nonsingular and its inverse can be written as

$$\Phi^{-k} = \Phi(-kmt) = e^{-kt\gamma}\begin{pmatrix} \mu_k^- & S_k \\ -S_k D & \mu_k^+ \end{pmatrix}, \tag{5.40}$$

(d) If $k \geq 1$ and 1 is not an eigenvalue of the matrix Φ^k, then the inverse of matrix $\Phi^k - I$ can be written as

$$\left(\Phi^k - I\right)^{-1} = \frac{1}{d(t,\gamma)}\begin{pmatrix} \mu_k^- e^{kt\gamma} - 1 & S_k e^{kt\gamma} \\ -S_k e^{kt\gamma} D & \mu_k^+ e^{kt\gamma} - 1 \end{pmatrix}, \tag{5.41}$$

where the function $d(kt, \gamma)$ is given by

$$d(kt,\gamma) = \det\left(\Phi^k - I\right) = 1 - 2C_k e^{kt\gamma} + e^{2kt\gamma}. \tag{5.42}$$

Proof. To show statements (a), it is sufficient to consider the equality $C_k^2 - m^2 S_k^2 = 1$. Taking into account the equalities

$$\mu_k^+ + \mu_k^- = 2C_k, \quad \mu_k^+ \mu_k^- + S_k^2 D = C_k^2 - m^2 S_k^2 = 1,$$

we obtain directly (5.39) and statement (b) follows.
To show statement (c) it is sufficient to consider the equalities $\mu_{-k}^{\pm} = \mu_k^{\mp}$ and $S_{-k} = -S_k$. Statement (d) is a direct consequence of statement (b) by putting $\lambda = 1$. □

Remark 77. *Regarding statement (b) in Proposition 76, note that if there exists a n-periodic orbit with $\gamma^2 - m^2 > 0$ and $\gamma < 0$ then the n-periodic is stable.*

The function d defined in (5.42) can be written as

$$d\,(kt,\gamma) = \begin{cases} e^{2kt\gamma} - 2e^{kt\gamma}\cos(kt) + 1, & \text{if} \quad m = i, \\ e^{2kt\gamma} - 2e^{kt\gamma}\cosh(kt) + 1, & \text{if} \quad m = 1, \\ e^{2kt\gamma} - 2e^{kt\gamma} + 1, & \text{if} \quad m = 0. \end{cases} \tag{5.43}$$

Therefore, for any $t, k > 0$, it is sufficient to study the function d with $k = 1$, see Figure 5.2. In the next result, we show some properties of the function $d\,(t,\gamma)$.

Proposition 78. *Given $m \in \{0, 1, i\}$ and $t > 0$. Consider the function d defined as in (5.43) with $k = 1$. The following statements hold if we except the case of pure rotation $\gamma = 0$ and $m = i$.*

(a) For $\gamma^2 - m^2 \neq 0$ we have

$$\operatorname{sgn}\left(d\,(t,\gamma)\right) = \operatorname{sgn}\left(\gamma^2 - m^2\right),$$

and when $\gamma^2 - m^2 = 0$ we obtain $d_1\,(t,\gamma) = 0$.

(b) For all $t > 0$ we get

$$\lim_{\gamma\to-\infty} d\,(t,\gamma) = 1, \quad \lim_{\gamma\to\infty} d\,(t,\gamma) = \infty.$$

Proof. If $m = 0$, the conclusion follows from the factorization $d\,(t,\gamma) = \left(e^{t\gamma} - 1\right)^2$. For $m = i$, it is sufficient to consider the inequalities

$$\left(e^{2t\gamma} - 1\right)^2 < e^{4t\gamma} - 2e^{2t\gamma}\cos 2t + 1 < \left(e^{2t\gamma} + 1\right)^2.$$

In the case $m = 1$, after some algebra, we obtain the identity

$$d\,(t,\gamma) = (e^{t\gamma} - e^{t})(e^{t\gamma} - e^{-t}).$$

Now, it is direct to get that $d\,(t,\pm1) = 0$, $d\,(t,\gamma) \neq 0$ for all $\gamma \neq \pm1$ and $d\,(t,\gamma) > 0$ if $\gamma^2 - 1 > 0$ and statement (a) follows. Statement (b) is a direct computation. □

In what follows, to reduce notation, we will write for $k \in \mathbb{N}$

$$d_k := d\,(kt,\gamma). \tag{5.44}$$

Remark 79. *Note that, as a consequence of Proposition 78, if we exclude the case $\gamma = 0$ and $m = i$ then for all $k \geq 1$ and $t > 0$ the matrix $\Phi^k - I$ is nonsingular if and only if $\gamma^2 - m^2 \neq 0$.*

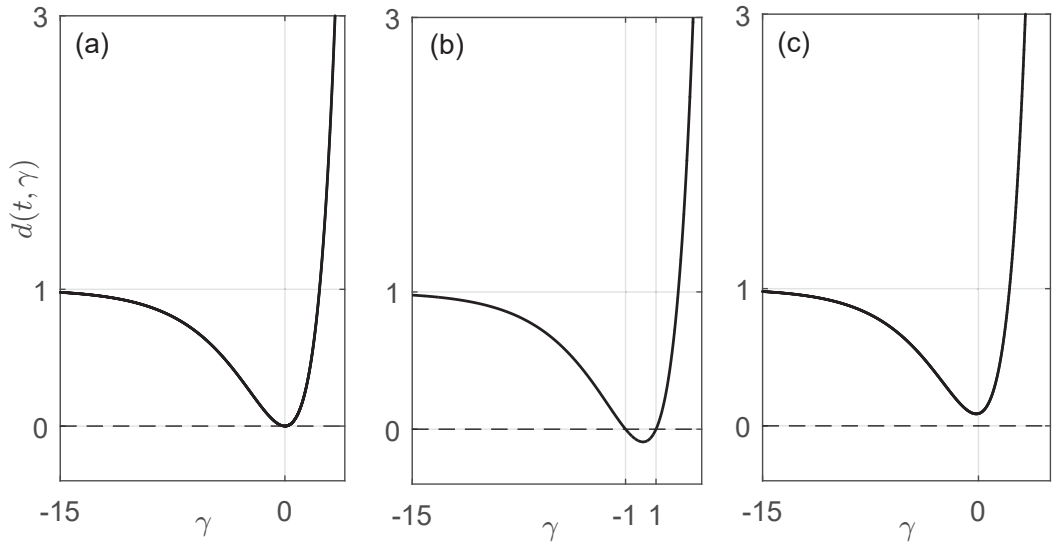

Figure 5.2: The function d defined as in (5.43) with $k = 1$ and $t = 0.1$. The cases $m = 0, 1, i$ correspond with (a),(b) and (c) respectively.

5.4 The discontinuous stroboscopic map when $A_L = A_R$

In this section, the stroboscopic map generated by the normalized canonical form (5.16)-(5.17) is analized . We concentrate our attention in the case where matrices A_L and A_R are equal and nonsingular and they correspond to anti-saddle dynamics, that is

$$A_L = A_R = A, \quad \gamma_L = \gamma_R = \gamma, \quad m_L = m_R = m, \quad \text{and} \quad D = \gamma^2 - m^2 > 0.$$

In this case, the solution of system (5.16)-(5.17) for $\mathbf{x}(t_0) = \mathbf{x}_0 \in \Sigma_j$ with $j \in \{L, R\}$ is

$$\mathbf{x}(t) = \Phi \mathbf{x}_0 - \Upsilon \mathbf{b}_j, \quad j = \{L, R\}, \tag{5.45}$$

where the matrix Φ is given in (5.23) and the matrix Υ is defined by

$$\Upsilon = \Upsilon(mt) = \int_0^t e^{(t-\tau)A} d\tau = (\Phi - I) A^{-1}, \tag{5.46}$$

Given $m \in \{0, 1, i\}$ and the sets Σ_L and Σ_R defined in (5.7), we consider the two-dimensional stroboscopic map P for a fixed value $t > 0$ associated to the normalized canonical form (5.16)-(5.17),

$$P(\mathbf{x}; t) = \begin{cases} P_L(\mathbf{x}; t) = \Phi \mathbf{x} - (\Phi - I) A^{-1} \mathbf{b}_L, & \text{if} \quad \mathbf{x} \in \Sigma_L, \\ P_R(\mathbf{x}; t) = \Phi \mathbf{x} - (\Phi - I) A^{-1} \mathbf{b}_R, & \text{if} \quad \mathbf{x} \in \Sigma_R, \end{cases} \tag{5.47}$$

where the matrix Φ is given in (5.23) and the vectors $\mathbf{b}_j$ in (5.17).

In what follows, we assume $b \neq 0$ in the vector $\mathbf{b}_R$ defined in (5.17), so that the stroboscopic map (5.47) is discontinuous always, even when $a_L = a_R$.

Points $\mathbf{x}_j^*$ with $P_j\left(\mathbf{x}_j^*\right) = \mathbf{x}_j^*$ are fixed points of map P. If the fixed point $\mathbf{x}_j^* \in \mathbf{\Sigma}_j$, the point is termed real, where the sets $\mathbf{\Sigma}_j$ are defined in (5.7); otherwise, it will be termed virtual fixed point. The map P has the two fixed points given by

$$\mathbf{x}_L^* = \frac{1}{\gamma^2 - m^2}\begin{pmatrix} a_L \\ 2\gamma a_L \end{pmatrix}, \quad \mathbf{x}_R^* = \frac{1}{\gamma^2 - m^2}\begin{pmatrix} a_R \\ 2\gamma a_R + (\gamma^2 - m^2)\, b \end{pmatrix}. \tag{5.48}$$

The fixed point $\mathbf{x}_L$ is virtual when $a_L > 0$ and the fixed point $\mathbf{x}_R$ is virtual when $a_R < 0$.

5.5 Polar description of the parameter plane (a_R, a_L)

In this section we show that for the map (5.47), the regions on the parameter plane (a_R, a_L) with different dynamic behavior are separated by straight lines passing through the origin. First, we consider the parameter γ as a fixed value, and we introduce the new parameters r and θ defined by the polar coordinates as follows

$$a_R = r\cos\theta, \quad a_L = r\sin\theta, \quad \text{with} \quad r > 0 \quad \textit{and} \quad \theta \in [0, 2\pi].$$

The map P defined in (5.47) has the following homothetic property, whose proof is direct and it is omitted.

Proposition 80. *Given $r > 0$, the map P defined in (5.47)-(5.23)-(5.17), satisfies the equality*

$$P\left(r\mathbf{x}; t, rb, r, \theta\right) = rP\left(\mathbf{x}, t, b, 1, \theta\right)$$

As usual, the orbit of $\mathbf{x}$ under the map P will be called $\mathrm{Or}\left(\mathbf{x}; t, b, r, \theta\right)$ and it is defined by

$$\mathrm{Or}\left(\mathbf{x}; t, b, r, \theta\right) = \left\{\mathbf{x}_k \in \mathbb{R}^2 : \mathbf{x}_k = P^k(\mathbf{x}; t, b, r, \theta), \quad k \geq 0\right\},$$

where P^k is the k-th iterate of map P. As a direct consequence of Proposition 80 we have the following result.

Proposition 81. *Given $r > 0$, the orbit of a point $\mathbf{x}$ verifies*

$$\mathrm{Or}\left(\mathbf{x}; t, b, r, \theta\right) = r\left(\mathrm{Or}\left(r^{-1}\mathbf{x}; t, b, 1, \theta\right)\right). \tag{5.49}$$

From this result, we see that it suffices to consider the map P with the parameter $r = 1$. Moreover, points on the same straight line through the origin on the parameter plane (a_R, a_L) have the same dynamical behavior, and so, the bifurcation curves on the parameter plane are straight lines passing through the origin, see Figure 5.3(a).

Note that the vector $\mathbf{b}_L$ defined in (5.17) does not depend of the parameter b. Thus, making explicit the functional dependence, the map P can be written in the form

$$P\left(\mathbf{x}; t, b, \theta\right) = \begin{cases} P_L\left(\mathbf{x}; t, \theta\right) = \Phi\mathbf{x} - (\Phi - I)A^{-1}\mathbf{b}_L, & \text{if} \quad \mathbf{x} \in \mathbf{\Sigma}_L, \\ P_R\left(\mathbf{x}; t, b, \theta\right) = \Phi\mathbf{x} - (\Phi - I)A^{-1}\mathbf{b}_R, & \text{if} \quad \mathbf{x} \in \mathbf{\Sigma}_R, \end{cases} \tag{5.50}$$

where Φ is given in (5.23) and the new vectors are

$$\mathbf{b}_R = \begin{pmatrix} -b \\ \cos\theta \end{pmatrix}, \quad \mathbf{b}_L = \begin{pmatrix} 0 \\ \sin\theta \end{pmatrix}. \tag{5.51}$$

The fixed points of map P can be rewritten in terms of the parameter θ, as follows

$$\begin{aligned} \mathbf{x}_L^*(\theta) &= \frac{1}{\gamma^2 - m^2} \begin{pmatrix} \sin\theta \\ 2\gamma \sin\theta \end{pmatrix}, \\ \mathbf{x}_R^*(\theta) &= \frac{1}{\gamma^2 - m^2} \begin{pmatrix} \cos\theta \\ 2\gamma\cos\theta + (\gamma^2 - m^2)\, b \end{pmatrix}. \end{aligned} \tag{5.52}$$

In Figure 5.3(a) we show the border collision bifurcation lines separating existence regions of periodic orbits on the parameter plane (a_R, a_L) for the map (5.47)-(5.23)-(5.17) and for parameters values $t = 0.1$, $m = 1$, $\gamma = -2$ and $b = -0.5$. On the red lines, the fixed points given in (5.52) change from real to virtual, that is, $\mathbf{e}_1^T \mathbf{x}_L^*(\theta) = 0$ or $\mathbf{e}_1^T \mathbf{x}_R^*(\theta) = 0$. The blue line is a circular arc with radius $r = 1$ on the two-parametric plane. Also, the region of the period two orbit is shown. In (b) we show a bifurcation diagram along the circular arc parametrized by the angle θ. In Figure (c) we show a period diagram of the bifurcation diagram given in (b).

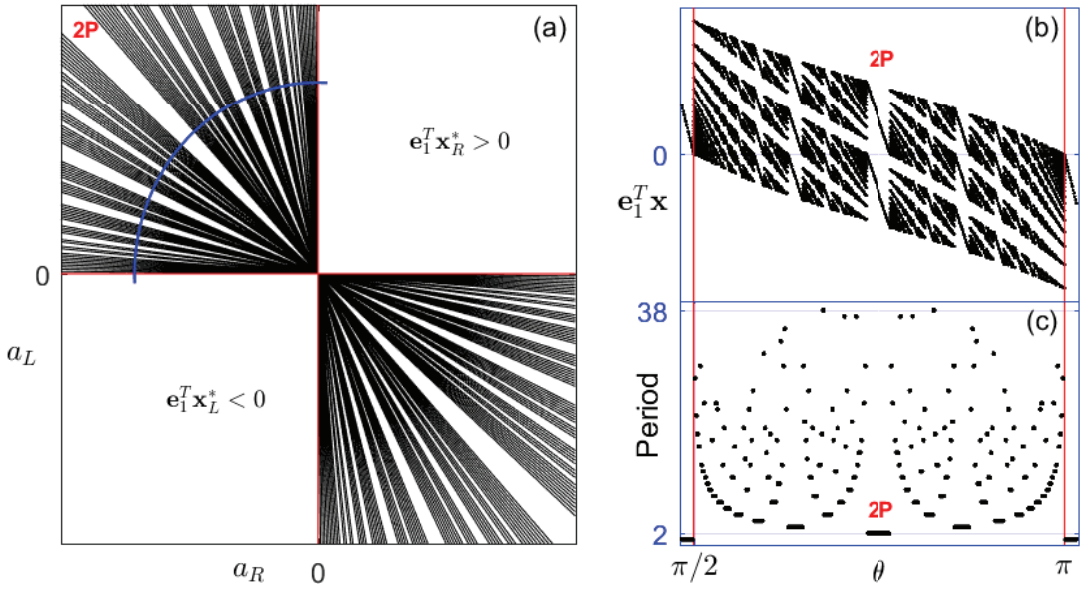

Figure 5.3: (a) On the parameter plane (a_R, a_L) and for the map (5.47)-(5.23)-(5.17) with parameters $t = 0.1$, $m = 1$, $\gamma = -2$ and $b = -0.5$, the straight lines given by Proposition 80, which separate the different regions of periodic orbits are shown. (b) Bifurcation diagram calculated along the blue curve given in (a) parametrized by the angle θ. (c) Periods (numerically computed) of the periodic orbits found in the bifurcation diagram given in (b).

5.6 Periodic solutions

Having in mind, the generalization of the conjecture described at the beginning of this chapter, In this section we will consider two specific families of periodic orbits, and we will show that it is sufficient to characterize only one of these families. In order to study the existence of such families of periodic orbits, we concentrate our attention in the case where both equilibrium points are stable and virtual (see (5.52)), that is

$$\gamma^2 - m^2 > 0, \quad \gamma < 0, \quad \text{and} \quad \cos\theta < 0 < \sin\theta. \tag{5.53}$$

The above inequalities imply that if there exists a periodic orbit, then such periodic orbit is stable, see Remark 77. For convenience, we consider the parameter $\theta \in (\pi/2, \pi)$.

As usual, given a map $P : \mathbb{R}^2 \longrightarrow \mathbb{R}^2$, we consider the symbolic representation of an orbit starting at $\mathbf{x}$, also called the itinerary of $\mathbf{x}$, as $I_P(\mathbf{x}) \in \{L, R\}^N$, where

$$I_P(\mathbf{x})(k) = \begin{cases} L & \text{if } \mathbf{e}_1^T P^k(\mathbf{x}) < 0, \\ R & \text{if } \mathbf{e}_1^T P^k(\mathbf{x}) \geq 0. \end{cases} \qquad k \geq 1.$$

In the following, we use the upper index with parentheses to denote a succession of elements. If $\mathbf{x}$ belongs to a n-periodic orbit of a map P, then we write $I_P(\mathbf{x}) = \left(I^{(1)}, I^{(2)}, \ldots, I^{(n)}\right)$ for some finite sequence of the length n consisting of symbols L and R. As in Avrutin et al. [2011] and Gardini et al. [2010], we concentrate our attention in two finite specific symbolic sequences, namely $RL^{n-1} = (R, L, L, \ldots, L)$ and $LR^{n-1} = (L, R, \ldots, R)$. In what follows, we use a subscript to denote that the points belongs to a n-periodic orbit, for example, a 3-periodic orbit is the set $\mathrm{Or}(\mathbf{x}_3^{(1)}) = \{\mathbf{x}_3^{(1)}, \mathbf{x}_3^{(2)}, \mathbf{x}_3^{(3)}\}$.

If there exists a n-periodic orbit $\mathrm{Or}(\mathbf{x}_n^{(1)})$ with $\mathbf{e}_1^T \mathbf{x}_n^{(1)} > 0$ and $\mathbf{e}_1^T \mathbf{x}_n^{(k)} < 0$ for $2 \leq k \leq n$, then its itinerary is RL^{n-1} and we will say that the n-periodic orbit is admissible and of type RL^{n-1}. Analogously, we define the admissible n-periodic orbit of type LR^{n-1}.

In the next proposition, we obtain the form of the maps corresponding to those symbolic sequences.

Proposition 82. *Consider the map P defined in (5.50)-(5.51). Then the following statements hold for $n \geq 2$.*

(a) Assume that $\mathbf{x} \in \Sigma_R$ and $I_P(\mathbf{x}) = RL^{n-1}$. The n-iterate defines the following map

$$P_{RL^{n-1}}(\mathbf{x}) := \left(P_L^{n-1} \circ P_R\right)(\mathbf{x}) = \Phi^n \mathbf{x} - \Phi^{n-1}(\Phi - I)A^{-1}\mathbf{b}_R - \left(\Phi^{n-1} - I\right)A^{-1}\mathbf{b}_L. \tag{5.54}$$

(b) Assume that $\mathbf{x} \in \Sigma_L$ and $I_P(\mathbf{x}) = LR^{n-1}$. The n-iterate defines the following map

$$P_{LR^{n-1}}(\mathbf{x}) := \left(P_R^{n-1} \circ P_L\right)(\mathbf{x}) = \Phi^n \mathbf{x} - \Phi^{n-1}(\Phi - I)A^{-1}\mathbf{b}_L - \left(\Phi^{n-1} - I\right)A^{-1}\mathbf{b}_R. \tag{5.55}$$

Proof. The sequence RL^{n-1} corresponds to the composition $P_L^{n-1} \circ P_R$. By induction, we obtain

$$P_L^{n-1}(\mathbf{y}) = \Phi^{n-1}\mathbf{y} - \left(\sum_{i=0}^{n-2} \Phi^i\right)(\Phi - I)A^{-1}\mathbf{b}_L.$$

Having in mind that

$$\left(\sum_{i=0}^{n-2} \Phi^i\right)(\Phi - I) = \Phi^{n-1} - I,$$

and taking $\mathbf{y} = P_R(\mathbf{x})$ we get (5.54) and statement (a) follows. The proof of statement (b) is analogous. □

As a direct consequence of Proposition 82, we obtain an analytical expression for the fixed point of the maps (5.54) and (5.55).

Proposition 83. *Assume $\gamma^2 - m^2 > 0$ and $\gamma < 0$. The following statements hold for $n \geq 2$.*

(a) If there exist a n-periodic orbit $\mathrm{Or}(\mathbf{x}_n^{(1)})$ of type RL^{n-1}, then this periodic orbit is unique and $\mathbf{x}_n^{(1)}$ corresponds with the fixed point of map (5.54) which is given by

$$\mathbf{x}_n^{(1)} = (\Phi^n - I)^{-1}\left[\Phi^{n-1}(\Phi - I)A^{-1}\mathbf{b}_R + \left(\Phi^{n-1} - I\right)A^{-1}\mathbf{b}_L\right]. \tag{5.56}$$

(b) If there exist a n-periodic orbit $\mathrm{Or}(\mathbf{x}_n^{(1)})$ of type RL^{n-1}, then this periodic orbit is unique and $\mathbf{x}_n^{(1)}$ corresponds with the fixed point of map (5.55) which is given by

$$\mathbf{x}_n^{(1)} = (\Phi^n - I)^{-1}\left[\Phi^{n-1}(\Phi - I)A^{-1}\mathbf{b}_L + \left(\Phi^{n-1} - I\right)A^{-1}\mathbf{b}_R\right]. \tag{5.57}$$

In the next two propositions, we give an analytic expressions of the elements of the n-periodic orbits of type RL^{n-1} and RL^{n-1}.

Proposition 84. *Assume that $\gamma^2 - m^2 > 0$ and $\gamma < 0$. If there exist a n-periodic orbit $\mathrm{Or}(\mathbf{x}_n^1)$ of type RL^{n-1}, we have*

$$\begin{aligned} \mathbf{x}_n^{(1)} &= W_n^{(1)}A^{-1}(\mathbf{b}_R - \mathbf{b}_L) + A^{-1}\mathbf{b}_L, \\ \mathbf{x}_n^{(k)} &= P_{RL^{n-1}}^k(\mathbf{x}_n^{(1)}) = W_n^{(k)}A^{-1}(\mathbf{b}_R - \mathbf{b}_L) + A^{-1}\mathbf{b}_L, \quad 2 \leq k \leq n, \end{aligned} \tag{5.58}$$

where the matrices $W_n^{(1)}$ and $W_n^{(k)}$ are

$$\begin{aligned} W_n^{(1)} &= (\Phi^n - I)^{-1}\Phi^{n-1}(\Phi - I), \\ W_n^{(k)} &= \Phi^{k-2}(\Phi W_n^{(1)} - \Phi + I), \quad 2 \leq k \leq n. \end{aligned} \tag{5.59}$$

Moreover, the first component of $\mathbf{x}_n^{(k)} = (x_n^{(k)}, y_n^{(k)})$ is

$$x_n^{(k)}(\theta) = bw_{12}^{(k)} + \frac{1 - 2\gamma w_{12}^{(k)} - w_{11}^{(k)}}{\gamma^2 - m^2}\sin\theta + \frac{2\gamma w_{12}^{(k)} + w_{11}^{(k)}}{\gamma^2 - m^2}\cos\theta \tag{5.60}$$

where $\left[w_{11}^{(k)}, w_{12}^{(k)}\right]$ is the first row of the matrix $W_n^{(k)}$.

Proof. From Proposition 76 matrix $\Phi^n - I$ is nonsingular, so that map (5.54) has a unique fixed point $\mathbf{x}_n^{(1)}$ given by (5.54) and taking account that

$$\Phi^{n-1}(\Phi - I) + \Phi^{n-1} - I = \Phi^n - I,$$

we obtain $\mathbf{x}_n^{(1)}$ defined in (5.58). Since $\mathrm{Or}(\mathbf{x}_n^{(1)})$ is a n-periodic orbit of type RL^{n-1}, by induction we obtain $\mathbf{x}_n^{(k)}$ as in (5.58). □

The proof of the next result is analogous to the proof of Proposition 84.

Proposition 85. *Assume that $\gamma^2 - m^2 > 0$ and $\gamma < 0$. If there exist a n-periodic orbit $\mathrm{Or}(\mathbf{x}_n^{(1)})$ admissible of type LR^{n-1}, then*

$$\begin{aligned} \mathbf{x}_n^{(1)} &= W_n^{(1)} A^{-1}(\mathbf{b}_L - \mathbf{b}_R) + A^{-1}\mathbf{b}_R, \\ \mathbf{x}_n^{(k)} &= P_{LR^{n-1}}^k(\mathbf{x}_n^{(1)}) = W_n^{(k)} A^{-1}(\mathbf{b}_L - \mathbf{b}_R) + A^{-1}\mathbf{b}_R, \quad 2 \le k \le n, \end{aligned} \tag{5.61}$$

Moreover, the first component of $\mathbf{x}_n^{(k)} = (x_n^{(k)}, y_n^{(k)})$ is

$$x_n^{(k)}(\theta) = -bw_{12}^{(k)} + \frac{1 - 2\gamma w_{12}^{(k)} - w_{11}^{(k)}}{\gamma^2 - m^2}\cos\theta + \frac{2\gamma w_{12}^{(k)} + w_{11}^{(k)}}{\gamma^2 - m^2}\sin\theta, \tag{5.62}$$

where $\left[w_{11}^{(k)}, w_{12}^{(k)}\right]$ is the first row of the matrix $W_n^{(k)}$ defined in (5.59).

Now, we show a symmetry property between the orbits the type RL^{n-1} and LR^{n-1}, its proof is a consequence of Propositions 84 and 85.

Proposition 86. *Assume that $\gamma^2 - m^2 > 0$ and $\gamma < 0$. Then, the n-periodic orbit $\mathrm{Or}(\mathbf{x}_n^{(1)}(\theta))$ is admissible of type RL^{n-1} if and only if $\mathrm{Or}(\mathbf{x}_n^{(1)}(3\pi/2 - \theta))$ is admissible of type LR^{n-1}.*

Proof. Suppose that the n-periodic orbit $\mathrm{Or}(\mathbf{x}_n^{(1)}(\theta))$ is admissible of type RL^{n-1}, that is $x_n^{(1)}(\theta) > 0$ and $x_n^{(k)}(\theta) < 0$ for $2 \le k \le n$, where $x_n^{(k)}(\theta)$ is defined in (5.60). Now, taking into account that

$$\sin(3\pi/2 - \theta) = -\cos\theta, \quad \cos(3\pi/2 - \theta) = -\sin\theta,$$

we get

$$x_n^{(k)}(3\pi/2 - \theta) = bw_{12}^{(k)} - \frac{1 - 2\gamma w_{12}^{(k)} - w_{11}^{(k)}}{\gamma^2 - m^2}\cos\theta - \frac{2\gamma w_{12}^{(k)} + w_{11}^{(k)}}{\gamma^2 - m^2}\sin\theta = -x_n^{(k)}(\theta),$$

so that,

$$x_n^{(1)}(3\pi/2 - \theta) < 0, \quad x_n^{(k)}(3\pi/2 - \theta) > 0, \quad 2 \le k \le n,$$

thus $\mathrm{Or}(\mathbf{x}_n^{(1)}(3\pi/2 - \theta))$ is admissible of type LR^{n-1} and the conclusion follows. □

As a first consequence of Proposition 86, we see that to study periodic orbits of type RL^{n-1} and type LR^{n-1} it is sufficient to study only one type of sequences. Therefore, in the following, according to above proposition and without loss of generality, we concentrate our attention on the sequences of type RL^{n-1}.

5.7 Border-collision bifurcation curves

In this section we will study the first component of a n-periodic orbit of type RL^{n-1}, this component is ruled by the functions $x_n^{(k)}$ defined in (5.60). The sign of these functions determine the admissibility of a n-periodic orbit, for instance, a 2-periodic orbit is admissible at θ, if the two functions $x_2^{(1)}$ and $x_2^{(2)}$ have different sign at θ, that is $x_2^{(1)}(\theta) \cdot x_1^{(2)}(\theta) < 0$. In what follows, we concentrate our attention in the case where both equilibrium points are stable and virtual, that is the condition

A n-periodic orbit undergoes a border collision bifurcation (BC bifurcation, for short) when a periodic point of the n-periodic orbit collides with $x = 0$. The term was introduced in Nusse and Yorke [1992] (see also Gardini and Tramontana [2011], Sushko et al. [2016]).

Therefore, given a n-periodic orbit of type RL^{n-1} and the functions $x_n^{(k)}$, if there exist $2 \leq k \leq n$ and $\theta \in (\pi/2, \pi)$ such that $x_n^{(k)}(\theta) = 0$ then we have a BC bifurcation. The functions $x_n^{(k)}$ are called border collision bifurcation curves.

In order to study the existence of a BC bifurcation, of a n-periodic orbit of type RL^{n-1}, we need to obtain analytic expressions for the functions $x_n^{(k)}$. First, to alleviate notation, we introduce for $n \geq 2$ and $1 \leq k \leq n$ the auxiliary functions

$$h_n^{(k)}(\gamma) := 2\gamma w_{12}^{(k)} + w_{11}^{(k)}, \qquad r_n^{(k)}(\gamma) := w_{12}^{(k)}, \tag{5.63}$$

so that given $t, b \in \mathbb{R}$ the functions $x_n^{(k)}$defined in (5.60) can be rewritten for $1 \leq k \leq n$ as

$$x_n^{(k)}(\theta) = \frac{1}{D}(b r_n^{(k)}(\gamma) D + (1 - h_n^{(k)}(\gamma)) \sin\theta + h_n^{(k)}(\gamma) \cos\theta), \tag{5.64}$$

where $D = \gamma^2 - m^2$.

In order to study the admissibility of the n-periodic orbits, we will consider the case where functions $x_n^{(k)}(\theta)$ are strictly decreasing on the interval $(\pi/2, \pi)$.

We will study the admissibility of the n-periodic orbits, in the particular case in which the border collision bifurcation curves $x_n^{(k)}$ are strictly decreasing on the interval $(\pi/2, \pi)$.

In the following result, sufficient conditions in terms of functions $h_n^{(k)}$ will be given so that functions $x_n^{(k)}$ are strictly decreasing for all $n \geq 2$,. In addition, given two border-collision bifurcation curves $x_n^{(s)}$ and $x_n^{(w)}$, we show two conditions such that $x_n^{(s)}(\theta) < x_n^{(w)}(\theta)$ on the interval $(\pi/2, \pi)$.

Proposition 87. *Given $m \in \{0, 1, i\}$, $\gamma \in \mathbb{R}$ such that $D = \gamma^2 - m^2 > 0$ and $\gamma < 0$ and $n \geq 2$. Consider the functions $x_n^{(k)}$ defined as in (5.64). The following statements hold.*

(a) If there exists $k \in \{1, 2, \ldots, n\}$ and $\gamma \in \mathbb{R}$ such that $0 < h_n^{(k)}(\gamma) < 1$, then $x_n^{(k)}$ is strictly decreasing on the interval $(\pi/2, \pi)$, see figures 5.4(a) and 5.5(a)-(b).

(b) If there exist $s, w \in \{1, 2, \ldots, n\}$, and $\gamma, b \in \mathbb{R}$ satisfying the condition

$$h_n^{(s)}(\gamma) - h_n^{(w)}(\gamma) > 0, \quad \text{and} \quad \frac{b(r_n^{(s)}(\gamma) - r_n^{(w)}(\gamma))D}{h_n^{(s)}(\gamma) - h_n^{(w)}(\gamma)} < 1, \tag{5.65}$$

or the condition

$$h_n^{(s)}(\gamma) - h_n^{(w)}(\gamma) < 0, \quad \textit{and} \quad \frac{b(r_n^{(s)}(\gamma) - r_n^{(w)}(\gamma))D}{h_n^{(s)}(\gamma) - h_n^{(w)}(\gamma)} > \sqrt{2}, \tag{5.66}$$

for all $n \geq 2$, *then we have* $x_n^{(s)}(\theta) < x_n^{(w)}(\theta)$ *for all* $\theta \in (\pi/2, \pi)$.

Proof. If $\theta \in (\pi/2, \pi)$ we get $\sin\theta > 0$ and $\cos\theta < 0$, and so

$$\frac{\partial x_n^{(k)}(\theta)}{\partial \theta} = \frac{(1 - h_n^{(k)}(\gamma))\cos\theta - h_n^{(k)}(\gamma)\sin\theta}{D} < 0,$$

and statement (a) follows.

After some algebra, we obtain that the inequality $x_n^{(s)}(\theta) < x_n^{(w)}(\theta)$ is equivalent to

$$b(r_n^{(s)}(\gamma) - r_n^{(w)}(\gamma))D < (\sin\theta - \cos\theta)\,(h_n^{(s)}(\gamma) - h_n^{(w)}(\gamma)).$$

Now, having in mind that $1 \leq \sin\theta - \cos\theta \leq \sqrt{2}$, for $\theta \in (\pi/2, \pi)$, statement (b) follows. □

In Figure 5.4, we show the functions $h_n^{(k)}$ and $r_n^{(k)}$ when $m = 1$, $n = 3$ and $t = 0.9$.

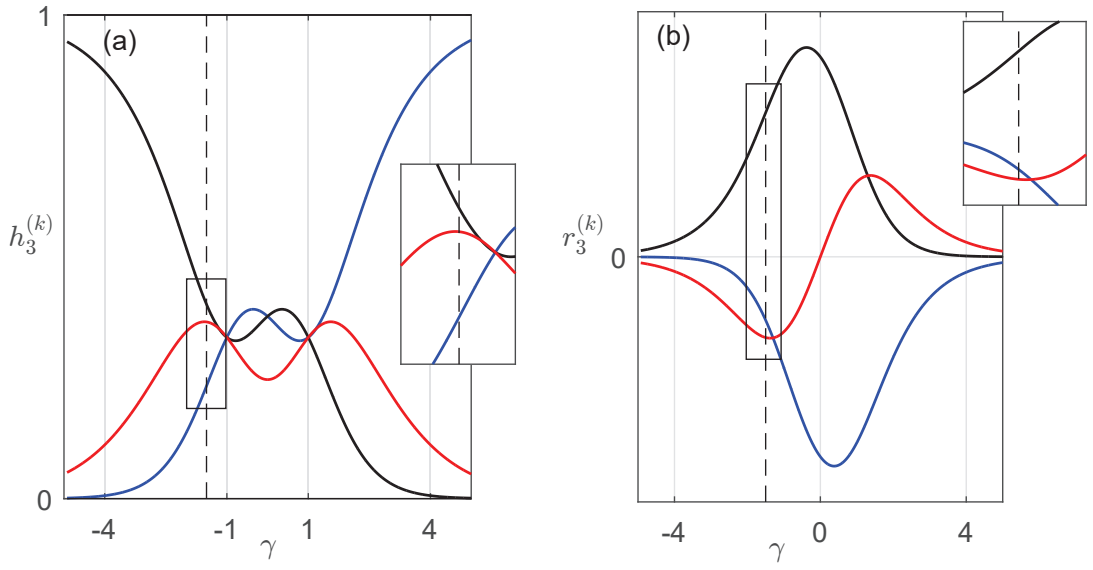

Figure 5.4: Functions $h_3^{(k)}$ and $r_3^{(k)}$ defined as in (5.63) with parameters $t = 0.9$ and $m = 1$. (a) The blue, black and red lines represent functions $h_3^{(1)}$,$h_3^{(2)}$ and $h_3^{(3)}$ respectively. The dashed line is the value $\gamma = -1.5$ where $h_3^{(1)}(\gamma) < h_3^{(3)}(\gamma) < h_3^{(2)}(\gamma)$. (b) The blue, black and red lines are the functions $r_3^{(1)}$,$r_3^{(2)}$ and $r_3^{(3)}$ respectively. The dashed line is the value $\gamma = -1.5$ such that $r_3^{(3)}(\gamma) < r_3^{(1)}(\gamma) < r_3^{(2)}(\gamma)$.

Now, we need to determine the elements of the matrices $W_n^{(k)}$ defined in (5.59). In the next result we omit the dependence on the parameters γ and t.

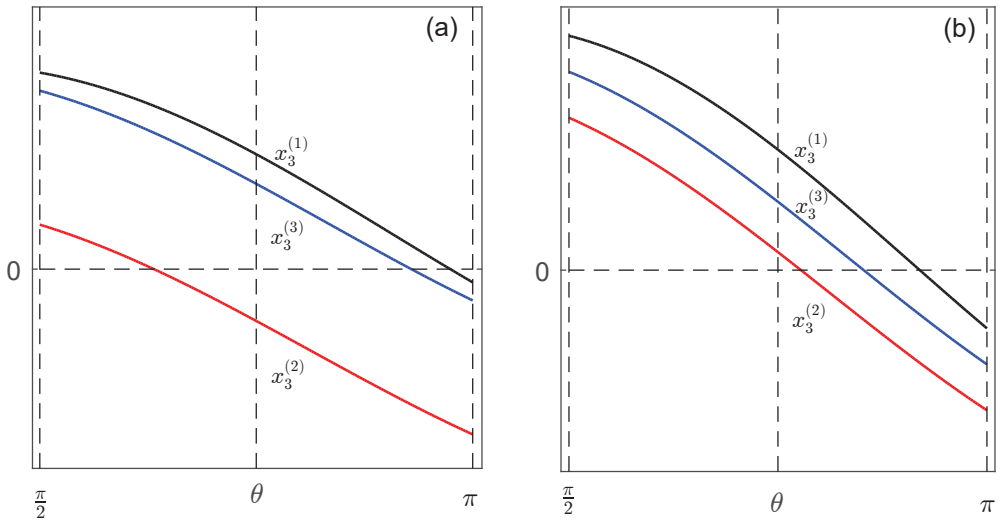

Figure 5.5: Functions $x_3^{(k)}$ given in (5.64) with parameters as in Figure 5.4, that is $t = 0.9$, $m = 1$. In black, red and blue we show the functions $x_3^{(1)}$, $x_3^{(2)}$ and $x_3^{(3)}$ respectively. (a) Taking $b = -1.5$ and from Proposition 87(b) we get $x_3^{(2)}(\theta) < x_3^{(3)}(\theta) < x_3^{(1)}(\theta)$ for all $\theta \in (\pi/2, \pi)$. (b) Taking $b = -0.3$ and from Proposition 87(b) we obtain $x_3^{(2)}(\theta) < x_3^{(3)}(\theta) < x_3^{(1)}(\theta)$ for all $\theta \in (\pi/2, \pi)$ and $0 < x_3^{(2)}(3\pi/4) < x_3^{(3)}(3\pi/4) < x_3^{(1)}(3\pi/4)$.

Proposition 88. *Given $m \in \{0, 1, i\}$, $\gamma \in \mathbb{R}$ such that $D = \gamma^2 - m^2 > 0$, $\gamma < 0$ and $n \geq 2$. Consider for $2 \leq k \leq n$ the matrices $W_n^{(k)}$ defined in (5.59). Then the matrix $W_n^{(1)} = \left[w_{ij}^{(1)}\right]$ is given by*

$$W_n^{(1)} = \frac{1}{d_n} \begin{pmatrix} e^{nt\gamma}\left(1 - e^{-t\gamma}\mu_1^-\right) + e^{-t\gamma}\mu_{n-1}^+ - \mu_n^+, & S_n - e^{-t\gamma}(e^{nt\gamma}S_1 + S_{n-1}) \\ -d_n w_{12}^{(1)} D, & d_n(2\gamma w_{12}^{(1)} + w_{11}^{(1)}) \end{pmatrix}, \tag{5.67}$$

where the functions C_k, S_k, μ_k and d_n are defined in (5.19)-(5.20)-(5.22) and (5.43)-(5.44) respectively. Moreover, for $2 \leq k \leq n$, the first row $\left[w_{11}^{(k)}, w_{12}^{(k)}\right]$ of the matrix $W_n^{(k)}$ is given by

$$\begin{aligned} w_{11}^{(k)} &= e^{(k-1)t\gamma}\left((w_{11}^{(1)} - 1)\mu_{k-1}^+ - w_{21}^{(1)}S_{k-1} + e^{-t\gamma}\mu_{k-2}^+\right), \\ w_{12}^{(k)} &= e^{(k-1)t\gamma}\left((1 - w_{22}^{(1)})S_{k-1} + w_{12}^{(1)}\mu_{k-1}^+ - e^{-t\gamma}S_{k-2}\right). \end{aligned} \tag{5.68}$$

Proof. From (5.23) and (5.41) we obtain the matrices Φ^n and $(\Phi^n - I)^{-1}$, so that

$$\begin{aligned} W^{(1)} &= (\Phi^n - I)^{-1}\left(\Phi^n - \Phi^{n-1}\right) = \\ &= \frac{e^{nt\gamma}}{d_n} \begin{pmatrix} \mu_n^- e^{nt\gamma} - 1 & S_n e^{nt\gamma} \\ -DS_n e^{nt\gamma} & \mu_n^+ e^{nt\gamma} - 1 \end{pmatrix} \begin{pmatrix} \mu_n^+ - e^{-t\gamma}\mu_{n-1}^+ & e^{-t\gamma}S_{(n-1)} - S_n \\ D\left(S_n - e^{-t\gamma}S_{n-1}\right) & \mu_n^- - e^{-t\gamma}\mu_{n-1}^- \end{pmatrix} \end{aligned}$$

After some algebra and taking into account the identities

$$C_n^2 - \gamma^2 S_n^2 = \mu_n^+ \mu_n^-, \quad S_n C_{n-1} - C_n S_{n-1} = S_1, \quad C_n C_{n-1} - m^2 S_n S_{n-1} = C_1, \tag{5.69}$$

we obtain (5.67).

By considering the identities (5.28), (5.29) and (5.31) given in Proposition 75, we get

$$\begin{aligned}\frac{1}{e^{(k-1)t\gamma}} w_{11}^{(k)} &= (w_{11}^{(1)} - 1)\left(\mu_k^+ \mu_1^- + D S_k S_1\right) + w_{21}^{(1)}\left(\mu_k^+ S_1 - S_k \mu_1^+\right) + e^{-t\gamma}\left(\mu_k^+ \mu_2^- + D S_k S_2\right) = \\ &= (w_{11}^{(1)} - 1)\mu_{k-1}^+ - w_{21}^{(1)} S_{k-1} + e^{-t\gamma}\mu_{k-2}^+.\end{aligned}$$

Analogously, considering the identities (5.28), (5.29) and (5.32) given in Proposition 75, we obtain

$$\begin{aligned}\frac{1}{e^{(k-1)t\gamma}} w_{12}^{(k)} &= (w_{22}^{(1)} - 1)\left(\mu_k^+ S_1 - S_k \mu_1^+\right) + w_{12}^{(1)}(\mu_k^+ \mu_1^- + D S_k S_1) + e^{-t\gamma}(\mu_k^+ S_2 - S_k \mu_2^+) = \\ &= (1 - w_{22}^{(1)}) S_{k-1} + w_{12}^{(1)} \mu_{k-1}^+ - e^{-t\gamma} S_{k-2}.\end{aligned}$$

and then (5.68) follows.

□

Using the above result, we can give an algebraic expression for auxiliary functions $h_n^{(k)}$ and $r_n^{(k)}$.

Theorem 89. *Given $m \in \{0, 1, i\}$, $\gamma \in \mathbb{R}$ such that $D = \gamma^2 - m^2 > 0$, $\gamma < 0$ and $n \geq 2$. The functions $r_n^{(k)}$ and $h_n^{(k)}$ defined in (5.63) can be rewritten as follows; for $k = 1$,*

$$\begin{aligned} d_n h_n^{(1)} &= e^{2nt\gamma} - e^{(2n-1)t\gamma}\mu_1^+ + e^{(n-1)t\gamma}\mu_{n-1}^- - e^{nt\gamma}\mu_n^-, \\ d_n r_n^{(1)} &= e^{nt\gamma} S_n - e^{(2n-1)t\gamma} S_1 - e^{(n-1)t\gamma} S_{n-1}, \end{aligned} \tag{5.70}$$

and for $2 \leq k \leq n$ we get

$$\begin{aligned} d_n h_n^{(k)} &= e^{(k-2)t\gamma}\left(e^{(n+1)t\gamma}\mu_{n+1-k}^+ - e^{nt\gamma}\mu_{n+2-k}^+ - e^{t\gamma}\mu_{k-1}^- + \mu_{k-2}^-\right), \\ d_n r_n^{(k)} &= e^{(k-2)t\gamma}\left(e^{(n+1)t\gamma} S_{n+1-k} - e^{nt\gamma} S_{n-k+2} + e^{t\gamma} S_{k-1} - S_{k-2}\right), \end{aligned} \tag{5.71}$$

where the functions S_k, μ_k and d_n are defined in (5.19)-(5.20)-(5.22) and (5.43)-(5.44) respectively.

Proof. From (5.67) and (5.63), we obtain (5.70). Now, from (5.68),(5.63) and after some algebra we get

$$\begin{aligned} d_n h_n^{(k)} &= e^{(2n+k-2)t\gamma}\left(\mu_{k-2}^- - \mu_1^+ \mu_{k-1}^- - S_1 D S_{k-1}\right) \\ &+ e^{(n+k-2)t\gamma}\left(\mu_{n-1}^- \mu_{k-1}^- - S_{n-1} D S_{k-1} - 2C_n \mu_{k-2}^-\right) \\ &+ e^{(n+k-1)t\gamma}\left(S_n S_{k-1} D - \mu_n^- \mu_{k-1}^- + 2C_n \mu_{k-1}^-\right) + e^{(k-2)t\gamma}\mu_{k-2}^- - e^{(k-1)t\gamma}\mu_{k-1}^-. \end{aligned}$$

Taking into account the identities (5.30), (5.34) and (5.35) given in Proposition 75, we obtain for $2 \leq k \leq n$, the expression for the functions $h_n^{(k)}$ given in (5.71). Finally, after some algebra and from (5.68) and (5.63) we have

$$\begin{aligned} d_n r_k = {} & e^{(2n+k-2)t\gamma}\left(\mu_1^+ S_{k-1} - \mu_{k-1}^+ S_1 - S_{k-2}\right) + e^{(n+k-1)t\gamma}\left(\mu_{k-1}^+ S_n + S_{k-1}\mu_n^- - 2C_n S_{k-1}\right) + \\ & + e^{(n+k-2)t\gamma}\left(2C_n S_{k-2} - \mu_{k-1}^+ S_{n-1} - S_{k-1}\mu_{n-1}^-\right) + e^{(k-1)t\gamma} S_{k-1} - e^{(k-2)t\gamma} S_{k-2}, \end{aligned}$$

and having in mind the identities (5.32), (5.36) and (5.37) given in Proposition 75, we get

$$\begin{aligned} \mu_1^+ S_{k-1} - \mu_{k-1}^+ S_1 - S_{k-2} &= C_1 S_{k-1} - S_1 C_{k-1} - S_{k-2} = 0, \\ \mu_{k-1}^+ S_n + S_{k-1}\mu_n^- - 2C_n S_{k-1} &= S_n C_{k-1} - C_n S_{k-1} = S_{n+1-k}, \\ 2C_n S_{k-2} - \mu_{k-1}^+ S_{n-1} - S_{k-1}\mu_{n-1}^- &= 2C_n S_{k-2} - C_{k-1} S_{n-1} - C_{n-1} S_{k-1} = -S_{n-k+2}. \end{aligned}$$

we obtain (5.71) and the proposition follows. □

Although the map defined in (5.50) is discontinuous, the functions $x_n^{(k)}$ are continuous for all $\gamma^2 - m^2 \neq 0$, since the function $d_n \neq 0$ at such points, see Remark 79.

Using the equivalent definition of functions $h_n^{(k)}$ and $r_n^{(k)}$, founded in (5.70) and (5.71), we give some identities of those functions. The proofs are a direct computation and so they are omitted.

Proposition 90. *Given $m \in \{0, 1, i\}$, $\gamma \in \mathbb{R}$ such that $D = \gamma^2 - m^2 > 0$ and $\gamma < 0$ and $n \geq 2$. Consider the functions $h_n^{(k)}$, $r_n^{(k)}$ rewritten in (5.70) and (5.71) respectively, and the function d_n defined in (5.44). The following identities hold.*

$$h_n^{(1)}(\gamma) = h_n^{(2)}(-\gamma), \quad r_n^{(1)}(\gamma) = -r_n^{(2)}(-\gamma), \tag{5.72}$$

$$d_n(h_n^{(1)} + h_n^{(2)}) = d_n + e^{(n+1)t\gamma}\mu_{n-1}^+ - e^{(2n-1)t\gamma}\mu_1^+ + e^{(n-1)t\gamma}\mu_{n-1}^- - e^{t\gamma}\mu_1^-, \tag{5.73}$$

$$d_n(r_n^{(1)} + r_n^{(2)}) = \left(e^{t\gamma} - e^{(2n-1)t\gamma}\right) S_1 + \left(e^{(n+1)t\gamma} - e^{(n-1)t\gamma}\right) S_{n-1}. \tag{5.74}$$

5.8 Periodic two orbits

In this section we will study the 2-periodic orbit. We will give a sufficient condition for the existence and admissibility of such orbits. We start by considering in the next remark some properties of the functions $h_2^{(k)}$ and $r_2^{(k)}$, these functions define the border-collision bifurcation curves studied in the previous section.

Remark 91. *Note that from Theorem 89, the functions $r_2^{(1)}$ and $h_2^{(1)}$ defined in (5.63) can be rewritten as*

$$\begin{aligned} h_2^{(1)}(\gamma) &= \frac{e^{4t\gamma} - e^{3t\gamma}\mu_1^+ - e^{2t\gamma}\mu_2^- + e^{t\gamma}\mu_1^-}{d_2(\gamma)}, \\ r_2^{(1)}(\gamma) &= \frac{e^{2t\gamma} S_2 - \left(e^{3t\gamma} + e^{t\gamma}\right) S_1}{d_2(\gamma)}, \end{aligned} \tag{5.75}$$

where the function d_2 is defined as in (5.43), that is

$$d_2(\gamma) = 1 + e^{4t\gamma} - 2C_2 e^{2t\gamma}. \tag{5.76}$$

Also, from Proposition 90 we get

$$h_2^{(1)}(\gamma) + h_2^{(2)}(\gamma) = 1, \quad r_2^{(1)}(\gamma) + r_2^{(2)}(\gamma) = 0. \tag{5.77}$$

Thus, functions $h_2^{(2)}$ and $r_2^{(2)}$ at $x_2^{(2)}$ defined in (5.64) satisfy

$$x_2^{(2)}(\theta) = -x_2^{(1)}(\theta) + \frac{1}{D}(\sin\theta + \cos\theta), \tag{5.78}$$

so that, $x_2^{(1)}(\beta) = 0$ if and only if $x_2^{(2)}(3\pi/2 - \beta) = 0$. In particular we have the identities

$$x_2^{(2)}(3\pi/4) = -x_2^{(1)}(3\pi/4) = 0, \quad x_2^{(2)}(\pi/2) = -x_2^{(1)}(\pi), \quad x_2^{(2)}(\pi) = -x_2^{(1)}(\pi/2), \tag{5.79}$$

if and only if $x_2^{(2)}(3\pi/4) = 0$.

Regarding Remark 91, we have that it is sufficient to study the behavior of the functions $h_2^{(1)}$ and $r_2^{(1)}$. In the following result we show that if $0 < t < 1$ and $\gamma \in \mathbb{R}$ such that $\gamma^2 - m^2 \neq 0$, we obtain the inequalities $0 < h_1(\gamma) < 1$ and $r_1(\gamma) < 0$, see Figure 5.6.

Proposition 92. *Given $m \in \{0, 1, i\}$. Consider the functions $h_2^{(1)}$ and $r_2^{(1)}$ given in (5.75). Then, for all $0 < t < 1$ and $\gamma \in \mathbb{R}$ such that $\gamma^2 - m^2 \neq 0$ we have the inequalities*

$$0 < h_2^{(1)}(\gamma) < 1, \quad r_2^{(1)}(\gamma) < 0. \tag{5.80}$$

Proof. First, note that after a direct computation we obtain for all $m \in \{0, 1, i\}$

$$\lim_{\gamma\to\infty} h_2^{(1)}(\gamma) = 0, \quad \lim_{\gamma\to-\infty} h_2^{(1)}(\gamma) = 1.$$

Assume that $m = 0$, then

$$h_2^{(1)}(\gamma) = \frac{e^{t\gamma}(e^{t\gamma} - t\gamma + 1)}{(e^{t\gamma} + 1)^2}, \quad r_2^{(1)}(\gamma) = \frac{-te^{t\gamma}}{(e^{t\gamma} + 1)^2}.$$

It is direct that for all $\gamma \in \mathbb{R}$ and $t > 0$ we have $r_2^{(1)}(\gamma) < 0$. If there exists $\gamma \in \mathbb{R}$ such that $h_2^{(1)}(\gamma) = 1$ then $e^{t\gamma} + t\gamma e^{t\gamma} + 1 = 0$, which is an addition of positive terms and we get a contradiction. Analogously, assume that there exists $\gamma \in \mathbb{R}$ such that $h_2^{(1)}(\gamma) = 0$, that is $e^{t\gamma} - t\gamma + 1 = 0$. Now, we consider the auxiliary function $f(\gamma) = e^{t\gamma} - t\gamma + 1$. The first and second derivatives of the function f are

$$\frac{\partial f(\gamma)}{\partial\gamma} = t\left(e^{t\gamma} - 1\right), \quad \frac{\partial^2 f(\gamma)}{\partial\gamma^2} = t^2 e^{t\gamma},$$

so that this function is concave up with a minimum value $f(0) = 2$ then function f does not vanish. Therefore, for all $\gamma \neq \pm 1$ and $m = 0$, we obtain $0 < h_2^{(1)}(\gamma) < 1$.

When $m = 1$ the function $h_2^{(1)}$ is not defined at $\gamma = \pm 1$ and

$$\lim_{\gamma \to -1^{\pm}} h_2^{(1)}(\gamma) = \lim_{\gamma \to 1^{\pm}} h_2^{(1)}(\gamma) = \frac{1}{2},$$

so that the function has an avoidable discontinuity at $\gamma = \pm 1$. Now, after some algebra, we obtain the equivalent expression

$$h_2^{(1)}(\gamma) = \frac{1}{2} + \frac{1}{2}\frac{\sinh(\gamma t) - \gamma \sinh t}{\cosh(\gamma t) + \cosh t} = \frac{1}{2} + g_1(\gamma).$$

Next, will show that $|g_1(\gamma)| < 1$. First, note that function g_1 has the properties

$$g_1(-\gamma) = g_1(\gamma), \quad \lim_{\gamma \to \infty} g_1(\gamma) = 1, \quad \lim_{\gamma \to -\infty} g_1(\gamma) = -1.$$

Due to the symmetry it is sufficient to show that for all $\gamma > 0$ we get $g_1(\gamma) < 1$. Suppose there exists $\gamma > 0$ such that $g_1(\gamma) = 1$, that is

$$\begin{aligned} 0 &= \cosh(\gamma t) - \sinh(\gamma t) + \cosh t + \gamma \sinh t = \\ &= e^{-\gamma t} + \cosh t + \gamma \sinh t, \end{aligned}$$

which ia an addition of positive terms and then we have contradiction. Analogously, for the case $m = i$ we obtain the equivalent expression

$$h_2^{(1)}(\gamma) = \frac{1}{2} + \frac{1}{2}\frac{\sinh(t\gamma) - \gamma \sin t}{\cosh(t\gamma) + \cos t} = \frac{1}{2} + g_2(\gamma).$$

Now, following the same previous reasoning we obtain

$$\begin{aligned} 0 &= \cosh(t\gamma) - \sinh(t\gamma) + \cos t + \gamma \sin t = \\ &= e^{-\gamma t} + \cos t + \gamma \sin t, \end{aligned}$$

and with $\cos t > 0$ and $\sin t > 0$, we obtain a contradiction, that is for $0 < t < \pi/2$. Next, we will show that $r_2^{(1)}(\gamma) < 0$ in the cases $m = 1, i$. When $m = 1$ we have

$$r_2^{(1)}(\gamma) = \frac{e^{t\gamma} \sinh t \left(2e^{t\gamma} \cosh t - e^{2t\gamma} - 1\right)}{d_2(\gamma)},$$

where $d_2(\gamma) = e^{4t\gamma} - 2e^{2t\gamma} \cosh 2t + 1$. We note that for $t > 0$

$$\operatorname{sgn}(r_2^{(1)}(\gamma)) = \operatorname{sgn}\left(f(\gamma)\, d_2(\gamma)\right),$$

where the auxiliary function $f(\gamma) = 2e^{t\gamma} \cosh t - e^{2t\gamma} - 1$. From Proposition 78 we have $d_2(\gamma) > 0$ for all $\gamma^2 - 1 > 0$ and $d_2(\gamma) < 0$ for $\gamma^2 - 1 < 0$. Also, for all $t > 0$ the function f has an absolute maximum at $\gamma^* = \ln(\cosh t)/t$ and

$$f(\pm 1) = 0, \quad f(\gamma^*) = \frac{1}{2}(\cosh 2t - 1) > 0,$$

then $f(\gamma) > 0$ for all $\gamma^2 - 1 < 0$ and $f(\gamma) < 0$ for all $\gamma^2 - 1 > 0$. Therefore, $r_2^{(1)}(\gamma) < 0$ for all $\gamma \neq 1$.

When $m = i$ we have

$$r_2^{(1)}(\gamma) = \frac{e^{t\gamma}\sin t\,(2e^{t\gamma}\cos t - e^{2t\gamma} - 1)}{d_2(\gamma)},$$

and from Proposition 78 we have $d_2(\gamma) > 0$ for all $\gamma \in \mathbb{R}$. If $0 < t < \pi$ we have

$$\operatorname{sgn}(r_2^{(1)}(\gamma)) = \operatorname{sgn}(f(\gamma)\, d_2(\gamma)),$$

where $f(\gamma) = 2e^{t\gamma}\cos t - e^{2t\gamma} - 1$. If $0 < t < \pi/2$ the function has an absolute maximus at $\gamma^* = \ln(\cos t)/t$ with $f(\gamma^*) < 0$. If $t \geq \pi/2$ we have $\frac{\partial f(\gamma)}{\partial \gamma} > 0$ for all $\gamma \in \mathbb{R}$ and $f(0) < 0$. Therefore, for $0 < t < \pi$ we have $r_2^{(1)}(\gamma) < 0$ for all $\gamma \in \mathbb{R}$ and the proposition follows. □

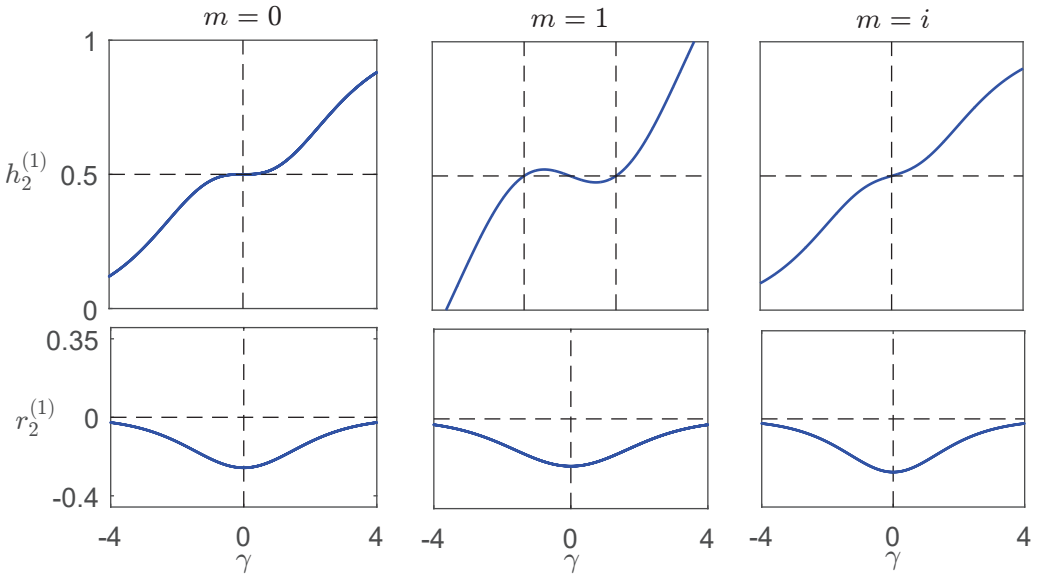

Figure 5.6: Functions $h_2^{(1)}$ and $r_2^{(1)}$ with the parameter $t = 0.5$ and by varying the parameter γ.

Now, we give sufficient conditions on the functions $h_2^{(1)}$ and $r_2^{(1)}$, such that for any $k = 1, 2$, the border collision bifurcation curves $x_2^{(k)}$ are strictly decreasing on the interval $(\pi/2, \pi)$ and $x_2^{(2)}(\theta) < x_2^{(1)}(\theta)$.

Proposition 93. *Given $m \in \{0, 1, i\}$, $0 < t < 1$ and $\gamma \in \mathbb{R}$ such that $D = \gamma^2 - m^2 \neq 0$. The following statements hold.*

(a) For $k = 1, 2$, the border collision bifurcation curves $x_2^{(k)}$ defined in (5.64) are strictly decreasing on the interval $(\pi/2, \pi)$.

(b) If the condition

$$b < \frac{2h_2^{(1)}(\gamma) - 1}{2r_2^{(1)}(\gamma) D}, \tag{5.81}$$

hold, we have $x_2^{(2)}(\theta) < x_2^{(1)}(\theta)$ for all $\theta \in [\pi/2, \pi]$.

Proof. From Proposition 92, we have the inequalities $0 < h_2^{(k)}(\gamma) < 1$, for $k = 1, 2$. Now, from Proposition 87(a), the functions $x_2^{(k)}$ are strictly decreasing on the interval $(\pi/2, \pi)$ and statement (a) follows.
From (5.77) we get

$$h_2^{(2)}(\gamma) + h_2^{(1)}(\gamma) = 1, \quad r_2^{(1)}(\gamma) = -r_2^{(2)}(\gamma).$$

Now, from hypothesis we have

$$b < \frac{2h_2^{(1)}(\gamma) - 1}{2r_2^{(1)}(\gamma)D} = \frac{1}{D}\frac{2h_2^{(1)}(\gamma) - (h_2^{(2)}(\gamma) + h_2^{(1)}(\gamma))}{r_2^{(1)}(\gamma) - r_2^{(2)}(\gamma)} = \frac{1}{D}\frac{h_2^{(2)}(\gamma) - h_2^{(1)}(\gamma)}{r_2^{(2)}(\gamma) - r_2^{(1)}(\gamma)}. \quad (5.82)$$

Taking into account that $0 < h_2^{(1)}(\gamma) < 1$ and $r_2^{(1)}(\gamma) < 0 < r_2^{(2)}(\gamma)$, we obtain

$$h_2^{(2)}(\gamma) - h_2^{(1)}(\gamma) = 1 - 2h_2^{(1)}(\gamma) > 0, \quad r_2^{(2)}(\gamma) - r_2^{(1)}(\gamma) = -2r_2^{(1)}(\gamma) > 0.$$

Therefore, we can rewrite (5.82) as

$$\frac{b(r_2^{(2)}(\gamma) - r_2^{(1)}(\gamma))D}{h_2^{(2)}(\gamma) - h_2^{(1)}(\gamma)} < 1,$$

and from Proposition 87(b), we obtain $x_2^{(2)}(\theta) < x_2^{(1)}(\theta)$ for all $\theta \in [\pi/2, \pi]$ and the proposition follows. □

Remark 94. *From Proposition 93, if* $x_2^{(1)}(3\pi/4) > 0$ *we obtain*

$$b < \frac{1}{\sqrt{2}}\frac{2h_2^{(1)} - 1}{2r_2^{(1)}D} < \frac{2h_2^{(1)} - 1}{2r_2^{(1)}D}.$$

Therefore, if $x_2^{(1)}(3\pi/4) > 0$ *we have* $x_2^{(2)}(\theta) < x_2^{(1)}(\theta)$ *for all* $\theta \in [\pi/2, \pi]$.

The main result of this section is a complete characterization of the 2-periodic orbits. Taking the parameter $0 < t < 1$, the modal parameter $m \in \{0, 1, i\}$ and $\gamma \in \mathbb{R}$ such that $\gamma^2 - m^2 > 0$ and $\gamma < 0$, the following theorem allows us give conditions on the parameter b such that there exists an interval $I \subseteq [\pi/2, \pi]$, where for all $\theta \in I$ a 2-periodic orbit is stable and admissible of type RL.

Theorem 95. *Given* $m \in \{0, 1, i\}$, $0 < t < 1$ *and* $\gamma \in \mathbb{R}$ *such that* $D = \gamma^2 - m^2 > 0$ *and* $\gamma < 0$. *Consider the functions* $x_2^{(1)}$, $h_2^{(1)}$ *and* $r_2^{(1)}$ *given in* (5.64) *and* (5.75) *respectively. The following statements hold for map* P *given in* (5.50)-(5.51).

(a) If $x_2^{(1)}(\pi) \geq 0$ *or equivalent, if there exist* $b \in \mathbb{R}$ *such that*

$$bDr_2^{(1)}(\gamma) - h_2^{(1)}(\gamma) \geq 0,$$

then map P *has a unique stable 2-periodic orbit for all* $\theta \in [\pi/2, \pi]$.

(b) If $x_2^{(1)}(\pi) < 0$ *and* $x_2^{(1)}(3\pi/4) > 0$ *or equivalently, if there exist* $b \in \mathbb{R}$ *such that*

$$bDr_2^{(1)}(\gamma) - h_2^{(1)}(\gamma) < 0, \quad 2bDr_2^{(1)}(\gamma) + \sqrt{2}(1 - 2h_2^{(1)}(\gamma)) > 0,$$

then there exists a unique $\beta \in (3\pi/4, \pi)$ *such that* $x_2^{(1)}(\beta) = 0$ *and for all* $\theta \in (3\pi/2 - \beta, \beta)$ *map* P *has a unique stable 2-periodic orbit.*

Proof. From statement (a) of Proposition 93, functions $x_n^{(k)}$ defined in (5.64) are strictly decreasing on the interval $[\pi/2, \pi]$ for $k \in \{1, 2\}$. Then, if $x_2^{(1)}(\pi) \geq 0$ we have $x_2^{(1)}(\theta) > 0$ for all $\theta \in [\pi/2, \pi)$. Also, $x_2^{(1)}(\pi) > 0$ if and only if $x_2^{(2)}(\pi/2) < 0$ and so we obtain $x_2^{(2)}(\theta) < 0$ for all $\theta \in (\pi/2, \pi)$ and statement (a) follows.
If $x_2^{(1)}(\pi) < 0$ and $x_2^{(1)}(3\pi/4) > 0$, there exists a unique $\beta \in (3\pi/4, \pi)$ such that for all $\theta \in (\pi/2, \beta)$ we obtain $x_2^{(1)}(\theta) > 0$. Finally, we have that $x_2^{(2)}(\pi/2) > 0$ and $x_2^{(2)}(3\pi/2 - \beta) = 0$, so that for all $\theta \in (3\pi/2 - \beta, \pi)$ we obtain $x_2^{(2)}(\theta) < 0$ and taking the open interval $(3\pi/2 - \beta, \beta)$ statement (b) follows. The stability in both statements comes from Proposition 76(b) and this concludes the proof. □

Remark 96. *Regarding statement (b) of the previous theorem, the numerical value of* $\beta \in (3\pi/4, \pi)$ *can be computed by solving the equation* $x_2^{(1)}(\beta) = 0$, *that is*

$$0 = br_2^{(1)}(\gamma) D + (1 - h_2^{(1)}(\gamma)) \sin\beta + h_2^{(1)}(\gamma) \cos\beta,$$

and after some algebra we obtain that

$$\beta = \arcsin\left(\frac{-br_2^{(1)}(\gamma) D}{\sqrt{(1 - h_2^{(1)}(\gamma))^2 + (h_2^{(1)}(\gamma))^2}}\right) - \pi - \arctan\left(\frac{h_2^{(1)}(\gamma)}{1 - h_2^{(1)}(\gamma)}\right).$$

The equalities $x_2^{(1)}(\pi) = 0$ and $x_2^{(1)}(3\pi/4) = 0$ are equivalent to

$$br_2^{(1)}(\gamma) D - h_2^{(1)}(\gamma) = 0 \quad \text{and} \quad 2br_2^{(1)}(\gamma) D - 2\sqrt{2}h_2^{(1)}(\gamma) + \sqrt{2} = 0. \tag{5.83}$$

Solving for b in (5.83), and by fixing the parameter t, we obtain on the two-parametric plane (γ, b) the functions b_1 and b_2 defined by

$$b_1(\gamma) = \frac{h_2^{(1)}(\gamma)}{r_2^{(1)}(\gamma) D}, \quad b_2(\gamma) = \frac{2h_2^{(1)}(\gamma) - 1}{\sqrt{2}r_2^{(1)}(\gamma) D}. \tag{5.84}$$

Remark 97. *Note that given* $m \in \{0, 1, i\}$, $0 < t < 1$ *and* $\gamma \in \mathbb{R}$ *such that* $D = \gamma^2 - m^2 > 0$ *and* $\gamma < 0$, *we obtain* $0 < h_2^{(1)}(\gamma) < 1/2$ *and* $r_2^{(1)} < 0$, *thus*

$$b_1(\gamma) < 0 < b_2(\gamma). \tag{5.85}$$

Given the two-dimensional parameter space (γ, b), we define the sets Δ and Δ_β as

$$\begin{aligned} \Delta &:= \left\{(\gamma, b) \,:\, \gamma^2 - m^2 > 0,\, \gamma < 0,\, b \le b_1(\gamma)\right\}, \\ \Delta_\beta &:= \left\{(\gamma, b) \,:\, \gamma^2 - m^2 > 0,\, \gamma < 0,\, b_1(\gamma) < b < b_2(\gamma)\right\}. \end{aligned} \tag{5.86}$$

Regarding Theorem 95, if $(\gamma, b) \in \Delta$, the hypotheses of statement (a) are satisfied, and then map P has a unique stable 2-periodic orbit for all $\theta \in [\pi/2, \pi]$. Also, at $\theta = \pi/2$ and $\theta = \pi$ a border-collision bifurcation of 1-periodic orbit to 2-periodic orbit occurs. Moreover, if $b = b_1(\gamma, t)$ we get

$$\mathbf{e}_1^T \mathbf{x}_L^* \left(\pi/2\right) = x_2^{(1)} \left(\pi/2\right), \qquad \mathbf{e}_1^T \mathbf{x}_R^* \left(\pi\right) = x_2^{(2)} \left(\pi\right),$$

where $\mathbf{x}_L^*$ and $\mathbf{x}_R^*$ are the fixed points defined in (5.52).
On the other hand, if $(\gamma, b) \in \Delta_\beta$, the hypotheses of statement (b) are satisfied, thus, there exists a unique $\beta \in (3\pi/4, \pi)$ such that map P has a unique stable 2-periodic orbit for all $\theta \in (3\pi/2 - \beta, \beta)$. In Figure 5.7, we show the two-parametric space (γ, b) and a discussion of the above theorem.

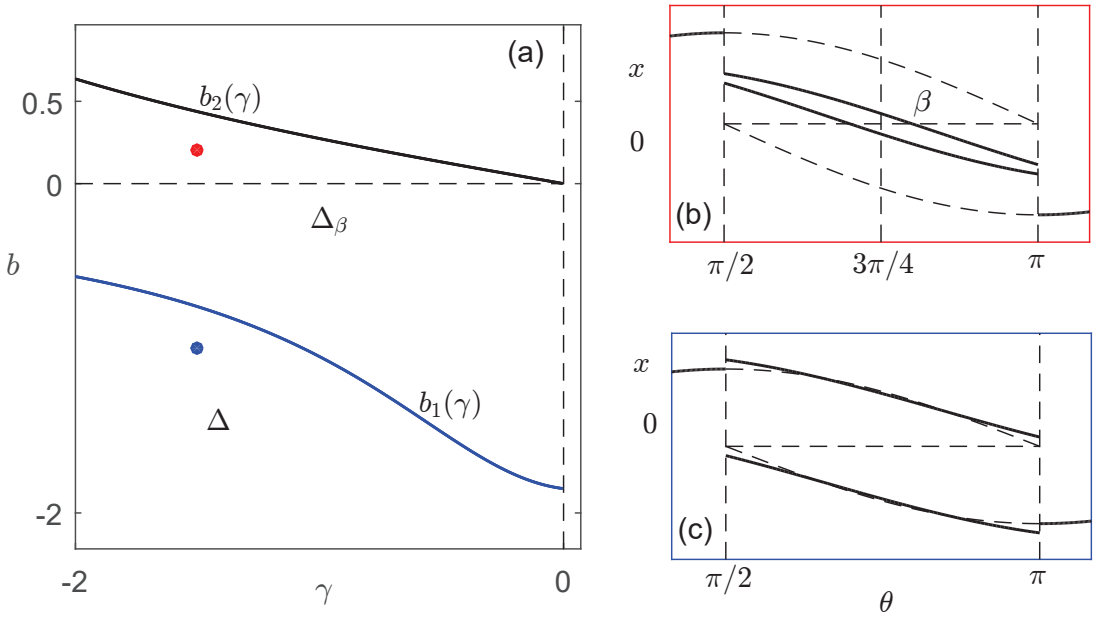

Figure 5.7: (a) Fixing the parameter $t = 0.9$, the two-dimensional parameter space is shown. The functions b_1 and b_2 defined in (5.84) are shown in blue and black respectively. Also, the set Δ and Δ_β defined in (5.86) are shown. The red and blue points correspond to the elements of the sets Δ_β and Δ respectively. (b) 2-periodic orbit corresponding to the red dot shown in (a). (c) 2-periodic orbit corresponding to the blue dot shown in (a).

5.9 On the BB bifurcation

The extension to n-periodic orbit with itinerary RL^{n-1} of the results so far presented for the periodic two orbits, it is a complex and non-trivial task that will not be completed in this thesis. In this section, we present a first approach to the study of the admissibility of the orbits mentioned and a conjecture about occurrence of BB bifurcation in discontinuous stroboscopic maps is established. We emphasize that this conjecture is a generalization of the conjecture given in Fossas and Granados [2013].

First, extending the strategy used in the study of orbits 2 periodic, we assume that for $n \geq 3$, and for all $\theta \in [\pi/2, \pi]$ the border collision bifurcation curves $x_n^{(k)}$ are strictly decreasing and the following inequalities hold (see Figure 5.9)

$$x_n^{(2)}(\theta) < x_n^{(3)}(\theta) < \cdots < x_n^{(n)}(\theta) < x_n^{(1)}(\theta). \tag{5.87}$$

Note that the inequalities given in (5.87) are sufficient but not necessary conditions for the admissibility of periodic orbits, see Figure 5.8.

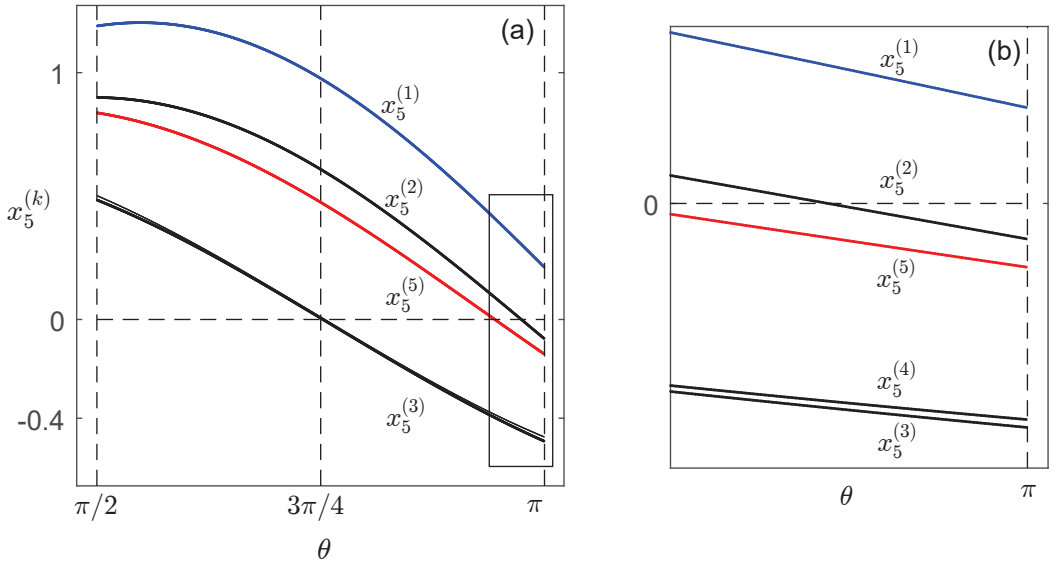

Figure 5.8: Border collision bifurcation curves for 5-periodic orbit with parameter fixed in $m = i$, $t = 0.9$, $\gamma = -0.15$ and $b = -0.1$. (a) Functions $x_5^{(1)}$ and $x_5^{(5)}$ in blue and red respectively. In black the functions $x_5^{(k)}$ with $k = 2, 3, 4$. (b) A zoom of (a) where the inequalities $x_5^{(3)}(\theta) < x_5^{(4)}(\theta) < x_5^{(5)}(\theta) < x_5^{(2)}(\theta) < x_5^{(1)}(\theta)$ hold.

In the following proposition, we show that given $n \geq 3$, $m \in \{0, 1, i\}$ and $0 < t < 1$, if we assume that there are two real numbers $\overline{\gamma}$ and $\overline{b}$, satisfying some conditions, then, we can guarantee the existence of an interval $I_n \subseteq (3\pi/4, \pi)$ such that for all $\theta \in I_n$ the n-periodic orbit with itinerary RL^{n-1} is stable and admissible.

Proposition 98. *Given $m \in \{0, 1, i\}$, $0 < t < 1$ and $n \geq 3$. Suppose that there exist $\overline{\gamma} \in \mathbb{R}$ with $D = \overline{\gamma}^2 - m^2 > 0$ and $\overline{\gamma} < 0$ such that for all $k \in \{1, 2, \ldots, n\}$ we*

have

$$0 < h_n^{(k)}(\overline{\gamma}) < 1, \tag{5.88}$$

where the functions $h_n^{(k)}$ *are given in* (5.70) *and* (5.71). *Additionally, suppose that for all* $\theta \in [\pi/2, \pi]$ *we have the inequalities* (5.87). *If there exists* $\overline{b} \neq 0$ *such that*

$$2\overline{b}r_n^{(2)}(\overline{\gamma})D - 2\sqrt{2}h_n^{(2)}(\overline{\gamma}) + \sqrt{2} > 0, \quad \overline{b}r_n^{(1)}(\overline{\gamma})D - h_n^{(1)}(\overline{\gamma}) < 0. \tag{5.89}$$

Then there exist an interval $I_n = (\mu_n, \upsilon_n) \subseteq (3\pi/4, \pi)$ *such that for all* $\theta \in I_n$ *the* n*-periodic orbit* $\mathrm{Or}(\mathbf{x}_n^{(1)}(\theta))$ *defined in* (5.58) *is admissible.*

Proof. From hypotheses and Proposition 87(a) functions $x_n^{(k)}$ are strictly decreasing on the interval $[\pi/2, \pi]$. Inequalities (5.89) are equivalent to $x_n^{(2)}(3\pi/4) > 0$ and $x_n^{(1)}(\pi) < 0$ respectively. Then from relations (5.87) we obtain

$$\begin{aligned} &0 < x_n^{(2)}(3\pi/4) < x_n^{(3)}(3\pi/4) < \cdots < x_n^{(n)}(3\pi/4) < x_n^{(1)}(3\pi/4), \\ &x_n^{(2)}(\pi) < x_n^{(3)}(\pi) < \cdots < x_n^{(n)}(\pi) < x_n^{(1)}(\pi) < 0, \end{aligned}$$

so that there exists a unique $\beta_k \in (3\pi/4, \pi)$ with $x_n^{(k)}(\beta_k) = 0$ and

$$3\pi/4 < \beta_2 < \beta_3 < \cdots < \beta_n < \beta_1 < \pi.$$

Taking $\mu_n = \beta_n$ and $\upsilon_n = \beta_1$, we have that, if $\theta \in (\mu_n, \upsilon_n)$

$$x_n^{(2)}(\theta) < x_n^{(3)}(\theta) < \cdots < x_n^{(n)}(\theta) < 0 < x_n^{(1)}(\theta).$$

Therefore, the n-periodic orbit $\mathrm{Or}(\mathbf{x}_n^{(1)}(\theta))$ defined in (5.58) is admissible of type RL^{n-1}. the stability of the periodic orbit it is a direct consequence of the Proposition 76(b). □

Taking $\overline{\gamma} = -1.1$ and $\overline{b} = -1$, we obtain for $m = 1$, $t = 0.9$ and $n = 5$ the inequalities (5.88), (5.87) and (5.89), so that, from the previous proposition there exists an interval $I_5 = (\mu_5, \upsilon_5) \approx (2.933, 2.954)$ such that for all $\theta \in I_5$ the 5-periodic orbit of type RL^{n-1} is stable and admissible, see Figure 5.9.

A complete result on the existence of the numbers $\overline{\gamma}$ and $\overline{b}$ is left as future work. We note that if there exist $\gamma \in \mathbb{R}$ and $b \neq 0$ such that for all $n \geq 3$ and $\theta \in [\pi/2, \pi]$, we have the inequalities (5.87) and (5.89), then, there exists a family of open intervals $\{(\mu_n, \upsilon_n)\}_{n=3}^{\infty}$ with

$$3\pi/4 < \mu_3 < \upsilon_3 < \mu_4 < \upsilon_4 \cdots < \mu_n < \upsilon_n < \cdots < \pi,$$

and such that the n-periodic orbit $\mathrm{Or}(\mathbf{x}_n^{(1)}(\theta))$ is stable and of type RL^{n-1} on the interval (μ_n, υ_n), in other words, we have for $n \geq 3$ the simultaneous admissibility of the sequence of type RL^{n-1} on the two-parameter plane (a_R, a_L), that is, map P defined in (5.47)-(5.23)-(5.17) has a big bang bifurcation point at $(0, 0)$.

Having in mind the extension to our stroboscopic map of the conjecture given in Fossas and Granados [2013], in the next result, we study the behavior of functions $h_n^{(1)}$ when n tends to infinity.

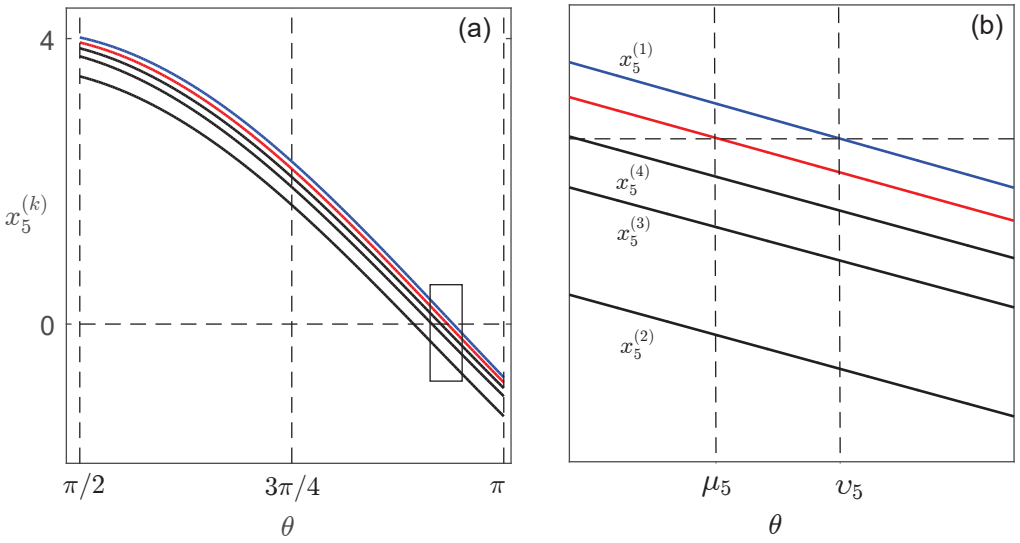

Figure 5.9: Border collision bifurcation curves for 5-periodic orbit with parameter fixed in $m = 1$, $t = 0.9$, $\gamma = -1.1$ and $b = -1$. (a) Functions $x_5^{(1)}$ and $x_5^{(5)}$ in blue and red respectively. In black the functions $x_5^{(k)}$ with $k = 2, 3, 4$. (b) A zoom of (a), the interval $I_5 = (\mu_5, \upsilon_5)$ given by Proposition (98) is shown.

Proposition 99. *Given $m \in \{0, 1, i\}$, $n \geq 3$, $0 < t < 1$ with $t \neq \pi/2n$ and $\gamma \in \mathbb{R}$ such that $\gamma^2 - m^2 \neq 0$. Consider the functions $h_n^{(1)}$ given in (5.70). The following statements hold.*

(a) For $m \in \{0, 1, i\}$ we have

$$\kappa(n) := \lim_{\gamma \to 0} h_n^{(1)}(\gamma) = \begin{cases} \dfrac{1}{n}, & \text{if } \ m = 0, \\ \dfrac{1 - C_n - C_1 + C_{n-1}}{2(1 - C_n)}, & \text{if } \ m \neq 0, \end{cases} \tag{5.90}$$

where C_n is defined in (5.19). Moreover,if $m = 1$ we get

$$\lim_{\gamma \to \pm 1} h_n^{(1)}(\gamma) = \frac{1}{n}.$$

(b) For all $n \geq 3$ and $t > 0$ we have $0 < \kappa(n) < 1/2$, and there exists $\kappa_\infty \in \mathbb{R}$ such that

$$\kappa_\infty = \lim_{n \to \infty} \kappa_n(t) = \begin{cases} \frac{1}{2}(1 - e^{-t}) & \text{if } \ m = 1, \\ 0 & \text{if } \ m = 0. \end{cases}$$

(c) If $m = i$ there exists $n_0 > 3$ such that $\kappa(n_0) < 0$.

Proof. Using the L'Hopital rule we obtain (5.90). If $m = 0$ we have that $\kappa(n) = 1/n$, then for all $n \geq 3$ we obtain $0 < \kappa(n) < 1/2$. Since $\cosh t$ is an strictly increasing

function, we have $\cosh t < \cosh t\,(n-1)$, also $\cosh(nt) - 1 < 0$, then we get

$$\frac{1 - \cosh(nt) - \cosh t + \cosh((n-1)\,t)}{1 - \cosh(nt)} < 1,$$

so that for $m = 1$ we obtain $0 < \kappa(n) < 1/2$ and statement (a) follows. To show statement (b) it is sufficient to consider that $1 - \cos(nt) > 0$ and that

$$\kappa(n) = \frac{1}{2}\left(1 + \frac{\cos((n-1)\,t) - \cos t}{1 - \cos(nt)}\right),$$

so that for n_0 sufficiently large we get

$$\frac{\cos((n_0-1)\,t) - \cos t}{1 - \cos(n_0 t)} < -1,$$

that is $\kappa(n_0) < 0$ and the proposition follows. □

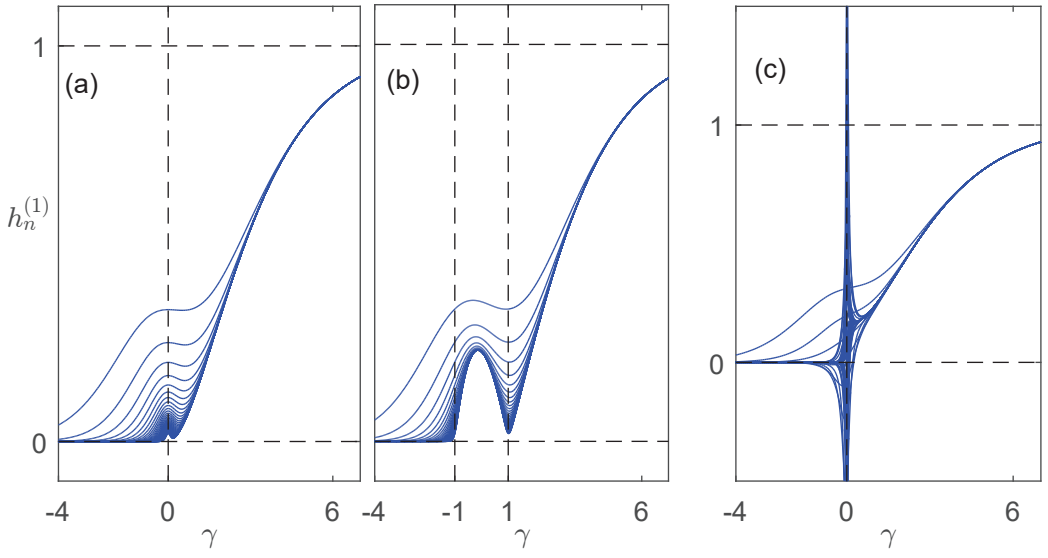

Figure 5.10: Functions $h_n^{(1)}(\gamma)$ with $3 \le n \le 50$ and $t = 0.6$ are shown. (a), (b) and (c) correspond to the cases $m = 0, 1, i$ respectively.

Regarding Proposition (87)(a), the inequalities $0 < h_n^{(k)}(\gamma) < 1$ are sufficient conditions for the border collision bifurcation curves to be strictly decreasing on the interval $[\pi/2, \pi]$, thus, as a first consequence of the previous proposition, we have that when $m = i$, that is, foci case, we cannot guarantee the inequalities mentioned above. Therefore, motivated by the previous reasoning and after extensive numerical simulations, we give the following conjecture about the cases $m = 0, 1$, that is, node case.

Conjecture 100. *Given $m \in \{0, 1\}$ and $n \ge 3$. Then for any $1 \le k \le n$, $0 < t < 1$ and $\gamma \in \mathbb{R}$ such that $\gamma^2 - m^2 \neq 0$ we get $0 < h_n^{(k)}(\gamma) < 1$.*

Now, we are in position to state a conjecture about the occurrence of a big bang bifurcation in the discontinuous stroboscopic map P defined in (5.47)-(5.23)-(5.17). Our conjecture involves only the node case, and a certain attractive sliding set, that is, $m \in \{0, 1\}$ and a certain negative value b. However, we emphasize that this does not exclude the presence of a big bang bifurcation in foci case.

Conjecture 101. *Given $m \in \{0, 1\}$ and $0 < t < 1$. Consider the stroboscopic map P defined in (5.47)-(5.23)-(5.17), the two-parameter plane (a_R, a_L), and the functions*

$$\begin{aligned} d_3(\gamma,t)h_3^{(2)}(\gamma,t) &= e^{4t\gamma}\mu_2^+ - e^{3t\gamma}\mu_3^+ - e^{t\gamma}\mu_1^- + 1, \\ d_3(\gamma,t)r_3^{(2)}(\gamma,t) &= e^{4t\gamma}S_2 - e^{3t\gamma}S_3 + e^{t\gamma}S_1, \\ d_3(\gamma,t) &= e^{6t\gamma} - 2C_3e^{3t\gamma} + 1, \end{aligned}$$

where the functions S_k, C_k and $\mu_k^{\pm}$ are defined in (5.19) and (5.20) respectively. Then for $\gamma + m < 0$ sufficiently small and

$$b = \min\left\{\frac{1}{\gamma + m},\, F(\gamma, t)\right\},$$

where the function F is defined as

$$F(\gamma,t) = \frac{1}{D}\frac{2h_3^{(2)}(\gamma,t) - 1}{\sqrt{2}r_3^{(2)}(\gamma,t)},$$

the stroboscopic map P has at $(0, 0)$ a big bang bifurcation point of codimension two.

As in Figure 5.3, we consider in Figures 5.11 and 5.12 a circular arc with radius $r = 1$ on the two-parametric plane (a_R, a_L). In Figure 5.11(a) we show a bifurcation diagram of the stroboscopic map P defined in (5.47)-(5.23)-(5.17) along the circular arc parametrized by the angle $\theta \in [3\pi/4, \pi + 0.01]$. For the set of parameters $m = 0$, $t = 0.9$ and $\gamma = -0.2$, we obtain from Conjecture 101 that $b = 1/\gamma$. In Figure 5.11(b) we show a period diagram of the bifurcation diagram given in (a). The case $m = 1$ is considered in Figure 5.12, taking $m = 1$, $t = 0.9$ and $\gamma = -1.05$ in Conjecture 101, we obtain that $b = F(\gamma, t) \approx -9.27$.

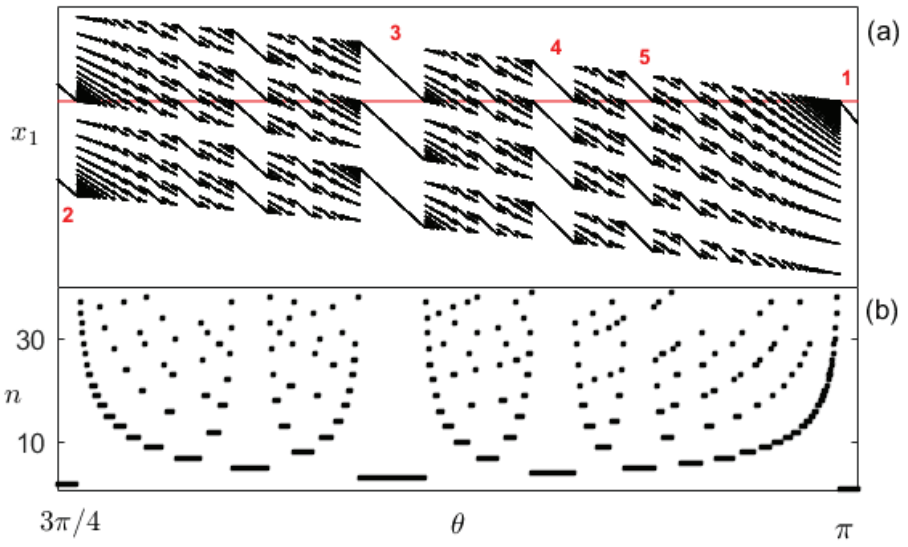

Figure 5.11: (a) Bifurcation diagram of map P defined in (5.50)-(5.51) is shown. Parameters fixed in $m = 0$, $t = 0.9$, $\gamma = -0.2$ and $b = 1/\gamma$. The parameters γ and b are taken from Conjecture 101. Parameter θ is varied. (b) Period diagram calculated numerically with parameters as in (a).

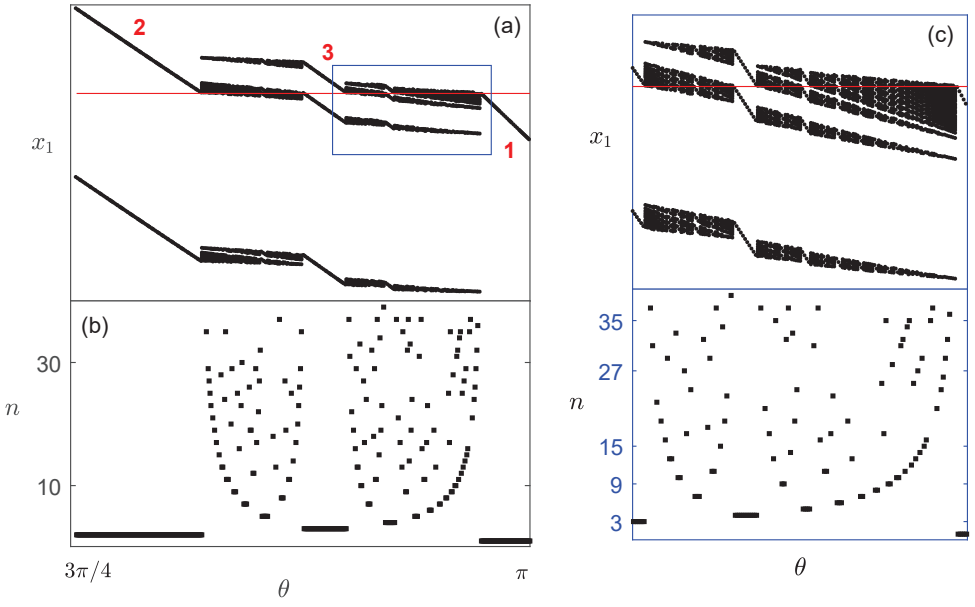

Figure 5.12: (a) Bifurcation diagram of map P defined in (5.50)-(5.51) is shown. Parameters fixed in $m = 1$, $t = 0.9$, $\gamma = -1.05$ and $b = -9.27$. The parameters γ and b are taken from Conjecture 101. Parameter θ is varied. (b) Period diagram calculated numerically with parameters as in (a). (c) A zoom of (a) and (b).

Bibliography

A. Amador, S. Casanova, G. Olivar, and J. Hurtado. Codimension-two big-bang bifurcation in a ZAD-controlled boost DC-DC converter. *Publicacions Matematiques*, 24:1450150, 2014. URL https://doi.org/10.1142/S0218127414501508.

V. Avrutin and M. Schanz. On multi-parametric bifurcations in a scalar piecewise-linear map. *Nonlinearity*, 19(3):531–552, 2006. URL http://stacks.iop.org/0951-7715/19/i=3/a=001.

V. Avrutin, M. Schanz, and S. Banerjee. Multi-parametric bifurcations in a piecewise-linear discontinuous map. *Nonlinearity*, 19(8):1875–1906, 2006. URL http://stacks.iop.org/0951-7715/19/i=8/a=007.

V. Avrutin, M. Schanz, and S. Banerjee. Codimension-three bifurcations: Explanation of the complex one, two, and three-dimensional bifurcation structures in nonsmooth maps. *Physical Review E*, 75:066205, Jun 2007. URL https://doi.org/10.1103/PhysRevE.75.066205.

V. Avrutin, A. Granados, and M. Schanz. Sufficient conditions for a period incrementing big bang bifurcation in one-dimensional maps. *Nonlinearity*, 24(9):2575, 2011. URL http://stacks.iop.org/0951-7715/24/i=9/a=012.

E. Fossas and A. Granados. Occurrence of big bang bifurcations in discretized sliding-mode controlled systems. *Differential Equations and Dynamical Systems*, 21:35–43, 2013. URL https://doi.org/10.1007/s12591-012-0121-y.

E. Freire, E. Ponce, and F. Torres. Canonical discontinuos planar piecewise linear systems. *SIAM Journal Applied Dynamical Systems*, 11:181–211, 2012. URL https://doi.org/10.1137/11083928X.

E. Freire, E. Ponce, and F. Torres. A general mechanism to generate three limit cycles in planar filippov systems with two zones. *Nonlinear Dynamics*, 78(1): 251–263, 2014. URL https://doi.org/10.1007/s11071-014-1437-7.

L. Gardini and F. Tramontana. Border collision bifurcation curves and their classification in a family of 1D discontinuous maps. *Chaos, Solitons & Fractals*, 44(4): 248 – 259, 2011. URL https://doi.org/10.1016/j.chaos.2011.02.001.

L. Gardini, F. Tramontana, V. Avrutin, and M. Schanz. Border-collision bifurcation in 1D piecewise-linear maps and leonov's approach. *International Journal of Bifurcation and Chaos*, 20(10):3085–3104, 2010. URL https://doi.org/10.1142/S021812741002757X.

A. Granados, M. Krupa, and F. Clément. Border collision bifurcations of stroboscopic maps in periodically driven spiking models. *SIAM Journal on Applied Dynamical Systems*, 13(4):1387–1416, 2014. URL https://doi.org/10.1137/13094637X.

A. Granados, L. Alsedà, and M. Krupa. The period adding and incrementing bifurcations: From rotation theory to applications. *SIAM Review*, 59(2):225–292, jan 2017. URL https://doi.org/10.1137/140996598.

Y. Kuznetsov, S. Rinaldi, and A. Gragnani. One-parameter bifurcations in planar Filippov systems. *International Journal of Bifurcation and Chaos*, 13(8):2157–2188, 2003. URL https://doi.org/10.1142/S0218127403007874.

H.E Nusse and J.A Yorke. Border-collision bifurcations including period 2 to period 3 for piecewise smooth systems. *Physica D: Nonlinear Phenomena*, 57(1-2):39–57, 1992. URL https://doi.org/10.1016/0167-2789(92)90087-4.

I. Sushko, L. Gardini, and V. Avrutin. Nonsmooth one-dimensional maps: some basic concepts and definitions. *Journal of Difference Equations and Applications*, 22(12):1816–1870, oct 2016. URL https://doi.org/10.1080/10236198.2016.1248426.

Chapter 6

Conclusions and future works

In this thesis, motivated by concrete engineering problems, some specific piecewise linear systems have been investigated. The achieved results have been presented along the document, structured in two blocks. First, in Part I of this work, we have provided for the first time rigorous mathematical results regarding the rich dynamics of memristor oscillators. Thus, we have discovered a conserved quantity for 3D and 4D models of memristor oscillators, a result that surprisingly had been not stressed before, being a consequence of the different electrical conservation laws. Furthermore, their long-term dynamical dependence on initial conditions has been emphasized, since the dynamics is stratified as a consequence of the conserved quantity. Consequently, we have shown that a dimensional reduction in the mathematical models is possible, although the price to pay is the introduction of an additional parameter to give account of initial conditions. Thus, our study put on a firm basis the extended feeling among researchers that chaotic regimes are only possible for 4D memristor oscillators.

During the process of writing this thesis, we have been aware of the work done by Fernando Corinto and Mauro Forti, which appeared in the papers Corinto and Forti [2016] and Corinto and Forti [2017]. They propose to model memristor oscillators in an incremental flux-charge framework, so avoiding the usual models in terms of currents and voltages. In such a framework, it is possible to avoid the unnecessary extra dimension and the lack of smoothness in the equations when dealing with piecewise linear characteristics. In fact, apart from giving an alternative approach, our main contribution in this subject is to show how it is possible to overcome such drawbacks for PWL memristor oscillators without abandoning the usual current-voltage setting.

In a second level of relevance, a much deeper insight on the dynamics of elementary memristor oscillators has been gained, thanks to the topologically equivalent continuous models derived in this thesis. For 3D PWL memristor oscillator models, the existence of bistable regimes has been detected for the first time, and what is much more important, it has been adequately mathematically characterized in terms of the model parameters. Some previous conjectures on the structure of the set of periodic orbits for such memristor oscillators have been rigorously shown, pointing out a few inconsistent assertions in previous works.

For the particular case of 3D memristor oscillators whose memristor character-

istics is a cubic polynomial, a case frequently studied in the electrical engineering literature, we also show the appearance of an infinity number of invariant manifolds, since the key point is the existence of a conserved quantity, and that does not depends on the shape of the memristor characteristics. In addition, we give a global approximation of the different bifurcation sets for the corresponding cubic planar differential systems, which are topologically equivalent to a symmetric Bogdanov-Takens canonical form. Curiously, the quoted cubic Bogdanov-Takens system had not been previously analyzed by resorting to the powerful first-order Melnikov method and so the detailed analysis of this pending case is another contribution of our work.

For 4D memristor oscillator models, our techniques give rise logically to 3D dynamical systems, and so the mathematical analysis of these models is much more involved. We are conscious that in this concrete field there is a lot of work to do. Here, our contribution is limited to explain and justify a new global bifurcation leading to the sudden generation of a hyper-sphere completely foliated by periodic orbits. We have so introduced in 4D piecewise linear systems a multiple Focus-Center-Cycle bifurcation, a rich phenomenon non reported in the literature, which in some sense constitutes the parametric onset of oscillations for the corresponding memristor oscillators. Several numerical simulations, also included in this document, not only confirm the theoretical results achieved but also stimulate future research by showing similar and even more complicated dynamics in the studied 4D memristor oscillators.

Finally, in the second part of the thesis, a conjecture given by Fossas and Granados, regarding the existence of a big bang (BB) bifurcation in the stroboscopic map of a second order relay control system Fossas and Granados [2013], has been investigated. For the stroboscopic map studied in the quoted paper, a topological equivalence with the normalized canonical form introduced in Freire et al. [2014] has been established. Next, by studying the main properties of the generic stroboscopic map defined by the mentioned canonical form, the orbits of period two has been fully characterized. At last, we have given an extension to our map of the conjecture mentioned above. Extensive simulations suggest the truth of such conjecture but its verification or falsification is left for future work.

Bibliography

F. Corinto and M. Forti. Memristor circuits: Flux-charge analysis method. *IEEE Transactions on Circuits and Systems I: Regular Papers*, 63(11):1997–2009, nov 2016. URL https://doi.org/10.1109/tcsi.2016.2590948.

F. Corinto and M. Forti. Memristor circuits: Bifurcations without parameters. *IEEE Transactions on Circuits and Systems I: Regular Papers*, 64(6):1540–1551, jun 2017. URL https://doi.org/10.1109/tcsi.2016.2642112.

E. Fossas and A. Granados. Occurrence of big bang bifurcations in discretized sliding-mode controlled systems. *Differential Equations and Dynamical Systems*, 21:35–43, 2013. URL https://doi.org/10.1007/s12591-012-0121-y.

E. Freire, E. Ponce, and F. Torres. A general mechanism to generate three limit cycles in planar filippov systems with two zones. *Nonlinear Dynamics*, 78(1): 251–263, 2014. URL https://doi.org/10.1007/s11071-014-1437-7.

List of Figures